CHARACTERISING THE IMMUNE RESPONSE TO COMBINED SKIN AND SOLID ORGAN TRANSPLANTS

Helen Stark

Green Templeton College

Nuffield Department of Surgery

University of Oxford

Thesis submitted as partial fulfilment of the requirements for the degree of Doctor of Philosophy

Supervisors: Professor Peter Friend, Professor Henk Giele,

Dr Joanna Hester, Professor Fadi Issa

College Supervisor: Dr Susan Burge

Michaelmas term 2022

ABSTRACT

Transplantation offers a life-saving solution for patients with end-stage organ failure. Despite advances in recent years, managing acute rejection episodes remains challenging. This is partly due to difficulties in recognising when acute rejection is taking place. The concept of a sentinel skin flap for monitoring of organ transplantation has recently been introduced as a potential solution for this. The advent of abdominal wall transplants for the reconstruction of large defects in patients undergoing small bowel transplantation has further highlighted the usefulness of skin for monitoring, particularly in differentiating organ rejection from infections. Sentinel skin flaps also provide a site that is easy to biopsy, and which patients can be trained to review.

There are limited data in the literature on the alloresponse to a combined skin and solid organ transplant. The aim of this thesis is to characterise in depth this immune response. In chapter 3 the systemic immune response is examined using a combination of flow cytometry and gene expression analysis to analyse blood samples. Chapters 4 and 5 investigate the local immune response in small bowel and skin samples respectively, using the multiplexed gene expression and spatial proteomic techniques. Finally in Chapter 6 a human transgenic mouse model is used to explore the role of Langerhans cell related pathways in skin transplant rejection.

This is the first study to characterise both the systemic and local immune response in a combined skin and solid organ transplant, offering unique insights into the dynamic changes in immune phenotype post-transplantation and during rejection. The data

provide support for the use of a sentinel skin flap for immune monitoring in solid organ transplantation and will be used to guide future clinical trials.

ACKNOWLEDGMENTS

I would like to start by thanking my supervisor Professor Giele, for giving me the opportunity to develop my academic career as his clinical research fellow and for his mentorship and advice in the last three years. I am eternally grateful to my supervisors Dr Hester and Professor Issa who have guided my research career, provided opportunities to develop my skills and taught me everything I know about immunology. Dr Hester has been instrumental in developing my experimental skills and very generous with her time. I am grateful to Professor Issa for always questioning and pushing me to develop my ideas and supporting me in wider collaborations outside of our lab. I am also thankful for the encouragement of my supervisor Professor Friend who has been a great supporter of my research and provided excellent feedback.

I have thoroughly enjoyed my time with the Translational Research in Immunology Group, mostly due to the excellent people who make up the lab. Special mention must go to Amy Cross who has often provided sound advice and problem-solving skills. Whilst it may not have made (much of) an appearance in this thesis my time in the animal house was brightened by Marie, Ollie, Guido, Sarah and Amy, with whom many hours have been spent. I would also like to thank all members of the lab for their thoughtful discussions, probing questions, and willingness to join me for coffee or lunch.

This thesis would not have been possible without the generosity of the patients who agreed to take part in our trial and were willing to donate tissue for research purposes. I would also like to acknowledge James Barnes, my predecessor in the lab who was

responsible for collection of many of the samples used in this thesis. I have also been the grateful recipient of funding from the Royal College of Surgeons (England), Nuffield Department of Surgery, Green Templeton College, and the JP Moulton Charitable Foundation.

Finally, I would like to say a big thank you to my family and friends who have supported me throughout. My parents for making me believe I could achieve anything, and my friends for encouraging me to keep going! Thank you all.

ABBREVIATIONS

abdominal wall transplant	AWTx
antigen presenting cell	APC
areas of interest	AOI
binding density	BD
deoxyribonucleic acid	DNA
digital spatial profiler	DSP
fields of view	FOV
formalin fixed paraffin embedded	FFPE
human leukocyte antigen	HLA
Human Tissue Authority	HTA
Langerhans cells	LCs
messenger ribonucleic acid	mRNA
microlitre	µl
micrometre	µm
milligram	mg
millilitre	ml
millimetre	mm
modified multivisceral transplant	MMVT
nanogram	ng
natural killer	NK
NHS Blood and Transplant	NHSBT
optimal cutting temperature	OCT

Oxford Centre for Histopathology Research	OCHRe
Oxford Radcliffe Biobank	ORB
pancreas transplant alone	PTA
peripheral blood mononuclear cell	PBMC
principal component analysis	PCA
quality control	QC
regional ethics committee	REC
regions of interest	ROI
relative centrifugal force	g
ribonucleic acid	RNA
sentinel skin flap	SSF
simultaneous pancreas and kidney	SPK
small bowel	SB
small bowel alone	SBA
skin and small bowel	SBS
standard deviation	SD
standard error of the mean	SEM
T cell receptor	TCR
T regulatory cells	Tregs
terminally differentiated memory T cells	TEMRA
ultraviolet	UV

Table of Contents

1 Chapter 1. General introduction

Transplantation has been established as a treatment for organ failure for many years. Despite this several challenges remain, not least managing the recipient's immune response to the allograft. The advent of powerful immunosuppressive therapy has enabled indications for transplantation to expand but comes with its own collateral damage of increased risk of infection and malignancy. Acute rejection episodes are known to be associated with increased risk of graft failure, yet for many organ transplants there is not a simple test to recognise when these episodes are occurring. Instead, there is a reliance on functional tests that only demonstrate when damage to the transplanted organ has occurred. To tackle this problem, Oxford has pioneered the use of a sentinel skin flap (SSF) for immune monitoring in solid organ transplantation. The aim of this thesis is to perform an in-depth characterisation of the immune response to these combined transplants.

1.1 A brief history of organ transplantation

In the late 1800s surgery was becoming more commonplace, aided by the development of anaesthetic drugs[1]. As a result, surgeons began to contemplate more invasive procedures. This led to the idea that certain conditions may be treated by removal of the diseased organ and replacement with an organ transplant[2]. In 1883, Kocher was one of the first to attempt this in humans, transplanting thyroid tissue into patients who had previously undergone total thyroidectomy[2]. However, it was Alexis Carrel, along with Charles Guthrie, who developed the technique of vascular anastomoses, such that organ transplantation could be reliably performed[3]. In an early communication from 1905, they detailed experiments performing successful thyroid, kidney, and heart transplants

in dogs[3]. Transplantation was no longer being limited by surgical technique, but by the lack of understanding of the immune response to transplants.

It has been suggested that Georg Schöne may be considered the first transplant immunologist for recognising in 1912 that allografts rarely worked as well as autografts and for developing the concept that the immune system was responsible for the rejection of these grafts[2,4]. However, this theory of cellular immunity was not widely accepted, and acute rejection continued to prevent successful human organ transplants. It was not until 1956 that Joseph Murray undertook kidney transplantation between identical twins, thereby avoiding the problem of allograft rejection[5]

Whilst this transplant had a good outcome, providing encouragement for the concept of transplantation, the problem of rejection remained. It was in 1960 that Roy Calne reported on the use of a new drug, 6-mercaptopurine, which showed promise for increasing kidney allograft survival in dogs[6]. Although prolonging survival to a certain extent, outcomes in human recipients of kidney transplantation remained poor[4]. Then, in 1963 Starzl et al demonstrated reliable immunosuppression in human kidney transplant recipients, using a combination of azathioprine and prednisone[7]. With better control of the immune response, transplantation became more common, and the development of extra-renal organ transplants took place[4]. Further developments of new immunosuppressive drugs, summarised in **Table 1-1**, have enabled organ transplantation to become the gold standard of care for patients with end stage organ failure[8–13].

Drug	Mechanism of action
1960s - prednisone	regulation of gene expression[7]
1960s - 6-MP/azathioprine	azathioprine is prodrug of 6-MP, incorporates into DNA, anti-proliferative[6]
1960s – antilymphocyte globulin (ALG)	depleting antibody, multiple targets T cell membrane proteins[14]
1970s - cyclophosphamide	alkylation of DNA - targets T cell proliferation[15]
1980s - tacrolimus	calcineurin inhibitor - targets T cell proliferation[16]
1990s - mycophenolate mofetil	inhibition of de novo purine synthesis, anti-proliferative[17]
1990s - sirolimus	mTOR inhibitor, decrease in cytokine driven T cell proliferation[18]
1990s - alemtuzumab	depleting antibody, targets CD52, prevents proliferation T and B cells[19]
1990s - basiliximab	non depleting antibody, prevents binding of IL2 to its receptor[20]
2000s - belatacept	fusion protein, blocks co-stimulation of T cells by binding CD80/86[21]

Table 1-1. Summary of immunosuppressive drugs, used in solid organ transplantation.

1.2 An overview of pancreas and small bowel transplantation

This thesis explores the immune response in patients undergoing pancreas and small bowel transplantation combined with either a sentinel skin flap (SSF) or abdominal wall transplant (AWTx). The next section of this chapter focuses on the current indications, outcomes, and immune monitoring strategies for patients undergoing either pancreas or small bowel transplant alone.

1.2.1 Indications for pancreas transplantation

The indications for pancreas transplantation include patients who have severe hypoglycaemic unawareness, ketoacidosis, or significant problems with using exogenous insulin to manage their diabetes, but with normal renal function[22]. These patients will be offered a pancreas alone transplant (PAT). A second indication is renal failure (eGFR < 20ml/min/1.73m^2) with insulin dependent diabetes mellitus, where a simultaneous kidney-pancreas transplant (SPK) or pancreas after kidney transplant (PAK) may be offered[22]. Most of these patients have type 1 diabetes mellitus, but it may also include those with type 2 diabetes mellitus who are insulin dependent. There are several significant sequelae associated with diabetes mellitus, including peripheral vascular disease and amputation, retinopathy leading to blindness, cardiovascular diseases such as myocardial infarction and stroke. Therefore, improving glycaemic control in these patients may have far-reaching beneficial effects.

1.2.2 Immune monitoring of pancreas transplants

When pancreas transplantation first started, the primary way to monitor the graft was based on non-specific clinical symptoms, such as fever or pain[23]. The immune monitoring of pancreas transplants varies depending on how the pancreas is draining. For patients who have a bladder drained pancreas, it is possible to monitor the urine for levels of amylase and lipase[23]. This option is not available for patients with an enterically (via the bowel) drained pancreas[23]. Pancreas graft biopsies are undertaken to provide a definitive tissue diagnosis of rejection. However, these biopsies are not without morbidity, there is a risk of intraperitoneal bleeding, pancreatitis, or pancreas fistula[24], therefore they are not recommended by all centres.

Research has focussed on finding a non-invasive test for rejection, that avoids the need for a tissue biopsy. Whilst imaging can provide useful information, there is no evidence at present that USS, CT or MRI can be used to diagnose rejection specifically in pancreas transplantation[23]. Histological analysis of pancreas biopsies had found an increase in granzyme and HLA-DR during acute rejection[25], therefore when looking for a biomarker in blood samples Cashion et al focused on these, plus perforin. In a very small group of seven patients they were able to demonstrate an increase in perforin, granzyme B and HLA-DR up to 5 weeks prior to clinically evident acute rejection[26]. However, a similar finding was also demonstrated when patients were diagnosed with pancreatitis, suggesting a lack of specificity for acute rejection[26]. The development of dnDSA (de novo Donor Specific Antibodies) has been associated with rejection episodes and poorer graft survival in a large cohort of simultaneous pancreas and kidney and isolated pancreas transplants, so it has been recommended that levels are monitored in all pancreas transplant patients[27,28]. There remains the need for an accurate, non-invasive way to monitor the immune response in pancreas transplant. This is an area that has been highlighted as requiring further research by the First World Consensus Conference on Pancreas Transplantation 2019[27].

1.2.3 Outcomes of pancreas transplantation

The most recent NHS Blood and Transplant report on outcomes following pancreas transplantation noted that patient survival following simultaneous pancreas and kidney transplant (SPK) transplant was 99% at one year and 98% at five years post transplantation[29]. For pancreas alone transplants (PAT) patient survival was 100% at one year and 84% at five years. Graft survival (pancreas) was 93% for SPK and 88% for PAT at one year and 80% for SPK and 56% for PAT at five years. This correlates well

with a large review of a US cohort, in which five-year graft survival for SPK was 72% and 55% for PAT[30]. It is not clear why the UK has slightly better outcomes but may reflect the fact that pancreas transplantation is only provided by eight centres within the UK, centralising the service and increasing the number carried out by each centre, in contrast to the US where there is not a centralised service.

Niederhause et al performed a large cohort study of pancreas transplant patients and found that 21% would have at least one episode of biopsy proven rejection within the first year of post transplantation. This was divided into acute cellular rejection (ACR), defined by the Banff criteria, antibody mediated rejection (AMR), defined as the combination of graft dysfunction, focal or diffuse C4d deposition and detectable DSA and mixed when both ACR and AMR were seen simultaneously. In the first 12 months 18% would have an episode of ACR, 10% an episode of AMR and 7% mixed[31]. These findings were supported in a different cohort, reported by Dong et al, who found a 14.7% chance of biopsy proven rejection in their cohort of pancreas transplant patients. Of note they found that although acute rejection was less common with the advent of improved immunosuppressive therapy, it was associated with an increased risk of graft loss[32].

1.2.4 Indications for small bowel transplantation

Small bowel transplantation is indicated in patients with irreversible small bowel failure in whom home parenteral nutrition is no longer possible[33]. Reasons why parenteral nutrition may fail include lack of vascular access, liver disease and recurrent line-related sepsis[34].

1.2.5 Immune monitoring of small bowel transplant

The gold standard for immune monitoring of intestinal transplants is regular endoscopies where tissue biopsies are taken. To standardise the process a consensus statement was published following the VIIIth International Small Bowel Transplant Symposium[35]. It recommended a minimum of three biopsy samples be reviewed for each episode, to maximise an accurate diagnosis, as it is known acute cellular rejection may not be present uniformly throughout the small bowel. Samples are then graded, according to the extent of injury seen, from 0-3, with 0 being normal and 3 equating to severe rejection. It should be recognised that biopsies are not without their risks, including potential ulceration and perforation of the bowel[36].

Cheng et al investigated the role of donor specific antibodies (DSAs) in their cohort of intestinal transplant patients[37]. They determined the rates of pre-formed DSAs (11%) and de novo DSAs (25% of remaining samples without pre-formed DSAs). They found patients who developed dnDSAs had an increased risk of acute rejection, and higher rates of graft loss (30% at 2 years) than those without DSAs. Although DSAs were not necessarily specific for a rejection episode, they provide useful information on the immune status of the recipient and are therefore used in a clinical setting to monitor patients.

1.2.6 Outcomes of small bowel transplantation

The Intestinal Transplant Registry reported on outcomes for patients operated on post 2000. They found a patient survival rate of 77%, 58% and 47% at one, five and ten years respectively. Graft survival rates were 71% at one year, 50% at five years, dropping to 41% at ten years. The most common cause for graft loss and patient death

was sepsis. The intestine has a high-density population of immune cells, which can pose challenges for transplantation, as these passenger leucocytes interact with the recipient's cells. This has been postulated to be responsible for the relatively high rate of graft versus host disease (GVHD) 7-13% seen in intestinal transplantation.[36].

Both pancreas and small bowel transplantation are lifesaving treatments for patients who have failure of these organs. While the early outcomes are excellent, longer-term survival has plateaued. An accurate way to monitor these patients for rejection is required, to prevent allograft failure later. In this thesis, the role of skin as a sentinel transplant for monitoring these transplants will be explored.

1.3 A brief history of skin transplantation

Skin transplantation dates to Egyptian times, with the first mention in the Ebert papyrus dated to around 1500BC, and later discussed in detail in Indian Ayurvedic manuscripts[38]. However, it was not until much later that skin grafting entered into the regular practice of surgeons. Reverdin described the use of "pinch grafts" to aid re-epithelialisation of ulcers[38]. Further developments were described by Ollier in 1872 and Thiersch in 1886, both describing variations of split skin grafts (SSGs), to overcome the problems of scar contracture noted with pinch grafts[38]. Whilst these developments improved on the initial outcomes, there were still reports of scar contracture, particularly problematic when they occurred across joints or around structures such as the eye. To address this Wolfe described use of a full thickness skin graft (FTSG) for treatment of ectropion[39]. These full thickness skin grafts included the dermis, reducing the rate of scar contracture, but with slightly increased risk of graft failure in

comparison to split thickness grafts[39], see **Figure 1-1** for layers taken in the different types of graft.

Autologous skin grafts became commonly used for the reconstruction of burns, with the strategy of early excision and immediate grafting, described by Janzekovic et al in 1970, still in use today[40]. Autologous skin grafts are not only used for the reconstruction of burns, but they may also be used to reconstruct wounds caused by trauma or resection of cancers. Indeed, they form one of the "rungs" of the reconstructive ladder or latterly "elevator", familiar to plastic surgeons[41].

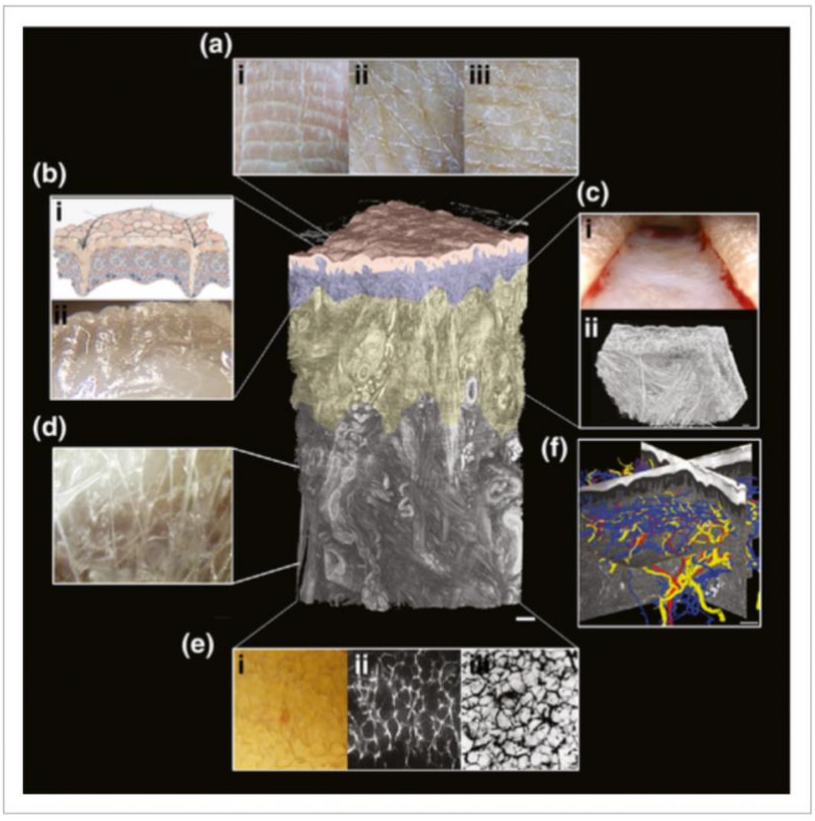

Figure 1-1. Architecture of the skin. *The central image shows a 3D reconstruction of human skin using episcopic rendering. The epidermis is shown in pink, papillary dermis in blue, reticular dermis in yellow and hypodermis in white. (a) demonstrates the*

differences found in the surface topography at different sites; (i) volar surface of finger, (ii) dorsum of hand, (iii) abdomen, which have differences in subunit shape. (b)(i) shows a schematic of the epidermis, and (ii) a cross section through human epidermis, with dermis showing as white due to collagen content. (c)(i) shows skin cut down to the reticular dermis and (ii) episcopic imaging of the dermis to show the collagen fibre orientations. (d) demonstrates the loose extendible and flexible collagenous microvacuolar network in the hypodermis. (e) shows hypodermal fat using different imaging modalities (i) operative endoscopy in living tissues, (ii) two photon excited fluorescence to view fibroelastic fibres (reproduced with permission, license no. 5535850745629, from Heuke et al 2013[42]), (iii) Indian ink injection of the lymphatics (reproduced with permission, license no. 5535851429945, from Ryan et al 1989[43]). (f) 3D rendering of skin vascularity using episcopic imaging, the branching arterial tree in red, venous plexus in blue, closely followed by nerves in yellow. When taking a split skin graft the epidermis and part of the dermis will be taken, whereas for a full thickness skin graft all the epidermis and dermis is taken. Figure reproduced with permission, license no. 5535850121169, from Wong et al 2016[44], with modification of the caption.

Also included in this ladder are flap reconstructions, including local, regional, and free flaps. The key difference between a skin graft and skin flap is blood supply, with flaps having an integral blood supply at the end of the surgical procedure.[45] Much like skin grafts, flaps were described early, with Susrata in India (around 1000-800BC) describing a forehead flap (loco-regional) for reconstruction of the nose[46]. It was not until the early 20th Century that flap reconstruction became commonly used again, with two World Wars resulting in a large amount of significant trauma and driving surgical

innovation[46]. This was followed by technological progress, with the development of operating microscopes and the necessary sutures and microsurgical instruments which enabled microsurgical free flap procedures to be developed.

The use of skin grafts or flaps from a separate donor (allografts) rather than autografts (from the same patient), has been limited in much the same way as solid organ transplants, by the development of acute rejection leading to graft loss. There are often alternative reconstructive options which may be used instead of allografts. Therefore, the morbidity associated with immunosuppressive medication, which would be required to maintain them is less acceptable and they are used less often than solid organ transplants[47].

1.4 Vascularised composite allografts.

In this section vascularised composite allografts (VCAs) are considered. This is a diverse group of allografts, which includes hand, face and abdominal wall transplants. In common they contain skin plus other soft tissue components and are primarily vascularised, like the SSFs in this study. This section will not include the wider range of non-skin containing VCAs such as uterus transplants.

1.4.1 Indications for VCAs

VCAs are indicated for patients with significant tissue loss, that may not otherwise be reconstructed[48]. For example, significant injuries to the hand or face involving most of their structures are challenging to replace. They are responsible for complex functions such as speech, eating, and the fine motor skills of the hand. The patient must also be willing to comply with lifelong immunosuppression and intensive rehabilitation[49].

There has been ethical debate about the use of VCAs for hand and face reconstruction due to the morbidity associated with the immunosuppression that is required to maintain the transplants, which are life-improving rather than lifesaving[49–51]. Abdominal wall transplants (AWTx) are used to reconstruct the abdominal wall in patients who are also undergoing abdominal organ transplantation (often small bowel or modified multivisceral transplants). The primary indication for AWTx is loss of the abdominal domain, which may be due to multiple prior surgeries with associated scar formation, extensive enterocutaneous fistulae, abdominal wall fibrosis following radiotherapy, or involvement of the abdominal wall by tumour (as in pseudomyxoma peritonei)[52]. Therefore, the requirement for immunosuppression in AWTx is mitigated somewhat by the life-saving solid organ transplant[48].

1.4.2 Immune monitoring of VCAs

Acute rejection in VCA is currently diagnosed using a combination of clinical and histological assessment[53]. If acute rejection occurs the transplanted skin develops a visible rash, typically a maculopapular erythematous rash. This may be accompanied by oedema. For definitive diagnosis a tissue biopsy is taken and undergoes histopathological examination, according to the Banff 2007 working classification for vascularised composite allografts (VCA)[54]. This is a consensus paper, designed to standardised diagnosis of acute rejection in VCA. It recommends a clinical assessment of the percentage of the transplanted skin involved, along with a tissue biopsy (minimum 4mm punch biopsy). This is graded from 0-4, as detailed in **Table 1-2** (from the original paper)[54]. At present this classification focuses on acute rejection, as the presentation of antibody mediated rejection and chronic rejection is less standardised and requires further investigation.

Grade	Description
Grade 0	No or rare inflammatory infiltrates
Grade I	Mild. Mild perivascular infiltration. No involvement of epidermis
Grade II	Moderate. Moderate-to-severe perivascular inflammation with or without mild epidermal and/or adnexal involvement. No epidermal apoptosis
Grade III	Severe. Dense inflammation and epidermal involvement with epithelial apoptosis and dyskeratosis and/or keratinolysis
Grade IV	Necrotizing acute rejection. Frank necrosis of epidermis or other skin structures

Table 1-2. Banff 2007 working classification. *Histopathological assessment of vascularised composite allografts*[54].

1.4.3 Outcomes of VCAs

The International Registry on Hand and Composite Tissue Transplant reported on outcomes for the first series of 49 VCA patients in 2010[55]. They found that 85% had at least one episode of acute rejection in the first-year post-transplantation. All patients developed protective sensation in their transplant and over 80% developed sensory and discriminative sensibility. One patient died, within the first year (3%) and 10 patients had lost their graft by 8 years (20%). Graft loss was mostly associated with poor compliance with immunosuppression.

Levi et al were the first to report on the use of abdominal wall transplantation[56]. In their cohort of eight patients (four adult, four children), six of the eight received abdominal wall transplants from the same donor as their intestinal transplant and had concurrent transplantation. At time of publication, follow up ranged from 1–23 months, five

patients had a functioning abdominal wall transplant, and six patients were still alive. Two patients died, after developing sepsis and multiorgan failure. They reported biopsy-proven intestinal rejection, without abdominal wall rejection in two patients and a further two patients who had abdominal wall rejection without intestinal rejection. It is unclear whether the patients who had intestinal rejection without skin rejection had received concurrent transplants from the same donor, or from different donors. This may be expected to result in differences in rejection.

In a recent review of outcomes for all reported abdominal wall transplants, which included the above study, Honeyman et al reported that estimated patient survival figures for 1- and 3-years post-transplantation were like those reported for abdominal organ transplants alone, with 53% alive at the time of publication (follow up ranging from 6 – 85 months)[52]. AWTx loss was 4.3% in the early period (one due to venous thrombosis and the other due to global hypoperfusion) and a late graft loss of 3% (of those surviving). In terms of acute rejection episodes, at least 35% of AWTx and 22% of small bowel transplants had biopsy proven rejection in the first 12 months. This finding is interesting as this is much lower than the acute rejection rate in the first year for hand transplantation, which is reported as 85%. There has only been one report in the literature of chronic rejection in an abdominal wall transplant[52].

1.5 Skin as an immune organ

The skin has a large surface area and acts as the primary interface between body and environment. It requires both active defence and tolerogenic pathways to ensure the appropriate immune response is generated, overactivation results in autoimmunity and

chronic inflammation, and under activation results in vulnerability to infection[57] . The concept of skin associated lymphoid tissue was first postulated in 1983[58]. It was noted that cells within the skin were able to recognise, process and present antigen, that there were peripheral lymph nodes able to receive signals from the skin, that there were T lymphocytes with an affinity for travelling to skin and that cells within the skin were able to produce signals that attracted these T cells. These elements together allowed the skin to carry out immune surveillance and monitoring[58].

It is helpful to consider the anatomy of the skin when thinking about this role. The outermost layer, the stratum corneum, is formed of dead keratinocytes with intercellular lipids. This layer prevents water from passing across it, preserving the integrity of the organism. Together with the strata lucidum, granulosum, spinosum and basale it forms the epidermis. Within the stratum spinosum resides a unique type of antigen presenting cell, Langerhans cells (LCs)[59]. These have their origin in macrophage precursors and are thought to act as sentinels at the skin barrier. They have been observed to have dendritic cell-like properties, with the ability to circulate to lymph nodes from the skin[60].

The stratum basale is where new keratinocytes are generated, before eventually cycling up to the stratum corneum. Keratinocytes have immune cell-like functions, with pattern recognition receptors and the ability to produce cytokines such as IL-1, TNFα and IL-33[59.] The stratum corneum is not a perfect barrier, various skin appendages, including hair follicles and sweat glands punctuate the surface, extending down into the dermis. Therefore, they are a potential site where skin integrity may be breached. However,

hair follicles are considered a site of immune privilege. Keratinocytes located here have reduced MHC class I, hindering presentation of antigen to $CD8^+$ T cells. They produce immunosuppressants such as IL-10 and TGFβ and have a unique extracellular matrix[61]. It is unknown exactly why hair follicles have these properties, but it is likely partly due to fact skin microbiota are common in this location. Under normal conditions, hair follicles attract monocytes, but not effector T cells. They do however promote skin resident $CD4^+$ and $CD8^+$ T memory cells, by secretion of IL-7 and IL-15. As they are a site of both dendritic cell and T cell trafficking, they form an important site for antigen presentation in the skin[59].

Below the epidermis is the dermis, a fibrous layer made up of collagen and elastin. It has a rich plexus of nerves and vessels running throughout. These vessels provide a network for circulating immune cells to enter and leave the skin. When inflammation is present, the postcapillary venules can become more permeable, allowing the extravasation of immune cells. Within the dermis reside several innate immune cells, including dermal dendritic cells (dDCs), γδ T cells and innate lymphoid cells (ILCs)[59]. Nerves within the dermis that express $TRPV1^+$ nociceptors have been found in a mouse model to interact with dDCs, regulating the IL-23/-17 pathway, and thereby the immune response to inflammation in the skin. When these receptors are pharmacologically ablated, IL-23 is reduced, thereby reducing activation of γδT cells. Furthermore, it has been noted that 75% of dDCs were spatially associated with the cutaneous nerves[62].

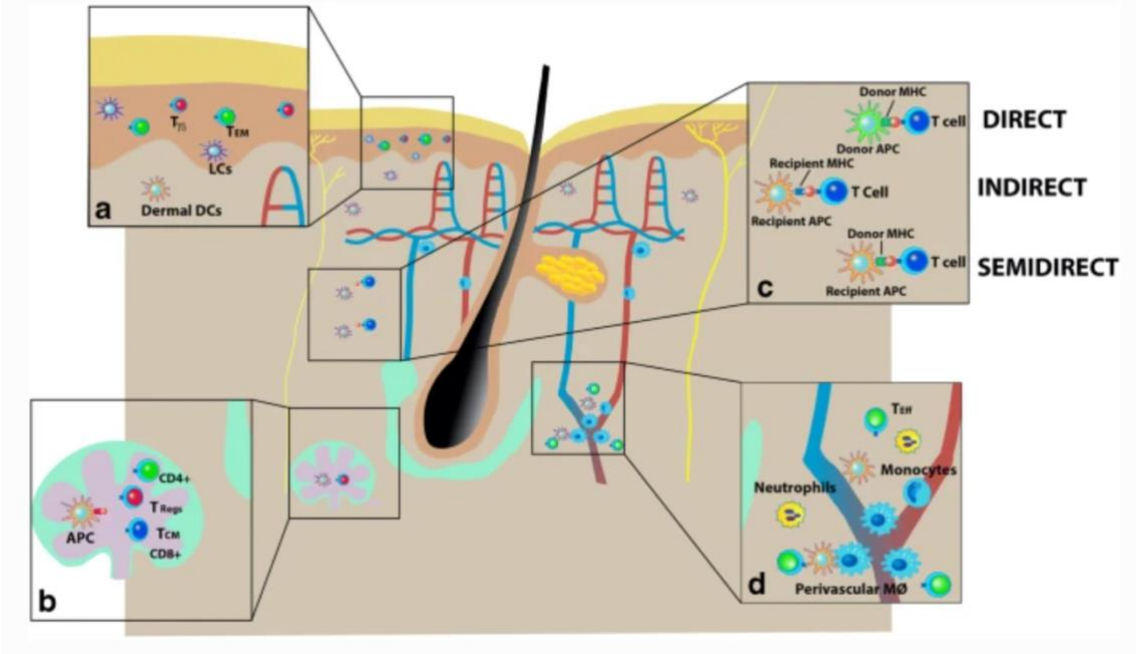

Figure 1-2. Skin as an immune organ. *(a) within the epidermis, below the stratum corneum are found Langerhans cells (LCs), γδ T cells (Tγδ) and effector memory T cells (T_{EM}). (b) Antigen presenting cells (APC) such as the dermal dendritic cells or LCs present antigen to naïve T cells, resulting in differentiation of $CD4^+$ and $CD8^+$ T cells as well as Tregs, in the dermatrophic lymph nodes. (c) Allorecognition may take place via direct, indirect and semi-direct routes, discussed in more detail in 1.6.2. (d) the post capillary venules are a site where perivascular macrophages and T cells can interact, increasing permeability and allowing for migration of other immune cells such as neutrophils. Figure reproduced from Leonard et al 2020[63], with modification of caption, used under license CC BY 4.0.*

Clark et al demonstrated that there is a large pool of resident memory T cells within healthy skin[64]. In fact, far higher than in peripheral circulation. The authors characterised these T cells and found they had a diverse TCR repertoire, with most of a Th1 type[64]. Further work by Watanabe et al, utilising alemtuzumab to deplete circulating T cells, has demonstrated the presence of two resident and two circulating T

cell populations with distinct functional activities and migration patterns which form part of the skin's immune defences[65] . These resident memory T cells offer the capacity for a speedy response to foreign antigen.

Clark et al also noted that around 10% of T cells found in normal skin are $CD3^{+}FOXP3^{+}$ regulatory T cells (Tregs). These Tregs could be induced to proliferate by the presence of IL-15 and fibroblasts, conditions found in inflamed skin, suggesting they may act to regulate the immune response in inflammatory conditions[66]. Seneschal et al have demonstrated that Langerhans cells (LCs) can induce proliferation of these skin resident T regulatory cells, via antigen presentation. They showed that the skin resident Tregs were mostly in the epidermis, allowing for the interaction with LCs. To investigate this further they cultured LCs and T cells with Candida albicans at high and low doses. They noted increased T effectors at high doses and increased Tregs at low doses, suggesting LCs were important in maintaining immune homeostasis in the skin[67]. Skin-homing T cells are recognised by the expression of cutaneous leukocyte antigens[68]. Hirahara et al noted that most of the peripheral blood Tregs had functional skin homing receptors, suggesting they play an important role in immune regulation in the skin[69]. It has subsequently been demonstrated in a humanised mouse model, that CLA^{+} Tregs are able to prolong skin graft survival longer than CLA^{-} Tregs[70]. Interestingly when these grafts are re-transplanted to mice reconstituted with fresh PBMC they survive longer than re-transplants that had not been treated with Tregs, suggesting Tregs within the grafts gave a survival benefit.

Typically, T cell activation occurs when Langerhans cells (LCs) and dermal DCs capture antigen and migrate to lymph nodes (LNs), where they present to naïve T cells. This is mediated by CCR7[71]. Of note it has been found that these skin specific antigen presenting cells (APCs) can also activate tissue resident T effector cells. In a mouse model of contact hypersensitivity, dDCs formed clusters in perivascular regions in response to macrophage signalling via IL-1Rα. These perivascular regions are sites where T cells can migrate to from the peripheral circulation, thereby providing evidence for inducible skin associated lymphoid tissue, where effector T cells rather than naïve T cells are activated[71].

It can be appreciated that the skin is a highly complex immune organ, associated with specialised immune cells. The spatial organisation of specific structures and specialised immune cells contributes to its ability to both monitor and respond to immune threats, whilst maintaining tolerance to innocuous organisms. Furthermore, this will also play a role in the complexity of the alloresponse to skin transplantation.

1.6 An overview of the immune response to transplantation

The immune system has developed to survey the body and provide a defence from invading microorganisms, infected cells, or tumours, by recognising foreign antigens (proteins) on their surface[72]. In general, transplants are donated by non-identical individuals. These transplants are known as allografts, as they come from genetically different individuals of the same species[73]. These allografts express alloantigens on their surface, which are recognised as foreign by the recipient's immune system. Whilst

transplantation is now a widely accepted medical therapy for failing organs, acute rejection secondary to the alloresponse is still challenging to manage.

The immune system can be broadly split into two, often interacting branches – the innate and the adaptive immune response. The innate response is highly conserved across mammals and represents the immediate line of defence[72]. It is mediated by immune cells (neutrophils, macrophages), complement and other acute phase proteins[72]. The adaptive immune response is more specific and is mediated by B and T lymphocytes[72]. The context in which an insult occurs may also affect how the immune system responds.

1.6.1 The innate immune response to an organ transplant

It is increasingly recognised that the innate immune response plays an important role in transplant rejection[74]. It is thought that non-self molecules, damage associated molecular patterns or DAMPs, on the surface of the allograft may be recognised by antigen presenting cells (APCs) via pattern recognition receptors (including Toll like receptors, TLRs), resulting in cytokine release and activation of the adaptive immune response[75]. Mice lacking signalling via the MyD88 pathway (which includes TLR4) were unable to reject a minor mismatch skin graft[76]. This finding was associated with a lack of both mature and immature dendritic cells in the draining lymph nodes[76]. This is the usual site of naïve T cell activation, highlighting a key link between the innate and adaptive immune response in transplant rejection.

Furthermore, it is understood that the innate immune response may be activated by "danger" signals, several of which may be present at the time of transplant, including heat shock proteins, alarmins, mammalian DNA and interferon-α[77,78]. This is supported by the finding that increased ischaemic time leads to delayed graft function in kidney transplantation[79]. Activation of APCs triggers an inflammatory response which leads to differentiation of myeloid cells into mature antigen presenting cells, which go on to activate T cells, via the presentation of foreign antigen and provision of co-stimulation, demonstrating another important link between the innate and adaptive immune systems[80].

1.6.2 The adaptive immune response to an organ transplant

Allograft rejection is known to be reliant on functioning T cells[81]. The hallmark of the adaptive immune response is specificity to a particular antigen. In transplantation, the main antigens recognised as foreign are the major histocompatibility antigens (MHCs), which are highly polymorphic between individuals. First the antigen is recognised by a specific T or B cell receptor, usually in a secondary lymphoid organ (spleen, lymph node or mucosal associated lymph tissue)[72]. Once activated, effector T cells leave the lymphoid tissue and home towards the disease site (or in this case the allograft) or activated B cells release antibodies into the blood where they then circulate to the affected tissue[72]. Antigen is often presented to T cells by dendritic cells (may also be by macrophages and B cells), in a complex with MHC molecules. There are two main classes of MHC molecule, class I typically presents endogenous antigens and class II presents exogenous antigens[72]. $CD4^+$ T cells recognise antigen with MHC class II and $CD8^+$ T cells recognise antigen with MHC class I[72]. T cell receptor (TCR) signalling requires binding of MHC and engagement of co-stimulatory receptors to produce

activation. TCR engagement without co-stimulation leads to anergy or cell death[72], therefore appropriate co-stimulation is essential for rejection to take place. Activation of $CD4^+$ and $CD8^+$ T cells leads to differing responses, with $CD4^+$ T cells described as "helper" cells and $CD8^+$ T cells as cytotoxic. The $CD4^+$ T cells may produce a variety of different cytokines, which lead to either a more proinflammatory or more allergic-type response[72].

The immune response to transplantation is unique in that both recipient and donor immune cells play a role in allorecognition. There are three main pathways of T cell activation involved in the alloresponse. The direct response in which recipient $CD8^+$ and $CD4^+$ T cells recognise MHC I and II on the surface of donor antigen presenting cells (APCs)[82]. The indirect response, which occurs when alloantigen from the graft is processed by recipient APCs and is presented to T cells in the conventional manner[82]. Thirdly, the semi-direct response where donor MHC is taken up by recipient dendritic cells (DCs) and presented intact on their surface, where they then interact with recipient T cells.[82] Once activated the $CD4^+$ T cells may go on to cause direct cytotoxicity or provision of help to cytotoxic $CD8^+$ T cells or B cells[83]. The $CD8^+$ T cells cause direct toxicity to the graft by the release of cytokines such as granzymes[83]. A fourth pathway has recently been described, in which donor $CD4^+$ T cells provide "help" to recipient B cells, leading to their activation[84].

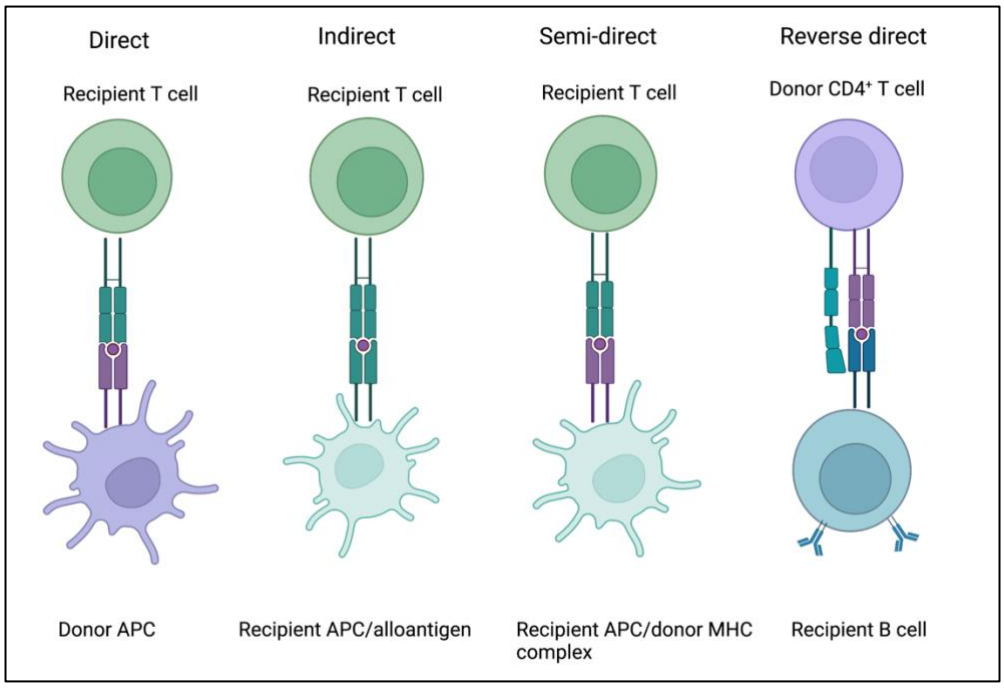

Figure 1-3. Types of allorecognition. *In direct allorecognition the donor APCs activate recipient T cells. Indirect allorecognition takes place when recipient APCs activate recipient T cells. In semi-direct allorecognition intact donor MHC-antigen complexes are presented to recipient T cells, by recipient APCs. Finally in reverse direct allorecognition donor CD4$^+$ T cells activate recipient B cells. Created with BioRender.com.*

1.7 The alloresponse to skin transplants

Much of the early work researching transplant immunology was undertaken using animal models of skin graft transplants. These models provided the advantage of orthotopic transplantation and easily visible sites for monitoring and biopsies, which could then be analysed using histology[85]. Medawar et al demonstrated the "second set" principle in both rabbits and mice, whereby a second graft from the same donor was rejected more quickly than the first, supporting the idea of immunological

"memory"[86,87]. This confirmed the observations they had made in a case report of pinch grafting in a burns patient, where the second set of allografts were rejected more quickly[88].

These early experiments took regular biopsies of the transplanted skin grafts and used histological staining techniques to explore the underlying mechanisms of acute rejection. These were somewhat limited to morphological descriptions of what was happening in the tissues, and the types of infiltrating cells, identified based on their appearance[88–90]. They described a cellular infiltrate, with perivascular infiltrates, spreading from dermis to involve the epidermis, ultimately ending in necrosis. Immunohistochemical (IHC) techniques allowed for a more in-depth assessment of the mechanisms underlying skin rejection. Using these techniques researchers were able to show that there was a T cell infiltrate, composed mainly of $CD4^+$ and $CD8^+$ T cells[91–95]. This was confirmed by Win et al, using immunofluorescence (IF), who demonstrated an increase in both total number and proliferative T cells in samples from face transplant patients at rejection[96]. They noted there were increases in $CD8^+$ T cells expressing both granzyme and perforin. It is known that adhesion molecules play a role in T cell migration from the circulation into tissues, increased levels have been found in skin biopsies at rejection[97]. Furthermore, when these adhesion molecules have been blocked in an animal model of skin transplant, increased rejection free graft survival has been found[97]. Immunoregulatory markers, such as IDO and FOXP3, were also found to be present at rejection in skin biopsies from hand transplant patients[91,97]. This likely reflects the complexity that is involved in the alloresponse, with both effector and regulatory cells both present simultaneously in tissues. Lian et al used both IHC and IF

techniques to differentiate between donor and recipient immune cells using a combination of HLA type and tissue residency markers[98]. The authors found a predominance of donor $CD8^+$ Trm (resident memory) cells in epidermal regions at rejection, suggesting these had potentially proliferated post-transplantation[98]. These techniques have contributed to the understanding of the mechanism of rejection in skin transplants, however they have limitations. For both, the number of markers that can be visualised concurrently is restricted by the availability of antibodies and fluorophores that can be differentiated from one another[99,100]. To gain more insight serial slides may be stained with different panels, but at the cost of using more of what may be small samples[99].

Several newer technologies have been developed to tackle this problem. These include techniques such as CODEX which uses DNA conjugated antibodies and can report on up to 60 different antibodies in a single slide[101], and Hyperion which uses metal-labelled antibodies, followed by laser ablation and mass spectroscopy[102]. Alternatively, laser capture microdissection (LCM) can specifically select an area of interest, separate this from the specimen slide and then RNA, DNA or protein analysis can be performed[103]. These techniques have been used to explore immune cell populations in chronic rejection in liver transplant demonstrating distinct immune populations ($CD8^+$ T cells and $CD68^+$ macrophages) spatially associated in chronic rejection[104]. Trailin et al used LCM to show there were differences in gene expression between glomeruli (*TGFB1*) and tubulointerstitial (*HAVCR1* and *IGHG1*) areas in kidney transplants, and further differences in those with chronic active antibody mediated rejection (*GNLY*)[105]. LCM was also used by Vergani et al in an islet cell transplant model where they

identified differences in cytokines expressed in graft samples at rejection in those treated with immunosuppression (decreases in IL2 and IFN γ) versus not treated, which were not noted in peripheral blood samples, supporting a role for examining both peripheral and graft responses in transplantation[106].

In 2016 Ståhl et al published the first description of spatial transcriptomics, when they described their technique for exploring mRNA expression in tissues[107]. Tissue sections are applied to slides which have arrays of oligonucleotides, positionally labelled. These are permeabilized and then hybridized, allowing for capture of the oligonucleotides in a spatially resolved manner. This allows for the simultaneous investigation of the expression of thousands of genes. They were able to apply this method to breast cancer biopsies and demonstrated unexpected heterogeneity in gene expression between areas[107]. There followed several commercially available platforms, including GeoMx Digital Spatial Profiler (DSP), Vizgen MERFISH and Visium 10X (a commercial development of Ståhl et al's method) culminating in Nature declaring spatial transcriptomics their "Method of the Year 2020"[108]. Whilst their potential for exploring mechanisms underlying transplant rejection has been recognised[109], there have been few publications in the organ transplant field which have used these methods. Salem et al used the whole exome GeoMx DSP platform to study acute cellular rejection in a single human kidney transplant biopsy, compared to a control from a nephrectomy[110]. They selected five tubular regions of interest (ROIs) and three glomerular ROIs. One of the benefits of this technique is the ability to choose areas that show changes, as rejection often occurs in patches throughout the tissue rather than homogenously. On comparison between the two they found that the rejection samples were associated with an increase

in immune associated processes, when compared to the control. Interestingly variability between the transplant sample ROIs was because of genes associated with kidney development or injury, rather than immune processes, suggesting potentially new pathways of interest in the development of acute rejection. This was however a small study with only one patient in each group, limiting the applicability of the findings. Rosales et al studied a mouse model of kidney transplant tolerance and used the immune protein panel GeoMx DSP platform to characterise intragraft Treg rich organised lymphoid structures (TOLS)[111]. They compared TOLS to non-TOLS cortex regions in the kidney and found an increased expression of T cell checkpoint molecules (Lag3, PD1, VISTA) and T cell and Treg markers (CD3e, CD8a, CD4, GITR, FOXP3) suggesting a regulatory role for these areas. These studies demonstrate the potential that spatial transcriptomic techniques have for exploring the mechanisms leading to both rejection and tolerance in transplantation.

It has been suggested that skin is the most immunologically challenging tissue to transplant, due to the immune response it provokes[112]. However, there is evidence that skin may not be more antigenic, but perhaps more susceptible to rejection[113]. There are several factors that may be contributing to this susceptibility. Skin contains both keratinocytes and endothelial cells which express MHC class II molecules, which may lead directly to activation of T cells[114]. It has also been suggested that skin-specific antigens are causing allograft rejection[115].

The idea that skin was the most “antigenic” tissue to transplant originated in the 1960s, with work carried out by Joseph Murray’s team[89]. They performed transplantation of

kidney and skin grafts in dogs, treated with immunosuppression. They noted that skin grafts on their own rejected on average by day 14, whereas kidney transplants alone generally survived greater than 50 days. This hierarchy of antigenicity was maintained until Wendt et al[116], who were the first to combine simultaneous skin grafts and kidney transplants from the same donor in the same human recipients. They found that the skin grafts survived long term under the same immunosuppression as would have been used for the kidney transplant alone. This contrasts with earlier animal studies in primates which had suggested far higher doses of immunosuppression would be required[117]. They also demonstrated recipient cells present in the skin graft many years after transplantation[116]. The finding that skin could be transplanted with the same level of immunosuppression as a solid organ transplant opened the opportunity to develop skin containing transplants, including hand and face transplants, otherwise known as vascularised composite allografts (VCAs). This has provided the opportunity to compare the alloresponse to primarily (VCAs) versus secondarily vascularised skin (skin grafts), further increasing our understanding of the mechanisms of allograft rejection.

Lee et al were the first to look systematically at the contribution of various parts of the VCA to rejection. They made several interesting observations regarding the antigenicity of skin. They noted that vascularised muscle provoked a more significant cell mediated immune response than skin. They also found that vascularised skin compared to vascularised subcutaneous tissues had similar outcomes. This was of note as it had previously been thought that epidermal Langerhans cells (specialised dendritic cells) were primarily responsible for the increased rejection seen in skin. Furthermore, the

whole limb VCA rejected more slowly than individual components alone. When comparing vascularised to non-vascularised skin they found differences in the type of immune response and the timing of this response[47]. This suggests the type of vascularisation affects the alloresponse to skin and implies that assumptions regarding antigenicity that were based on data from skin graft experiments may not be accurate.

There is some evidence for differences in immune cell trafficking between VCAs and skin grafts, which may in part explain the differences found in the alloresponse. Horner et al used a rat model of skin transplantation, using transgenic GFP rats as recipients and in vivo confocal microscopy to track cells. They demonstrated a higher number of recipient cells in post transplantation VCAs in comparison to skin grafts and commented that recipient dendritic cells could be found in the VCA dermis, but not in skin grafts. However, it was unclear how these dendritic cells were characterised[118]. Recipient T cells have also been found to rapidly enter the dermis of VCAs, in chimeric pigs, which had developed tolerance. Interestingly donor T cells were also seen in recipient skin, with no evidence of skin graft versus host disease (GvHD). $FOXP3^{+}$ Tregs were found in these tissues, suggesting a mechanism for local tolerance. Recipient T cell infiltration was also noted in the dermis of human VCA samples at 12 and 18 months, without signs of acute rejection[119].

Kant et al used a mouse model of skin transplant to demonstrate that rejection of non-vascularised skin grafts was a result of both direct and indirect T cell alloresponses (see *1.6.2.*), whereas primarily vascularised skin only provoked a direct response. To establish if this result was related to skin or vascularisation status, they also looked at

vascularised and non-vascularised heart transplants. They found a similar picture, with only a direct response noted in the vascularised heart transplant, suggesting that primary vascularisation is responsible for the type of alloresponse[120]. It is still not clear the exact mechanisms responsible for these differences. It has been suggested that the lack of primary vascularisation in skin grafts means donor APCs favour egress via lymph channels, with higher proportions reaching the draining lymph nodes leading to indirect allorecognition. The importance of these lymphatics has been demonstrated in experiments performed by Barker et al, who isolated a skin flap on a vascular pedicle alone, applied a full thickness skin graft and demonstrated increased survival[121]. More recently this view of passenger leucocytes has been challenged. Marino et al used imaging flow cytometry to demonstrate that there were few donor leucocytes in lymph nodes, regardless of vascularisation status. Instead, they found recipient APCs "cross-dressed" with donor MHC, derived from donor exosomes. These donor vesicles were able to travel to the lymph nodes via lymphatics[122]. It is likely the earlier experiments by Kant et al were not able to distinguish donor alloantigens/MHC complexes on donor versus recipient APCs accurately.

1.8 Immune monitoring via donor skin transplants

As has been highlighted earlier in this chapter the immune monitoring of both pancreas and small bowel transplants is currently very challenging, with most tests only positive when function has been impaired. There is a clear need for a better way to monitor these transplants. Here we consider the use of donor skin transplants for immune monitoring. SSFs leverage the easy visibility of skin rejection to provide a continuous monitor for distant organ transplants.

1.8.1 Donor skin transplants for immune monitoring of vascularised composite allografts

Donor skin transplants have most commonly been used to monitor VCAs. Zamfirescu et al used a rat model to investigate the use of a distant skin graft (secondarily vascularised) for the monitoring of VCAs[123]. They found that the sentinel skin graft showed signs of rejection on average a day before the VCA and did not appear to induce rejection compared to VCA alone. This study provided evidence that a sentinel skin graft may provide useful in the clinical setting.

Lanzetta et al demonstrated the use of full thickness skin grafts for monitoring hand transplants in human patients[124]. In support of the findings of Zamfirescu et al[123], rejection in the sentinel graft typically occurred earlier than in the hand transplant. However, the usefulness of this site for monitoring decreased over time as the donor skin was replaced by recipient skin in a process they termed "creeping substitution"[124].

Diefenbeck et al described the use of a SSF (primarily vascularised) for monitoring a vascularised composite knee joint graft[125]. This was designed to allow monitoring of knee joint VCAs, which are typically completely hidden. However, it also provided an easily available biopsy site, and did not undergo the creeping substitution that had affected the sentinel skin grafts. SSFs have been used for immune monitoring of face VCAs by several groups[93,126]. They are of particular benefit in these patients as they provide a separate site for immune monitoring and biopsy away from the face VCA. Biopsy sites of the face were a potential aesthetic concern. Furthermore, facial skin is more prone to inflammatory dermatoses that may be difficult to differentiate from

rejection on histopathological assessment, therefore a SSF, derived from non-facial skin, for monitoring and biopsies is useful[93,126]. These studies demonstrate that SSFs may be safely used for immune monitoring in VCAs and offer an easily accessible biopsy site, with good concordance for rejection. In fact, it seems the SSF may show signs of rejection preceding that of the VCA, offering a potential window of opportunity to adjust the immunosuppression and prevent damage to the VCA.

1.8.2 Donor skin transplants for monitoring of solid organ transplants

Whilst the short-term survival of many solid organ transplants is now very high, there remains a lack of improvement in the longer-term outcomes. It is well described that acute rejection episodes contribute to worse outcomes, including chronic rejection, therefore it is logical that recognising and treating these episodes may have a beneficial effect on graft survival [127]. Recent years have seen the development of more specific blood tests to diagnose acute rejection, such as donor-derived cell free DNA levels[128] and gene expression panels, like the Allomap for cardiac transplants[129]. However, these rely on taking a blood test at the time of rejection and can only give a result for that specific point in time.

The benefits of SSFs for immune monitoring were recognised in vascularised composite allografts and include the ability to provide a continual, visual monitoring site that the patient can observe for themselves. It also facilitates remote monitoring of patients by the medical team[130]. It is easy to biopsy, with a minimum of morbidity associated, unlike when taking a biopsy from the solid organ transplant [127].

Wendt et al were one of the first to recognise the potential of a skin graft for immune monitoring of solid organ transplants. They reported on six patients in whom they transplanted a split skin graft (SSG) and kidney transplant from the same donor. They found 100% correlation for rejection between skin graft and kidney transplant once the skin graft had completely taken[131]. Prior to this Haberal et al had used donor SSG prior to kidney transplantation in ABO incompatible patients (recipient O, living donor HLA compatible, but ABO incompatible), to identify patients who may be suitable for an ABO incompatible kidney transplant[132]. Interestingly no concern regarding sensitisation of patients by using this strategy was noted by the authors.

Despite these early forays into the use of donor skin for solid organ transplant immune monitoring, this strategy was not widely used, until the advent of abdominal wall transplants. Abdominal wall transplantation (AWTx) was first undertaken to solve a reconstructive problem[56]. As has been discussed in more detail earlier in this chapter, patients who required a small bowel or modified multivisceral transplant often had poor abdominal domains, due to previous surgery or radiotherapy. As they would require immunosuppression for small bowel transplantation, the addition of the abdominal wall transplant on balance became more acceptable. As experience with the combined AWTx and small bowel transplants grew, it was noted that the skin part of the VCA was providing useful information on the immune status of the transplants. Acute cellular rejection episodes were easily identified by a maculopapular rash on the donor skin. This also offered an easily biopsied site and allowed prompt treatment with an increase in immunosuppression that preventing rejection in the small bowel transplant [133]. In one case the patient delayed their presentation to the transplant team, developing

mild rejection in their small bowel transplant in the meantime. With the idea that skin is the most antigenic tissue, the concept of skin acting as an early rejecting sentinel for the small bowel transplant took hold. This was further reinforced by a patient who presented with graft-versus-host disease (GVHD), with clear sparing of the skin of their abdominal wall transplant[133]. It may be difficult to differentiate infection from rejection in small bowel transplantation as at presentation the symptoms are very similar. However, bowel symptoms without a rash on the abdominal wall skin can be treated more confidently as infection rather than rejection, preventing unnecessary immunosuppression and the potential morbidity that is associated[134].

The addition of a large skin containing VCA did not lead to a significant increase in the incidence of de novo DSA formation compared to small intestine alone[135]. This study provided reassurance that despite its reputation as the most antigenic tissue, the skin component of the VCA was not causing sensitisation of these patients. This suggested it would be safe to consider the addition of skin to a solid organ transplant for immune monitoring purposes.

1.9 Conclusion

Transplantation is the gold standard treatment for those patients who have organ failure. Despite advancements in both surgical and immunosuppressive treatment the long-term survival of organ transplants has plateaued. As it is known that acute rejection episodes contribute to earlier graft loss, immune monitoring of these patients is crucial to their longevity. A SSF has the potential to offer a continuously visible, easily biopsied site for immune monitoring. From preliminary studies it seems that despite concerns that

including skin may sensitise patients, a SSF can offer a safe and accurate way to monitor patients. In Oxford we are uniquely placed to explore the immune response to these combined transplants, due to the relatively large cohort of patients who have undergone either a SSF and pancreas transplant or an abdominal wall and small bowel transplant. To date there is not any published literature reporting in depth the immune response to combined skin and solid organ transplants or comparing the systemic response to the local response. Characterising the immune response in these combined transplants may allow us to understand why there are reduced rates of acute rejection in these combined transplants. It may also provide further evidence that a SSF may give an accurate reflection of the alloresponse to a solid organ transplant from the same donor.

1.10 Thesis aims.

The aims of this thesis are to:

- Characterise the systemic immune response to a combined skin and solid organ transplant (chapter 3)
- Characterise the local immune response in small bowel and in skin in combined transplants (chapters 4&5)
- Compare the local immune response in small bowel and skin (chapters 4&5)
- Explore the role of modifying a Langerhans cell related pathway in skin allograft rejection in a novel mouse model (chapter 6)

2 Chapter 2: Materials and methods

2.1 Vascularised sentinel skin flaps to detect rejection in pancreas transplantation – a pilot study.

2.1.1 Research and Ethics Committee approval

Approval was granted by the Southwest Research and Ethics Committee (15/SW/0333). The trial has been registered on www.clinicaltrials.gov (NCT03183258).

2.1.2 Study recruitment

Patients were recruited from the Oxford Transplant Centre, to have a combined pancreas and sentinel skin flap transplant. Patients were eligible for recruitment if they underwent a pancreas transplant alone (PTA) or simultaneous pancreas-kidney (SPK) transplant, were adults (>18 years old) and gave informed consent for participation. They were excluded if they had received an experimental medication in the preceding 30 days, had an enterically drained pancreas transplant alone, were unable to return to Oxford for follow up or if they had any other condition felt by the investigator to put at risk either the patient or the trial.

2.1.3 Sentinel skin flap (SSF) transplantation

The SSF was retrieved from the same donor as the pancreas transplant. It was a primarily vascularised flap, based on the radial artery, with a skin paddle approximately 12 x 4 centimetres in size. The flap was removed with the venae commitantes and if possible, the cephalic vein was also included. It was flushed with heparin and then University of Wisconsin preservation solution. Flaps were transported to the Oxford Transplant Centre on ice (as for the pancreas). Inset took place at the same time as the pancreas transplant, to reduce operative time for the patient. The SSF was inset in the recipient's non dominant forearm, **Figure 2-1**.

Figure 2-1. Sentinel skin flap in recipient's forearm. *This photo depicts a healthy skin flap, on the ulnar aspect of the left volar forearm.*

The donor radial artery was anastomosed as a flow-through flap, to the recipient's ulnar artery using 10.0 Ethilon sutures. The venae commitantes of the flap were anastomosed to the recipient ulnar venae commitantes, to provide venous drainage. This microsurgical procedure was performed by the plastic surgery team.

2.1.4 Sample procurement and postoperative management

Blood samples and SSF biopsies were taken from the participant on the day of transplant prior to transplantation. 50ml of blood was taken in a combination of EDTA and SST BD Vacutainer tubes. 4mm punch biopsies were taken from the SSF and flash frozen. Standard induction immunotherapy consisting of two doses of alemtuzumab, followed by maintenance therapy with tacrolimus (target trough levels 8-12 for the first six months, then 6-10 thereafter) and mycophenolate mofetil 750mg twice daily was given. Participants were followed up for 12 months post-transplantation. If rejection was suspected, patients were dosed once daily, for three days, with 500mg of intravenous methylprednisolone. Participants were followed up at four routine time points in the postoperative period: six weeks, three months, six months, and twelve

months. Protocol blood samples and tissue biopsies, as described previously, were taken for research purposes at each of these time points. Participants were also reviewed if there was suspicion of acute rejection, termed an "event". In a pancreas transplant alone (PTA) patient this would be a skin rash on the sentinel skin flap confirmed as rejection by histopathology (Banff 2007 criteria)[54], a clinically significant drop in urinary amylase (>50% below baseline), a clinically significant rise in oral glucose tolerance (new impaired glucose tolerance with no other cause) or high amylase/lipase with radiological features of graft pancreatitis. For simultaneous pancreas-kidney transplant recipients this would be as for the PTA, with the addition of a clinically significant rise in serum creatinine (>20% from baseline with no other cause). Event blood tests and a sentinel skin flap biopsy were taken for research purposes.

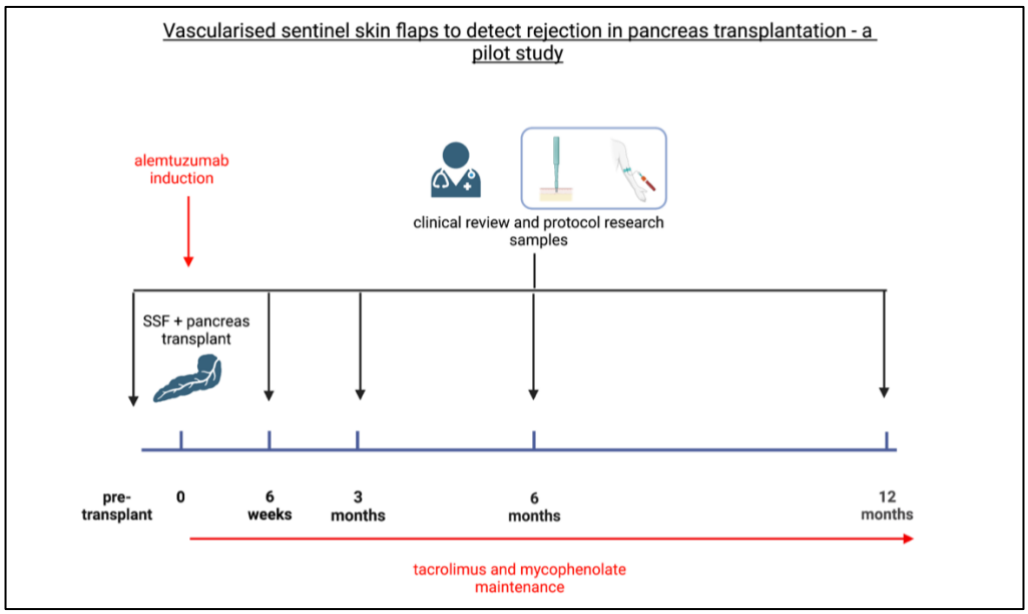

Figure 2-2. Overview of study protocol. *Patients undergo clinical review at five time points: pre-transplant, as well as 6 weeks, 3 months, 6 months and 12 months post-transplantation. At these times blood samples and skin flap biopsies are also taken for research purposes. Patients are under standard clinical review during this time.*

Induction immunosuppression consists of alemtuzumab, with maintenance immunosuppression on a combination of tacrolimus and mycophenolate mofetil. Created with BioRender.com

2.1.5 Patient demographics and outcomes [136]

Twenty participants were recruited to the study and received a sentinel skin flap at the same time as pancreas transplantation. One participant had sentinel skin flap necrosis secondary to venous thrombosis, requiring removal but remained in the clinical study, as the plan was to perform an intention to treat analysis. One participant who underwent SPK transplantation required early pancreatectomy but decided to keep their sentinel skin flap and remained in the study. The group consisted of 13 men and seven women. The mean age was 46.6 years (SD = 7.58). There were 17 SPK transplants, one PTA, one pancreas transplant after kidney transplant, and one pancreas after SPK. The median HLA (human leukocyte antigen) mismatch was 4 (range 3-5). Patient survival at 12 months was 100%. Pancreas and kidney allograft survival at 12 months was 95% and 100% respectively. Sentinel skin flap survival at 12 months was 95%.

Patient demographics	
Total number of patients	20
Male	13
Female	7
Mean age (standard deviation)	46.6 (7.58)
Patient survival at 12 months	100%
Pancreas allograft survival at 12 months	95%
Kidney allograft survival at 12 months	100%
SSF survival at 12 months	95%

Table 2-1. Demographics for patients in the pilot study "Vascularised Sentinel Skin Flaps to Detect Rejection in Pancreas Transplantation".

2.2 Abdominal wall (or SSF) and small bowel transplant

2.2.1 Research and Ethics Committee approval

The abdominal wall, sentinel skin flap and small bowel samples were retrieved by the Oxford Centre for Histopathological Research (OCHRe), following an ethics application to the Oxford Research Biobank (19/SC/0173).

2.2.2 Background

Small bowel transplantation is still an uncommon procedure, with only twelve being performed in the UK in 2020/21 (NHSBT Activity Report 2020/21)[137]. Oxford has developed a combined abdominal wall and small bowel transplant programme, approved by the Human Tissue Authority, licence 40038. Small bowel transplantation is indicated for patients who have intestinal failure and lack of vascular access for total

parenteral nutrition (TPN). Abdominal wall transplantation is indicated in patients whose abdominal domain is not sufficient for closure, post small bowel transplantation. The abdominal wall transplant (AWTx) is retrieved from the same donor as the small bowel transplant. The size will vary depending on the recipient's needs, but generally includes skin, subcutaneous tissue, fascia, and the rectus abdominis muscles, with the associated deep inferior epigastric vessels. The AWTx is inset following small bowel transplantation, by the plastic surgery team, **Figure 2-3**. Patients who did not require an AWTx transplant, received a sentinel skin flap (SSF) as described in *2.1.3*. Patients received induction immunosuppression with alemtuzumab, followed by tacrolimus monotherapy (target trough levels 8-12 for first six months, then 6-10 thereafter). Clinical follow up included protocol small bowel transplant biopsies, taken twice a week for the first three months. If there was a suspicion of rejection in either the small bowel or abdominal wall or SSF, then biopsies of both were taken for histology. Rejection episodes were treated with three doses, once daily, of 500mg methylprednisolone intravenously.

Figure 2-3. Abdominal wall transplant. *This photo shows a centrally placed abdominal wall transplant.*

2.2.3 Patient demographics and outcomes

Twelve patients were included in this study. Seven who had combined small bowel and AWTx or SSF and five who had a small bowel transplant alone. The average age of combined transplant patients was 47.3 years (SD 10.1), while for the small bowel alone patients it was 43.6 years (SD 10.7). In the combined group there were six men and one woman, compared to four and one respectively, in the small bowel transplant alone group. In the combined transplant group, there were three small bowel (SB) and SSF transplants, two small + large bowel and SSF transplants, one modified multivisceral transplant (MMVT) and SSF and one MMVT and AWTx. In the small bowel alone group there were two SB transplants, two SB and right colon transplants and one MMVT. The MMVTs did not include the liver. Patient survival at 12 months was 100%

in both the combined group and in the SB alone group. Small bowel survival at 12 months was 70% in the combined group and 80% in the SB alone group. SSF and AWTx survival at 12 months was 70%. Demographic data are summarised in **Table 2-2**.

	Small bowel and skin	**Small bowel alone**
Total number of patients	7	5
Mean age (standard deviation)	47.3 (10.1)	43.6 (10.7)
Male	6	4
Female	1	1
Patient survival at 12 months	100%	100%
Small bowel survival at 12 months	70%	80%
Skin survival at 12 months	70%	n/a

Table 2-2. Demographic data for patients with small bowel and skin transplant or small bowel transplant alone.

2.3 Flow cytometry analyses of human blood samples

2.3.1 Blood sample processing for flow cytometry

The samples analysed in this study were originally collected by James Barnes and the peripheral blood mononuclear cell (PBMC) isolation and staining were performed by him. Frozen PBMCs were thawed and processed in batches. Fluorochrome coupled antibodies were used to phenotypically profile cells. These panels are made by Beckman Coulter according to established protocols and have been validated in detailed immunological studies such as the ONE study[138]. Five panels were run on each sample

where sufficient cell numbers allowed. These panels were: Basic Phenotyping, T cell subsets, T cell receptors, T regulatory (Treg) cells, and B cells. 7.5 x 10^5 cells were used for all panels except the Treg panels where 1 x 10^6 cells were used. Samples were processed according to the manufacturer's instructions. The antibodies used, along with their clones are detailed in **Table 2-3**

Panel	Specificity	Conjugation	Clone	Species of Origin	Isotype
Basic phenotype	CD45	Krome Orange	J33	Mouse	IgG1
	CD3	APC-A750	UCHT-1	Mouse	IgG1
	CD4	APC	13B8.2	Mouse	IgG1
	CD8	Alexa Fluor 700	B9.11	Mouse	IgG1
	CD19	Texas Red (ECD)	J3_119	Mouse	IgG1
	CD56	PE	N901	Mouse	IgG1
	CD16	FITC	3GB	Mouse	IgG1
	CD14	PC7	RMO52	Mouse	IgG1

Panel	Specificity	Conjugation	Clone	Species of Origin	Isotype
T cell	CD45	Krome Orange	J33	Mouse	IgG1
	CD3	APC-A750	UCHT-1	Mouse	IgG1
	CD4	APC	13B8.2	Mouse	IgG1
	CD8	Alexa Fluor 700	B9.11	Mouse	IgG1
	CD45RA	FITC	2H4	Mouse	IgG1

	CD197 (CCR7)	PE	G043H7	Mouse	IgG1
	CD27	PC7	IA4CD27	Mouse	IgG1
	CD28	Texas Red	CD28.2	Mouse	IgG1
	CD279 (PD1)	PC5.5	PD1.3.5	Mouse	IgG2b
	CD57	Pacific Blue	NC1	Mouse	IgM

Panel	**Specificity**	**Conjugation**	**Clone**	**Species of Origin**	**Isotype**
TCR	CD45	Krome Orange	J33	Mouse	IgG1 kappa
	CD3	APC-A750	UCHT-1	Mouse	IgG1 kappa
	CD4	APC	13B8.2	Mouse	IgG1
	CD8	A700	B9.11	Mouse	IgG1
	TCR αβ	PE	IP26A	Mouse	IgG1 kappa
	TCR $\gamma\delta$	FITC	IMMU 510	Mouse	IgG1
	TCR Vδ1	PC7	R9.12	Mouse	IgG1
	TCR Vδ2	Pacific Blue	IMMU 389	Mouse	IgG1
	HLA-DR	Texas Red	IMMU 357	Mouse	IgG1

Panel	**Specificity**	**Conjugation**	**Clone**	**Species of Origin**	**Isotype**
B cell	CD45	Krome Orange	J33	Mouse	IgG1
	CD19	Texas Red (ECD)	J3-119	Mouse	IgG1
	IgD	FITC	IA6-2	Mouse	IgG2a
	IgM	Pacific Blue	SA-DA4	Mouse	IgG1
	CD27	PC7	IA4CD27	Mouse	IgG1
	CD24	APC	ALB9	Mouse	IgG1
	CD38	APC-A750	LS198-4-3	Mouse	IgG1
	CD21	PE	BL13	Mouse	IgG1

Panel	Specificity	Conjugation	Clone	Species of Origin	Isotype
Treg	CD45	Krome Orange	J33	Mouse	IgG1 kappa
	CD3	APC-A750	UCHT-1	Mouse	IgG1 kappa
	CD4	PC7	SFCI12T4D11(T4)	Mouse	IgG1
	CD39	PC5.5	BA54	Mouse	IgG1 kappa
	FoxP3	Alexa Fluor 647	259D	Mouse	IgG1 kappa
	Helios	Pacific Blue	22F6	Hamster	IgG
	CD45RA	FITC	2H4	Mouse	IgG1
	CD25	PE	B1.49.9	Mouse	IgG2a

Table 2-3. Antibody details for the Beckmann Coulter Duraclone flow cytometry panels.

Flow cytometric data were acquired from a NAVIOS flow cytometer (Beckman Coulter).

2.3.2 Analysis and statistical tests of flow cytometry data

Analysis was performed using Kaluza Analysis Software (Beckman Coulter). A detailed gating strategy may be found in Appendix 1. Absolute counts were calculated from the results of the white blood count taken at the same time as the research samples. The following equation was used:

absolute count (cells/μl) = (number of cells gated/number of lymphocytes gated) x actual lymphocyte count x 1000

Mean counts at each time point +/- standard error of the mean were calculated for each of the cell populations. Wilcoxon matched pairs signed rank test was used to calculate differences between samples at rejection and protocol time points and when comparing different time points post-transplantation to the pre-transplantation time point. Mann-Whitney tests were used to compare rejectors to non rejectors at the same time points. GraphPad Prism 9.4.0. was used to perform all calculations.

2.4 RNA isolation

2.4.1 Blood (Tempus™ tubes)

Samples were obtained from participants in the study "Vascularised Sentinel Skin Flaps to Detect Rejection in Pancreas Transplantation", REC 15/SW/0333. See *2.1*. for a description of the study. Whole blood was collected in Tempus™ tubes, chosen as they immediately lyse and stabilise blood, minimising the risk of inducing gene changes post collection[139]. Furthermore, they maintain integrity of RNA at room temperature for up to 5 days, giving adequate time for transport from patient to lab. RNA was isolated using MagMAX™ for stabilised blood tubes RNA isolation kit (ThermoFisher, UK), as per the manufacturer's instructions. RNA concentration was measured using a Qubit Fluorometer (ThermoFisher Scientific). On average 54.2ng/μl (range 1-179) of RNA has been obtained from 3ml of blood stabilised in Tempus™ tubes.

2.4.2 Skin (fresh frozen)

Samples were obtained from participants in the study "Vascularised Sentinel Skin Flaps to Detect Rejection in Pancreas Transplantation", REC 15/SW/0333. See *2.1*. for a description of the study. Samples were removed from -80°C and kept on ice. 350μl of lysis buffer was added to each sample. A TissueRuptor II (Qiagen, UK) was used to

mechanically disrupt tissues. 10µl proteinase K and 590µl RNase free water was added to each sample. These were then incubated for 10 minutes at 55°C. Then followed centrifugation at 15-25°C for three minutes at 10,000g. Next the supernatant was added to a new 2ml tube. Then half the supernatant volume (around 450µl) of 96-100% ethanol was added to the lysate and mixed by pipetting. The next steps used the columns and reagents from the RNeasy Micro kit (Qiagen, UK). 700µl of sample was transferred to a RNeasy spin column in a 2ml tube, centrifuged for 15 seconds >8000g. Flow through was discarded. The previous steps were repeated until no sample remained. Next 700µl of RW1 was added, then centrifuged for 15 seconds at >8000g before discarding the flow through. 500µl RPE was added, centrifuged for 15 seconds at >8000g and flow through discarded. Finally, 500µl of RPE was added and then centrifuged for 2 minutes at >8000g. The column was placed into a new 2ml tube, then placed in the centrifuge with lid open for one minute >8000g to air dry. The column was placed in a new 1.5ml tube and then 30µl of RNase free water was added. This was centrifuged for one minute at >8000g. This step was repeated, re-using the elute on the second time to increase concentration. RNA concentration was measured using a Nanodrop 2000 spectrophotometer (ThermoFisher, UK). On average 16.66ng/µl (range 0.3-91.2) of RNA have been obtained from 1mm^3 skin fresh frozen in optimal cutting temperature (OCT) compound.

2.4.3 Small bowel and skin (formalin fixed, paraffin embedded)

Samples were obtained from Oxford Centre for Histopathology Research (OCHRe). These included the punch biopsies of abdominal wall transplant or sentinel skin flaps and small bowel transplant biopsies. This followed ethical approval from the Oxford Radcliffe Biobank (ORB) research tissue banks ethics, reference 19/SC/0173. RNA was

isolated using RNeasy FFPE kit (Qiagen, UK), as per the manufacturer's instructions. RNA concentration was measured using a Nanodrop 2000 spectrophotometer (ThermoFisher, UK). On average 74.34ng/μl (range 12.2 – 327.5) of RNA has been obtained from two formalin fixed paraffin embedded (FFPE) curls cut at 10μm for the small bowel samples. On average 12.47ng/μl of RNA has been obtained from x4 FFPE curls cut at 10μm for the skin samples.

2.5 nCounter gene expression analysis

2.5.1 Overview of nCounter technology

The NanoString nCounter provides a direct, digital count of mRNA in samples, using a unique, barcode technology. It does not require any amplification and works particularly well for formalin fixed paraffin embedded (FFPE) samples. The capture probes consist of specific sequences (35-50 bases) targeting genes of interest. These are matched with reporter probes, with a colour coded sequence attached to their 5' end. After hybridisation these pairs are counted, resulting in a readout of gene count, **Figure 2-4**.

2.5.2 nCounter gene expression workflow

In brief, RNA was isolated from samples as detailed in 2.5. For fresh frozen skin and blood an RNA input of 50ng was used. For FFPE samples an RNA input of 150ng was used. Capture and reporter probe sets were added. Samples were hybridised in a thermal cycler for 20 hours at 65°C and then loaded onto the nCounter cartridge. The nCounter SPRINT was used to run the cartridge.

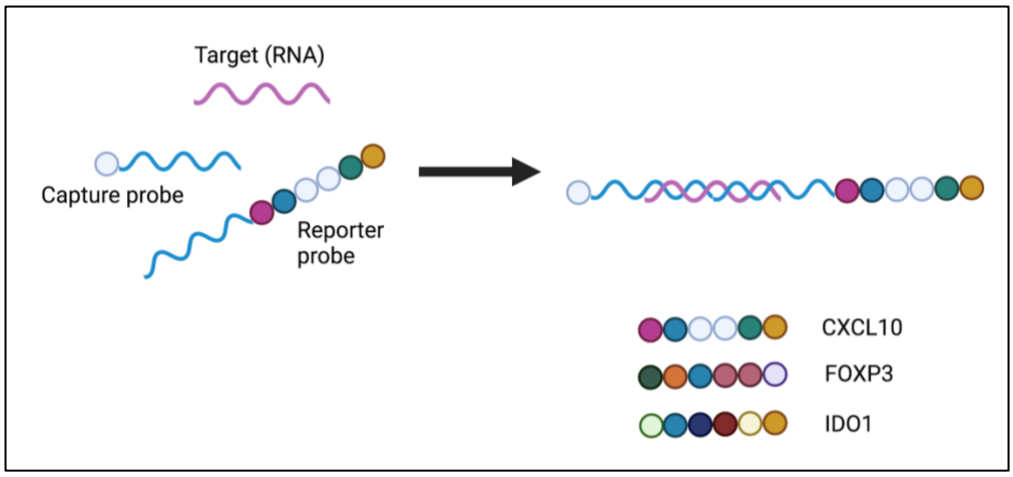

***Figure 2-4. Schematic of NanoString nCounter technology**. Capture and reporter probes are hybridised with mRNA. The reporter probes for each gene have a unique barcode (represented here by coloured dots) which are then counted by the nCounter, and a gene count for each gene in the panel is given. Created with BioRender.com.*

2.5.3 Banff Human Organ Transplant Panel

The Banff Human Organ Transplant panel was chosen, comprising of 770 gene targets focussed on organ rejection, tissue injury and immune response (full list of genes in Appendix 2). This panel has been developed by an international consortium of transplant experts and is produced by NanoString Technologies.[140]

2.5.4 Quality control of nCounter gene expression data

Data were subject to quality control and analysed using the nSolver software. Initial quality control (QC) was based on four factors: imaging QC (>75%), binding density (0.1-1.8), positive control linearity and limit of detection. Imaging QC measures how many fields of view (FOV) are recorded by the nCounter, divided by the total. It is an indicator of how well the cartridge was scanned. Binding density describes how many reporter codes are visible, if too high they will overlap, and accuracy of data is reduced. The binding density can be affected by RNA input, gene expression or the size of the

codeset. Positive control linearity is a check of the hybridisation efficiency. Every sample has six synthetic DNA controls, at decreasing concentrations, added. These should show decreasing counts according to their concentration. The positive controls are also used, together with negative controls, to calculate the limit of detection. The positive control E count should be two times higher than the background (calculated by looking at negative controls). If a sample raises a QC flag, the raw counts are examined and compared to other samples, before a decision is made on whether to exclude that sample. Samples are then normalised, to account for sample to sample (and differing run) variations. A check is made on signal to noise ratio i.e., how many probes are above the level of the negative probes. Then, counts are normalised between samples using housekeeping genes included in the panel. For housekeeper normalisation the geomean of the housekeeper gene count is calculated for each lane. Then the arithmetic mean of these geomeans is calculated. This arithmetic mean is divided by the geomean of each lane to produce a lane specific normalisation factor. Then all the gene counts in the lane are multiplied by the lane specific normalisation factor. The results of initial QC for the samples may be seen in **Table 2-4**.

Sample type	Number of samples	Initial QC flags	What was QC flag for?
Blood	23	8	binding density >1.8
Skin	30	0	n/a
Small bowel	16	1	binding density >1.8
Total	69	9	

Table 2-4. nCounter gene expression initial QC results.

A small proportion of samples had a QC flag raised, due to high binding density. However, on review of the rest of their parameters, no other QC flags were raised. When the data was analysed by PCA and hierarchical clustering these samples were not noted to be outliers, therefore they were kept for analysis.

2.5.5 Statistical analysis of nCounter gene expression data

Analysis of gene expression data was performed using the nSolver Analysis 4.0 and the nSolver Advanced Analysis 2.0 analysis software from NanoString. These are proprietary software packages that are provided by NanoString for use with nCounter data. One of the first analyses carried out is principal component analysis, to gain an unbiased overview of the data. Principal component analysis (PCA) reduces the dimensionality of data by transforming multiple variables into linear set of principal components. The first principal component is those with the most variance. The PCA plot is then coloured by the variable of interest (e.g., rejection status or time point) and it is possible to see if samples cluster according to the variable. As this is unsupervised clustering it may offer insight into trends within the data. Differential gene expression is calculated using a mixed negative binomial method. Data is presented in a volcano plot, with $-\log_{10}$(p-value) on y axis and $\log_2$ fold change on x axis. As there will be multiple comparisons within the same sample the p-values are adjusted using the Benjamini-Hochberg method to control for false discovery rate. Gene set analysis is based on the calculations performed when calculating differential gene expression. This is expressed as a directed global significance score, which summarises changes in regulation (both up and down) of genes within pre-defined gene sets relative to a chosen variable (e.g., rejection status or time point). The heatmap of pathway scores combines all the

pathways and samples in one visualization, by z transformation of scores so they can be displayed on the same scale.

2.6 GeoMx Digital Spatial Profiler

2.6.1 Overview of GeoMx Digital Spatial Profiler technology

The NanoString GeoMx Digital Spatial Profiler (DSP) enables highly multiplexed, spatially resolved proteomic analysis of tissue slides. It has been designed for either mRNA or protein readouts, using similar capture and reporter probe technology as the nCounter. The reporter probes are attached with a UV-cleavable bond, enabling specific collection by the GeoMx DSP, when UV light is shone on the regions of interest.

2.6.2 GeoMx DSP workflow

2.6.2.1 Slide preparation

Tissue samples were cut to <7μm thickness and placed on SuperFrost Plus™ slides. Slides were obtained from OCHRe (Oxford Centre for Histopathology Research), following ethical approval from the Oxford Radcliffe Biobank research tissue banks ethics, reference 19/SC/0173. Slides were baked at 60°C for 60 minutes. Automated slide preparation was performed by the BOND-RX (Leica Biosystems), using a Bake and Dewax protocol, with heat induced epitope retrieval of 20 minutes at ER1 (citrate-based buffer at pH 6).

2.6.2.2 Hybridisation

Slides were blocked with Buffer W for one hour at room temperature. Samples were incubated overnight at 4°C with the primary antibody mix. This included Immune Activation, Immune Cell Profiling, Drug Target, Immune Cell Typing and custom CXCL9 antibody modules, all supplied by NanoString, see appendix 3 for full details.

Post hybridisation, the slides underwent several washing and blocking steps: 1X TBS-T (3 x10 minutes), 4% paraformaldehyde (30 minutes at room temperature), 1X TBS-T (2 x 5 minutes).

2.6.2.3 Morphology marker staining

Slides were then stained, for two hours at room temperature, with the morphology marker mix, comprising SYTO13, CD45, pancytokeratin (panCK) and CD31. These were chosen to facilitate visualisation of tissue architecture and to identify immune cell populations of interest. See **Table 2-5** below for details of the antibodies used. Then a final set of washes with 1X TBS-T (2 x 5 minutes) was commenced prior to loading to the GeoMx DSP machine.

Specificity	Fluorochrome	Clone
panCK	Alexa-Fluor 532	AE1 + AE3
CD45	Alexa-Fluor 594	PD7/26
CD31	Alexa-Fluor 647	JC/70A
SYTO13	Alexa-Fluor 488	

Table 2-5. Details of antibodies used for morphology marker staining.

2.6.2.4 GeoMx DSP region of interest selection and collection

After scanning, regions of interest (ROIs) were chosen and collected. These were then segmented based on CD45 staining into $CD45^+$ and $CD45^-$ areas of interest (AOIs). The detection antibodies have a UV-cleavable oligonucleotide barcode attached, allowing specific ROIs to be collected and counted in a direct, digital process. After storage at 4°C overnight the collected ROIs were dried down in a thermocycler set to 65°C for one hour, then rehydrated with 7µl DEPC water.

2.6.2.5 nCounter DSP readout

A GeoMx Hybridisation Code master mix was made (consisting of Probe R, Probe U and GeoMx codes) and added to the samples, then placed in a thermocycler at 67°C for 20 hours. On the final day the hybridized samples were pooled according to column and loaded to an nCounter cartridge before running on the SPRINT. Counts were uploaded back to the GeoMx DSP machine, where quality control and analysis took place.

2.6.3 Region of interest selection strategy

2.6.3.1 Abdominal wall or SSF biopsies

The current gold standard for diagnosis of rejection in a vascularised composite allograft is histological analysis of a tissue biopsy. Histopathologists score the findings using the Banff 2007 working classification[54] which amongst other things looks for perivascular infiltrates and epidermal involvement. Therefore, regions of interest (ROIs) were chosen which were either centred on perivascular regions (recognised by staining for CD31) or in the epidermis (recognised by staining for panCK), **Figure 2-5**. As the goal was to investigate the immune response, these areas were then further segmented, based on CD45 staining, to look more specifically at the leukocyte population.

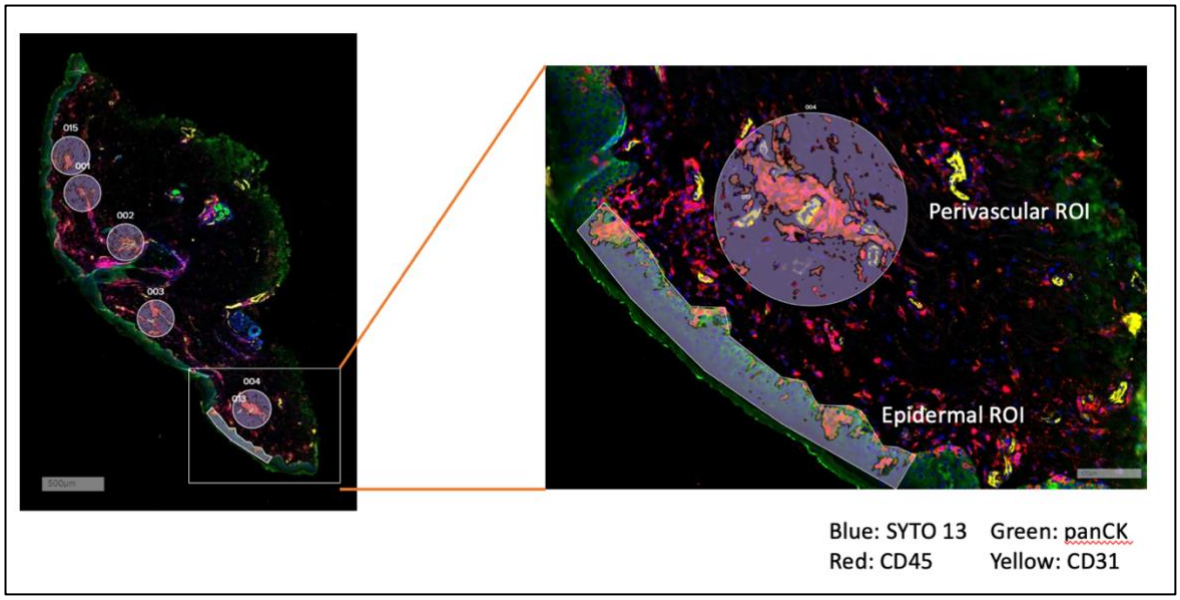

Figure 2-5. Region of interest selection, abdominal wall transplants. *This is an example of an AWTx biopsy taken at rejection. The following morphology markers have been used to visualise the architecture of the tissue: SYTO13 (nuclei), panCK (epithelium/connective tissue), CD31 (vascular endothelium), CD45 (leukocytes). Both perivascular and epidermal regions have been collected, using a combination of geometric and circular ROIs.*

2.6.3.2 Small bowel transplant

Similarly, to the abdominal wall transplants, diagnosis of rejection in small bowel transplants is based on histological findings, as defined by the International Small Bowel Transplant symposium[35]. This includes infiltrates and damage to the crypts, therefore ROIs in these areas were chosen, **Figure 2-6**. It should be acknowledged that the samples available have been cut in a number of different orientations, making it difficult to exactly replicate crypt areas between samples. Areas of denser CD45 staining were noted so it was decided to collect these as a second type of ROI. Both

these ROIs have been segmented based on CD45 staining, as in the abdominal wall or SSF transplants.

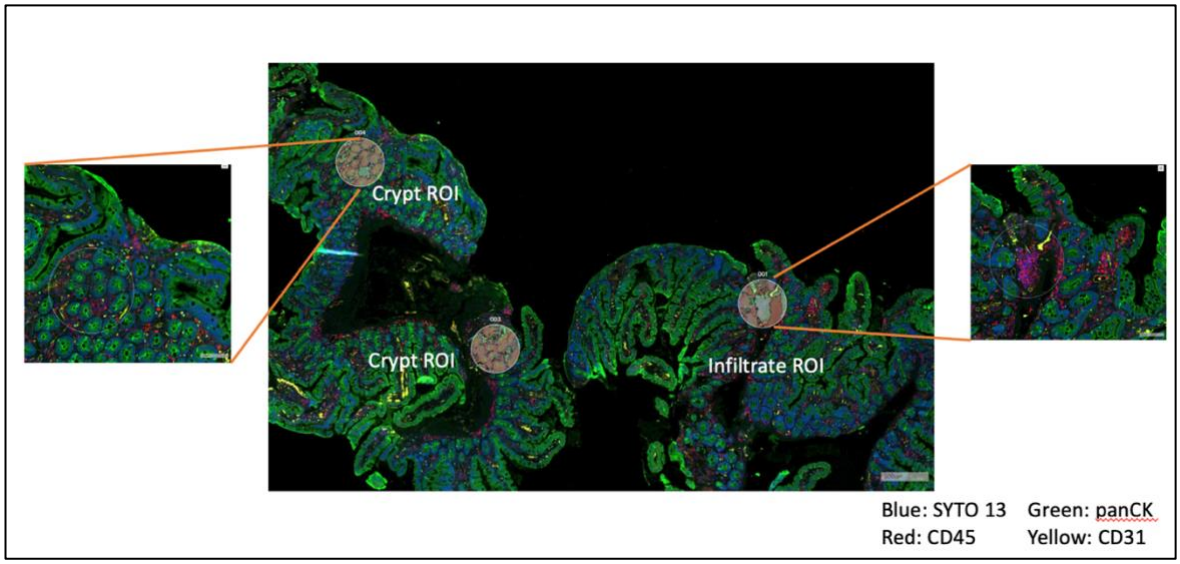

Figure 2-6. Region of interest selection, small bowel transplants. *This is an example of a small bowel biopsy taken at rejection. The following morphology markers have been used to visualise the architecture of the tissue: SYTO13 (nuclei), panCK (connective tissue), CD31 (vascular endothelium), CD45 (leukocytes). Both crypt and infiltrate regions have been collected, using circular ROIs.*

2.6.4 Quality control of GeoMx DSP data

The final readout of the GeoMx DSP ROI collection is performed on the nCounter. Therefore, the initial QC is the same as for the nCounter gene expression analysis, with checks of binding density, imaging QC and fields of view registered (described in detail in *2.5.4*). Positive control normalisation is also performed, a positive hybridisation code is spiked into all samples, aiding evaluation of the nCounter assay, and allowing calculation of a positive control normalisation factor, which can then be used across samples. After initial QC there were no flags for the skin samples (90 AOIs collected)

and eight flags for the small bowel samples (216 AOIs collected). These eight samples were reviewed and three removed as significant outliers on PCA plots. The rest were kept for further analysis. The next part of the analysis workflow is normalisation of the data. The housekeeper proteins GAPDH and S6 were used to perform housekeeper normalisation. These proteins are expressed similarly across samples and can be used to adjust for differences in the number of cells analysed between ROI or AOIs. Once normalisation is complete a background correction is performed, **Figure 2-7** and **Figure 2-8**. This eliminates non-specific signal, by using negative probes to measure background noise across samples.

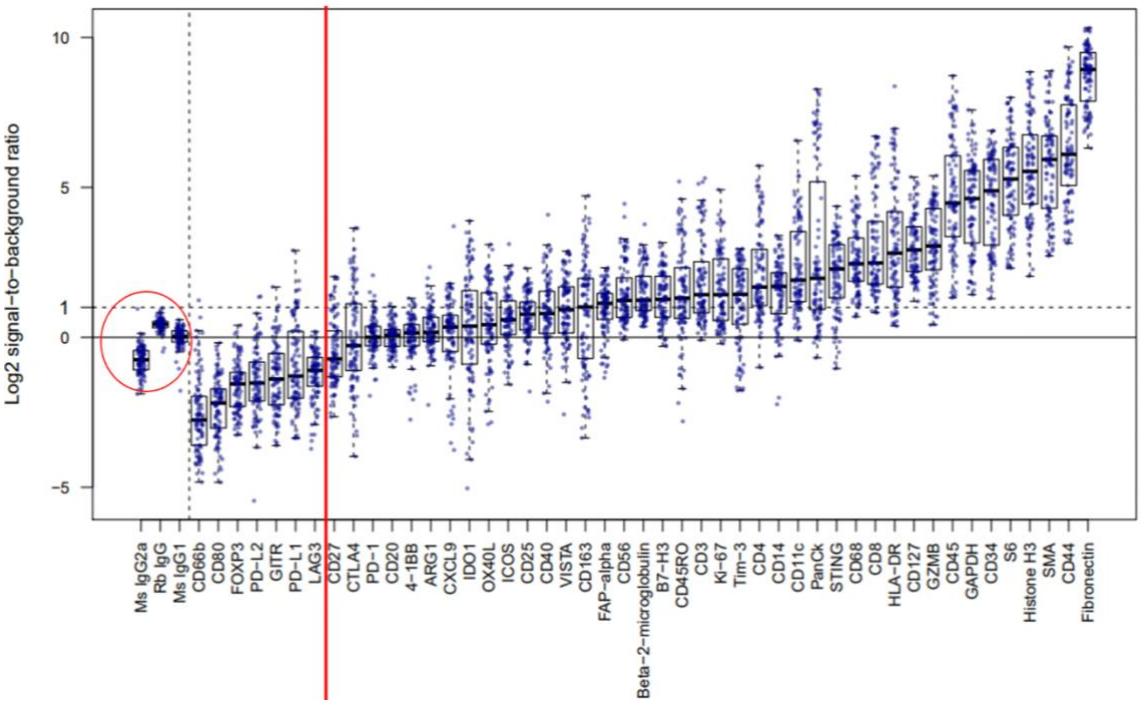

Figure 2-7. Background correction for abdominal wall samples. *The background level of signal is based on negative probes (Mouse IgG2a, Rabbit IgG and Mouse IgG1) circled on left of the chart. Probes to the left of the red line (CD66b, FOXP3, PD-L2, GITR, PD-L1 and LAG3) are deemed to be below background levels as most of the areas of interest (represented by a single dot) are lower than the negative controls.*

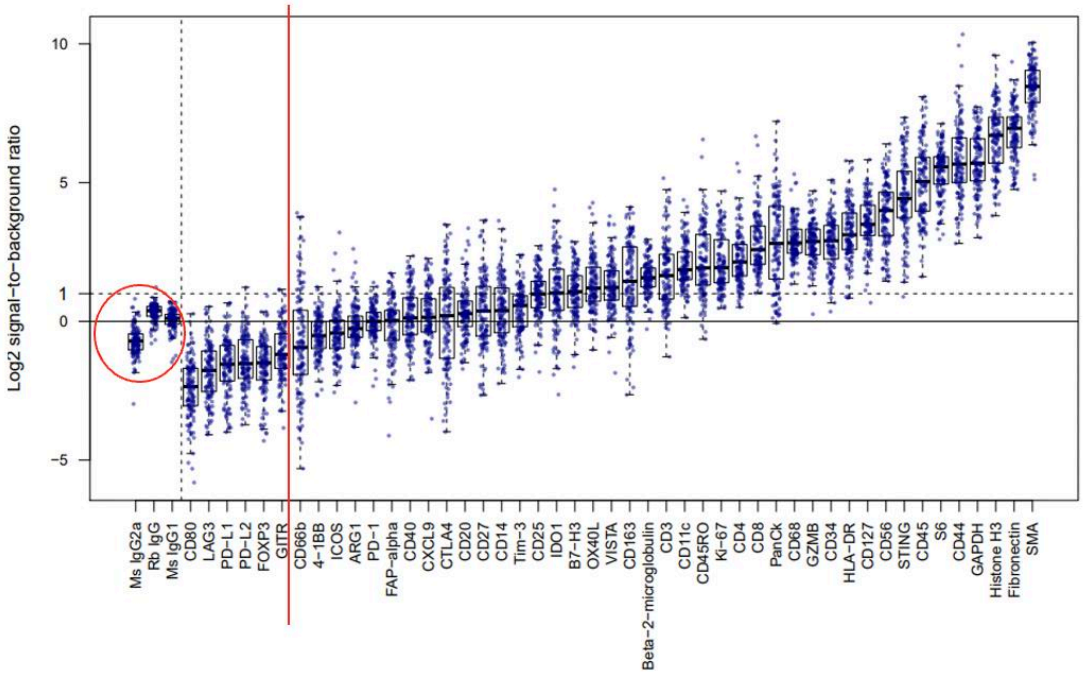

Figure 2-8. Background correction for small bowel samples. *The background level of signal is based on negative probes (Mouse IgG2a, Rabbit IgG and Mouse IgG1) circled on left of the chart. Probes to the left of the red line (CD80, LAG3, PD-L1, PD-L2, FOXP3 and GITR) are deemed to be below background levels as most of the areas of interest (represented by a single dot) are lower than the negative controls.*

2.6.5 GeoMx DSP data analysis

All data analysis was performed on the GeoMx DSP v2.4. This is a proprietary software provided by NanoString for the analysis of spatial data. Principal component analysis was performed to reduce the dimensionality of data and explore the data for potential clustering of samples according to the different variables (rejection, time). Data was then analysed using a linear mixed model, with Benjamini-Hochberg method to control for false discovery rate and volcano plots used to visualize the results.

2.7 Mouse skin transplant model

2.7.1 Mice

Mice were bred in a specific pathogen free (SPF) facility. Transgenic mice were generated by insertion of the human gene locus by microinjection. CBA mice were sourced from Charles River Laboratories and allowed to acclimatise for seven days prior to surgery. All procedures were carried out with Home Office approval, PPL P8869535A "Studies on transplant rejection and tolerance" and PIL C I72850948.

2.7.2 Intraperitoneal injections

Intraperitoneal (IP) injections of either placebo or an antibody to modify the Langerhans cell (LC) – associated pathway were given to transgenic mice at 72h intervals for one week prior to harvest of tail skin. IP injections were then continued in the recipient mice, split into two groups with 11 mice in each group. IP injections were given using an aseptic non touch technique.

2.7.3 Skin retrieval

Donor skin was harvested from transgenic mice. Skin was prepped using 2% chlorhexidine (with 70% isopropanol). A circumferential incision was made around the proximal tail, then longitudinally along the length of the tail. Once removed, the tail skin was placed on phosphate buffered saline (PBS) soaked gauze and cut into 1cm squares. It was stored in PBS, on ice and used the same day.

2.7.4 Skin transplant surgery

Prior to surgery mice were weighed and anaesthetised, using isofluorane 3% in a chamber, followed by maintenance with isofluorane 2-3%. Heat loss was minimised with the use of heat mats and drapes. Hair was removed from the left flank, followed by

an initial skin prep with 2% chlorhexidine. Chloramphenicol ointment was used to protect the eyes. Each mouse received a dose of Metacam (5mg/kg) subcutaneously. Surgery took place under aseptic conditions. The surgeon was scrubbed and wore sterile gloves and gown. Instruments were sterilised in an autoclave prior to use. Operating lights and microscope or loupes were used for magnification. Mice were placed in the right lateral position. Skin was prepped for a second time with chlorhexidine 2%. Sterile drapes were placed over the mouse. A one-centimetre square piece of skin was removed from the left flank/chest wall region. Donor skin was applied and secured using 8.0 prolene interrupted sutures. The graft was dressed with mepitel, inadine and gauze, affixed with fabric elastoplasts. The dressing was further reinforced with tape. Mice were placed into a heat box and monitored post operatively until fully recovered.

2.7.5 Skin graft monitoring

Skin grafts were monitored daily from day seven postoperatively. Bandages were removed under general anaesthetic (isofluorane 3%). Grafts were scored based on the percentage of graft area that was necrotic, **Table 2-6** [141].

Graft score	Description
5	<20% of graft necrotic
4	20-40% of graft necrotic
3	40-60% of graft necrotic
2	60-80% of graft necrotic
1	80-100% of graft necrotic, but remains in situ
0	Complete loss of graft

***Table 2-6. Description of graft scoring system, as described by Zhao et al*[141].**

2.7.6 Blood and tissue sampling techniques

Blood samples were retrieved from all mice on day five postoperatively via tail bleed. After warming for 30 minutes, mice were placed into a mechanical restraint tube. The tail skin was cleaned with 2% chlorhexidine. Tail veins were identified, and a scalpel was used to make a small cut, around 1/3 down the tail. Blood was collected in a microvette, and 50µl of heparin was added to each sample. Total blood volume taken did not exceed 10% of body weight.

Three mice from each group were sacrificed for tissue harvest at day five postoperatively. They underwent terminal anaesthesia with isofluorane. Both ipsilateral and contralateral axillary and groin lymph nodes were harvested, via a midline incision and placed in fetal calf serum (FCS) on ice, prior to processing.

3 Chapter 3: Systemic immune response to combined skin and solid organ transplantation

3.1 Introduction

In chapter 1, I discussed the importance of monitoring the immune response in organ transplants. It has been established that episodes of acute rejection contribute to poorer graft outcomes[142]. Close monitoring of transplanted organs is imperative, to prevent damage caused by unrecognised rejection. It is relatively easy to take a blood sample for monitoring purposes, without the associated morbidity that occurs with tissue biopsies. For this reason, blood samples have been widely used to investigate the immune response during transplantation, with the goal of using this knowledge to identify a potential biomarker for rejection or new therapeutic targets.

While there are many studies in the published literature reporting on both the repopulation of immune cells post kidney or simultaneous kidney pancreas transplantation and the changes that occur at rejection[143–145], there have not been any publications of in depth immunophenotyping of patients with combined skin and solid organ transplants. As discussed in Chapters 1 and 2, patients who underwent combined sentinel skin flap and pancreas transplantation or abdominal wall and small bowel transplantation had fewer episodes of acute rejection in the first 12 months, than had been expected. This is an area of great interest, given the need to understand why acute rejection episodes are less frequent in these combined transplants.

Flow cytometry has long been the method of choice for analysing blood samples. It is widely available and relatively affordable. One of its key benefits is the ability to offer

multiparametric analysis, facilitating in depth immunophenotyping of samples. It is possible to measure frequency of different immune cell types and their activation status. There are many studies in the published literature reporting on both the repopulation of immune cells post kidney or simultaneous kidney pancreas transplantation and the changes that occur at rejection[143–145], which are based on this method.

In recent years there has been increasing interest in developing a molecular test for rejection. Gene expression profiling offers the opportunity to examine many more pathways than flow cytometry alone, with the potential to offer crucial mechanistic insights into causes of rejection. It is likely that gene changes occur in blood prior to rejection taking place, offering the opportunity to recognise rejection before tissue damage has occurred. However due to the complex nature of the alloresponse, in combination with effects of immunosuppression and the confounding effect of infection, teams have been unable to identify a single biomarker that reliably predicts rejection. Instead, multiple genes are required to reach clinically useful predictive values[16–18].

3.2 Chapter 3 aims and hypotheses.

The aim of this chapter is to use flow cytometry and gene expression analysis to:

- characterise the systemic immune response to a combined skin and solid organ transplant in the first 12 months after transplant.
- characterise the systemic immune response at the time of a rejection episode.
- explore if there are differences in those who had a rejection episode in the first 12 months versus those who did not.

First, we hypothesise that analysis of blood samples from patients with a combined sentinel skin flap and pancreas transplant, who have received induction immunosuppression with alemtuzumab, will demonstrate similar repopulation of immune cells as has been reported in the literature for kidney transplants alone, including a prolonged depletion of $CD4^+$ T cells and transient depletion of other immune populations. Next, we hypothesise that at rejection blood samples from these patients will have increased expression of genes associated with T cell activation and proliferation, as well as chemokines such as CXCL9 and 10. Finally we hypothesise that patients who did not have an episode of rejection in the first 12 months will have differences in gene expression and immune cell subsets when compared to those patients who did have an episode of acute rejection.

3.3 Results

3.3.1 Effect of induction immunosuppression with alemtuzumab on immune cell repopulation post sentinel skin (SSF) and simultaneous pancreas and kidney (SPK) transplantation

It has been previously reported that the induction immunosuppression with alemtuzumab used to prevent rejection has a significant impact on leukocyte numbers, in some cases for more than 12 months following transplant[146]. Using flow cytometry, leukocyte populations at pre-transplantation and then 6 weeks, 3 months, 6 months, and 12 months post-transplantation were examined. See **Table 3-1** below for details of how many patients were included at each time point.

Time point	Number of patients
Pre-transplant	20
6 weeks post-transplant	17
3 months post-transplant	15
6 months post-transplant	16
12 months post-transplant	11

Table 3-1. Number of patients included in analysis at each time point.

As shown in **Figure 3-1** numbers of both T and B cells are significantly decreased at six weeks post-transplant compared to the pre-transplant numbers. Whilst the B cells returned to baseline by three months, the T cell numbers took until 12 months to recover.

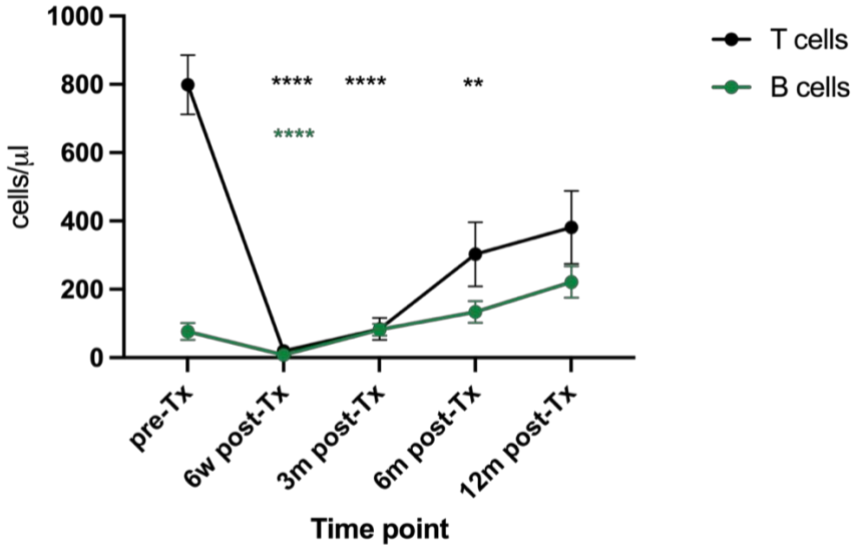

Figure 3-1. Repopulation of T and B cells post induction immunosuppression with alemtuzumab. *The mean +/- standard error of the mean (SEM) of the absolute number (cells/µl) of T cells ($CD3^+$) and B cells ($CD19^+$) is shown on this graph. The effect of*

*induction immunosuppression is clear, with a significant decrease in both T and B cells seen at 6 weeks post-transplantation. B cell numbers have recovered by 3 months post-transplant, but it takes until 12 months post-transplant for T cell numbers to recover. Time points include pre-Tx = pre-transplant, 6w post-Tx = 6 weeks post-transplant, 3m post-Tx = 3 months post-transplant, 6m post-Tx = 6 months post-transplant and 12m post-Tx = 12 months post-transplant. **** p <0.0001, ** p<0.01, when compared to pre-transplant time point. Black = T cells, green = B cells.*

Trzonkowski et al have previously reported similar findings of decreased T and B cells for a cohort of kidney transplant patients, under the same immunosuppressive treatment (alemtuzumab induction and maintenance with tacrolimus and mycophenolate mofetil)[145]. Both Noris et al and Knechtle et al also demonstrated significant depletion of T and B cells in cohorts of kidney transplant patients. Their patients received induction with alemtuzumab but were managed with different maintenance immunosuppression[144,147].

A significant decrease in NK cell numbers was also observed, these recovered by three months, see **Figure 3-2**. This is in keeping with Trzonkowski et al, who noted a transient decrease in NK cell numbers in their cohort of patients undergoing kidney transplant with alemtuzumab induction therapy[145]. Monocyte numbers did not decrease and in fact showed a significant increase at 12 months in comparison to pre-transplantation numbers, see **Figure 3-2**. This differs from the literature, where in general an initial decrease in monocyte numbers is reported, followed by recovery by 2-3 months post-transplantation[145–147].

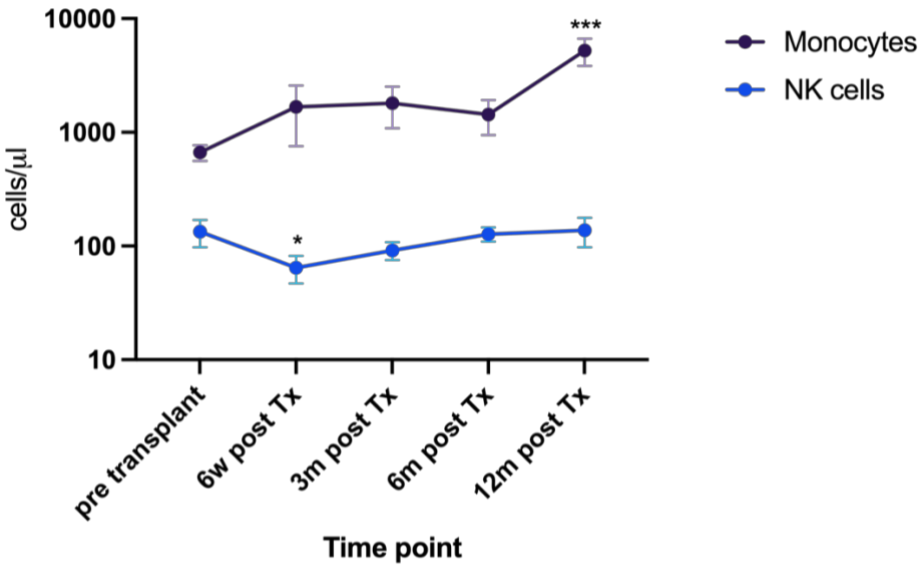

Figure 3-2. Repopulation of monocytes and NK cells post induction immunosuppression with alemtuzumab. *The mean +/- standard error of the mean (SEM) of the absolute number (cells/µl) of monocytes and NK cells is shown on this graph. Whilst the numbers of NK cells decrease compared to the pre-transplant time point, monocyte numbers are unaffected, until 12 months post-transplant when they are increased. Time points include pre-Tx = pre-transplant, 6w post-Tx = 6 weeks post-transplant, 3m post-Tx = 3 months post-transplant, 6m post-Tx = 6 months post-transplant and 12m post-Tx = 12 months post-transplant. *** p <0.001, * p<0.05, when compared to pre-transplant time point. Purple = monocytes, blue = B cells. Graph uses a logarithmic scale to aid visualisation.*

It is known that T cells are a key component of the alloresponse in transplantation, with both $CD4^+$ T helper and $CD8^+$ T effector cells contributing to rejection. Pre-transplantation there was a greater number of $CD4^+$ T cells compared to $CD8^+$ T cells,

however numbers of $CD4^+$ T cells appear disproportionately affected by induction immunosuppression compared to $CD8^+$ T cells, as shown in **Figure 3-3**. This results in the ratio of $CD4^+$:$CD8^+$ T cells being initially increased post-transplant, then reversed from six months, as shown in **Figure 3-4**, although this finding was not statistically significant. This finding is in keeping with the literature, which reports a more prolonged effect on the $CD4^+$ T cells than $CD8^+$ T cells[144,146].

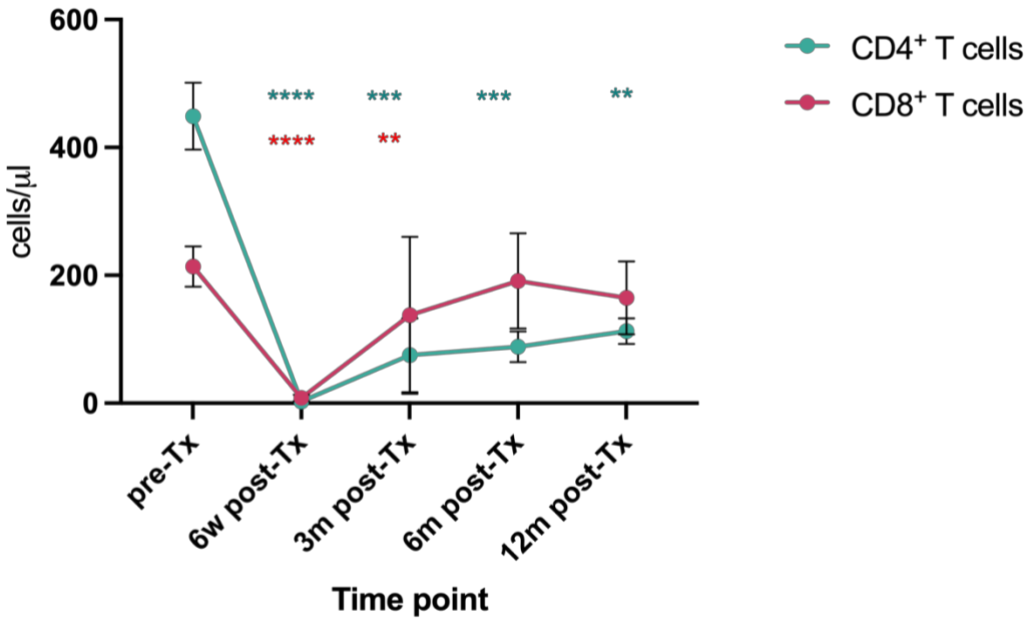

Figure 3-3. Repopulation of T cells post induction immunosuppression with alemtuzumab. *The mean +/- standard error of the mean (SEM) of the absolute number (cells/µl) of $CD4^+$ and $CD8^+$ T cells is shown on this graph. Both $CD8^+$ and $CD4^+$ T cells are significantly decreased at 6 weeks post-transplant, however $CD8^+$ T cells recover more quickly than $CD4^+$ T cells. Time points include pre-Tx = pre-transplant, 6w post-Tx = 6 weeks post-transplant, 3m post-Tx = 3 months post-transplant, 6m post-Tx = 6 months post-transplant and 12m post-Tx = 12 months post-transplant. **** p*

*<0.0001, *** p<0.01 and ** p<0.01, when compared to pre-transplant time point. Red = CD8⁺ T cells, green = CD4⁺ T cells.*

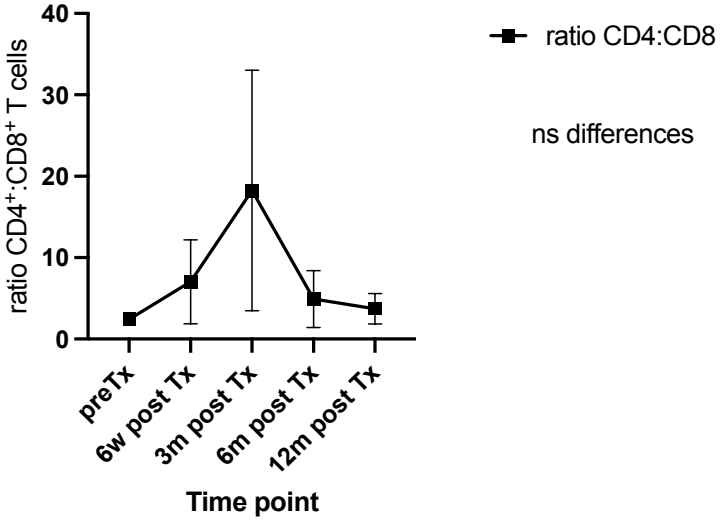

Figure 3-4. Ratio of CD4⁺:CD8⁺ T cells at protocol time points. *The mean ratio of CD4⁺:CD8⁺ T cells +/- standard error of the mean (SEM) is shown on this graph. There is initially an increase in the ratio, followed by a decrease, although this was not found to be statistically significant. Time points include pre-Tx = pre-transplant, 6w post-Tx = 6 weeks post-transplant, 3m post-Tx = 3 months post-transplant, 6m post-Tx = 6 months post-transplant and 12m post-Tx = 12 months post-transplant.*

As expected after alemtuzumab treatment, at six weeks post-transplantation, in both $CD4^+$ and $CD8^+$ T cell subsets the percentage of naïve cells was reduced, compensated by an expansion of the memory phenotypes. In $CD4^+$ T cells, this resulted in an increased proportion of the effector memory subtypes. Interestingly this pattern was not replicated in the $CD8^+$ T cells, although there was an increase in the effector memory

population, there were also relatively sizeable increases in the terminally differentiated population (TEMRA), **Figure 3-5** and **Figure 3-6**. The same skewing of memory phenotypes was also shown by Bouvy et al, in a cohort of kidney transplant patients following alemtuzumab induction immunotherapy[148]. Trzonowski et al also reported on a skewing of T cell populations towards memory phenotypes after induction with alemtuzumab[149]. They reported an initial increase in $CD4^+$ central memory T cells, which gradually were replaced by $CD4^+$ effector memory T cells. Meanwhile Borges et al have reported on three hand transplant patients, undergoing induction immunosuppression with rabbit antithymocyte globulin[150]. They found an initial increase in $CD4^+$ central memory T cells, followed by an increase in the effector memory population and an increase in $CD8^+$ TEMRA T cells, consistent with the results presented in this chapter.

Next the number of $CD4^+FOXP3^+$ Tregs was analysed. Tregs play an important role in immune tolerance, and act to suppress other immune cells, such as effector T cells[151]. As predicted by the data already presented for $CD4^+$ T cells, there was a significant decrease in the total number of Tregs at both 6 weeks and 3 months post-transplantation, see **Figure 3-7**. Whilst numbers returned to pre-transplantation levels at 6 months, they were significantly decreased again at 12 months. The Helios positivity, a marker of stability of human T regs,[152] of these T regulatory cells was also reviewed, and it was found that the proportion of Treg Helios negative cells increased over time post-transplant, **Figure 3-8**.

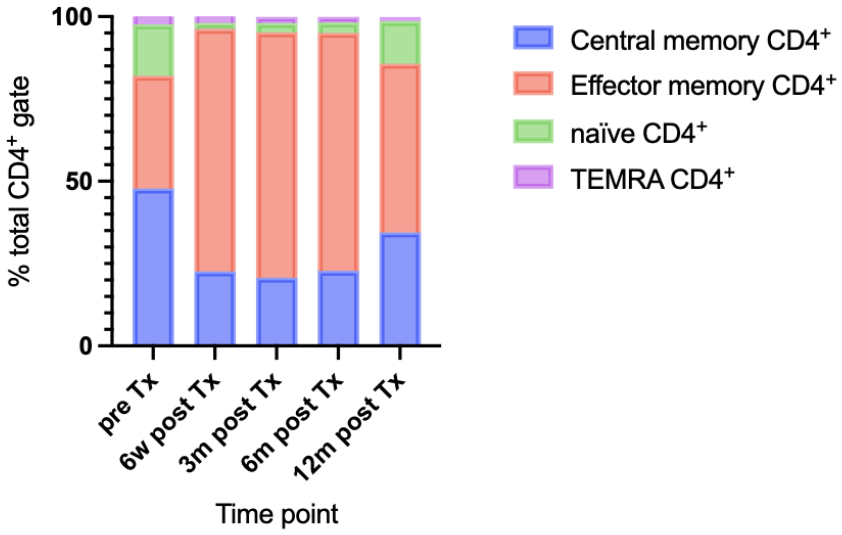

Figure 3-5. Repopulation of CD4$^+$ T cell subsets post-transplantation. *Repopulation is shown as a proportion of the total CD4$^+$ gate. Central memory (CD45RA$^-$CCR7$^+$), effector memory (CD45RA$^-$CCR7$^-$), naïve (CD45RA$^+$CCR7$^+$) and TEMRA (CD45RA$^+$CCR7$^-$) subsets are shown at each of the protocol time points. There is a greater proportion of memory subsets post-transplantation following induction immunosuppression.*

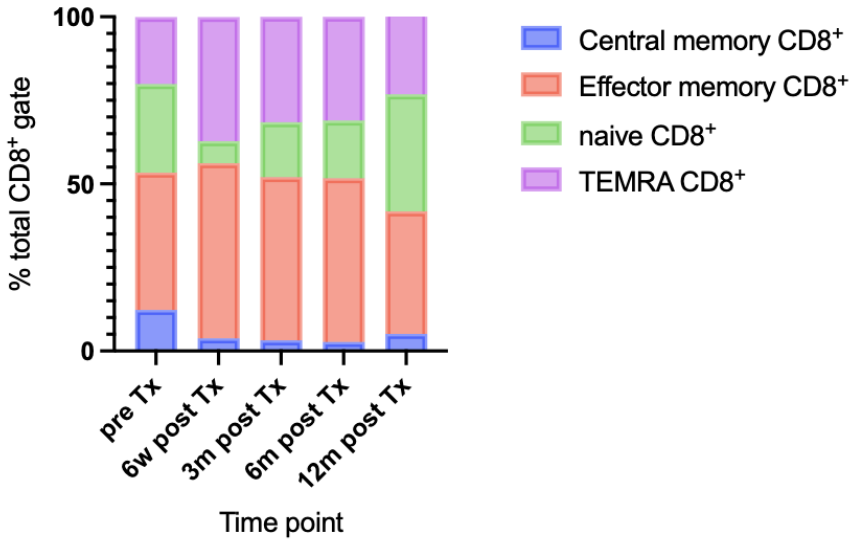

Figure 3-6. Repopulation of CD8$^+$ T cell subsets post-transplantation. *Repopulation is shown as a proportion of the total CD8$^+$ gate. Central memory (CD45RA$^-$CCR7$^+$), effector memory (CD45RA$^-$CCR7$^-$), naïve (CD45RA$^+$CCR7$^+$) and TEMRA (CD45RA$^+$CCR7$^-$) subsets are shown at each of the protocol time points.*

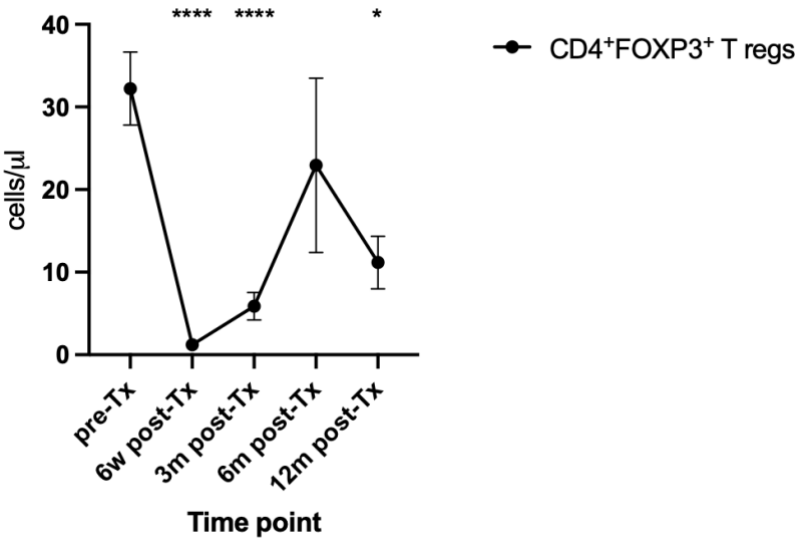

Figure 3-7. Repopulation of Tregs post induction immunosuppression with alemtuzumab. *The mean +/- standard error of the mean (SEM) of the absolute number (cells/µl) of CD4$^+$FOXP3$^+$ Tregs is shown on this graph. A significant decrease in the number of Tregs is shown at both 6 weeks and 3 months post-transplantation. Time*

*points include pre-Tx = pre-transplant, 6w post-Tx = 6 weeks post-transplant, 3m post-Tx = 3 months post-transplant, 6m post-Tx = 6 months post-transplant and 12m post-Tx = 12 months post-transplant. **** p <0.0001, * p< 0.05, when compared to pre-transplant time point.*

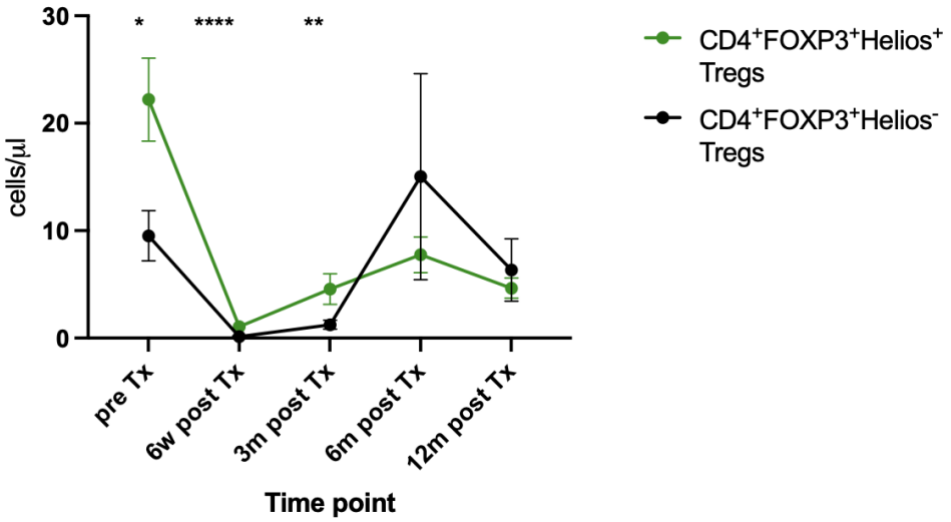

Figure 3-8. Repopulation of Treg subsets post induction immunosuppression with alemtuzumab. *The mean +/- standard error of the mean (SEM) of the absolute number (cells/µl) of Helios$^+$ and Helios$^-$ Tregs is shown on this graph. There are significantly fewer numbers of Helios$^-$ Tregs at the pre-transplant, 6 weeks, and 3 months post-transplant time points, compared to Helios$^+$ Tregs. Time points include pre-Tx = pre-transplant, 6w post Tx = 6 weeks post-transplant, 3m post Tx = 3 months post-transplant, 6m post Tx = 6 months post-transplant and 12m post-Tx = 12 months post-transplant. **** p <0.0001, ** p<0.01, * p< 0.05, comparison of number in each group at that time point.*

It is widely accepted that the ratio of T conventional to T regulatory cells has an impact on the likelihood of rejection post-transplantation, therefore this was the next area that has been investigated. At three months post-transplantation this ratio was significantly decreased compared to pre-transplantation, suggesting a relative increase in Tregs at this point, see **Figure 3-9**. This is consistent with the findings of Bloom et al, that induction with alemtuzumab results in an increased proportion of Tregs[153].

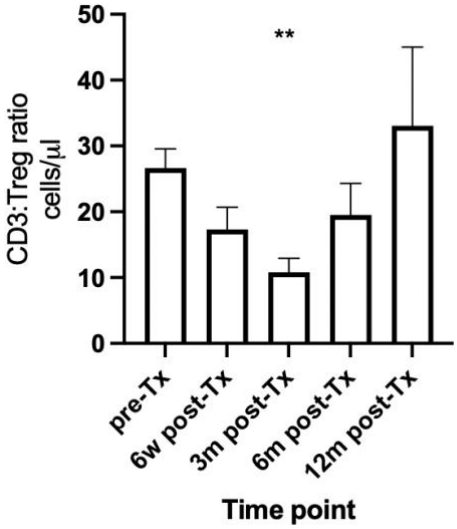

Figure 3-9. CD3: Treg ratio post-transplantation. *The mean +/- standard error of the mean (SEM) of the CD3: Treg ratio is shown on this graph. At 3 months post-transplantation there is a significant decrease in this ratio, suggesting a relative increase in the number of Tregs. ** $p<0.01$, in comparison to the pre-transplantation ratio.*

Most T cells were conventional αβ T cells, with a smaller proportion of γδ T cells noted. The frequency of these post-transplantation mirrored the numbers of $CD3^+$ T cells, with a significant decrease in the initial post-operative period, and slow recovery

over the next 12 months, shown in **Figure 3-10**. Next, the ratio of vδ1 to vδ2 in γδ T cells was calculated. In healthy blood vδ1 γδ T cells are in the majority, with vδ2 more often found in the skin, intestine, and lung[154]. In this cohort the ratio of vδ1: vδ2 increased compared to the pre-transplant time point, suggesting an expansion of vδ1 γδ T cells, **Figure 3-11**.

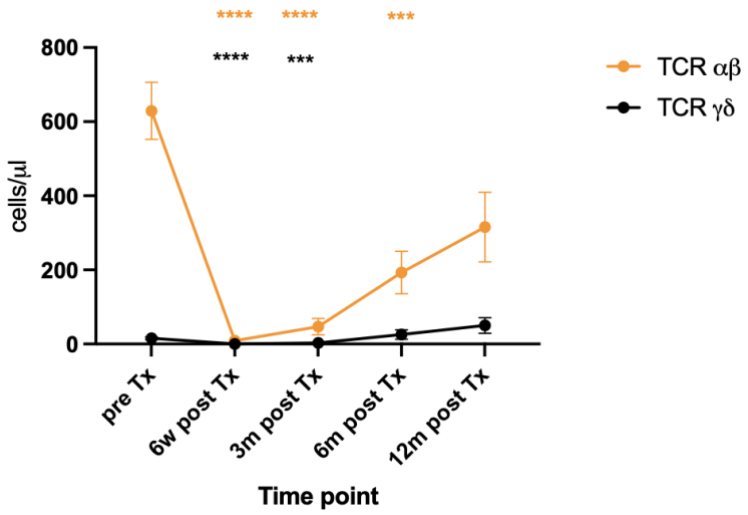

Figure 3-10. Repopulation of TCR subtype over time post-transplantation. *Graph shows absolute numbers +/- SEM at each of the protocol time points post-transplantation. Separated into two groups: TCRαβ (orange) and TCRγδ (black). While numbers of TCRγδ cells had returned to pre-transplant levels at 6 months, it took to 12 months for TCRαβ cells to recover. **** p< 0.0001, *** p<0.001 in comparison to the pre-transplant time point.*

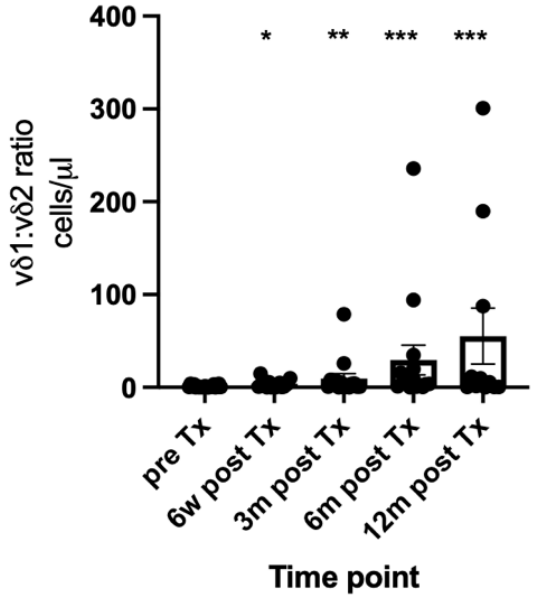

Figure 3-11. Ratio of vδ1 to vδ2 in γδ T cells over time post-transplantation. *Graph shows the ratio of absolute number of cells +/- SEM, at each of the protocol time points post transplantation. The ratio significantly increases over time post-transplant, suggesting an increase in vδ1 cells. *** $p < 0.001$, ** $p < 0.01$, * $p<0.05$ in comparison to pre-transplant time point.*

The different subsets of B cell were examined after transplantation to establish how they repopulated. All the subsets demonstrated a significant decrease at the six-week time point, except for transitional B cells. Naïve B cells made the quickest recovery back to pre-transplant levels, whereas class-unswitched memory B cells and plasmablasts had not yet fully recovered at 12 months post transplantation, **Figure 3-12**. Interestingly transitional B cells were significantly increased at 3- and 12-months post transplantation (**Figure 3-12** B, green). This is consistent with the reported literature for kidney transplants alone[143,155].

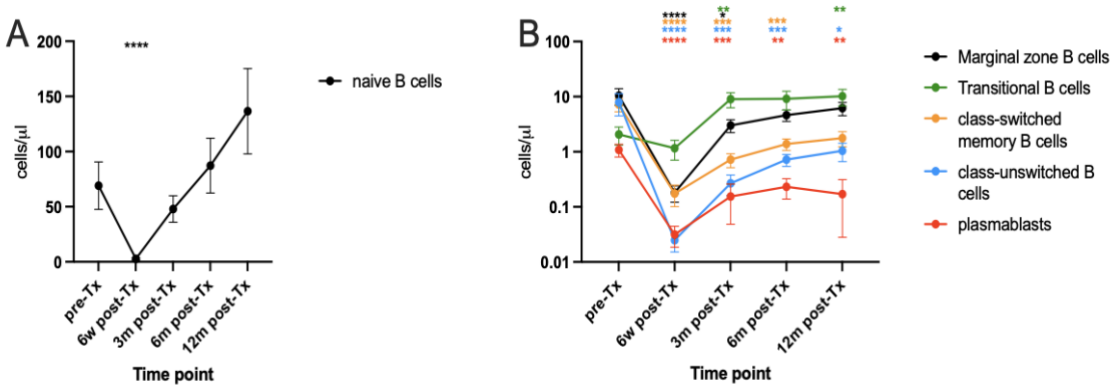

Figure 3-12. B cell subset repopulation over time post-transplantation. *Graph A shows absolute numbers +/- SEM of naïve B cells ($CD19^+IgD^+CD27^-$), Graph B shows marginal zone B cells ($CD19^+IgD^+CD27^+$), transitional B cells ($IgD^+IgM^+CD27^+CD38^{hi}CD24^{hi}$), class-switched memory B cells ($IgD^-IgM^-CD38^-CD27^+$), class unswitched memory B cells ($IgD^+IgM^+CD38^-CD27^+$) and plasmablasts ($IgD^-IgM^-CD38^{hi}CD27^+$). **** $p < 0.0001$, *** $p < 0.001$, ** $p < 0.01$, * $p < 0.05$ when compared to pre-transplant time point.*

These findings were confirmed by gene expression analysis using a multiplexed gene expression panel from NanoString, performed on a subset of the same patients. Initial principal component analysis (PCA) showed that samples tended to cluster according to time point, the pre-transplant samples separated away from the three- and six-month post-transplant samples. PCA analysis by patient and batch, demonstrates that these did not seem to be responsible for clustering of the samples, **Figure 3-13**.

Gene expression at three months post-transplant was compared to pre-transplantation gene expression and demonstrated 29 genes that were statistically differentially

expressed (downregulated) at this time (adjusted p value <0.05, log2 fold change < -1.5), predominantly in T cell related pathways, **Figure 3-14**. These included components of the T cell receptor (*CD3 D/E/G*), co-stimulatory molecules (*CD27* and *CD28, ICOS*), transcription factors (*TCF7*), chemokine receptors (*CCR7*) and cytokine receptors (*IL7R*).

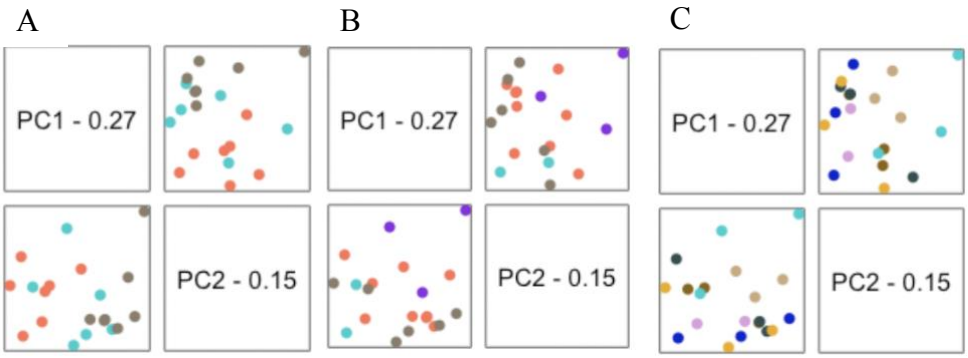

Figure 3-13. Principal component analysis of multiplexed gene expression counts. *Shows the first two components, PC1 captures the most variation and PC2 the second most variation in the data. Demonstrates clustering by A; time point (red = pre-transplant, grey = three months post-transplant and blue = six months post-transplant), B; batch (grey = 1, red = 2, blue = 3, purple = 4) and C; patient (yellow = S3, pink = S7, beige = S8, brown = S9, green = S11, aqua = S12, blue = S13).*

On comparison of the six months post-transplant time point to pre-transplant time point there were fewer differentially expressed genes, with only five significantly downregulated (adjusted p value <0.05, log2 fold change < -1.5), all of which were noted to be downregulated at three months, **Figure 3-15**. This corroborates the finding that T cell numbers have started to recover by six months, although are not yet back to pre-transplant levels.

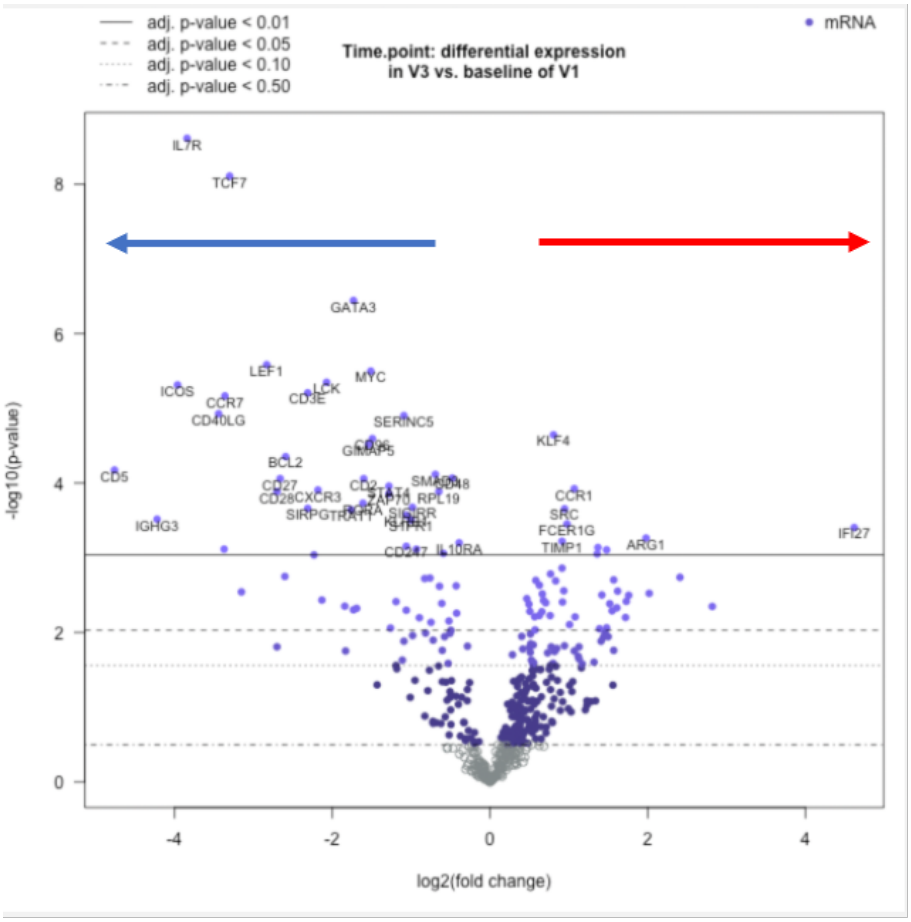

Figure 3-14. Volcano plot of the differentially expressed genes at three months compared to pre-transplantation. *Blue arrow shows genes that are downregulated at three months and red arrow shows those that are upregulated. The solid black line highlights an adjusted p-value <0.01 and the large, dashed line an adjusted p-value <0.05. Genes above these lines are considered significantly differentially expressed.*

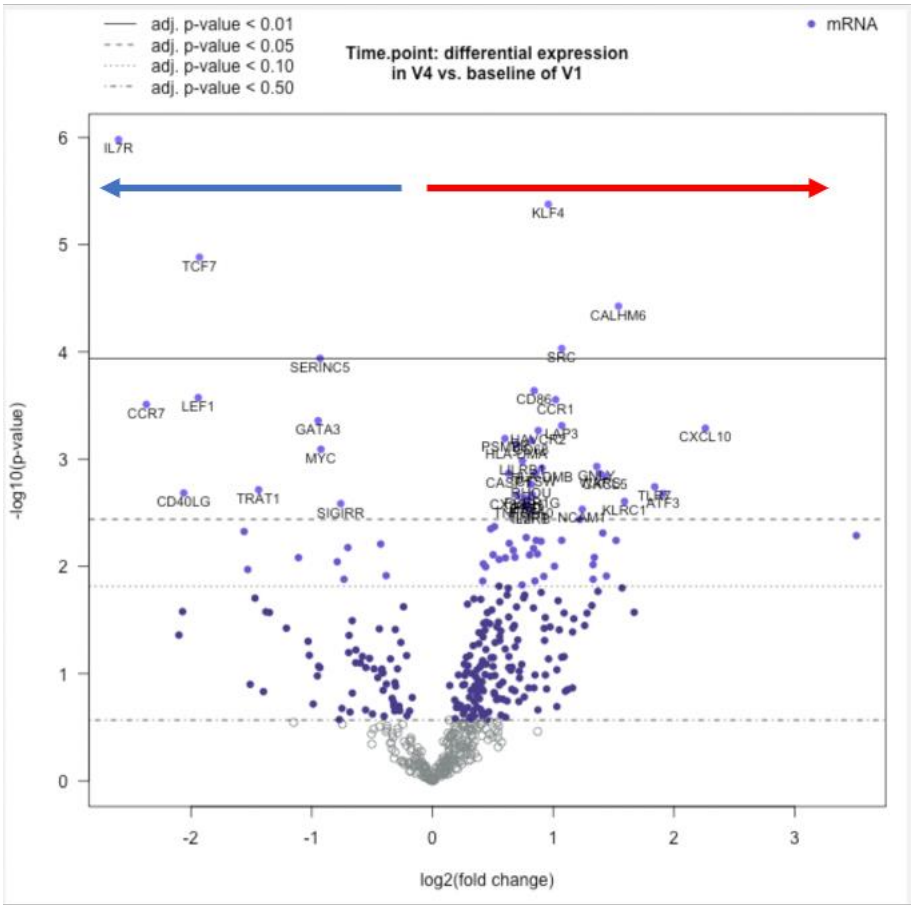

Figure 3-15. Volcano plot of the differentially expressed genes at six months compared to pre-transplantation. *Blue arrow shows genes that are downregulated at six months and red arrow shows those that are upregulated. The solid black line highlights an adjusted p-value <0.01 and the large, dashed line an adjusted p-value <0.05. Genes above these lines are considered significantly differentially expressed.*

To gain a higher-level overview of gene expression at the different time points directed global significance scores were calculated for the 37 pathways annotated in gene expression panel, **Figure 3-16**. These pathways can be broadly divided into tissue damage, immune response, and organ rejection. The scores give a measure of the extent to which a particular pathway's genes are up- or down-regulated, in comparison to a

chosen variable, in this case the pre-transplant time point. Unsurprisingly, the pathways related to T cell receptor signalling, T cell checkpoint signalling, and T cell differentiation were all down regulated at three months post-transplant in comparison to six months post-transplant. Furthermore, there were decreases in B cell receptor signalling, cytokine signalling and the adaptive immune system. These pathways were all showing relative increases in expression by six months post-transplant, in line with the flow cytometry data, which demonstrated evidence of immune cell repopulation from three months.

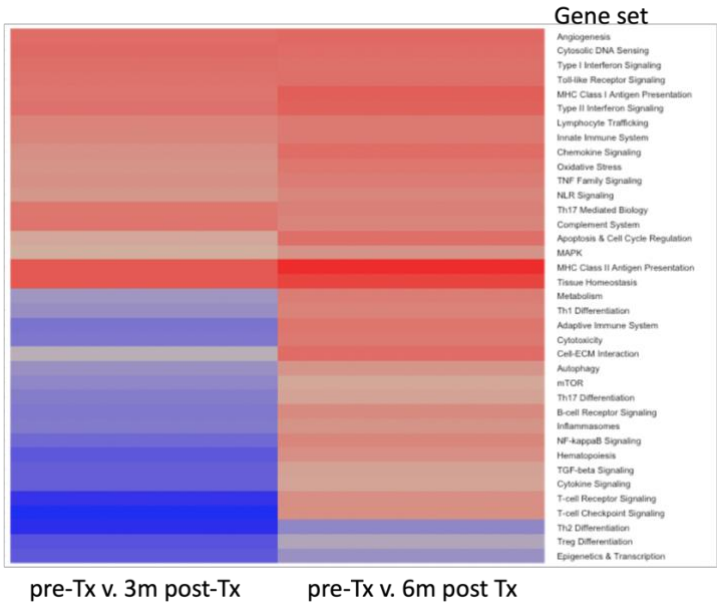

Figure 3-16. Heatmap of directed global significance scores*. The directed global significance score summarises changes in regulation (both up and down) of genes within pre-defined gene sets relative to a chosen variable. In this heatmap the variable is time, pre-transplant (pre-Tx) compared to three months post-transplant (3m post-Tx) and pre-transplant compared to six months post-transplant (6m post-Tx). The prespecified gene sets are on the y axis and the variable comparisons on the x axis. The heatmap of pathway scores combines all the pathways and samples in one visualization,*

by z transformation of scores so they can be displayed on the same scale. Red is upregulated and blue is down regulated. This heatmap shows more downregulation at three months post-transplant than at six months post-transplant, consistent with recovery of immune cell populations.

In summary results from this section support the hypothesis that repopulation of immune cell subsets in patients with a combined sentinel skin flap and SPK transplant, who receive induction immunosuppression with alemtuzumab, is similar to that reported in the literature for patients who have a SPK alone and receive the same immunosuppression.

1.1.1 Phenotype of the immune response at rejection in sentinel skin flap and simultaneous pancreas and kidney transplantations

In the previous section the immune cell repopulation in our cohort of patients who had a sentinel skin flap (SSF), and simultaneous pancreas-kidney transplant (SPK) was characterised. Next, the immune response during rejection will be characterised. Rejection in the SSF was diagnosed by histopathology, using the Banff working classification 2007. There were no episodes of pancreas rejection in the first 12 months. Only two patients in our initial cohort of twenty had an episode of skin flap rejection. The first had one SSF rejection at two months post-transplant, the second had a total of three episodes of SSF rejection, at six months, nine months, and 18 months post-transplantation. See **Table 3-2** for summary of samples analysed in this section.

This small number of samples restricts the conclusions that can be drawn, but it still provides us with some insights. Due to the significant effect that induction immunosuppression has on many of the immune cells, and the fact that all the rejection

episodes took place at two months or later, the rejection samples were compared to protocol samples taken in the same patients at three, six and 12 months.

Immune cell type	Number of rejection samples (patient n=2)	Number of protocol samples (patient n=2)
T cells	3	4
T regs	3	4
B cells	3	4
Monocytes	4	4
NK cells	4	4

Table 3-2. Summary of samples analysed at rejection. *Samples taken from the two patients who had a rejection episode in the first 12 months. Protocol samples are from the 3-month, 6 month and 12-month post-transplant time points.*

T cell populations were examined by flow cytometry, our hypothesis was that there would be an increase in T cell numbers at rejection. There were no significant differences in either $CD4^+$ or $CD8^+$ T cell numbers at the time of rejection, **Figure 3-17**. The ratio of Tregs to T conventional cells ($CD4^+$ and $CD8^+$), the ratio of vδ1: vδ2 γδ T cells, **Figure 3-18**, and finally numbers of total B cells, marginal zone B cells and transitional B cells, were examined, but there were no significant differences at rejection in any of these populations, **Figure 3-19**. Furthermore, there were no significant differences found in numbers of monocytes or NK cells at rejection versus protocol time points **Figure 3-20**.

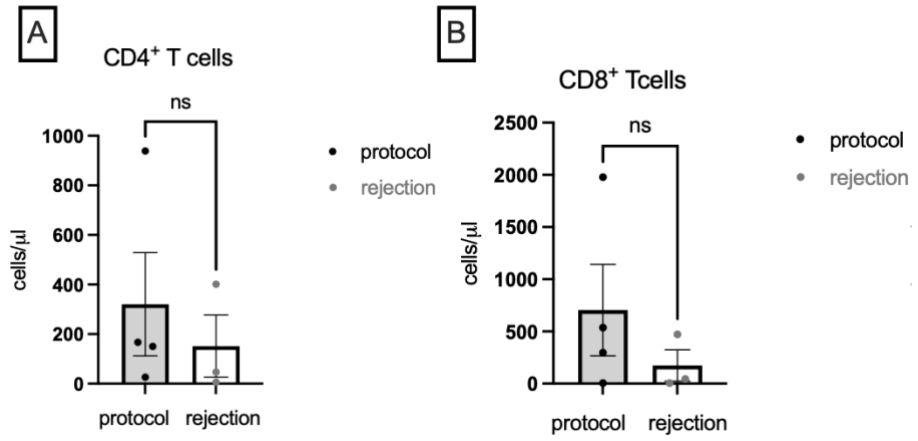

Figure 3-17. CD4+ and CD8+ T cells at rejection versus protocol time points for patients who had a rejection episode. *A. Absolute numbers of CD4+ T cells at protocol and rejection time points (+/- SEM), showing no significant difference. B. Absolute numbers of CD8+ T cells at protocol and rejection time points (+/- SEM), showing no significant differences.*

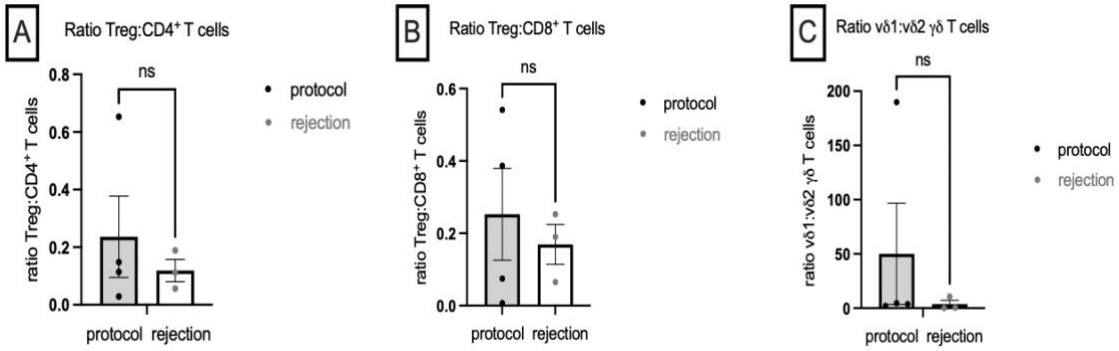

Figure 3-18. Ratios of Treg:Tconv and vδ1:vδ2 γδ T cells at rejection versus protocol time points. *A. Ratio of Treg:CD4+ T cells at protocol and rejection time points (+/- SEM), showing no significant difference. B. Ratio of Treg:CD8+ T cells at protocol and rejection time points (+/- SEM), showing no significant differences. C. Ratio of vδ1:vδ2*

γδ T cells at protocol and rejection time points (+/- SEM), showing no significant difference.

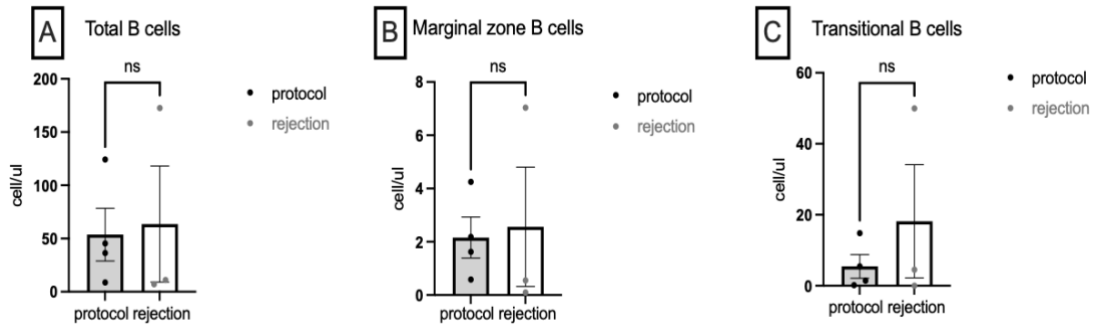

Figure 3-19. Total B cells, marginal zone B cells and transitional B cells at rejection versus protocol time points. *A. Absolute numbers of total B cells ($CD19^+$) at protocol and rejection time points (+/- SEM), showing no significant difference. B. Absolute numbers of marginal zone B cells ($CD19^+IgD^+CD27^+$) at protocol and rejection time points (+/- SEM), showing no significant differences. C. Absolute numbers of transitional B cells ($IgD^+IgM^+CD27^+CD38^{hi}CD24^{hi}$) at protocol and rejection time points (+/- SEM), showing no significant difference.*

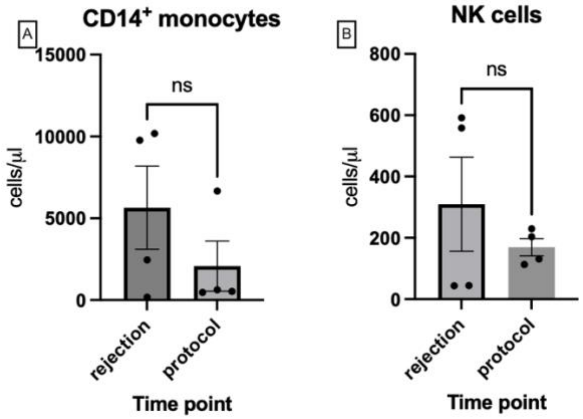

Figure 3-20. Monocytes and NK cells at rejection versus protocol time points. *A. Absolute numbers of monocytes at protocol and rejection time points (+/-SEM),*

showing no significant difference. B. Absolute numbers of NK cells at protocol and rejection time points (+/-SEM), showing no significant difference.

The two patients with rejection demonstrate different baseline T cell numbers, so each were reviewed separately over time, shown in **Figure 3-21**, but this did not identify any consistent patterns between the two.

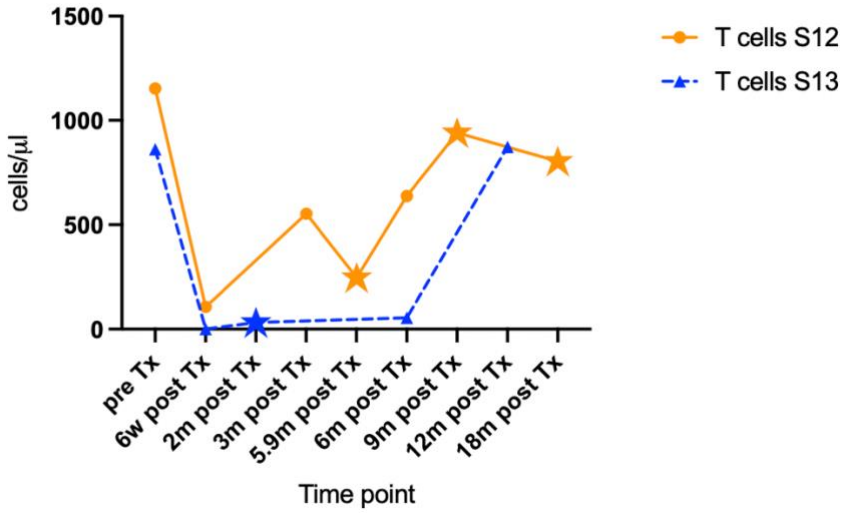

Figure 3-21. T cell repopulation in the two patients with rejection episodes in the first 12 months post-transplantation. *Circle/triangle symbols represent protocol samples, the star symbol represents episodes of rejection. Absolute counts are shown.*

This patient variation was also evident in the gene expression data. Initial PCA analysis shows the samples clustering more by patient than rejection status, **Figure 3-22**.

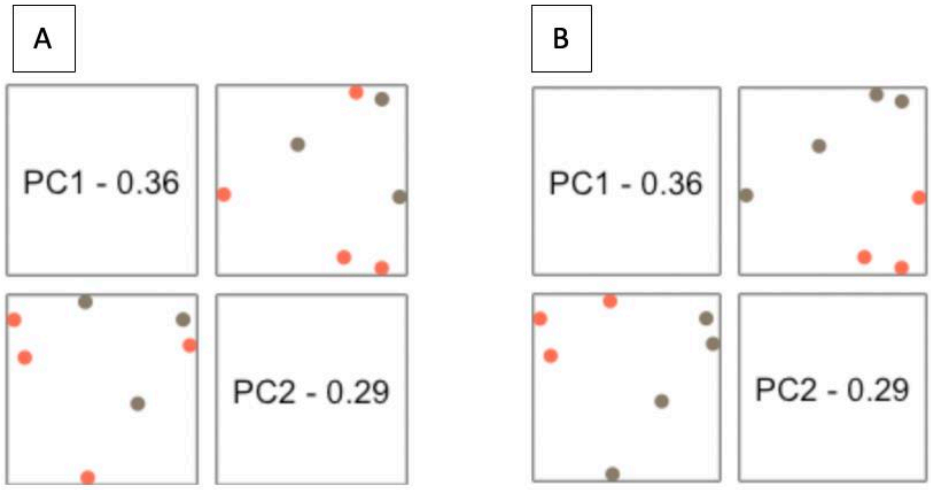

Figure 3-22. Principal component analysis of multiplexed gene expression counts from samples at rejection versus protocol time points. *Analysis of protocol (n=3) and rejection (n=4) samples from the two patients who had a rejection episode in the first 12 months post-transplantation. In A, red = rejection episode and grey = protocol sample. In B, red = patient S12 and grey = patient S13. There is more clustering seen in B, suggesting that variance is predominantly due to patient rather than rejection status.*

Differential gene expression analysis of rejection versus protocol samples was performed, but as may be expected following the PCA and flow cytometry results, did not find any significantly differentially expressed genes, **Figure 3-23**. Finally, pathway analysis was performed, comparing rejection to protocol samples. It was interesting to note that genes associated with Th2 differentiation and Treg pathways were both downregulated at rejection, as shown in **Figure 3-24**.

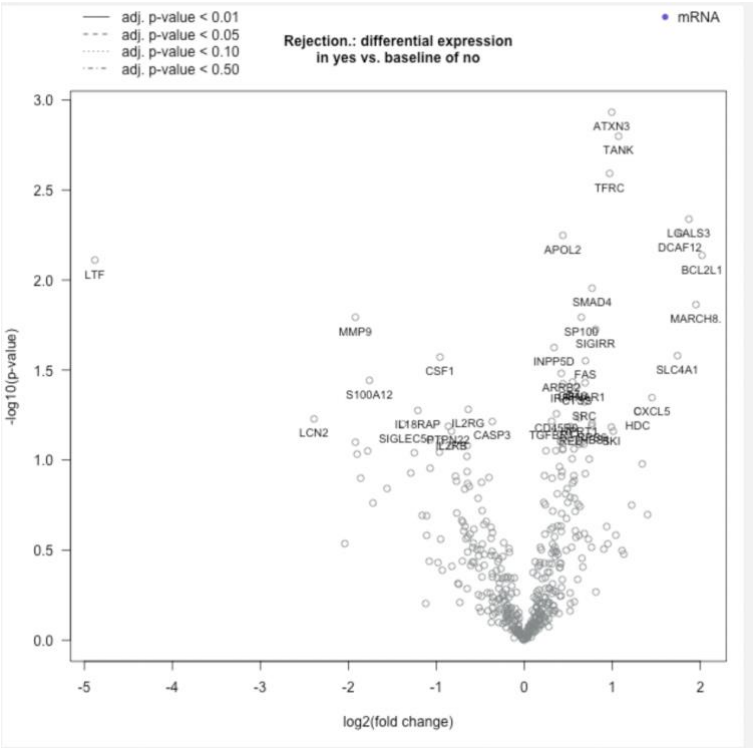

Figure 3-23. Volcano plot of the differentially expressed genes at rejection compared to protocol time points. *None of the genes reached a statistically significant level of difference (defined as an adjusted p value <0.05 and log_2 fold change >-1.5/1.5). This fits with the PCA and flow cytometric data which also did not find any statistically significant differences.*

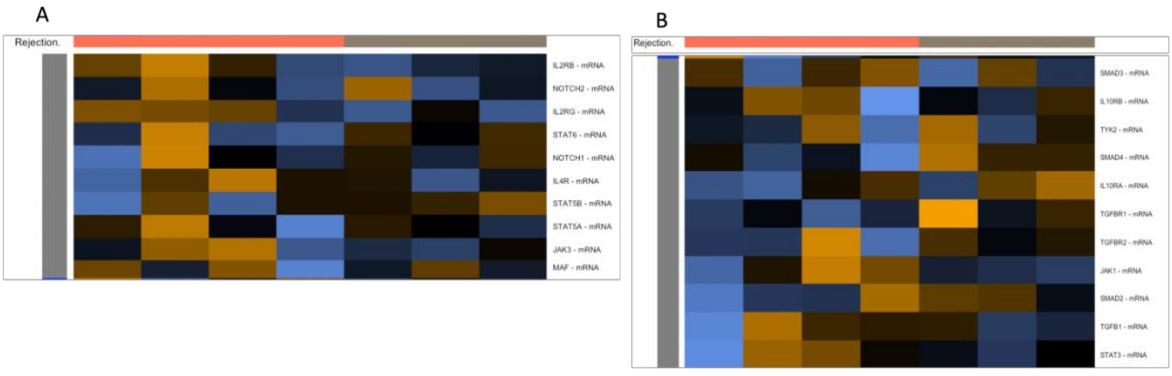

Figure 3-24. Heatmaps of Th2 and Treg differentiation pathways at rejection versus protocol time points. *A. Th2 pathway. B. Treg differentiation pathway. The genes annotated for each pathway are listed on the y axis and individual patients are separate*

columns on the x axis. Orange indicates high scores; blue indicates low scores. Scores are displayed on the same scale via a Z-transformation. The bar at the top indicates how the samples are clustered, red = rejection and grey = protocol time point. These two pathways show evidence of clustering according to rejection status.

Therefore, the results presented in this section do not support the hypothesis that there would be differences found in gene expression at rejection compared to protocol time points. As will be discussed later in this chapter, this is likely due to the sample size available for analysis.

1.1.2 Immune cell repopulation rejectors versus non rejectors

As highlighted at the start of this chapter, there were fewer episodes of rejection than we had anticipated for our cohort of sentinel skin flap (SSF) and pancreas transplant patients. Although the sample size is small, a subset analysis was performed of patients who had a rejection episode (rejectors), compared to those who did not (non rejectors). This analysis only included protocol samples, with the goal to establish if it were possible to differentiate between the two groups, see **Table 3-3** for number of samples in each group.

Time point	**Non- rejectors (n = 18 patients)**	**Rejectors (n = 2 patients)**	**Total**
Pre-Transplant (Tx)	18	2	20
6 weeks post-Tx	15	2	17
3 months post-Tx	14	1	15
6 months post-Tx	14	2	16
12 months post-Tx	10	1	11

Table 3-3. Number of samples in each group at each time point.

PCA analysis of gene expression in rejectors versus non rejectors, showed no evidence of clustering at the pre-transplant time point, but there was more convincing clustering at the three-month time point, as shown in **Figure 3-25**. It was not possible to perform differential gene analysis due to the small number in the rejector group, but it was possible to gain an overview by calculating pathway scores, **Figure 3-26**. At three months post-transplant there was clear evidence of clustering in the rejector group, with upregulation in type I interferon signalling, complement system, lymphocyte trafficking and Th17 mediated biology. However, despite the unsupervised clustering, on close review the two patients who were rejectors were very different to each other as well as being different to those who did not reject. It was interesting to note that several T cell related pathways were down regulated in rejectors compared to non rejectors at this time point.

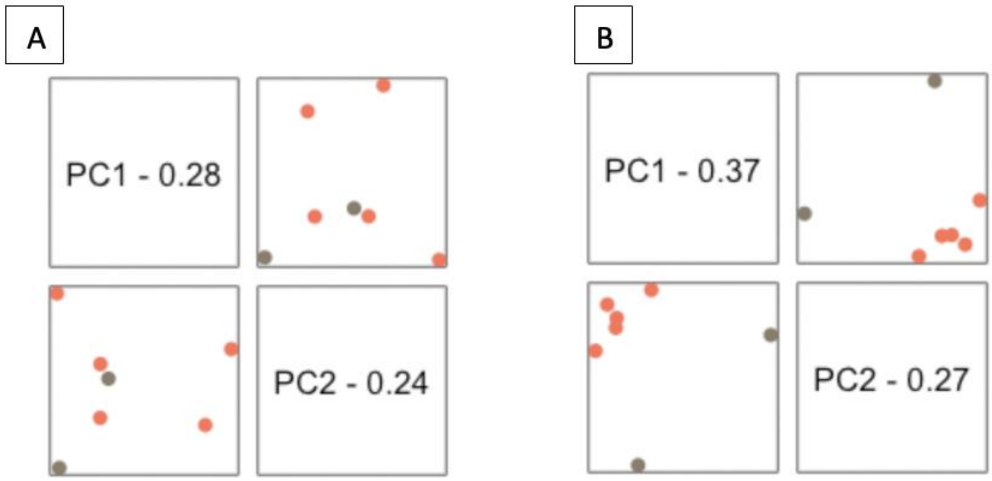

Figure 3-25. Principal component analysis of multiplexed gene expression counts from rejectors versus non rejectors at pre-transplant versus three months post-transplant time points. *Analysis of rejector (n=2) and non rejector (n=5) samples at*

pre-transplant (A) and three months post-transplant (B) time points. Red = non rejector and grey = rejector. There is more clustering seen in B, suggesting that there is more variance between the rejectors and non rejectors at three months post-transplant.

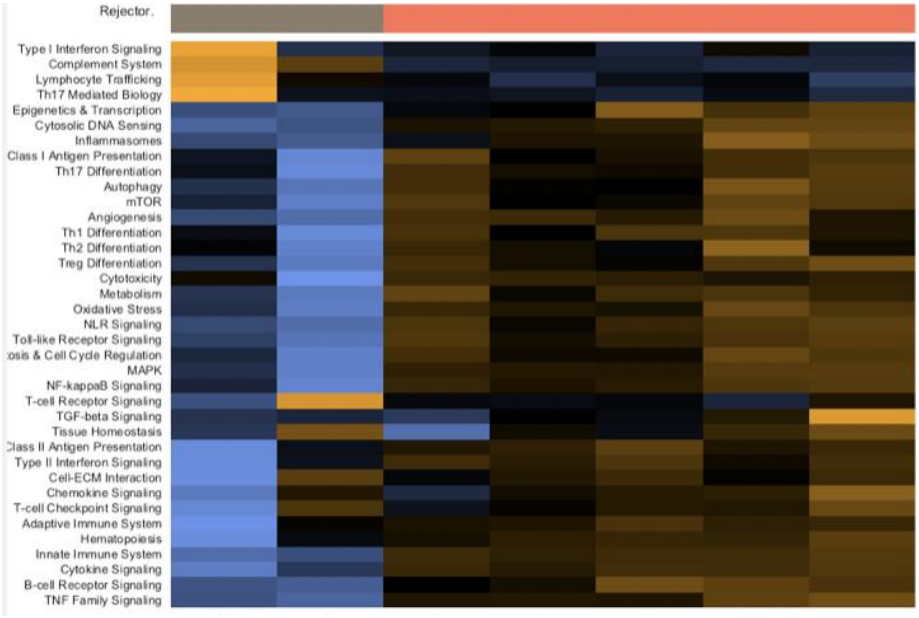

Figure 3-26. Heatmap of all pathways, demonstrating unsupervised clustering of rejectors and non rejectors. *The pathways are listed on the y axis and individual patients are on the x axis (each column represents a patient). Orange indicates high scores; blue indicates low scores. Scores are displayed on the same scale via a Z-transformation. The bar at the top indicates how the samples are clustered, red = non rejectors and grey = rejectors. Rejectors demonstrated upregulation of type 1 interferon signalling, complement system and lymphocyte trafficking. However, it is also clear that the two patients had different gene expression to each other, despite clustering together.*

The flow cytometry basic phenotype panel was examined over time post-transplantation. The number of total B cells was similar in the two groups at all time points. At three- and 12-months post-transplant, there was a trend towards higher numbers of T cells in the rejector group, **Figure 3-27**, however this represented a single

sample in the rejector group and therefore statistical significance could not be established. There was no difference in numbers of NK cells at any of the time points. A significant increase ($p<0.05$) in monocytes was found at the pre-transplant time point in the rejectors group, **Figure 3-28**.

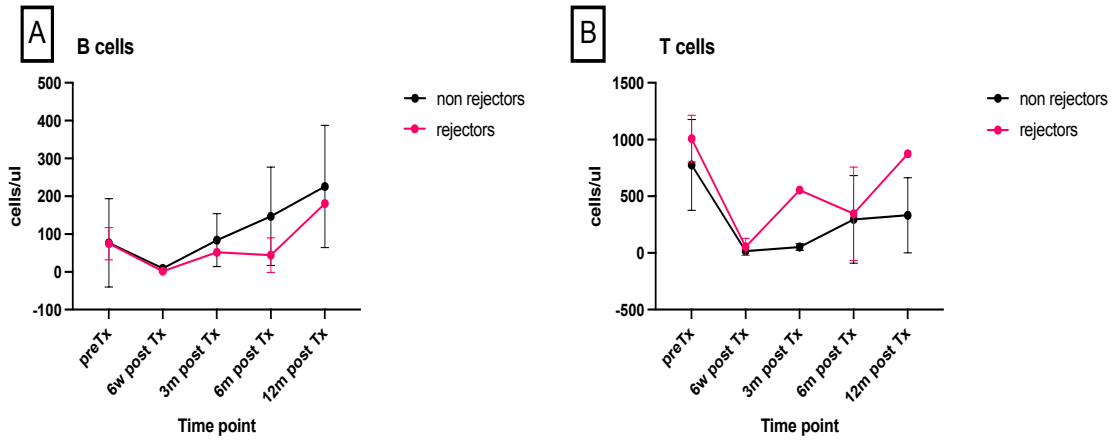

Figure 3-27. Repopulation of B and T cells, rejectors versus non rejectors*. Graph shows absolute numbers +/- SEM at each of the protocol time points post-transplantation. Separated into two groups, black = non rejectors and red = rejectors. There were no significant differences between rejectors and non rejectors at any of the measured time points. It should be noted statistical analysis could only be performed for pre-Tx, 6 weeks and 6 months post-transplant time points as at 3months and 12 months post-transplant there was a single sample in the rejector group.*

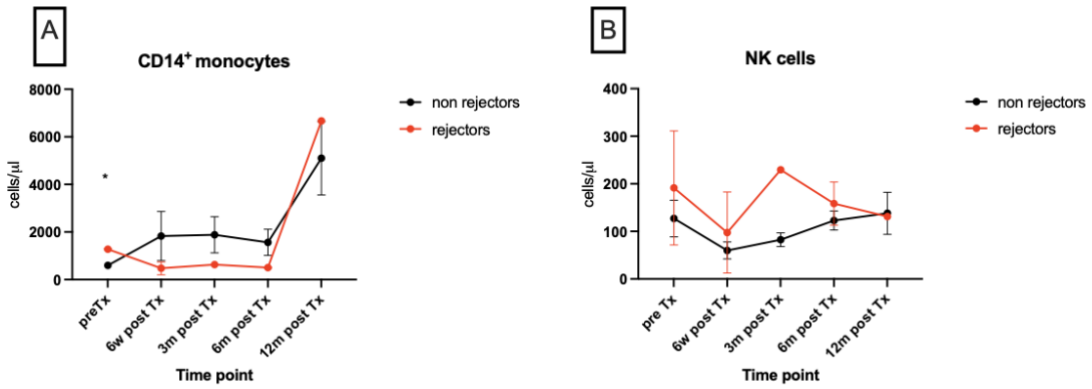

Figure 3-28. Repopulation of monocyte and NK cells, rejectors versus non rejectors*. Graph shows absolute numbers +/- SEM at each of the protocol time points post-transplantation. A shows monocytes, B shows NK cells. Separated into two groups, black = non rejectors and red = rejectors. There was a significant ($p<0.05$) increase in monocytes pre-transplant in patients who went on to have a rejection episode. This was the only statistically significant difference found between rejectors and non rejectors. It should be noted statistical analysis could only be performed for pre-Tx, 6 weeks and 6 months post-transplant time points as at 3 months and 12 months post-transplant there was a single sample in the rejector group.*

Next, the T cell subsets were reviewed, starting with $CD4^+$ T cells. At the pre-transplant time point the rejector group had an increase in the proportion of central memory T cells and a decrease in the proportion of naïve and terminally differentiated memory T cells (TEMRA T cells), in comparison to the non rejectors, **Figure 3-29**. Thereafter there is a predominance of memory cells in both cohorts, reflecting their relative resistance to the induction immunosuppression (absolute numbers shown in **Figure 3-30**).

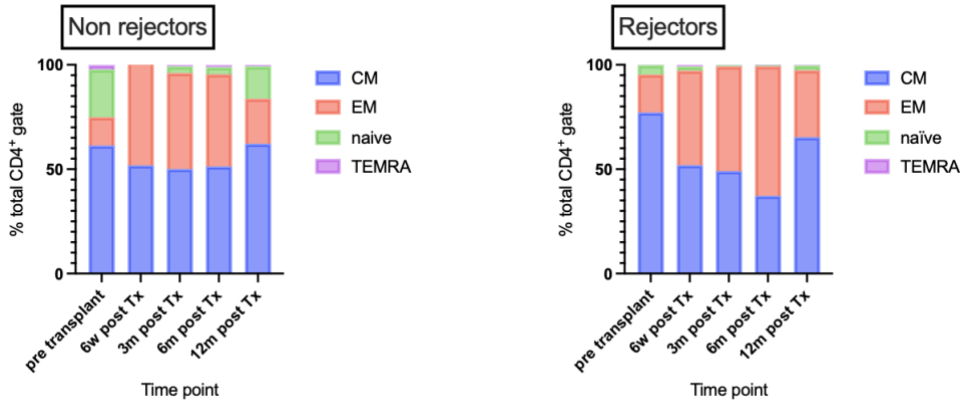

Figure 3-29. Repopulation of CD4$^+$ T cell subsets post-transplantation in non rejectors versus rejectors. *Repopulation is shown as a proportion of the total CD4$^+$ gate. Central memory (CD45RA$^-$CCR7$^+$), effector memory (CD45RA$^-$CCR7$^-$), naïve (CD45RA$^+$CCR7$^+$) and TEMRA (CD45RA$^+$CCR7$^-$) subsets are shown at each of the protocol time points. There is an expansion of central memory CD4$^+$ T cells at the pre-transplant time point in rejectors compared to non rejectors.*

There were also clear patterns in the rejector group CD8$^+$ T cell subset composition, when compared to non rejectors. The non rejectors had an even split between naïve, central and effector memory T cells and TEMRA cells pre-transplantation, shown in **Figure 3-31**. In contrast the rejectors had mostly central and effector memory T cells, evenly split between those two groups. In the rejector group, post-transplant, nearly all the CD8$^+$ T cells were of the effector memory subtype, potentially representing allospecific cells, responsible for rejection. There were significant increases in the absolute number of naïve and TEMRA CD8$^+$ T cells pre transplant in patients who did not have a rejection episode, shown in **Figure 3-32**.

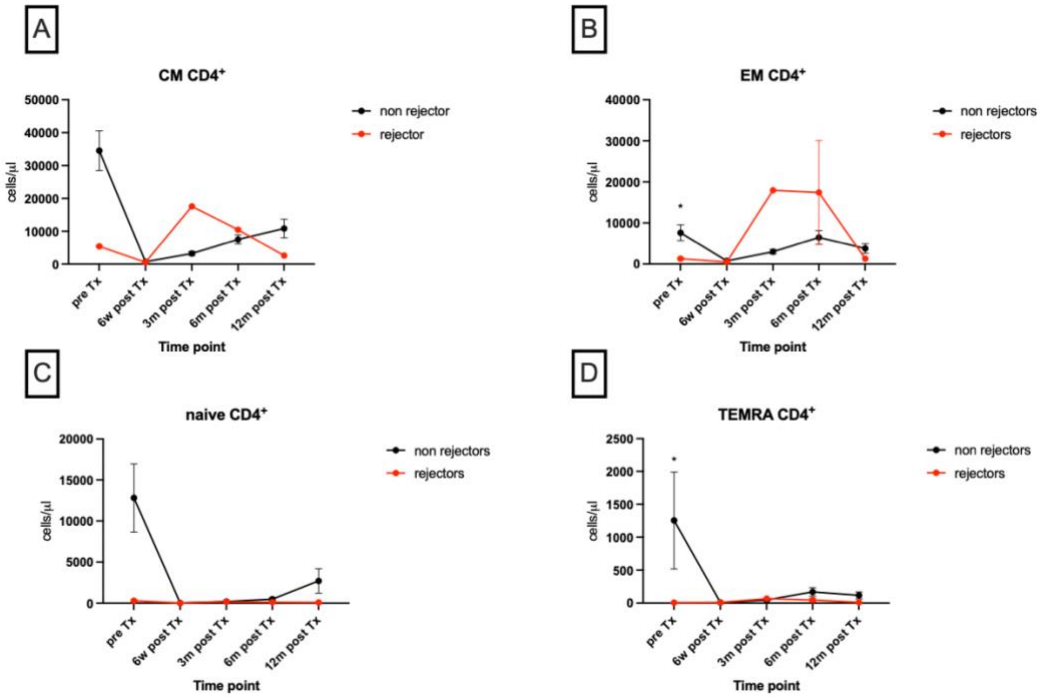

Figure 3-30. Absolute numbers of CD4+ T cell subsets, rejectors versus non rejectors.

Graph shows absolute numbers +/- SEM at each of the protocol time points post-transplantation. A shows central memory, B shows effector memory, C shows naïve and D shows terminally differentiated. Separated into two groups, black = non rejectors and red = rejectors. There was a significant increase in effector memory and terminally differentiated CD4+ T cells in patients who did not reject at the pre-transplant time point. It should be noted statistical analysis could only be performed for pre-Tx, 6 weeks and 6 months post-transplant time points as at 3 months and 12 months post-transplant there was a single sample in the rejector group.

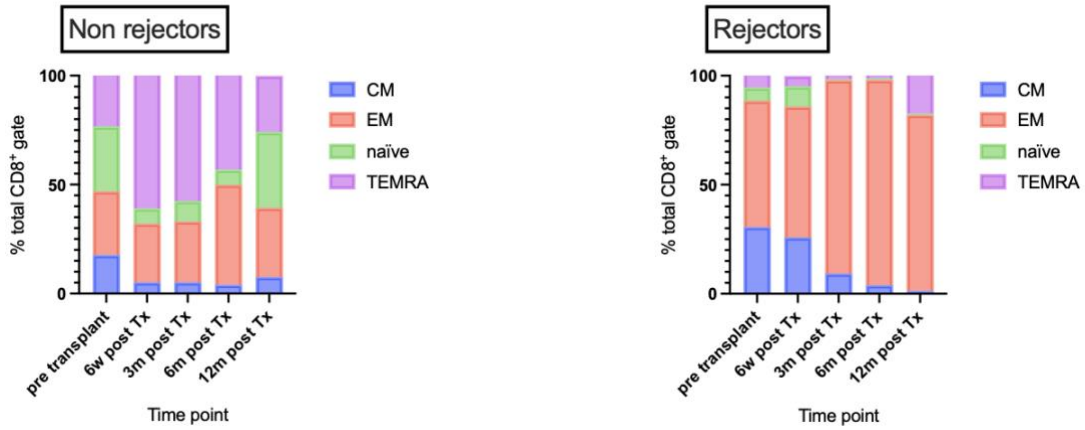

Figure 3-31. Repopulation of CD8$^+$ T cell subsets post-transplantation in non rejectors versus rejectors. *Repopulation is shown as a proportion of the total CD8$^+$ gate. Central memory (CD45RA$^-$CCR7$^+$), effector memory (CD45RA$^-$CCR7$^-$), naïve (CD45RA$^+$CCR7$^+$) and TEMRA (CD45RA$^+$CCR7$^-$) subsets are shown at each of the protocol time points. Post-transplantation the rejector group had an increased proportion of effector memory cells, compared to the non rejectors, who had higher proportions of TEMRA cells.*

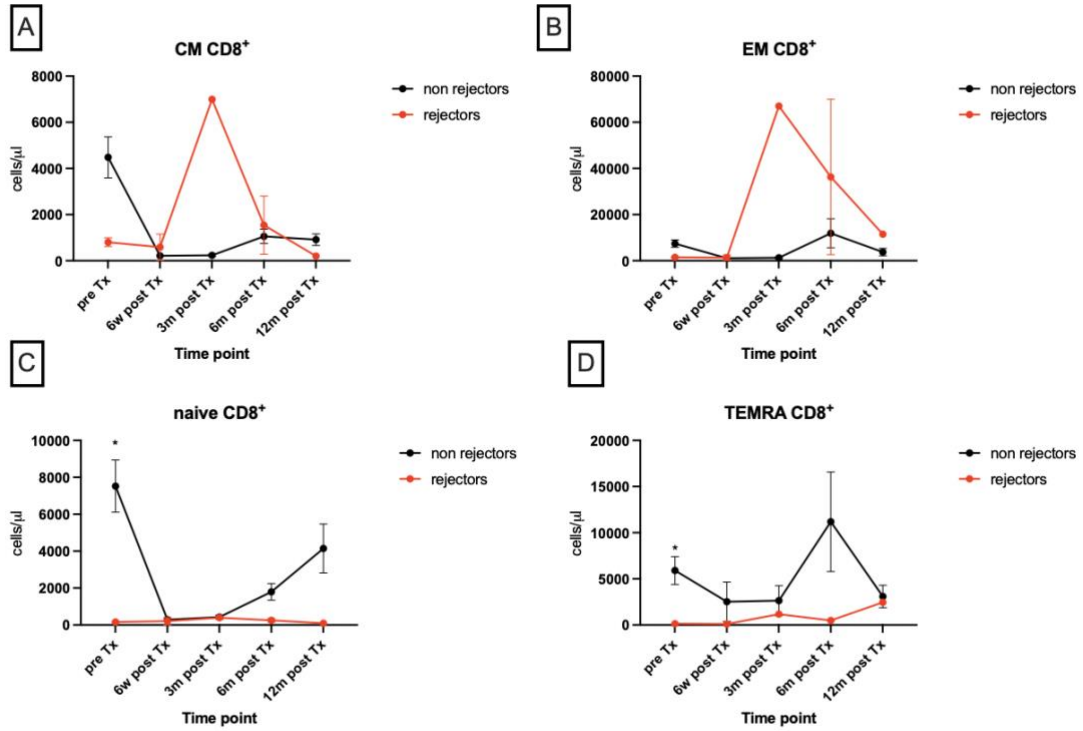

Figure 3-32. Absolute numbers of CD8⁺ T cell subsets, rejectors versus non rejectors. *Graph shows absolute numbers +/- SEM at each of the protocol time points post-transplantation. A shows central memory, B shows effector memory, C shows naïve and D shows terminally differentiated. Separated into two groups, black = non rejectors and red = rejectors. There was a significant increase in naive and terminally differentiated CD8⁺ T cells in patients who did not reject at the pre-transplant time point. It should be noted statistical analysis could only be performed for pre-Tx, 6 weeks and 6 months post-transplant time points as at 3 months and 12 months post-transplant there was a single sample in the rejector group.*

The results presented in this section provide some support for the hypothesis that there are differences in immune cell subsets in those patients who have a rejection episode. Of note significant differences were found in $CD4^+$ and $CD8^+$ memory T cell subsets at

the pre-transplantation time point. However, for many of the other immune cell subsets and time points no significant difference was found.

3.4 Discussion

At present the use of a sentinel skin flap (SSF) or abdominal wall transplant for immune monitoring is a novel technique, with Oxford being the only unit in the UK to undertake these procedures. This chapter reports on the first in depth immunophenotyping of these patients. Firstly, the repopulation of immune cells was documented. Induction immunotherapies are designed to reduce the risk of early acute rejection, mediated by T cells. In this study the effect of induction immunosuppression with alemtuzumab was most evident at six weeks post-transplantation, with a significant decrease in both T and B cells noted. This has been widely reported in the literature, for patients undergoing a similar treatment regimen[144,145,147,148]. Alemtuzumab is an anti-CD52 antibody. CD52 is expressed on most mature leukocytes, therefore it is unsurprising that induction immunosuppression with alemtuzumab causes depletion of these cells, and indeed seems to be the main driver of immune cell depletion in the early post-transplant period.

The effect of immunosuppression on immune cell repopulation in vascularised composite allotransplantation (VCA) has not been explored in as much detail as for solid organ transplants. In part this is due to the smaller number of patients who have had a VCA. Furthermore, immune monitoring in these patients typically focuses on skin samples from the allograft as these are easily available with reduced morbidity in comparison to solid organ transplants. Borges et al have reported on a cohort of six face transplant patients, who had significant depletion of $CD4^+$ and $CD8^+$ T cells in the

blood in the first 24 hours post-transplant, with signs of recovery by three months[156]. Like the findings of this study, albeit the first time point post transplantation was at 6 weeks and recovery starting to be evident at six months. It should be noted that these patients received different immunosuppression to the patients in this study (induction with rabbit antithymocyte globulin and maintenance with mycophenolate mofetil and methylprednisolone), which may explain the differences found and mean it is hard to make direct comparisons.

In this study, B cell numbers recovered more quickly post-transplantation, attaining pre-transplant levels by six months post-transplant, in comparison to T cell numbers which had not fully recovered by 12 months. This was also noted by Heidt et al in their study of immune cell repopulation following kidney transplantation[143]. Their patients received the same induction immunosuppression as in this study (alemtuzumab) and were maintained with a combination of tacrolimus and prednisolone. Heidt et al also noted an expansion of naïve B cells compared to memory B cells at three months[143], as has been found in this cohort of sentinel skin flap and SPK transplants. Of interest the transitional B cell subset was also found both by Heidt et al, and in this study, to have recovered by three months to higher levels than pre transplantation. Transitional B cells are of particular interest as they may represent a source of regulatory B cells[157]. The combination of expanded naïve and transitional B cells was also noted by Newell et al[155] in patients who had achieved operational tolerance in kidney transplantation. This may be due to the depletion of T cells, which would normally lead to activation of B cells.

More recently it has been recognised that while current induction immunosuppression works well against naïve populations, it seems memory cells are more resistant, or perhaps are disproportionately produced because of homeostatic proliferation[158]. This is problematic for transplant patients if they include T cells which recognise the transplant. Therefore, memory subsets in both the $CD4^+$ and $CD8^+$ T cell compartments were explored. In $CD4^+$ T cells, there was an increased proportion of the effector memory subtypes, post-transplantation. Bearing in mind this is the population that circulates in blood and can travel to peripheral organs, this could be a population contributing to organ rejection. $CD8^+$ T cells had decreased proportions of central memory cells, but an increase in naïve and TEMRA (terminally differentiated) subsets. Similar findings have been reported in other cohorts with kidney transplantation and face or hand transplant alone[145,148,150,156].

Initially the proportion of Tregs (defined as $CD4^+$ $CD25^+$ $FOXP3^+$) increased in comparison to both $CD4^+$ and $CD8^+$ T cells post-transplant, with this proportion decreasing from around six months post-transplant. This likely reflects the unequal effect of induction immunosuppression on the conventional T cells. This finding has also been reported by several teams in the literature[144,148,159]. It has been suggested that this altered ratio is another way that induction immunosuppression protects the allograft from rejection[159]. However, it is worth noting that the converse has been reported by Macedo et al[160]. They used a different definition of T regulatory cell, including low expression of CD127 in addition to $CD25^+$ and $FOXP3^+$, making the valid observation that effector T cells may also express CD25 and FOXP3 when activated.

γδ T cells are known to act both in innate and adaptive immune pathways and may be activated without classic activation from MHC[161]. Increased numbers of vδ2 γδ T cells have been associated with poorer outcomes in solid organ transplantation[154]. In this study it was found that the vδ1 proportion increased over time post transplantation, perhaps interesting to note considering the reduced number of rejection episodes seen in these patients. It is not clear exactly how γδ T cells may be acting in this setting, but it has been speculated that these may have a regulatory role[154]. This is the first report of γδ T cell repopulation post alemtuzumab induction therapy in solid organ transplantation.

There are few studies which have looked at gene expression over time post-transplant, with most focussing on rejection episodes[162,163]. This study has shown that at three months post-transplant there are a significant number of downregulated genes, the majority of which are associated with T cell pathways. These pathways show evidence of recovery by six months post-transplantation. This is consistent with results from Dorr et al[163], who performed RNAseq of PBMC from 32 patients with kidney transplants with thymoglobulin induction. Five of their top ten downregulated genes at the three-month time point were the same as in this cohort (*IL7R, LEF1, CD3E, TCF7* and *CD3D*)[163]. IL7R is expressed on naïve T cells and activation via IL7 is necessary for T cell survival[164]. CD3E and CD3D are found on T cell surface membrane in association with the TCR, where they signal activation on activation[165]. LEF1 and TCF7 are transcription factors and have been shown to play a key role in the maintenance of $CD8^+$ T cells[166]. These are all associated with T cells, which were also the most downregulated in the flow cytometry data. Furthermore, Dorr et al also noted a decrease in the number of differentially expressed genes over time, attributed to lymphocyte

recovery post induction immunosuppression. These findings are supported by those reported by Zhang et al in a cohort of 32 kidney transplant patients[162]. They noted a decrease in the number of differentially expressed genes over time, which they attributed to recovery of immune cells post immunotherapy. They reported that T cell related pathways were significantly impacted. It was less clear which immunosuppression was used, a key factor when trying to compare results.

This study includes 20 patients, with samples taken at five different time points, across the spectrum from pre-transplantation up to 12 months post-transplantation. This compares favourably with the literature for studies where alemtuzumab has been used for induction, sample sizes in the studies referenced here range from 10-29 patients[144,145,147,148]. Whilst there are other larger studies, these cannot be directly compared as they have either different maintenance immunosuppression or are not from patients undergoing solid organ transplant, both factors which may affect the immune cell repopulation.

At the beginning of this chapter, the observation was made that there have been fewer episodes of rejection in the cohort of sentinel skin flap and SPK transplant patients. Whilst this is a positive finding for these patients, it has made analysis of this group harder as there are fewer samples, and therefore less power to the calculations. It also became clear that the two patients who experienced at least one episode of acute rejection had very different immune cell populations to each other. This was particularly noticeable in the gene expression data, where PCA analysis found the samples clustered

more by patient than rejection. As a result, there were not any statistically significant differences between rejection and protocol samples in this cohort.

Finally, a subgroup analysis was performed, based on whether patients had an episode of rejection in the first 12 months. It should be highlighted that only two of the twenty patients had an episode of rejection in this time, therefore the rejector group was small. There were noticeable differences in $CD4^+$ and $CD8^+$ T cell subsets when they were divided into rejector and non rejector groups. There was a higher proportion of effector memory $CD4^+$ T cells, at the pre-transplant time point, persisting for the first 12 months, in patients who went on to reject. It is known that effector memory T cells are more resistant to induction immunosuppression and that $CD4^+$ T effector memory cells can activate cytotoxic $CD8^+$ T cells[167]. Furthermore, the non rejector group were found to have an increased proportion of TEMRA $CD8^+$ T cells. This fits well with data from Betjes et al who found an increase in TEMRA $CD8^+$ T cells was associated with fewer episodes of acute rejection[168]. It is thought that these TEMRA $CD8^+$ T cells are less alloresponsive as they have lost expression of CD28, an important co-stimulatory molecule for T cell activation. These results must be viewed with caution as the numbers involved are very low, but it would be interesting to explore this further.

A significant limitation to this study is the small number of patients, and even fewer who had an acute rejection episode. This has restricted the analyses that have been performed. As will be discussed later in this thesis, a further clinical trial of SSF for immune monitoring in lung transplantation has both funding and ethical approval (REC 20/WM/0026, see appendix 4). Blood samples will be taken from patients at the same

time points pre- and post-transplantation as in this study. These samples will undergo analysis using the same immunological assays, allowing comparison with this pilot data.

Furthermore, a second study to gather a control group of blood samples from patients who have a pancreas transplant alone has also been granted ethical approval (REC 21/EE/0213, see appendix 4). These samples will once again be taken at the same time points and undergo the same immunological assays. The results from this proposed study will be used to gain an insight into how the addition of a sentinel skin flap may be contributing to the altered clinical outcomes.

In summary the results presented in this chapter support the hypothesis that in patients who have a SSF and pancreas transplant, with alemtuzumab induction immunosuppression, have similar immune cell repopulation to that reported in the literature for kidney transplantation. There were no significant differences in either gene expression or immune cells noted at rejection, however this is likely due to the small number of rejection samples available for analysis. However, there were significant differences in pre-transplantation numbers of effector memory $CD4^+$ T cells and TEMRA $CD8^+$ T cells in those who went on to reject versus those who did not.

This is the first longitudinal immunomonitoring study in a sentinel skin flap and solid organ transplantation and one of the few studies looking at the dynamics of immune changes after alemtuzumab induction therapy. In the next chapter the local alloresponse

to small bowel samples from patients with a combined skin and small bowel transplant will be explored.

4 Chapter 4. Immune response in the small bowel transplant to a combined skin and small bowel transplant

4.1 Introduction

The previous chapter focused on the peripheral systemic alloresponse to a combined skin and solid organ transplant, by analysing blood samples obtained from patients who had a sentinel skin flap and simultaneous pancreas-kidney transplant (SPK). As discussed in Chapter 1, it is not routine practice to protocol biopsy pancreas or kidney transplants in Oxford. Therefore, to explore the local alloresponse in the solid organ itself, archived samples from patients who had received a combined skin (either abdominal wall or sentinel skin flap) and small bowel transplant were obtained, as it is standard practice to regularly biopsy the small bowel transplant to monitor rejection.

The small bowel is an immunologically complex organ. It contains many leukocytes and is continuously exposed to foreign antigens, whether from food, the microbiome, or pathogens[169]. Tertiary lymphoid structures, also known as gut-associated lymphoid tissues (GALT) are scattered throughout the small bowel. These contain many B cells and are key sites for T cell priming and IgA production[169] . Whilst this immune cell network is vital for monitoring and mediating these interactions with the outside world, these donor cells may become problematic after transplantation. Like other barrier organs, such as the skin and lungs, small bowel transplants have higher rates of acute rejection and decreased 5-year graft survival compared to other solid organs[36].

The gold standard for diagnosing acute rejection in small bowel transplants is histopathology. A consensus criterion for diagnosis was published following the VIIIth International Small Bowel Transplant Symposium[35]. As well as detailing standard practices for biopsy sampling and processing, it also described a scoring system for acute rejection. There was a recognition that acute rejection was associated with a predominantly mononuclear inflammatory cell population and apoptosis, the degrees of which varied depending on the grade of rejection. This damage was centred on the crypts. At the most severe acute rejection a diffuse infiltrate composed of activated lymphocytes, eosinophils and neutrophils is found[35]. This standard was based on a study from Lee et al who used histological methods to examine over 3000 biopsies from 62 human intestinal transplant patients[170]. Included in this sample were 318 samples taken at the time of acute rejection episodes (diagnosis based on clinical and histological findings). They noted a predominantly mononuclear population of infiltrating cells, along with crypt damage and apoptosis. The ileum was most often affected, although in most cases findings were similar throughout the small bowel.

Hayashi et al used a rat model of small bowel transplantation to examine the histological and cytokine gene expression in acute rejection[171]. They found similar histological findings (crypt apoptosis, lymphocyte infiltration) to those described by Lee et al[170]. At day 2-3 post-transplantation they found that expression of IFN-γ mRNA was significantly increased in allograft versus isografts. This finding was blocked by the administration of tacrolimus. Toogood et al also used a rat model to explore differences in cytokine expression between small bowel and heart transplants[172]. They used RT-PCR to analyse tissue samples and found that while heart transplants had elevation of

IL2, *IL6*, *IL10* and *IFN-γ* at time of rejection, the small bowel transplants only had a significant increase in *IFN-γ.* This elevation was notable before clinical or histological changes of rejection were seen, suggesting a potential role for *IFN-γ* as a biomarker for rejection.

Newell et al found that acute rejection of small bowel allografts relied on the presence of αβ T cells, but not γδ T cells, by using transgenic mice with a TCR β chain knockout or TCR δ chain knockout[173]. With the use of monoclonal antibodies to $CD4^+$ and $CD8^+$ T cells they found that both $CD4^+$ and $CD8^+$ T cells were needed for acute rejection of small bowel transplants. Zhang et al used a transgenic mouse model of small bowel transplant (where the donor $CD4^+$ T cells express a TCR specific for chicken OVA) to demonstrate that activation of donor $CD4^+$ T cells by foreign antigen (chicken OVA) caused an increase in recipient T cell activation and an increased number of recipients $CD8^+$ T cells in mesenteric lymph nodes (the draining lymph nodes of the small bowel)[174]. This was associated with an increase in *IFN-γ, CXCL9* and *CXCL10* mRNA, along with histological signs of acute rejection. CXCL9 and 10 are induced by IFN-γ and are involved in T cell migration via CXCR3, suggesting they may contribute to recipient T cell migration into the allograft. Furthermore, administering a monoclonal antibody to block CXCL10 increased the survival of small bowel transplants, which were found to have decreased numbers of host $CD4^+$ T cells, $CD8^+$ T cells and NK cells in the lamina propria, the initial site of acute rejection.

Increased levels of IFN-γ and CXCL9/10 have also been found in human intestinal transplants at rejection[175–177]. Zambernardi et al examined samples from a cohort of 15

patients, finding raised levels of *IFN-γ, CXCL9* and *CXCL10* mRNA at rejection, levels which decreased when a third immunosuppressive agent was added to their treatment. This is consistent with results from an earlier single patient study, which found an upregulation of genes related to IFN regulation, cytotoxic T cells, chemotaxis (including CXCL10 and 11) and cell cycle activation at acute rejection[176]. Furthermore, they matched the signature found at acute rejection with that from activated dendritic cells, which are known to produce IFNα, suggesting a role for DC activation of T cells in rejection. Using a larger PCR-array, Asaoka et al found several differentially expressed genes at acute rejection in human small bowel samples[177]. These included genes related to T cells, chemotaxis of macrophages (*CCL2, CCL3*), Th1 expression (*Tbet, GZMB, IFN-γ*) and immunoregulatory genes (*IL1-R2, CTLA4* and *IL10*).

To date, only 46 abdominal wall and small bowel transplants have been reported in the literature[52]. Most publications have focused on the clinical outcomes[52,56,133,178], with only one reporting on immunological outcomes (the incidence of de novo donor specific antibody formation)[179]. In this chapter a combination of targeted gene expression analysis and spatial protein analysis are used to explore the immune response post-transplantation in small bowel biopsies from both combined skin and small bowel transplants and small bowel transplants alone.

4.2 Chapter 4 aims and hypotheses

The aim of this chapter is to use a combination of gene expression analysis and spatial proteomic methods to:

- characterise the local alloresponse in acute rejection in small bowel transplant samples, from patients who had received a combined skin and small bowel transplant.
- compare the results of the gene expression analysis to samples from patients who had a small bowel transplant alone, with the goal of identifying if the addition of skin leads to any changes in gene expression.

First, we hypothesise that there will be differences in gene expression in the small bowel samples taken at rejection compared to protocol time points, with increases in IFNγ related genes, including CXCL9 and 10 at rejection. Next, we compare samples from small bowel transplants both with, and without a skin transplant. We hypothesise that there will be differences in gene expression between these two groups with an increase in regulatory genes such as CTLA4 and IL10, along with decreases in Th1-related genes in the combined small bowel and skin group, reflecting the decreased rate of rejection found clinically. Finally, we hypothesise that the gene expression results will be supported by spatially resolved protein analysis of small bowel samples, with increases in markers of T cell activation and expression of CXCL9 seen in crypt regions of interest at rejection.

4.3 Results

Gene expression analysis has the potential to highlight molecular pathways responsible for rejection early in the rejection process. It is particularly interesting to take samples from the site of rejection and small bowel transplants are often biopsied in the first few months post-transplant as part of routine clinical monitoring. The nCounter Banff

Human Organ Transplant (HOT) gene panel was used (see appendix 2 for full details), as in Chapter 3 for the analysis of blood samples. These results are based on 22 samples from 13 patients (16 samples from seven patients with combined transplants and six samples from five patients with a small bowel transplant alone). These patients were not part of a clinical trial; therefore, samples were taken as per clinical guidelines, with regular protocol samples in the first weeks and rejection samples taken based on clinical suspicion. Number of samples and the time points they were taken are shown in the table below.

Time sample taken.	**Small bowel and skin transplant**	**Small bowel alone transplant**	**Total number of samples**
early protocol (<150 days)	6	3	9
mid protocol (150-356 days)	4	2	6
late protocol >356 days	2	1	3
early rejection (<150 days)	3	0	3
mid rejection (150 - 356 days)	1	0	1
Total number of samples	16	6	22

Table 4-1. Time points of samples taken from small bowel transplant patients.

4.3.1 No significant differences in gene expression were found at rejection in small bowel samples from patients with a combined skin and small bowel transplant.

Principal component analysis (PCA) was used to explore samples from patients with a combined small bowel and skin transplant, to see if samples clustered by rejection status.

Interestingly, the one rejection sample which appears as an outlier (see **Figure 4-1**, B) was the only sample to be reported as severe acute rejection. The other samples in this experiment were reported as early acute rejection. Clustering does not appear to be solely due to patient (**Figure 4-1**, A), rejection (**Figure 4-1**, B) or time point (**Figure 4-1**, C). Two samples from patient 3 are noted to be outliers on the PCA, these were samples taken at later times post-transplantation. Results from analysis in blood samples in Chapter 3 have demonstrated the effect that time point post-transplantation may have on gene expression and this may be contributing to this finding. As expected from review of the PCA plots, when comparing rejection to protocol samples there were no significantly differentially expressed genes, **Figure 4-2**.

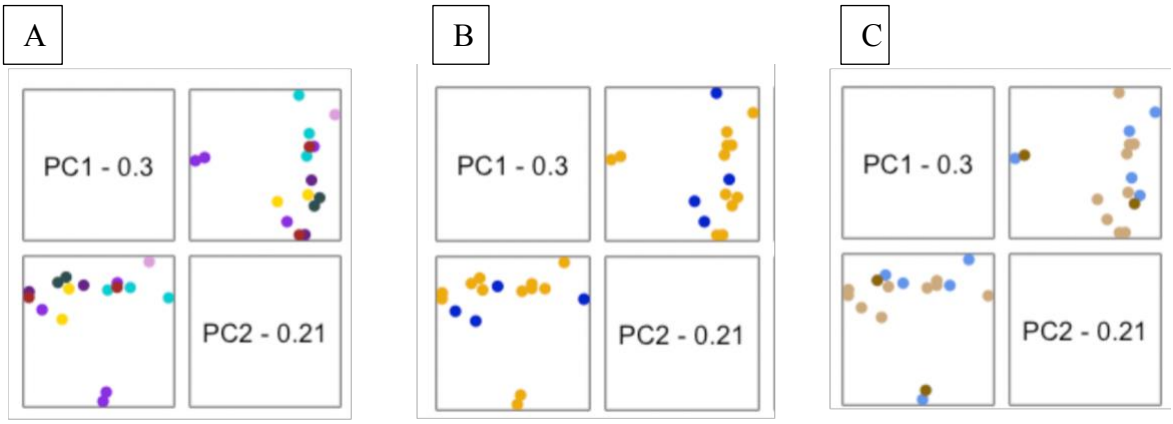

Figure 4-1. Principal component analysis of multiplex gene expression counts from small bowel transplant samples. *These charts show the first two components, PC1 captures the most variation and PC2 the second most variation in the data. A = coloured by patient (yellow patient 1, red patient 2, light purple patient 3, dark purple patient 4, pink patient 5, green patient 6, aqua patient 7), B = coloured by rejection (blue yes, yellow no) and C = coloured by time post-transplantation (beige <150 days, blue 150-365 days, brown > 365 days). Variation in PC1 and PC2 does not appear to*

be based solely on patient, rejection status or time post-transplant. Based on 16 samples, 12 at protocol and 4 at rejection time points.

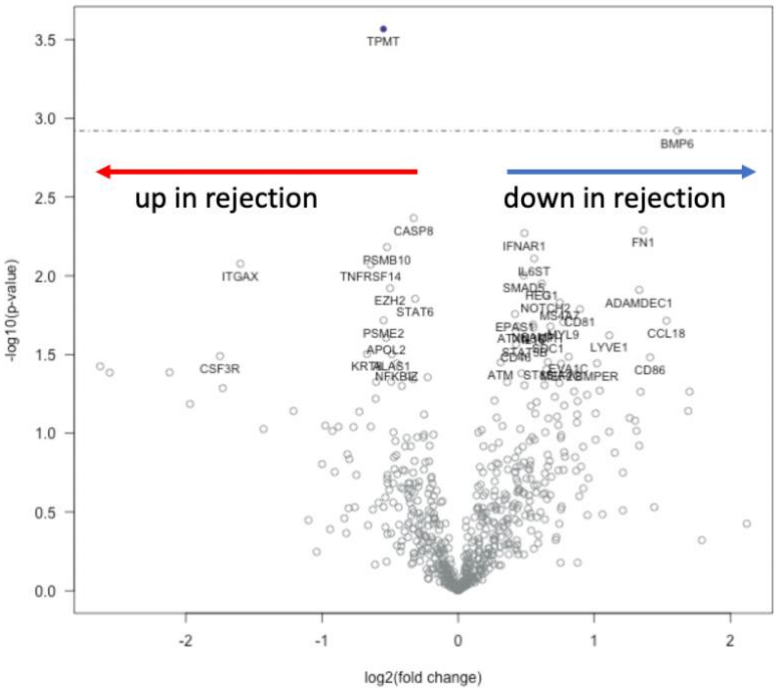

Figure 4-2. Volcano plot of differential gene expression in small bowel transplant biopsies taken at rejection and protocol time points. *None of the differentially expressed genes reached a statistically significant level (defined as an adjusted p value < 0.05 and fold change >-1.5/1.5). The dot/dashed line represents an adjusted p value of < 0.5. Based on 16 samples from 7 patients. 12 samples at protocol and 4 samples at rejection time points.*

The results in this section do not support the hypothesis that there will be differences in gene expression at rejection in the small bowel samples, however, as will be discussed later this is likely due to the small number of samples in this study.

4.3.2 There were no significant differences in gene expression in small bowel biopsies from combined skin and small bowel transplants compared to small bowel transplants alone.

Next, gene expression in small bowel transplants samples from combined skin and small bowel transplants (SBS) was compared to samples from small bowel transplants alone (SBA). As described in Chapter 2 rates of rejection were lower than expected in the SBS group so the two groups were compared to look for differences. Once again, principal component analysis (PCA) was used to explore the data for factors contributing to clustering. Patient (**Figure 4-3**, C), batch (relating to when samples were processed (**Figure 4-3**, D)), time point (**Figure 4-3**, B) and tissue type (**Figure 4-3**, A) were all explored, but none of these showed clear evidence of clustering. There were no significantly differentially expressed genes on comparison between the SBS and SBA groups, **Figure 4-4**.

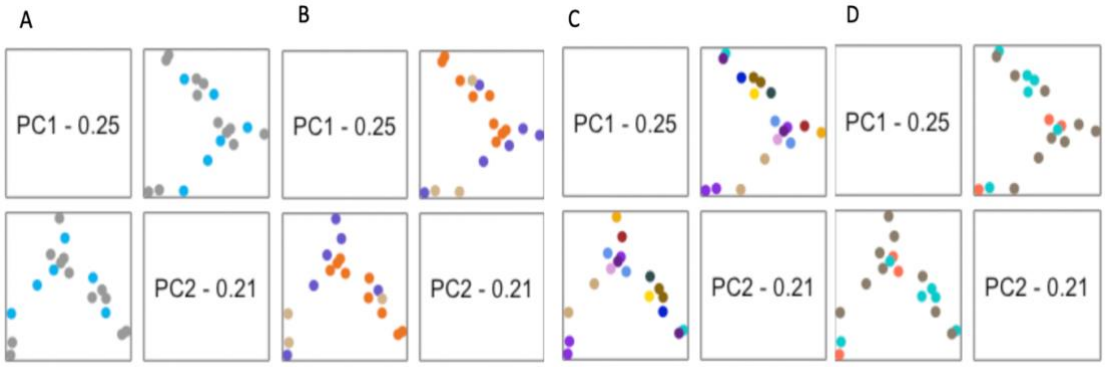

Figure 4-3. Principal component analysis of multiplex gene expression counts from small bowel transplant samples from combined small bowel and skin (SBS) and small bowel transplant alone (SBA). *These PCAs show the first two components, PC1 captures the most variation and PC2 the second most variation in the data. A = coloured by tissue type (grey SBS, blue SBA), B = coloured by time post-transplantation*

(orange < 150 days, purple 150-365 days, beige > 365 days), C = coloured by patient, D = coloured by batch (red 1, grey 2, blue 3). None of the PCA plots shows evidence of strong clustering related to the factors above. Based on 22 samples from 12 patients (samples: SBS n=12, SBA n=6, patients: SBS n=7, SBA n=5).

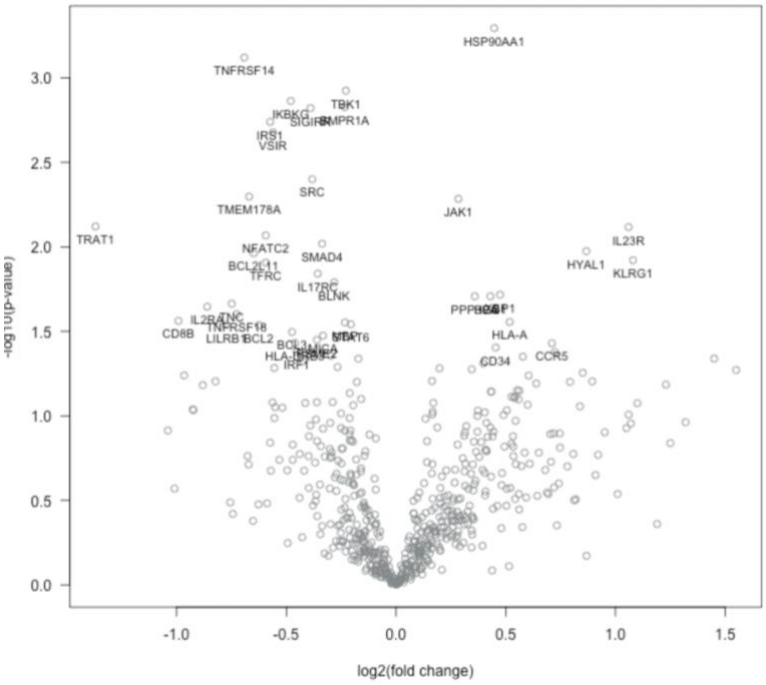

Figure 4-4. Volcano plot of differential gene expression in small bowel transplant biopsies from small bowel and skin (SBS) versus small bowel alone (SBA) transplants*. None of the differentially expressed genes reached a statistically significant level (defined as an adjusted p value < 0.05 and fold change >-1.5/1.5). These were samples taken at protocol time points, with no evidence of rejection. Based on 22 samples from 12 patients (samples: SBS n=12, SBA n=6, patients: SBS n=7, SBA n=5).*

The results in this section do not support the hypothesis that there will be differences in gene expression when comparing samples from participants with combined skin and small bowel transplants to those who had a small bowel transplant alone.

4.3.3 Characterisation of the immune response to rejection in small bowel transplants using spatially resolved protein analysis.

Spatially resolved protein analysis offers the possibility of exploring the immune response in the tissues and specific regions where rejection is occurring. Morphology markers were used to visualize the tissue anatomy and facilitate region of interest (ROI) selection. For the small bowel samples, ROI selection was based on the histopathological criteria[180], see table below, that are used to diagnose rejection combined with selecting areas of dense $CD45^+$ infiltrate that were noted in several of the samples, **Figure 4-5**. It may be possible to identify differences in these specific areas that were lost on the bulk gene expression analysis.

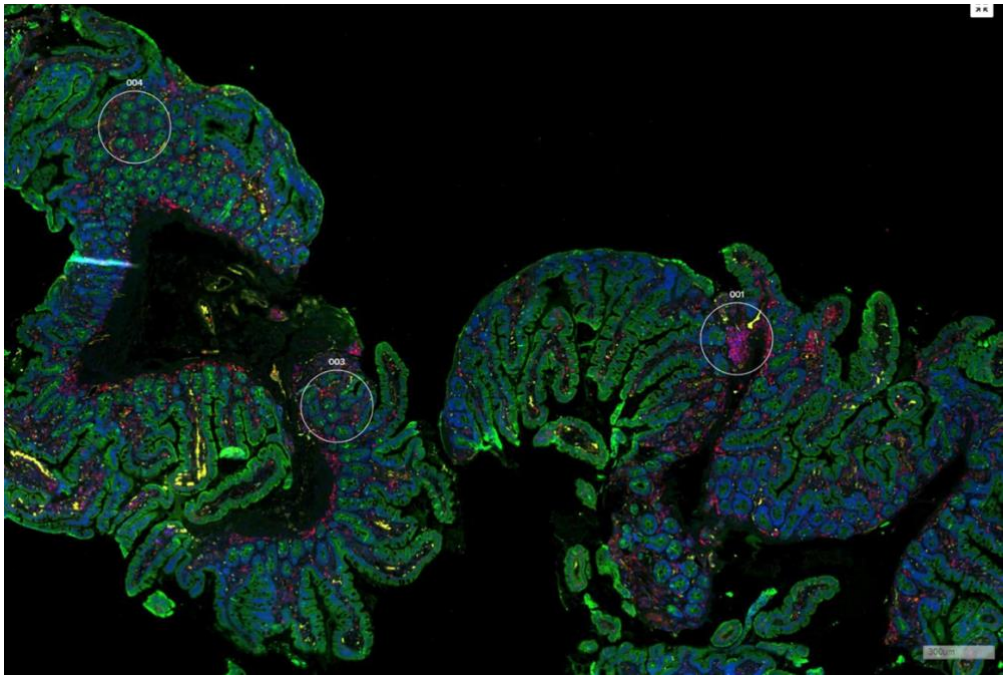

Figure 4-5. GeoMx DSP scan of small bowel transplant biopsy, demonstrating ROI selection strategy. *The following morphology markers were used: SYTO13 (blue, nuclei), CD45 (red, leukocytes), panCK (green, epithelium/connective tissue) and CD31 (yellow, vascular endothelium). Showing two crypt regions of interest (ROI), 003 and 004, and one infiltrate ROI, 001. The ROI is the white circle.*

A combination of protein panels (n = 44 proteins) from NanoString Technologies were used, with a focus on immune activation and immune cell typing, see appendix 3. These results are based on 11 samples from 5 patients. All these patients had a small bowel and skin transplant. For each patient one sample taken at the time of rejection (diagnosis based on histology) was included. In total 126 ROIs were collected, 38 from infiltrate regions and 88 from crypt regions. These ROIs were further subdivided based on CD45 status, as a marker of leukocytes. Areas of interest (AOIs) were collected from within ROIs that were either $CD45^+$ or $CD45^-$, **Figure 4-6**.

Grade	Description	Histological findings
0	No evidence of acute rejection	Unremarkable histological changes, essentially normal
Ind	Indeterminate	Small amount of epithelial injury, principally in crypts
1	Acute cellular rejection, mild	Crypt injury, including decreases in cell height/shape, increased mitotic activity, crypt destruction with apoptosis
2	Acute cellular rejection, moderate	Notable crypt injury and destruction, more diffusely distributed than in 1, focal crypt loss, mononuclear inflammatory population
3	Acute cellular rejection, severe	Marked crypt damage and destruction, accompanied by crypt loss. Diffuse mucosal ulceration. Marked diffuse inflammatory infiltrate

Table 4-2. Description of the histopathological criteria for small bowel rejection, based on the results of the pathology workshop at the VIIIth International Small Bowel Transplant Symposium[35]***.***

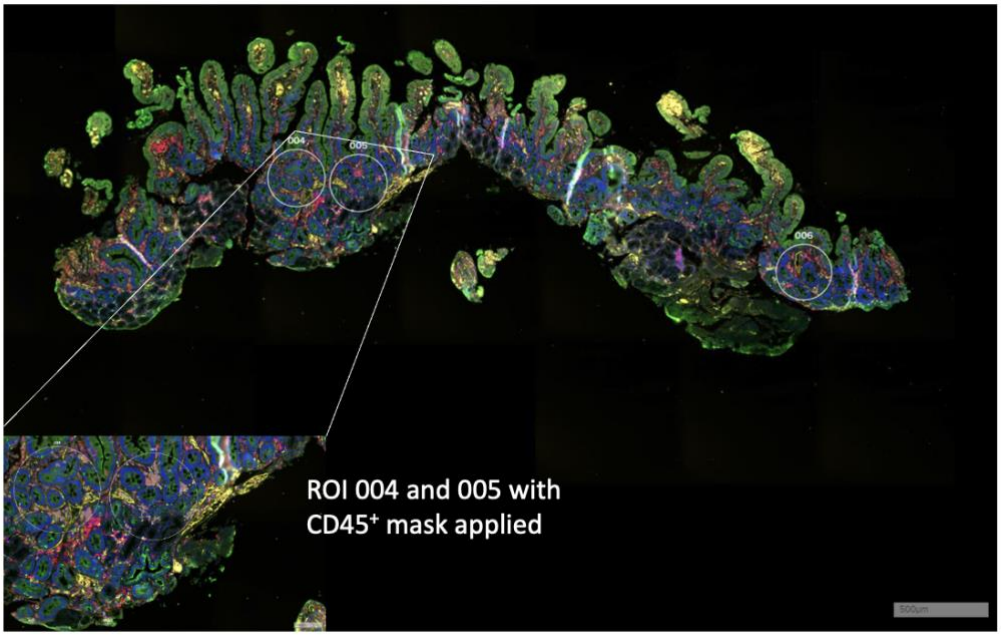

Figure 4-6. GeoMx DSP scan demonstrating region of interest (ROI) and area of interest (AOI) selection in small bowel transplantation*. Image shows a small bowel*

biopsy, stained with the following morphology markers, SYTO13 (blue, nuclei), CD45 (red, leukocytes), panCK (green, epithelium/connective tissue) and CD31 (yellow, vascular endothelium). The numbered circles are regions of interest (ROIs) that will be collected by the GeoMx for further analysis. The box inset shows selection of CD45$^+$ areas (shaded in red), these will be collected separately as an area of interest (AOI).

4.3.4 Principal component analysis of data from small bowel biopsies did not demonstrate any clear clustering by either rejection status or ROI location.

Principal component analysis was used to explore the data, to see if there were any contributing factors to sample clustering. There were some differences that appeared related to rejection status (**Figure 4-7**, B) and region of interest location (**Figure 4-7**, C). However, samples did not clearly separate based on these factors alone. Neither patient nor batch appeared to cause clustering.

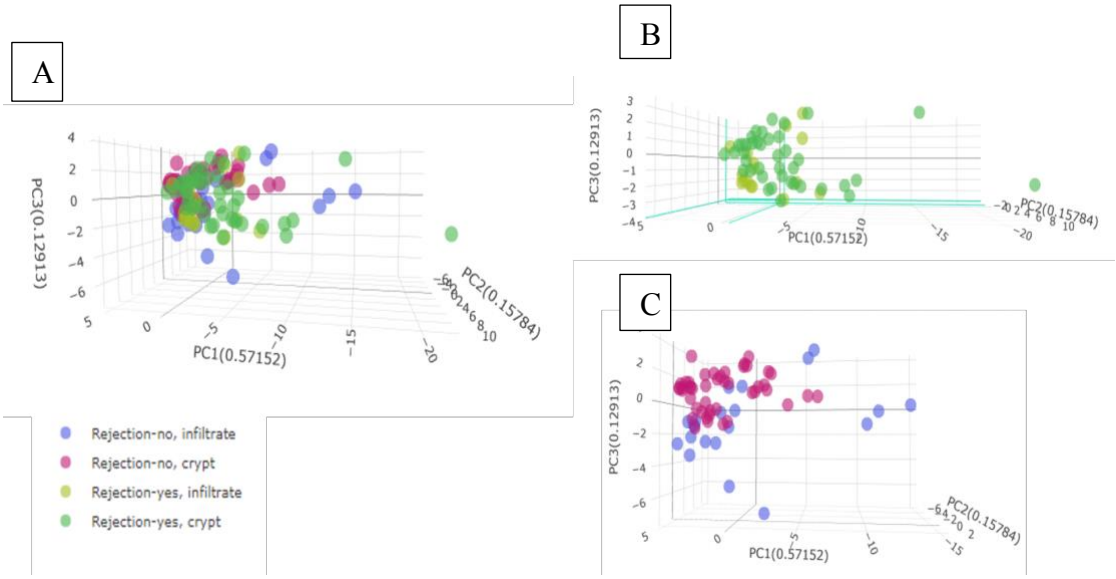

Figure 4-7. Principal component analysis of GeoMx DSP protein counts from small bowel transplant samples (SBS). *These charts show the first three principal components (PC1, PC2 and PC3), contributing to variation. A. Shows results coloured by both rejection status (yes or no) and the type of region collected (crypt or infiltrate), B. shows rejection samples and C. shows the protocol samples. Each dot represents a separate region of interest (ROI). There is no clear clustering either by ROI location or rejection status.*

4.3.5 Crypt CD45$^+$ AOIs are enriched for HLA-DR at rejection.

Crypt infiltration and damage is a key component of the histological diagnosis of acute rejection therefore, crypt regions of interest were the first to be examined. In **Figure 4-8** CD45$^+$ areas of interest (AOIs) have been compared with CD45$^-$ AOIs, from crypt ROIs. This demonstrated an upregulation of CD45, along with other mostly lymphocyte markers in the CD45$^+$ AOI, in comparison to the CD45$^-$ AOI in which panCK was upregulated, validating the selection technique. Next, the differences in the CD45$^+$

AOIs in crypt ROIs at rejection versus protocol time points were reviewed. HLA-DR protein was significantly enriched at rejection in crypt AOIs, as shown in **Figure 4-9**.

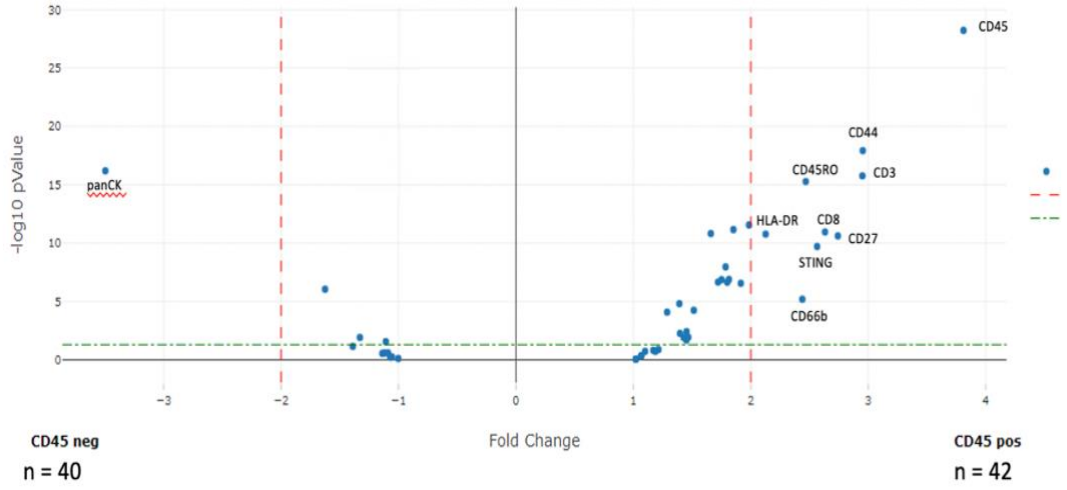

Figure 4-8. Volcano plot of differential protein expression in crypt regions of interest. *In this graph, CD45$^+$ areas of interest (AOIs) are compared to CD45$^-$ AOIs. There are several significantly differentially expressed proteins (taken as an adjusted p value <0.05 and fold change > -2/2), including. CD45 is most highly expressed in the CD45$^+$ AOI, and panCK was most highly expressed in the CD45$^-$AOI, providing confirmation that AOI selection was accurately performed by the GeoMx DSP. Red dashed line = significant fold change, green dashed line = significant adjusted p value <0.05.*

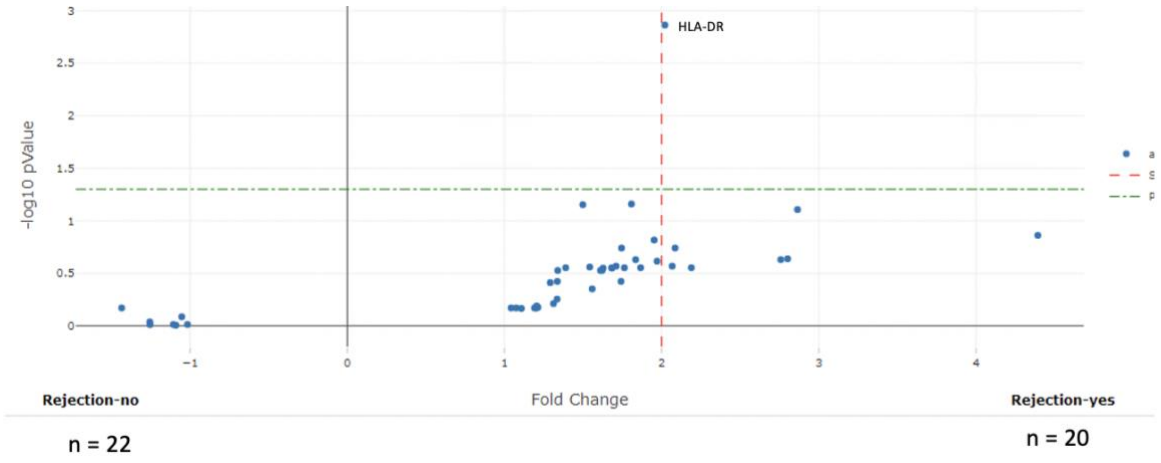

Figure 4-9. Volcano plot of differential protein expression in crypt regions of interest at rejection versus protocol time points. *HLA-DR was the only protein significantly enriched in crypt ROIs at rejection (adjusted p value <0.05, fold change >2). Red dashed line = significant fold change, green dashed line = significant p value.*

4.3.6 Crypt CD45$^+$ AOIs are enriched with myeloid markers, when compared to infiltrate AOIs.

The crypt CD45$^+$ AOIs were compared with those collected from infiltrate CD45$^+$ AOIs. The crypt AOIs had significant upregulation of myeloid markers (CD68, CD163), whereas CD20, a B cell marker, was upregulated in infiltrate AOIs, **Figure 4-10**. Finally, crypt CD45$^+$ AOIs were compared to infiltrate CD45$^+$ AOIs in the subset of samples taken at rejection, **Figure 4-11**. The crypt AOIs retained an upregulation in monocyte/myeloid markers and showed an upregulation in proteins associated with T cell activation and interferon pathways.

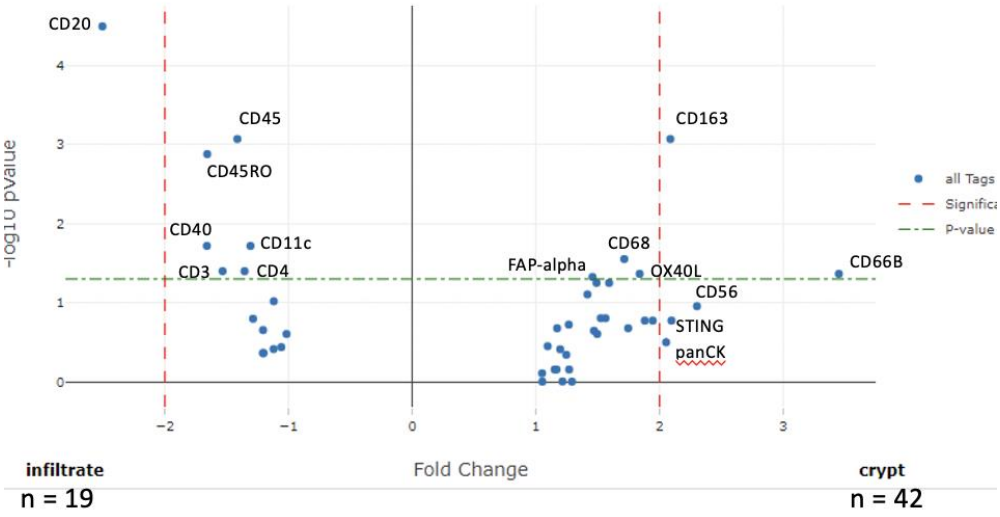

Figure 4-10. Volcano plot of differential protein expression in crypt CD45+ areas of interest compared to infiltrate CD45+ areas of interest*. The infiltrate AOIs are significantly enriched for CD20, a B cell marker. The crypt AOIs are significantly enriched for markers associated with myeloid cells (CD163 and CD66B). Red dashed line = significant fold change, green dashed line = significant p value (adjusted p value <0.05, fold change >-2/2).*

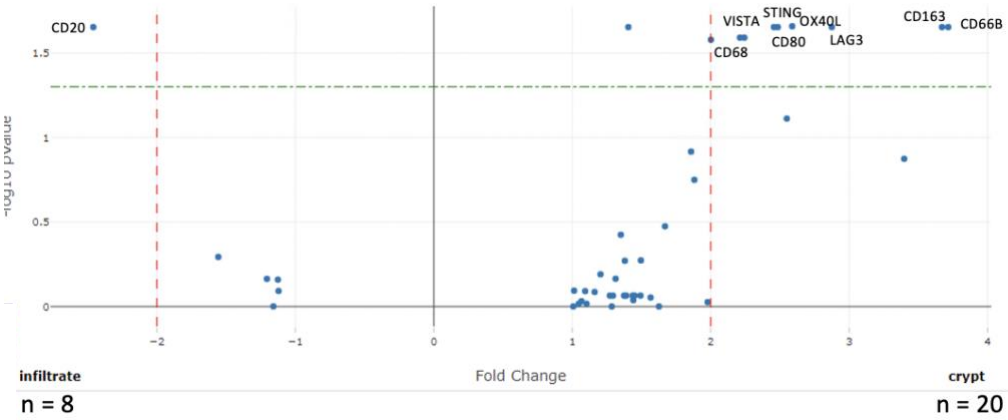

Figure 4-11. Volcano plot of differential protein expression in crypt CD45+ AOIs compared to infiltrate CD45+ AOIs at rejection time points. *At rejection the infiltrate*

AOIs remain significantly enriched for CD20, a B cell marker. The crypt AOIs continue demonstrate significant enrichment of myeloid markers, along with markers of T cell activation and interferon pathways. Red dashed line = significant fold change, green dashed line = significant p value (adjusted p value <0.05, fold change >-2/2).

The results from this section demonstrate that there were significant differences to be found at rejection in the samples from participants with combined skin and small bowel transplants, even though no differences were found in the previous sections looking at gene expression analysis in these samples. This supports a role for spatially resolved protein analysis in uncovering differences that may not be found using targeted gene expression analysis techniques. However it does not support our hypothesis that gene expression analysis results would be reflected by the spatially resolved protein results.

4.4 Discussion

In this chapter the local immune response to a combined skin and solid organ transplant within the graft itself was explored. As there were no paired skin and pancreas biopsies from the original study, samples were utilised from patients who had undergone a combined skin (abdominal wall or sentinel skin flap) and small bowel transplant. This is the first-time samples from combined small bowel and skin transplants have been analysed in this way.

Previous work has demonstrated significant increases in expression of T cell markers, IFN-γ and CXCL9/10 mRNA in small bowel transplant biopsies taken at rejection[175–177]. Therefore, the expectation was that there would be differences in these genes in the small bowel samples at the time of rejection. However, no significantly differentially

expressed genes were detected in this cohort. This could be linked to several factors. Only four rejection samples were included in this study. These were all from different patients, at different time points post-transplant and with different grades of rejection. The rejection samples in this cohort were taken at a range of time points from 39 days post-transplant up to 200 days post-transplant. From the results reported in chapter 3, it is clear that time post-transplantation has a significant effect on the immune cell compartments in the blood. This is often linked to the use of induction immunosuppression but is also likely due to the evolving immune response to the transplant.

In terms of rejection grade, three of the samples were reported as early acute rejection. Two of these three were noted to have "patchy" or "focal" involvement. The fourth sample was reported as severe acute rejection. Similarly, the control group of samples taken for comparison, reported as no rejection were also from a wide range of time points and seven different patients. A pragmatic approach to analysing these samples was taken, as patient variation is to be expected in human studies, and all the patients received the same immunotherapy. Unfortunately, it was not possible to identify any significant differences with this number of samples.

Next, samples from the combined skin and small bowel transplant (SBS) patients with those taken from patients who had a small bowel transplant alone (SBA) were compared. This was to provide a comparison of a single organ transplant without skin. A major limitation at this point was only having access to samples without evidence of rejection in the small bowel transplant alone group. Samples were from thirteen

different patients, at a wide range of time points (16 – 390 days post-transplant). Once again, no significantly differentially expressed genes were detected. There are several factors that likely contribute to this. The small sample size means the experiment is underpowered and unable to detect small differences. There are a wide range of time points included in this experiment, and as discussed earlier in this chapter, the effects of induction immunosuppression result in significant changes over time.

It may be that using a bulk gene expression technology has limited ability to identify small differences between samples. The nCounter technology has been chosen as it offers direct counting of mRNA (in comparison to RNAseq methods which require library prep), reducing potential for errors and good reported outcomes for formalin fixed paraffin embedded samples. An alternative would have been to use bulk RNAseq methods, which give a much higher resolution of mRNA expression, but require good quality and high yield of RNA or use single cell RNAseq, however this technique is more expensive, requires an access to fresh samples and the requirement to dissociate cells can lead to changes in their transcriptional profile[181]. It is also important to acknowledge that the choice of the nCounter Human Organ Transplant panel, whilst relevant to the pathways that are likely to be altered in these patients, has the limitation of being a targeted gene expression panel of only 758 genes. This necessarily restricts potential findings to these pathways and may not be sensitive enough to elucidate differences in this cohort.

The GeoMx Digital Spatial Profiler (DSP) offers the opportunity to explore in depth the immune response to rejection in small bowel transplantation. From a transplant

perspective, rejection does not happen at a uniform rate across the organ. Whilst acute rejection has been visualized using histological techniques, these are restricted in the depth of information they can provide. As there were a limited number of samples the goal was to gain as much information as possible from them. It was possible to analyse 44 different protein markers, related to immune cell function in one slide, using this technique.

This is the first time that small bowel transplant samples have been examined using spatially resolved protein analysis. The focus was predominantly on crypt regions as these are the areas which are used to diagnose rejection histologically. This study demonstrated that the segmentation had worked well by comparing $CD45^+$ to $CD45^-$ areas of interest (AOIs) and showing that CD45 was most highly expressed in the $CD45^+$ AOI. Focusing specifically on the $CD45^+$ AOIs, as transplant rejection is mediated by immune cells, a statistically significant upregulation of HLA-DR protein was found in the $CD45^+$ crypt AOIs at rejection compared to protocol time points. HLA-DR is a class II MHC protein, expressed on antigen presenting cells which interact with $CD4^+$ T cells to initiate an antigen specific immune response[182]. HLA-DR expression was shown to be increased at acute rejection in renal transplant biopsies and correlated with the degree of infiltration of lymphocytes and monocytes[183]. This was supported by Bishop et al who also noted an increase in HLA-DR expression in renal transplant biopsies at the time of rejection[184]. However, it should be noted that HLA-DR expression does not seem specific to transplant rejection, McDonald et al found that HLA-DR is expressed by intestinal epithelial cells in a number of inflammatory bowel diseases, including both Crohn's disease and ulcerative colitis[185].

On histological review of these samples, areas of denser immune infiltrate were noted, seen in more than one patient's samples. Interestingly, a recent manuscript described T regulatory cell rich organised lymphoid structures (TOLS) in tolerant kidney transplant biopsies[111]. $CD45^+$ ROIs from infiltrate regions were compared to those from crypt regions and demonstrated that there was a significant increase in CD20 found in the infiltrate ROIs. In contrast the crypt ROIs had an upregulation of myeloid and NK cell markers (CD66b, CD163, CD56). This suggests the infiltrates had higher populations of B cells whereas the crypt regions had higher populations of monocytes and NK cells, potentially signifying different roles for these areas. It was not possible to comment on T regulatory cells as the markers for these were not found to be above background levels after normalisation. This does not mean these cells were not present, rather the GeoMx DSP requires a certain number of cells to be selected in order for signal to be picked up. It is possible that these B cell-rich infiltrate areas may represent germinal centres, known to be found throughout the small bowel, forming part of the gut associated lymphoid tissue[186].

Next a subset of samples, taken at the timepoint of rejection were reviewed. The infiltrate AOIs remained enriched for $CD20^+$ cells, suggesting a B cell population. The crypt AOIs maintained a monocyte/myeloid rich phenotype, but also had elevated markers associated with T cell activation and interferon pathways. In a mouse model of small bowel transplant Zhang et al also found increases in the interferon gamma pathway at rejection, which induced CXCL10 and resulted in an increase in the number of host T cells and NK cells infiltrating the small bowel allograft[174]. Interferon gamma

production is controlled by cytokines released by antigen presenting cells[187]. This study also found that the crypt CD45$^+$ AOIs at rejection were enriched for CD68 and CD80, both expressed on antigen presenting cells. Asaoka et al used gene expression analysis to characterise the immune response in small bowel transplant biopsies[177]. At rejection they found an increase in CD80 expression, and an overexpression of Th1 associated molecules including interferon gamma[177], consistent with the results reported in this chapter. These findings are supported by work by Zambernardi et al who also explored gene expression in small bowel transplant biopsies at rejection, and found elevated levels of interferon gamma, CXCL10 and CXCL11[188].

In this study STING, stimulator of interferon genes, was also found to be enriched in the crypt CD45$^+$ AOIs at rejection in comparison to infiltrate CD45$^+$ AOIs. STING acts as an indirect sensor of cytosolic DNA[189]. Its role in transplantation has mostly been investigated in the context of haematopoietic stem cell transplantation, where it has been found to be an important regulator of GVHD[189]. There is speculation that it may play an important role in solid organ transplant rejection[189], but to date this has not been explored further in the literature, suggesting this may be a novel finding. The fact that changes are noted in the crypt rather than infiltrate areas suggest that crypt areas are preferentially involved in rejection, and correlates well with histological data.

Knight et al performed a large systematic review of donor-derived cell free DNA (dd-cfDNA) as a biomarker in solid organ transplantation[128]. The authors found that dd-cfDNA was associated with acute rejection episodes, with levels resolving after treatment. They also noted some evidence that higher levels of dd-cfDNA were

associated with worse graft outcomes. Of interest they considered it a potential biomarker across all types of organ transplant. Dholakia et al reviewed the evidence that dd-cfDNA may in fact be a stimulus for the immune response in transplantation and hypothesised that one of the possible effector pathways would be via STING[190]. The cGAS-STING pathway has emerged as a key mediator of the innate immune response, recognising the "danger signal" of extracellular DNA, with elevated levels found in diverse scenarios, including autoimmune disease, cancers, metabolic and ischaemic diseases[191]. It has been recognised as a potential therapeutic target in these disorders and therefore its finding in a transplant setting may offer a novel target for reducing the risk of acute rejection. Here we propose a hypothesis that dd-cfDNA stimulates the cGAS-STING pathway in transplantation, leading to upregulation of the interferon pathway, which in turn results in acute rejection via priming of the T cell response, **Figure 4-12**.

The findings from this chapter will form the basis for further work in this area and provide the opportunity to compare results to samples taken at the same time from the skin. This is a unique dataset of paired samples taken from combined small bowel and skin transplants and will be discussed in the next chapter. In this chapter the capability of these methods to generating relevant data has been demonstrated and has the potential for uncovering new mechanisms of rejection by sampling regions of interest more specifically using spatial profiling, as evidenced by the novel finding of STING upregulation in the crypt $CD45^+$ areas of interest at rejection.

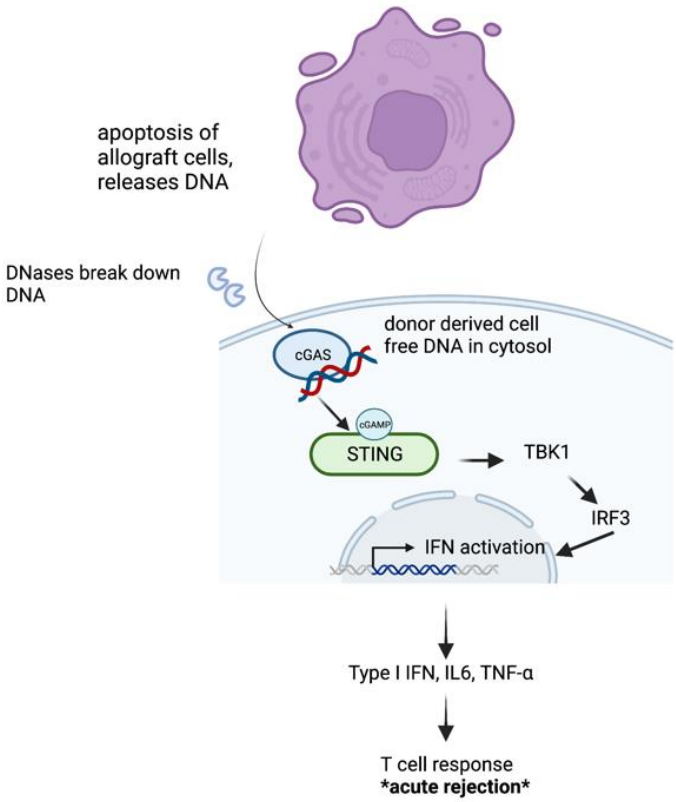

Figure 4-12. Potential model for role of cGAS-STING pathway in acute rejection.

Damage to allograft cells may occur via several routes, including the ischaemia-reperfusion injury associated with transplantation. This results in release of dd-cfDNA, which is taken up by macrophages which in turn is recognised by cGAS and results in activation of STING and TANK binding kinase 1 (TBK1) and interferon regulator factor 3 (IRF3). These translocate to the nucleus where they result in interferon activation and subsequent release of type I interferon, IL6 and TNF-α which prime a T cell response. Created by BioRender.com.

5 Chapter 5. Immune response in primarily vascularised skin transplants combined with solid organ transplants.

5.1 Introduction

Combining multiplexed gene expression and spatially resolved protein analysis techniques offers the opportunity to unravel the mechanisms underlying rejection in transplantation. As I have discussed in Chapter 1, the skin contains a complex immune system, with several anatomically distinct compartments with specific roles. It is clear from the histological data that rejection takes place in different locations at different time points[92,192]. Immunohistochemical analysis of hand transplant biopsies has confirmed that rejection is associated with an immune cell infiltrate consisting of $CD3^+$ T cells, along with expression of both FOXP3 and IDO, immunoregulatory molecules[91,97,156]. Hautz et al found upregulation of adhesion molecules ICAM-1 and E-selectin, involved in T cell migration, at rejection in hand transplant samples[97]. Using a rat model of hindlimb transplantation they used a topical agent to block E-selectin and demonstrated that when combined with standard immunosuppression this prolonged allograft survival. Studies of samples from face transplant patients, which measured mRNA expression, have shown that there is an influx of $CD8^+$ T cells at rejection, along with increases in granzyme and perforin[96]. Furthermore, Banff grade 3 rejection is characterised by IFN-γ driven inflammation, APC activation and proliferation of T cells[96,156]. Most recently Borges et al have used multiplexed gene expression analysis to explore mRNA expression in samples from hand transplant patients, finding increases in T cell recruiting chemokines (*CXCL13*, *CCL18*, *CCL17*, *CXCL9*) and effector molecules (*GZMB*, *GZMA*, *GNLY*) at rejection[150]. These studies benefit from large

sample sizes, due to the accessibility of skin for biopsies, however they are restricted in the number of patients included due to the small number of patients who have received a face or hand transplant. While providing an insight into the immune response in a vascularised skin transplant, they do not include those combined with a solid organ transplant.

In this chapter I will continue to explore the local immune response to a combined skin and solid organ transplant, this time focussing on the skin component. The original purpose of adding skin to a solid organ transplant was to provide an easily visible monitor for the transplanted organ(s). There are many advantages to using skin for monitoring: it develops a visible rash with rejection, it can be monitored by the patient with little training, and it is easy to biopsy, with minimal morbidity[127]. At the advent of combining skin and solid organ transplants, there were concerns about the addition of skin as it was thought to be the most "antigenic tissue"[193], with the potential to sensitise patients to their life-saving solid organ. It was also unknown how well skin rejection would correlate with solid organ rejection. This is the first study that investigates both gene and protein expression in skin biopsies from sentinel skin flaps.

5.2 Chapter 5 aims and hypotheses.

In this chapter I aim to:

- characterise the local immune response to skin from a combined skin and solid organ transplant, using a combination of gene expression analysis and spatially resolved protein analysis.

- consider how the response in skin compares both to small bowel transplants (based on the results from Ch4) and the systemic response in the blood (based on the results from Ch3).

We hypothesise that at rejection skin samples from AWTx and SSFs will have higher mRNA expression of T cell – associated genes (e.g. *CD8*, *CD4*), chemokines (e.g. *CXCL9*, *CXCL10*, *CXCL18*), T cell effector molecules (e.g. *GZMB*, *GZMA*) and immunoregulatory molecules (e.g. *FOXP3* and *IDO*). We will also explore the changes in gene expression in the skin over time post-transplant and predict that there will be decreases in gene expression related to T cells, B cells, and their associated signalling because of induction immunosuppression. Finally, we hypothesise that the changes found in the gene expression analysis will be reflected in spatially resolved protein analysis, with increases in proteins related to T cell activation, immune regulation and T cell migration upregulated in skin samples at rejection.

5.3 Results

To explore the mechanisms underlying rejection the nCounter Human Organ Transplant (HOT) panel was used to compare gene expression in skin samples at protocol and rejection time points, see appendix 2 for details of genes included. First the patients who underwent a sentinel skin flap (SSF) and simultaneous pancreas-kidney (SPK) transplant were analysed. This data set includes skin biopsies from two patients who each had at least one episode of rejection. In total four samples without rejection (protocol biopsies taken at 3- and 6-months post-transplantation) and three at the time of

rejection (2 months, 6 months, and 18 months post-transplantation) were included, see **Table 5-1**.

Patient	Rejection samples	Protocol samples
S12	2	2
S13	1	2

Table 5-1. SSF samples included in initial gene expression analysis. *Patient S12 had two episodes of rejection at 6- and 18-months post-transplantation respectively and Patient S13 had one episode of rejection at 2 months post-transplantation. The protocol samples used for comparison were taken at 3- and 6-months post-transplantation. These patients had a combined SSF and pancreas transplant.*

PCA analysis demonstrated clustering of the samples by rejection status, **Figure 5-1**. However, there were no genes that were significantly differentially expressed, using mixed negative binomial method to calculate differential expression, and then adjusting the p value to account for multiple comparisons. This was a very small sample size, which was likely the reason that no significant differences in gene expression were found.

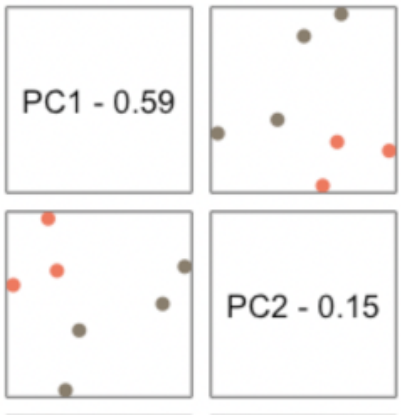

Figure 5-1. Principal component analysis of multiplexed gene expression counts from skin samples from the two patients with a combined sentinel skin flap and simultaneous pancreas-kidney transplants, who experienced an episode of rejection. *The graph shows the first two components, PC1 captures the most variation and PC2 the second most variation in the data. Dots coloured red are from samples at rejection (n=3) and dots coloured grey are at protocol (n=4) time points. This PCA plot demonstrates that the samples cluster by rejection status. Data from two patients.*

5.3.1 Differential gene analysis of skin transplant biopsies demonstrated >100 genes upregulated at rejection, including CXCL9 and CXCL10.

To increase the sample size, with the goal of discovering which genes were differentially expressed at rejection, the inclusion criteria was widened to include skin samples from both abdominal wall and sentinel skin flaps, transplanted in combination with either small bowel or simultaneous pancreas-kidney transplants. This resulted in a sample size of 23 skin biopsies, seven at rejection and sixteen at protocol time points, from twelve different patients. As for the smaller sample described previously, principal component analysis demonstrated clustering by rejection, **Figure 5-2**. Differential gene expression analysis revealed 134 significantly differentially expressed genes (adjusted p

value < 0.05 and log2 fold change +/- 1.5), **Figure 5-3**. The majority of these differentially expressed genes were upregulated at rejection. *CXCL9* and *CXCL10* were the most upregulated (log2 fold change of 6). Several other genes associated with chemokine signalling pathways were also noted to be upregulated (*CXCL1/2, CXCR4, CCL2, CCL19, CXCL16*), **Figure 5-4**. Genes associated with effector immune molecules (*KLRK1*), leukocyte trafficking (*VCAM1*), antigen processing and presentation (*HLA-DPB, HLA-DMB, PSMB, TAP1/2*), and innate immunity (*C1QB, CD68, CD14*) were also found to be upregulated at rejection. Genes associated with the cGAS-STING pathway were also noted to be upregulated (*CGAS*, *IRF1*), in keeping with the findings from Chapter 4 in small bowel samples at rejection. For a full list of the significantly differentially expressed genes see appendix 5.

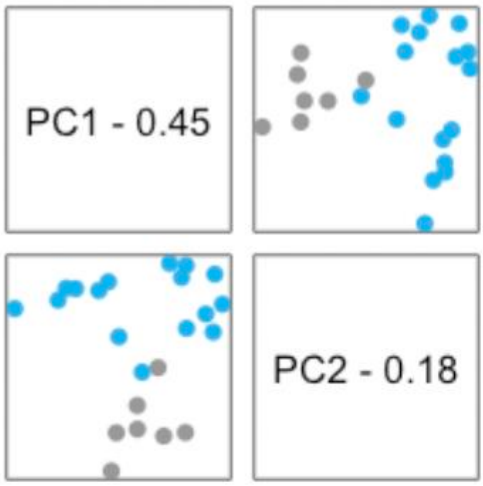

Figure 5-2. Principal component analysis of multiplexed gene expression counts in AWTx and SSF samples. *The graph shows the first two components, PC1 captures the most variation and PC2 the second most variation in the data. Dots coloured grey are from samples at rejection and dots coloured blue are at protocol time points. This PCA plot demonstrates that the samples cluster by rejection status. Based on 23 samples from 12 different patients.*

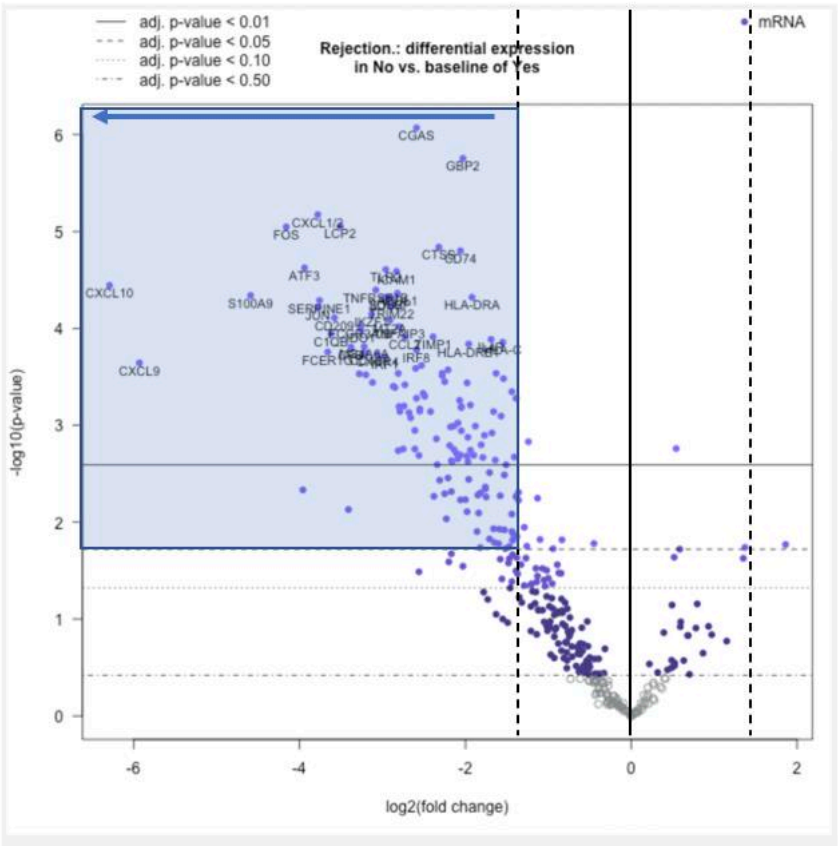

Figure 5-3. Volcano plot of differentially expressed genes at rejection versus protocol time points, AWTx and SSF samples. *The solid black line highlights an adjusted p-value <0.01 and the large, dashed line an adjusted p-value <0.05. Genes in the highlighted blue box are significantly upregulated at rejection compared to protocol time points (adjusted p value <0.05 and log2 fold change <-1.5). For a full list of the DEG see appendix 5. Based on 23 samples from 12 patients (12 at rejection, 11 at protocol time points).*

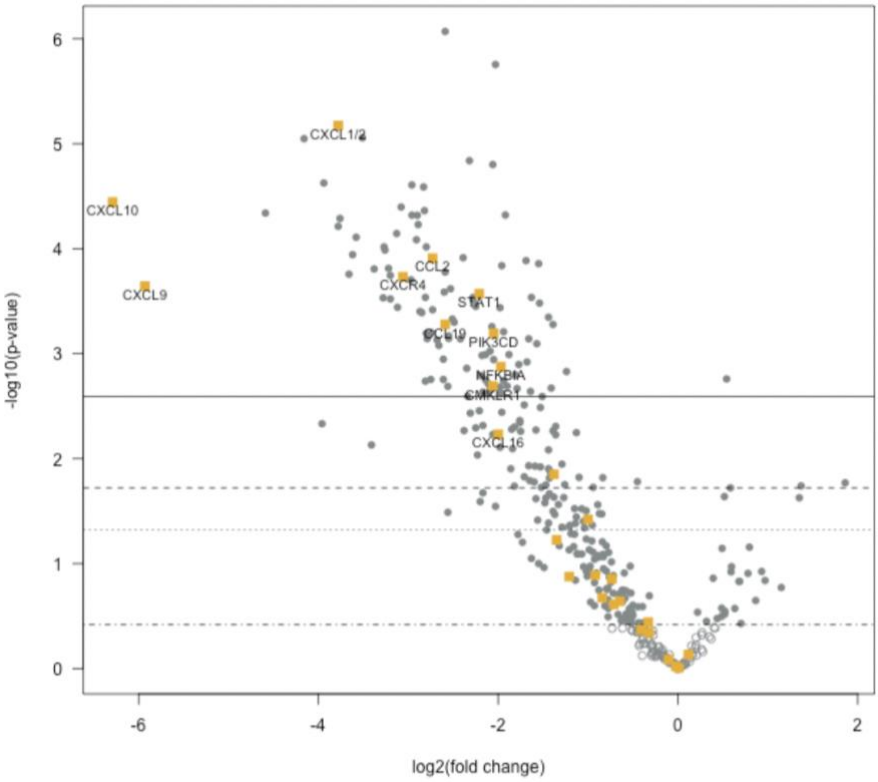

Figure 5-4. Volcano plot of differentially expressed genes, related to chemokine pathways, at rejection versus protocol time points in AWTx and SSF samples. *Several chemokines, including CXCL9 and 10 were found to be upregulated at rejection. Yellow dots highlight the genes that are part of chemokine pathways. The solid black line highlights an adjusted p-value <0.01 and the large, dashed line an adjusted p-value <0.05. Genes above these lines, and <-1.5 log2 fold change are considered significantly differentially expressed. Based on 23 samples from 12 patients (12 at rejection, 11 at protocol time points).*

Pathway analysis was performed to gain a higher order overview of this data. As is shown in **Figure 5-5**, a heatmap of the pathway data shows distinct clustering by rejection. Many of these pathways were upregulated at rejection, including both the

innate and adaptive immune system and associated signalling pathways such as T and B cell receptor signalling, chemokine and cytokine signalling and interferon signalling. These findings support known mechanisms underlying an acute rejection episode and are consistent with the findings discussed earlier in this chapter for vascularised skin transplants alone[91,96,150].

A subset of protocol samples was noted to have upregulation of mTOR, angiogenesis and autophagy pathways. Autophagy is a cellular process, in which damaged cells are repaired or recycled. It may be associated with ischaemia-reperfusion injury and has been associated with allograft rejection in an animal model of liver transplantation[194]. It is therefore interesting to see this pathway upregulated in samples that were not undergoing rejection, given that cellular damage would be expected to be part of the rejection process. Furthermore, these were samples from patients who did not have a rejection episode in the first 12 months of follow up. However, it is consistent with work from Lin et al, who using a mouse model of skin transplantation demonstrated that inducing autophagy in dendritic cells prolonged the survival of skin allografts[195]. The authors found that these dendritic cells produced more IL10 in vitro, which potentially results in a reduced T cell effector response.

The results in this section support the hypothesis that there would be upregulation of genes associated with T cells, chemokines and effector molecules at rejection in the skin from participants with combined skin and solid organ transplants.

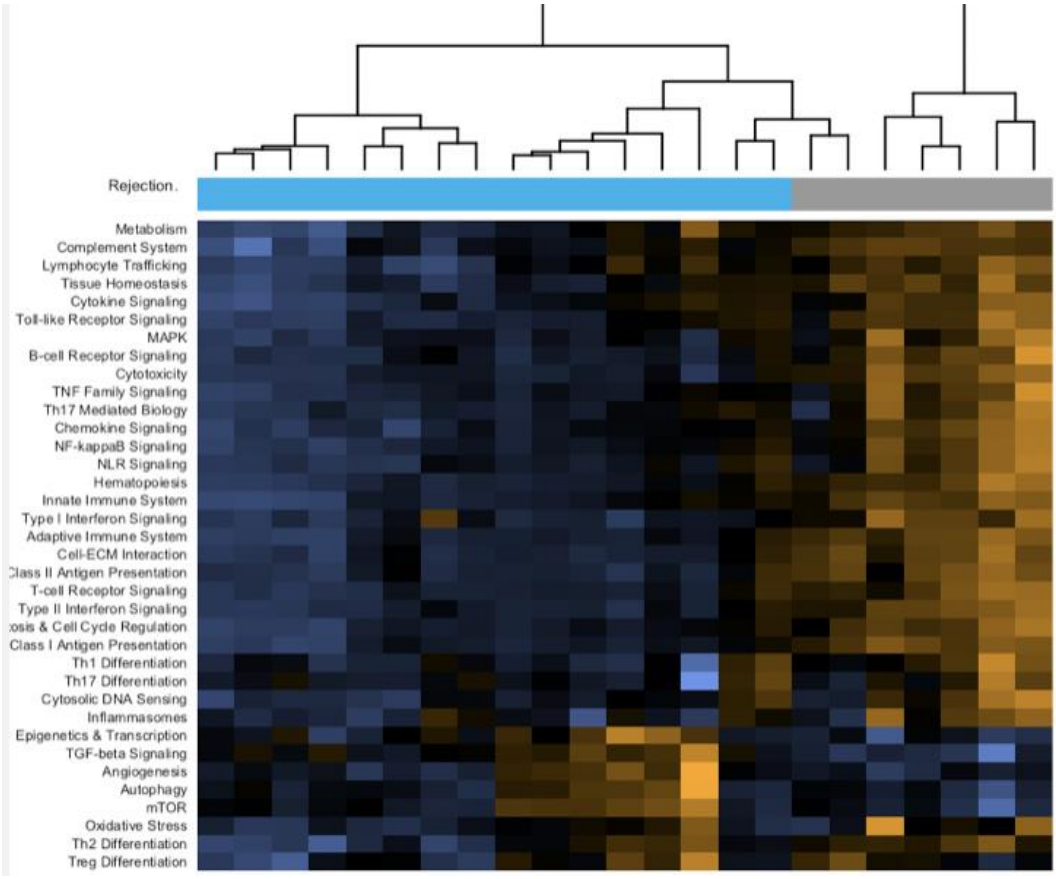

Figure 5-5. Heatmap of all pathways, demonstrating unsupervised clustering of rejection versus protocol samples in AWTx and SSF skin biopsies. *Pathway analysis demonstrates that samples cluster by rejection status. The pathways are listed on the y axis and each column on the x axis represents an individual sample. Orange indicates high scores; blue indicates low scores. Scores are displayed on the same scale via a Z-transformation. The bar at the top indicates how the samples are clustered, blue = protocol and grey = rejection. There appear to be two subsets within the protocol samples, with a group of samples demonstrating upregulation of pathways including autophagy, mTOR and angiogenesis compared to the rest of the group.*

5.3.2 Gene expression changes in the skin in the first 6 months following a combined skin and simultaneous pancreas-kidney transplant were different to those seen in the blood.

To explore how gene expression changes in the skin in the first 6 months after a combined sentinel skin flap and simultaneous pancreas-kidney transplant, the nCounter Banff Human Organ Transplant panel was used. This panel targets genes relevant to organ rejection, immune response, and tissue damage. Skin samples from seven patients, taken as per protocol before transplantation, 3 and 6 months after transplantation were included. These samples are from the same patients as those analysed in Chapter 3 looking at gene expression in the blood at the same time points post-transplantation. It was demonstrated in Chapter 3 that at three months post-transplantation 29 genes were downregulated in the blood, recovering so that at 6 months post transplantation only 5 were found to be downregulated. Our hypothesis was that similar results would be found in the skin samples.

On initial review of the data, using principal component analysis, there was no clear evidence of clustering related to time post-transplant, see **Figure 5-6**. Despite this there were several genes that were significantly differentially expressed at 3- and 6-months post-transplant when compared to pre-transplantation. In contrast to results in Chapter 3, when at 3 months post-transplant the most downregulated genes in blood samples were related to T cell pathways, in the skin samples the downregulated genes included markers of innate immune cells, including Langerhans cells (*CD44*), macrophages (*CD163*), and neutrophils (*SOD2*) along with various molecules involved in signalling pathways (*BCL3, FOS, STAT3*), **Figure 5-7**. The only gene significantly upregulated at

3 months post-transplant was *COL1A-1*, which encodes for collagen I production, a key component of skin extracellular matrix, perhaps indicating evidence of wound healing in the skin post-surgery.

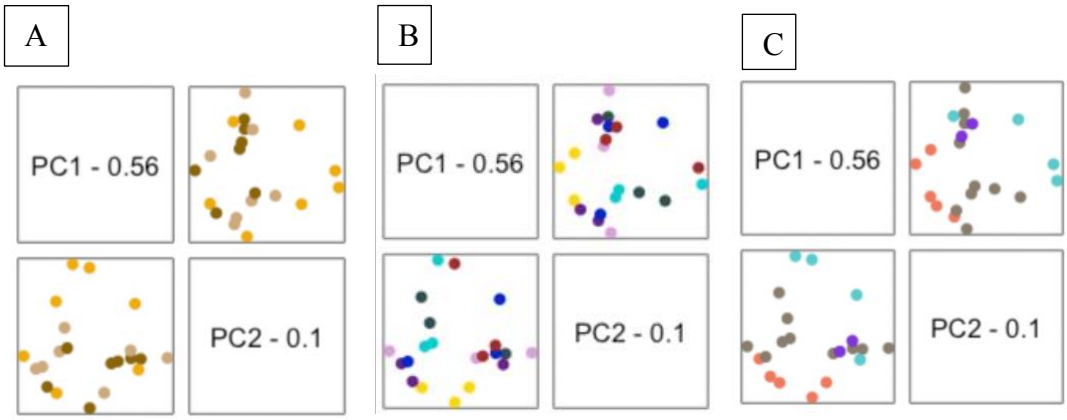

Figure 5-6. Principal component analysis of multiplexed gene expression counts from skin samples. *Each graph shows the first two components, PC1 captures the most variation and PC2 the second most variation in the data. A. Samples coloured by time point (pre-transplant yellow, 3 months post-transplant beige, 6 months post-transplant brown). B. Samples coloured by patient (S3 pink, S7 green, S8 aqua, S9 blue, S11 burgundy, S12 yellow, S13 purple). C. Samples coloured by batch number (1 red, 2 grey, 3 aqua, 4 purple). There is no clear clustering seen in these groups. Based on 21 samples from 7 patients.*

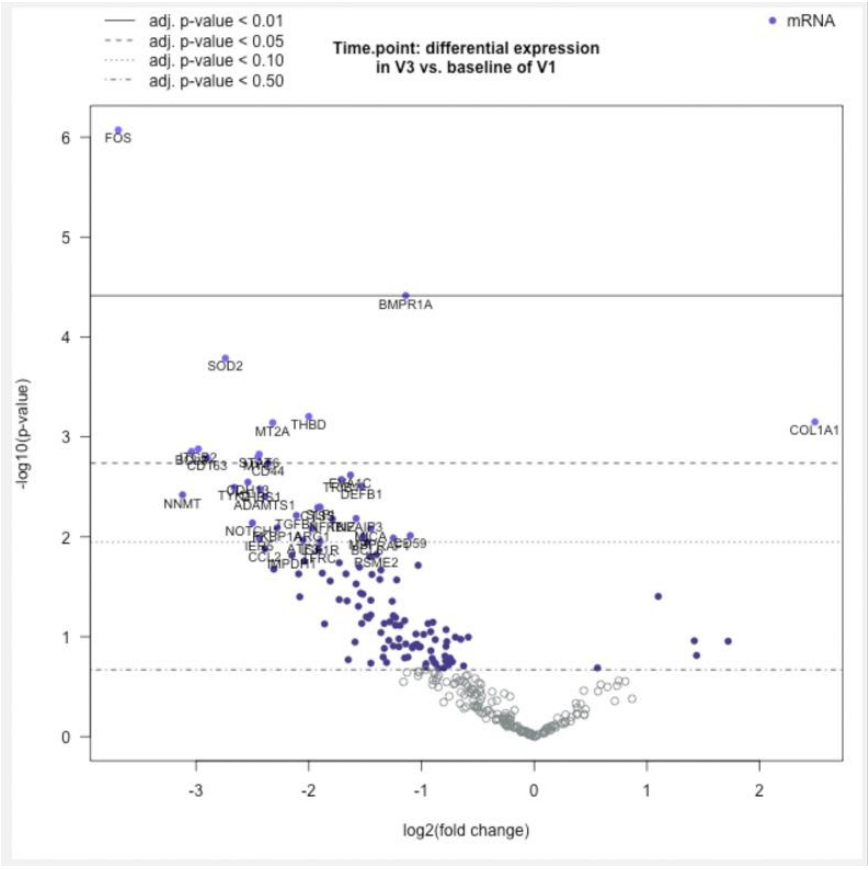

Figure 5-7. Volcano plot of differential gene expression at 3 months post-transplant compared to pre-transplant. *The solid black line highlights an adjusted p-value <0.01 and the large, dashed line an adjusted p-value <0.05. Genes above these lines and with a log2 fold change > 1.5 or <-1.5 are considered significantly differentially expressed. Based on 21 samples from 7 patients.*

At six months post-transplant there was evidence of further downregulation of genes in the skin biopsies, in comparison to the pre-transplant time point, with 25 significantly downregulated genes. These included more innate immune cell associated genes (*LCN2, BCL3, THBS1*), several macrophage associated genes (*LTBR, NOTCH1, CCL2, TAP1*) and additional signalling pathway genes (*IER5, NFIL3*), shown in **Figure 5-8**.

Furthermore, eight of the ten genes that were downregulated at three months, remained downregulated at this point see appendix 6 for full list of genes downregulated in skin and blood. In comparison at 6 months post-transplant when analysing blood samples using the same gene expression panel, there were fewer genes downregulated. This may be due to the reduced effect of induction immunosuppression on T cell subsets at this time. It also demonstrates that using blood alone to monitor the immune response post-transplantation in skin does not necessarily reflect what is happening in the skin accurately.

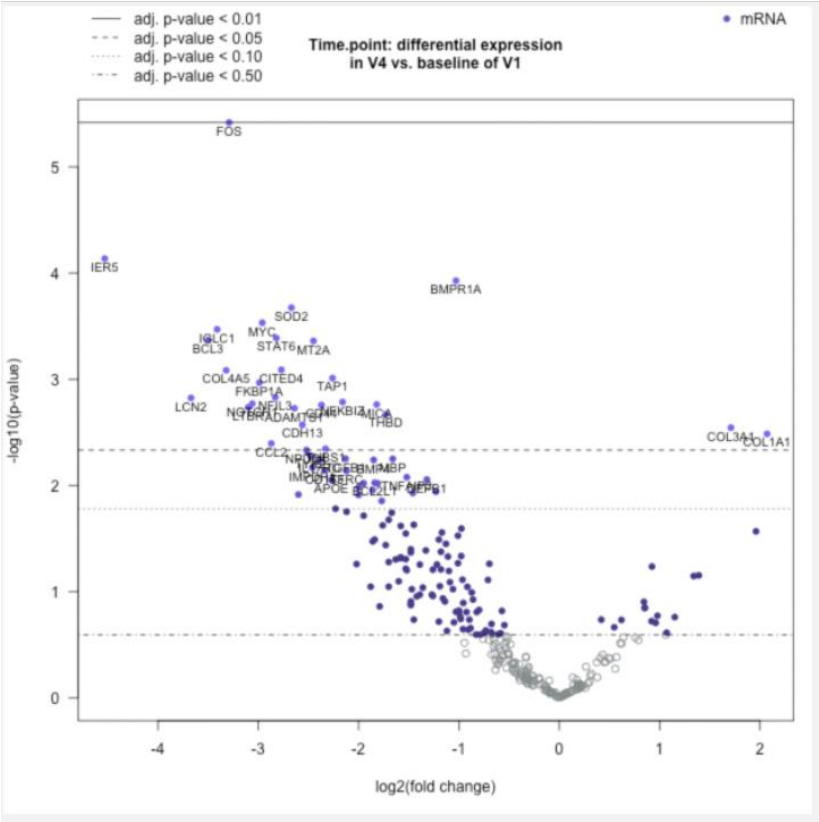

Figure 5-8. Volcano plot of differentially expressed genes at 6 months post-transplant compared to pre-transplant. *The solid black line highlights an adjusted p-value <0.01 and the large, dashed line an adjusted p-value <0.05. Genes above these lines and with a log2 fold change +/- 1.5 are considered significantly differentially expressed.*

Whilst the results presented in this section support the hypothesis that there would be decreases in gene expression in the skin over time post transplantation, they were not found to be related to the T and B cell pathways predicted.

5.3.3 Characterisation of the immune response to rejection in abdominal wall or SSF transplants using spatial proteomics

Next the local immune response to rejection in skin transplants, was explored using spatially resolved protein expression, with an immune focused panel used to analyse samples (see appendix 3 for full details of the protein panel). Having found evidence of upregulation in several genes at rejection the aim was to confirm these findings using protein expression and to also visualise where expression was found in the skin. Skin samples from five patients, who had undergone an abdominal wall or SSF and small bowel transplant, were included in this study. Four of these samples were at rejection. Corresponding small bowel samples from all these patients were analysed in Chapter 4. Rejection takes place in the skin in distinct anatomical regions, which makes spatially resolved protein analysis the ideal method for exploring the alloresponse. Protein counts were collected from both perivascular and epidermal regions of interest (ROIs) using the GeoMx DSP. Perivascular infiltrates are an early feature of rejection on histology, and as severity progresses the epidermis is later involved. To specifically characterise the immune response, regions of interest were segmented using a CD45 morphology marker, to enable separation of areas of interest (AOIs) that are $CD45^+$ and $CD45^-$, as CD45 is expressed on leucocytes. In total 38 perivascular ROIs and 17 epidermal ROIs were collected, see **Table 5-2**.

Region of interest (ROI) location	Rejection (number of ROIs segmented)	Protocol (number of ROIs segmented)
perivascular	31 (28/31)	7 (3/7)
epidermal	13 (4/13)	4 (0/4)

Table 5-2. Summary of the regions of interest (ROIs) collected from the skin transplant samples. *ROIs were collected from perivascular and epidermal regions, identified with the help of morphology markers. Most of the ROIs were then segmented based on CD45 positivity, with separate areas of interest (AOIs) collected that were either $CD45^+$ or $CD45^-$. These have been separated in samples taken at rejection (from four different patients) or at protocol (one patient) time points. The fraction in brackets details how many of the ROIs were segmented into AOIs.*

Principal component analysis, was used initially used to explore the data, looking for clustering in the samples. On review of different variables, **Figure 5-9**, it was found that the most difference was due to region of interest location and rejection status. As can be seen in **Figure 5-9C** and **Figure 5-9D**, the perivascular ROIs were clustering away from the epidermal ROIs and then separating out by rejection.

Next, differential protein expression analysis was performed, starting with the perivascular regions of interest, examining $CD45^+$ AOIs versus $CD45^-$ AOIs. Validating the selection strategy, CD45 was the most differentially expressed protein in the $CD45^+$ AOI, **Figure 5-10**. Furthermore, markers of extracellular matrix, including fibronectin, ARG1 and panCK were all upregulated in the $CD45^-$ AOIs, **Figure 5-10**.

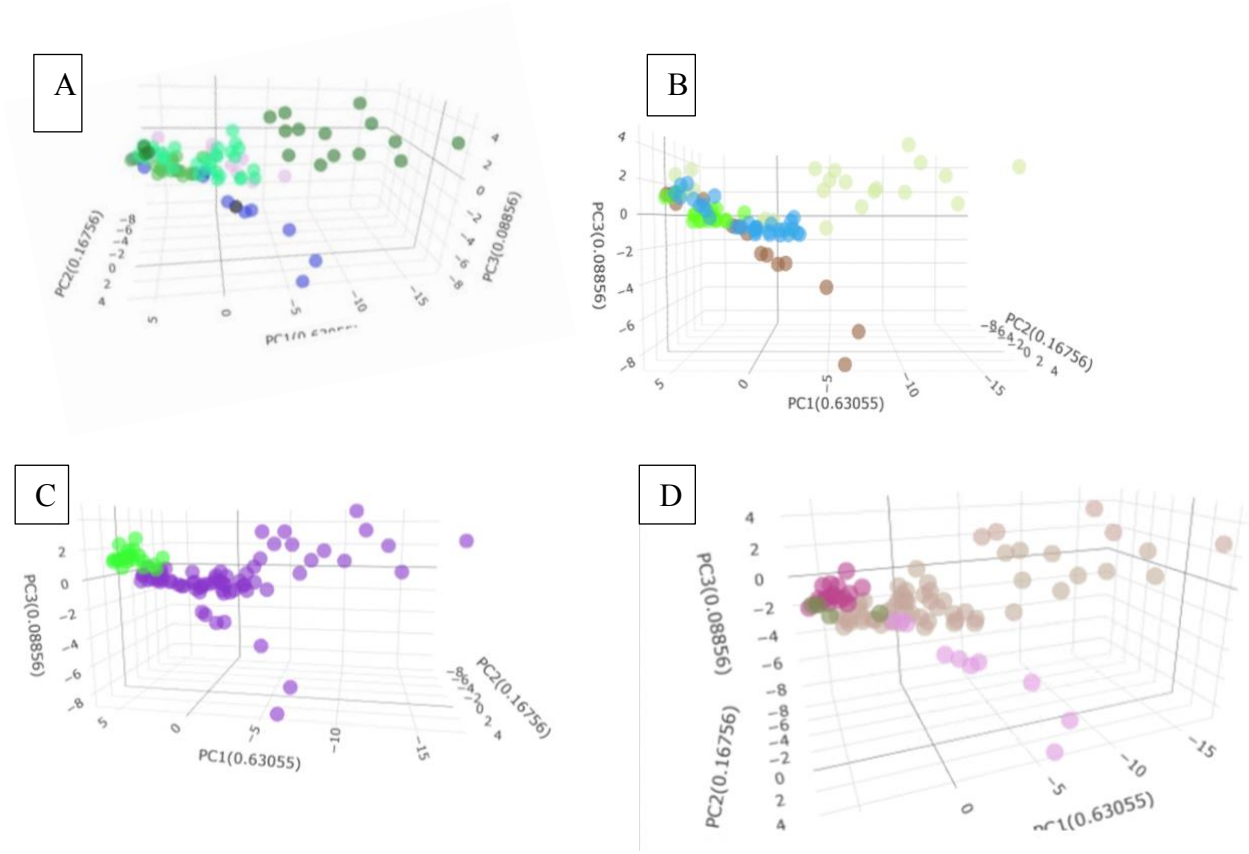

Figure 5-9. Principal component analysis of GeoMx DSP protein counts from AWTx/SSF samples. *The graph shows the first three components, PC1 captures the most variation, PC2 the second most variation and PC3 the third most variation in the data. A; coloured by patient, B; coloured by batch, C; coloured by ROI location (green = epidermal, purple = perivascular), D; coloured by ROI location and rejection status (dark pink = rejection, epidermal ROI, green = no rejection, epidermal ROI, light beige = rejection, perivascular ROI, light pink = no rejection, perivascular ROI). Variation is mostly due to ROI location and rejection status, shown by clustering in C and D. Based on data from 5 patients, 55 ROIs collected.*

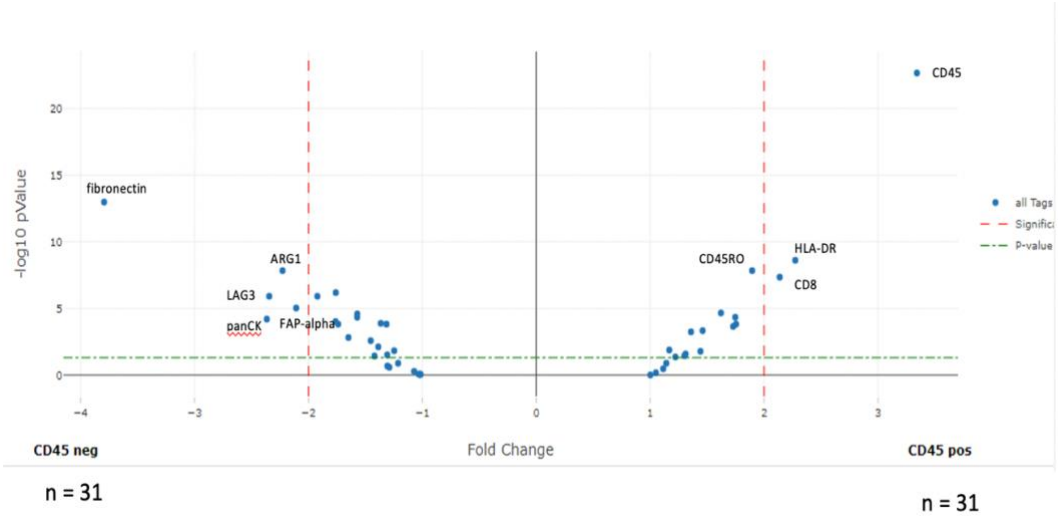

Figure 5-10. Volcano plot of differential protein expression in perivascular areas of interest. *In this graph, CD45$^+$ areas of interest (AOIs) are compared to CD45$^-$ AOIs. There are several significantly differentially expressed proteins (taken as an adjusted p value <0.05 and fold change > -2/2). CD45 is most highly expressed in the CD45$^+$ AOI, and fibronectin was most highly expressed in the CD45$^-$AOI, providing confirmation that AOI selection was accurately performed by the GeoMx DSP. Red dashed line = significant fold change, green dashed line = significant p value.*

At rejection the perivascular ROIs had an upregulation of proteins associated with both T cell and monocyte activation, **Figure 5-11**. Of interest CXCL9 was also upregulated. This is a chemotaxis-inducing cytokine, which was also found to be highly upregulated in rejection in the gene expression analysis reported earlier in this chapter. It binds to CXCR3 on T cells and promotes migration to sites of injury, in this instance the perivascular regions at rejection. When no rejection is taking place the perivascular regions of interest had an increase in inhibitory markers (PD-1, CTLA-4) and B cells (CD20).

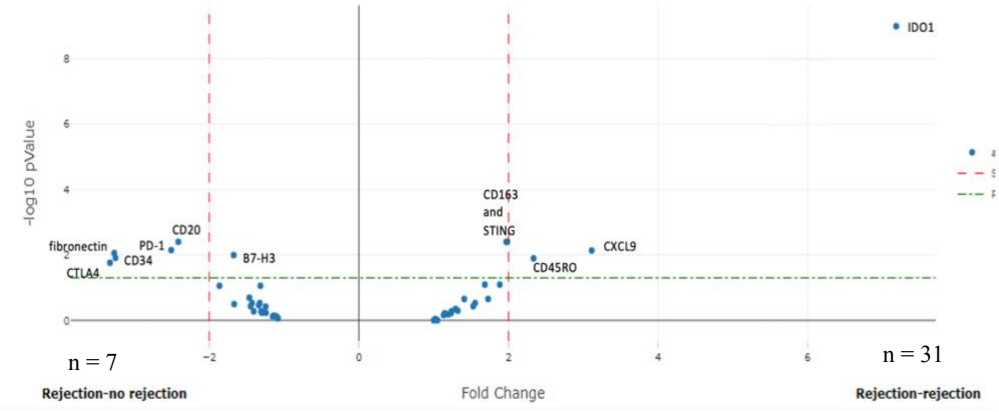

Figure 5-11. Volcano plot of differential protein expression in perivascular ROIs at protocol versus rejection time points. *In this graph, perivascular ROIs at rejection are compared to those at protocol time points. There is upregulation of IDO1, CXCL9 and CD45RO at rejection. Whilst at protocol time points the perivascular ROIs have upregulation of CD20, CTLA4, CD34 and PD-1. Red dashed line = significant fold change, green dashed line = significant p value.*

To look more specifically at the immune response, the $CD45^+$ segments from the perivascular ROIs alone were examined. At rejection IDO1 remained the most differentially expressed protein, **Figure 5-12**. IDO1 is known to catalyse the breakdown of tryptophan, a key metabolite required for T cell activation[196]. It is produced by activated dendritic cells, CD11c a marker of dendritic cells, was also noted to be significantly upregulated in rejection. IDO1 mRNA expression was also found to be significantly upregulated in the skin biopsies at rejection (adj p value < 0.002, log2 fold change -3.26). The upregulation of IDO1 at rejection perhaps reflects an attempt to regulate the T cell response.

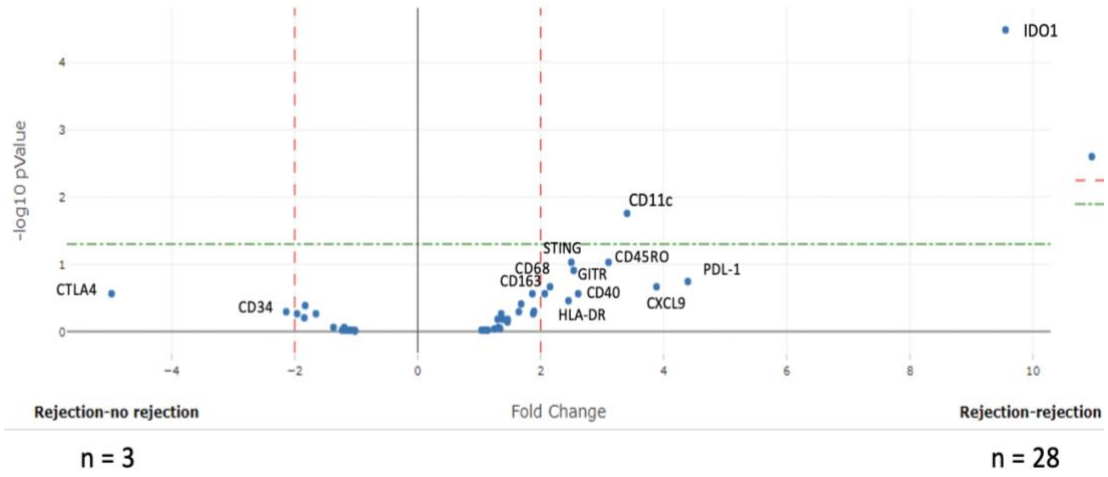

Figure 5-12. Volcano plot of differential protein expression in perivascular CD45$^+$ AOIs at protocol versus rejection time points. *In this graph, perivascular CD45$^+$ AOIs at rejection are compared to those at protocol time points. IDO1 remains significantly upregulated, along with CD11c. Red dashed line = significant fold change, green dashed line = significant p value.*

Having analysed the perivascular regions of interest (ROIs) the epidermal ROIs were explored. All the samples in this study were reported as Grade 3 rejection, so would include some involvement of the epidermis. The PCA suggested that there was less difference to be found in the epidermal ROIs, although this could in part be due to the smaller numbers for this group. Comparison of CD45$^+$ to CD45$^-$ areas of interest (AOIs) once again demonstrated satisfactory segmentation of the ROIs, **Figure 5-13**.

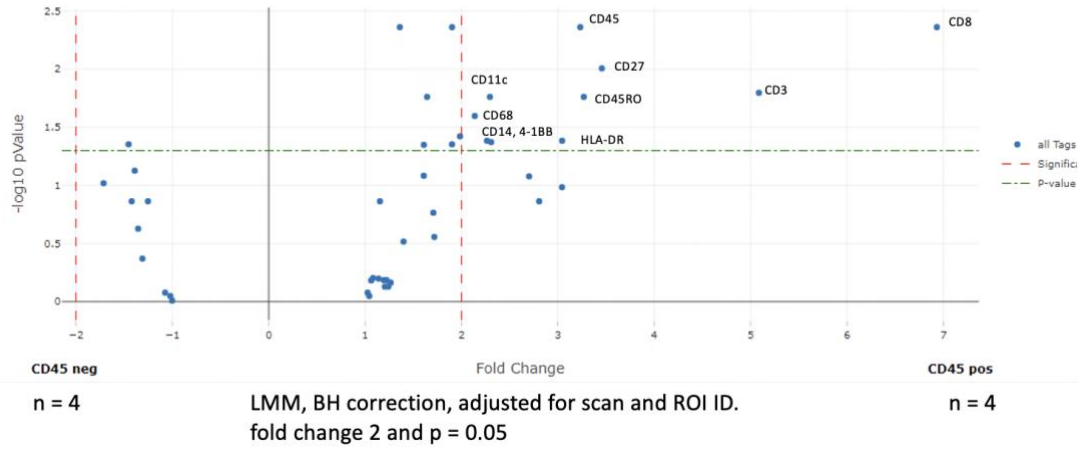

Figure 5-13. Volcano plot of differential protein expression in epidermal AOIs. *In this graph, epidermal CD45$^+$ AOIs are compared to epidermal CD45$^-$ AOIs. CD45 is most highly expressed in the CD45$^+$ AOIs, confirming accuracy of segmentation. Red dashed line = significant fold change, green dashed line = significant p value <0.05.*

At rejection there was an upregulation of CD40 and CD44 proteins. CD40 is a member of the TNF superfamily and is expressed on antigen presenting cells. CD40 mRNA was also found to be significantly upregulated in the skin biopsies at rejection (adjusted p value 0.02, log2 fold change -1.75). CD44 is another receptor which plays a role in cell adhesion and migration and is suggestive of activation. Interestingly STING was also noted to be upregulated in epidermal ROIs at rejection, reflecting the results from small bowel crypt ROIs discussed in Chapter 4. In contrast at protocol time points an increase in the inhibitory molecules, CTLA4 and PD-1 was found, as shown in **Figure 5-14**. CTLA4 is a co-inhibitory molecule, which binds to CD80 on antigen presenting cells, and prevents activation of T cells[197]. PD-1 is another inhibitory molecule, which acts as an inhibitory checkpoint on T cells and regulates their activation[198].

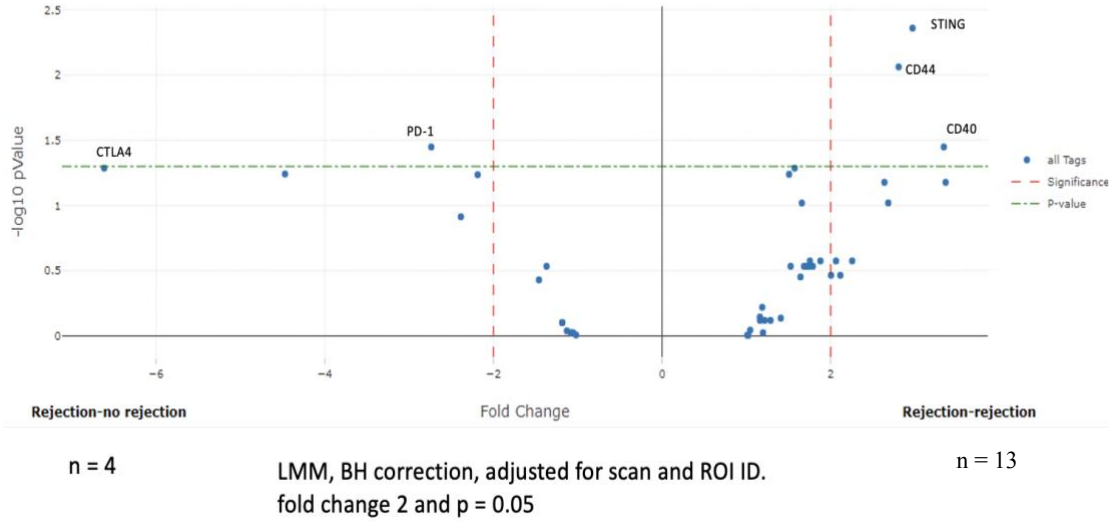

Figure 5-14. Volcano plot of differential protein expression in epidermal ROIs at rejection versus protocol time points. *In this graph, epidermal ROIs at rejection are compared to epidermal ROIs at protocol time points. CD40, CD44 and STING are significantly upregulated at rejection time points in the epidermal ROIs. At protocol time points CTLA4 and PD-1 are upregulated. Red dashed line = significant fold change, green dashed line = significant p value.*

When comparing perivascular to epidermal regions of interest (ROIs), there was an upregulation of nearly every protein in the panel in the perivascular ROIs, suggesting that the perivascular regions were the predominant sites of immune activation. The only exception was panCK, which was more highly enriched in the epidermal ROIs, **Figure 5-15**.

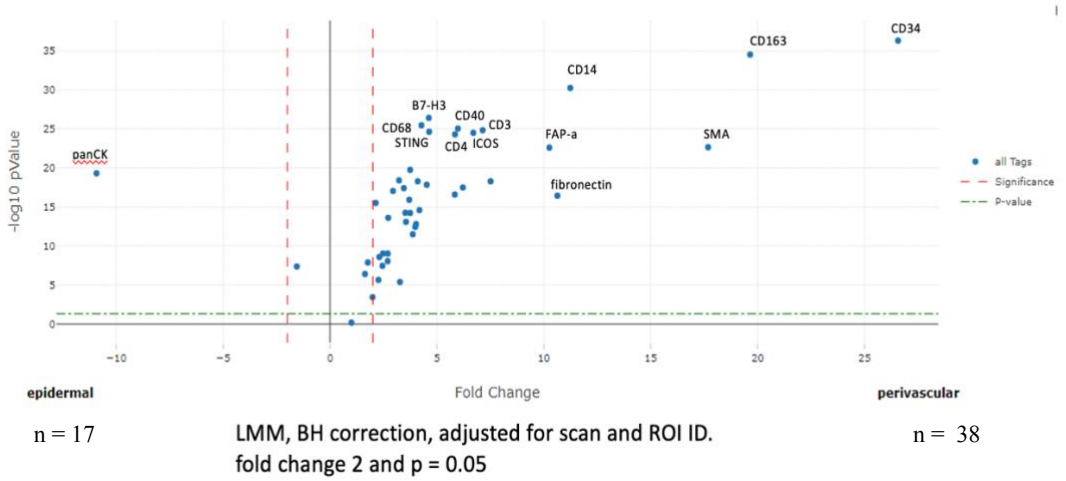

Figure 5-15. Volcano plot of differential protein expression in epidermal ROIs versus perivascular ROIs. *In this graph, epidermal ROIs are compared to perivascular ROIs at all time points (rejection and protocol). Nearly all the proteins are more highly expressed in the perivascular ROIs, except for panCK which is most upregulated in the epidermal ROIs. Red dashed line = significant fold change, green dashed line = significant p value.*

The results in this section support the hypothesis that the changes seen in gene expression at rejection in the skin, will be reflected in the spatial analysis of protein expression, demonstrated by increases in CXCL9 found in perivascular ROIs also noted to be one of the most significantly differentially upregulated genes.

5.4 Discussion

In this chapter, the local immune response in skin samples from patients who have had a combined skin and solid organ transplant was examined. Samples from patients who had a sentinel skin flap and simultaneous pancreas-kidney (SPK) transplant were combined with those who had an abdominal wall or SSF and small bowel transplant.

Samples have been examined to explore what happens at rejection, and to examine how gene expression changes over time post-transplantation.

There are no reports in the literature of how gene expression changes over time after a primarily vascularised skin transplant, rather most studies focus on what happens at rejection. However, it is valuable to understand what the likely baseline expression is at different time points after transplant, when trying to evaluate which changes are due to immunosuppression and which due to the alloresponse. In comparison to the findings in the blood (see Chapter 3), there were fewer differentially expressed genes found at three months post-transplant in the skin, when compared to a baseline of pre-transplant. Only one of these, *MYC*, was also downregulated in the blood at the same time. As this is an essential transcription factor, found in both innate and adaptive immune cells, this is perhaps unsurprising[199] . It is interesting to note that in the blood there was downregulation of far more genes, with a strong T cell pathway association, whereas in skin there were fewer genes, and these were mostly innate immune cell related. Furthermore, the number of genes downregulated increased in the skin at six months, whereas in the blood they decreased. There are a few explanations for this difference. I found fewer genes overall above threshold in the skin samples than the blood, **Figure 5-16**, so there was a smaller pool to look at in the skin. However, there was still a good number of probes above threshold in the skin. It may also reflect differences in the genes that expressed in the blood versus the skin.

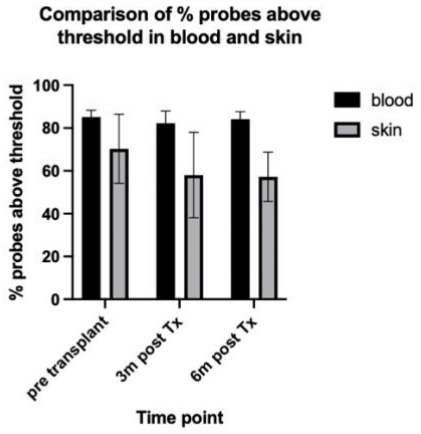

Figure 5-16. Graph to show the % of probes in the nCounter HOT panel above threshold, comparing blood to skin samples. *This bar chart shows the % of probes above threshold at the different protocol time points for blood (black) and skin (grey) samples. Mean +/- standard deviation. Based on matched samples from 7 patients.*

Differential gene expression, by its nature is a relative assessment, so the fact the skin had fewer differentially expressed genes, suggests that immune cells in the skin were less affected by immunosuppression that in the blood. This would fit well with the knowledge that there is a proportionally larger number of memory T cells in the skin than blood and these are less affected by immunosuppression than naïve T cells[200]. The samples from small bowel are harder to compare as they were not taken at protocol time points like the blood and skin. There were no significant differences in gene expression in the small bowel when comparing samples at less than six months post-transplant to more than six months post-transplant.

When using gene expression in samples for immune monitoring, there is a suggestion that it may be beneficial to look at skin in preference to the blood, for evidence that rejection is taking place. The skin samples taken at rejection in SSF patients showed more evidence of clustering on PCA analysis than the blood samples. As discussed in the previous paragraph it also seems that gene expression in the skin is less affected by immunosuppression than it is in the blood. As the techniques to analyse tissues develop, it is possible to explore the local immune response to transplantation in more depth and biopsies from SSF offer the ideal way to both monitor solid organ transplants and learn more about the alloresponse to skin transplantation.

In this chapter I was able to combine the two cohorts of abdominal wall and sentinel skin flap patients to gain insights into the transplanted skin at rejection. It was interesting to identify *CXCL9* and *10* as the most differentially expressed genes at rejection. CXCL9 and 10 are chemotaxis-inducing cytokines, which attract activated T cells to sites of inflammation[201,202]. Upregulation of these genes at rejection correlates with an increase in T cells infiltrating the allograft. Both CXCL9 and 10 bind to the CXCR3 receptor, found on T cells. They are induced by interferon-γ, which itself is regulated by IRF1. Interferon-γ signals via the JAK-STAT pathway[203]. Both IRF1 and STAT1 were found to be upregulated in this cohort at rejection. These results are consistent with results published by Borges et al, who found an increase in several chemokines, including CXCL9, at rejection in hand transplant biopsies[150]. The GeoMx DSP analysis also found an increase in CXCL9 protein expression at rejection in the perivascular regions of interest, suggesting that this marker does indeed play a role specifically at the site of rejection in the skin. It should be noted that CXCL9 and 10 are

not specific for rejection but are also upregulated in other inflammatory skin conditions[204].

In general, the results from the gene expression analysis of skin samples in this chapter, align well with those already published in the literature looking at face and hand transplant biopsies.[96,150] This includes upregulation of genes associated with T cell activation, infiltration, and chemokine-mediated signalling. In previous chapters which analysed blood and small bowel samples, a significant difference in gene expression at rejection was not found, although this was potentially due to the small number of samples available for analysis. It should be mentioned that the use of a targeted gene expression panel here has limited what is able to be found, with a bias towards immune pathways, organ rejection and tissue damage.

Spatially resolved protein analysis has allowed a more in-depth review of specific areas in the skin during rejection. It has been demonstrated that both T cell activation and monocyte markers were upregulated in perivascular regions of interest (ROIs) at rejection. This is in keeping with early histological studies, both Kanitakis et al (looking at hand transplant biopsies) and Cendales et al (looking at hand transplant and abdominal wall biopsies) found that infiltrates of leukocytes originated in perivascular regions, before migrating into the dermis and involving the epidermis[92,192]. This is perhaps not surprising as a key route for circulating cells to enter tissues is via blood vessels. It also correlates with a study from Borges et al, which analysed samples from face VCA patients and found an increase in both $CD14^+$ monocytes and $CD3^+$ T cells in skin biopsies at rejection[156].

In this study there was an increase in IDO1 in perivascular ROIs at rejection, and in the gene expression data at rejection. This is consistent with findings from Hautz et al, who demonstrated an upregulation of IDO staining on histological examination of skin samples from hand transplant patients[97]. Elevated levels of IDO have also been found in kidney biopsies during acute rejection in kidney transplant patients[205].

Whilst Hautz et al also noted an increase in HLA-DR expression in perivascular regions at rejection[97], there was not a significant increase noted in the perivascular regions in this cohort. However, the gene expression data did show that there was a significant upregulation of HLA-DR at rejection in the skin samples. It may be that the smaller sample of skin biopsies analysed using spatially resolved protein analysis meant this was not found, or perhaps that in these samples the cells expressing HLA-DR are elsewhere in the skin.

On comparison with small bowel crypt ROIs, similar proteins were found to be upregulated at rejection in the skin perivascular ROIs namely those related to T cell and monocyte signatures. On direct comparison of $CD45^+$ AOIs at rejection between the skin and small bowel samples, there were no significant differences in protein expression, **Figure 5-17**. This further supports the concept that skin may be a useful monitor for the immune response in the small bowel transplant.

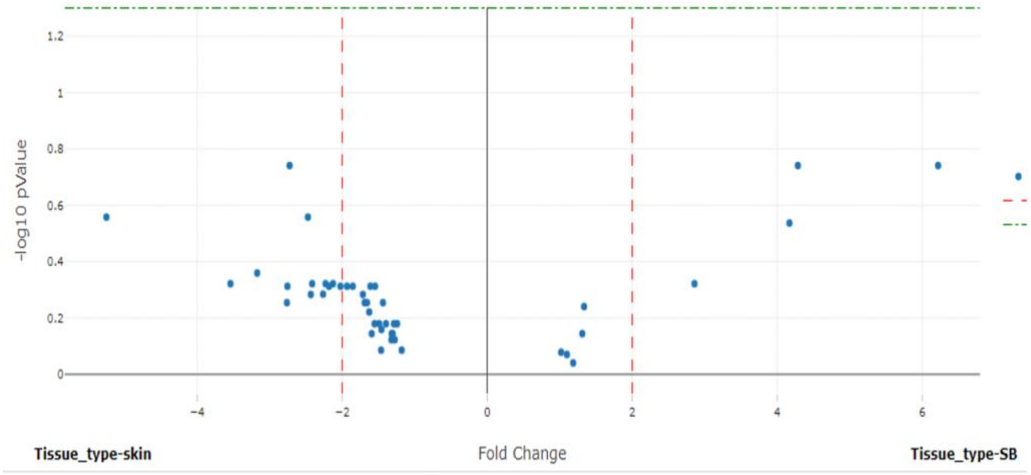

Figure 5-17. Volcano plot of differential protein expression in small bowel ROIs versus skin ROIs. *In this graph, small bowel ROIs are compared to skin ROIs. There are no significantly differentially expressed proteins. Red dashed line = significant fold change, green dashed line = significant p value.*

In this chapter it has been demonstrated that biopsies from the skin in combined skin and small bowel transplantation have a similar gene profile at rejection to those already published in the literature. Spatially resolved protein analysis has confirmed that perivascular regions of interest are important at rejection and have differential protein expression. The findings in the blood and skin are different, highlighting the importance of including the local alloresponse when trying to unravel the mechanisms involved in rejection. It is reassuring to see that the immune profile at rejection appears similar in skin and small bowel on molecular analysis and provides further support for the concept of sentinel skin flaps for immune monitoring in solid organ transplantation.

6 Chapter 6. The use of a novel mouse model to explore the role of Langerhans cells in skin allograft rejection.

6.1 Introduction

A unique feature of skin is the presence of Langerhans cells (LCs), a population of mononuclear phagocytes, which reside specifically in the epidermis[60]. These cells were first described in 1868[206], but it was not until the 1980s that their role as potent antigen presenting cells (APCs) was recognised[207]. Further research has found they have important sentinel functions, sampling antigen at the epidermis, upregulating Class II MHC and co-stimulatory molecules and migrating to lymph nodes where they activate naïve T cells[208–211].

There is therefore an assumption that LCs play a key role in skin graft donor LCs migrating from the graft to the draining lymph nodes to present antigen via the direct pathway[212]. The importance of lymphatics in acute skin graft rejection was noted in experiments in the 1960s, where the recipient graft bed was isolated on a vascular pedicle with and without lymphatic drainage[121]. Skin graft survival was increased when the lymphatic drainage was interrupted, indicating that afferent lymphatic drainage was required for acute rejection to take place. It has also been demonstrated that in the absence of secondary lymphoid tissues (lymph nodes, Peyer's patches, and spleen) cardiac allografts in a mouse model are accepted indefinitely[213]. This further supports a role for LC migration in allograft rejection. The significance of lymphatic drainage was not fully understood until later, when it became clear that antigen presenting cells in the skin such as Langerhans cells or dermal dendritic cells migrate via lymphatics to draining lymph

nodes[214–216] where they present antigen to naïve T cells, promoting T cell activation before they traffic back to skin[216].

Further support for the role of LCs in acute skin graft rejection was the finding by Chen et al that the density of LCs in the skin related to the rate of graft rejection, with rat trunk skin grafts rejecting faster than tail or ear skin grafts (which have fewer LCs in them)[217]. He et al studied the differences in rejection between heart and skin allografts in a mouse model[218], noting that skin grafts were rejected more quickly than heart allografts. This was attributed to the presence of LCs in the skin along with the differences in vascularisation of the transplants.

Contrary to the studies discussed so far, Obhrai et al demonstrated that LCs were not required for acute skin graft rejection in a mouse model in which LCs were deleted by the insertion of the diphtheria toxin receptor at the site of langerin expression (specific for LCs) [212]. Skin grafts from these mice were compared to wild type skin grafts in a fully allogenic model, in which both were rejected in a similar time frame. When they performed the same experiment in an H-Y mismatch they found that the LC-deficient grafts were rejected, whereas the wild type grafts were not, suggesting a role for LCs in graft tolerance.

There is growing recognition that LCs may have a tolerogenic role to play in skin immunity[206]. The skin is an important barrier organ and LCs are constantly being exposed to foreign antigens. Hemmi et al demonstrated in a mouse model that in non-inflammatory conditions, melanin granules were trafficked from the skin to regional lymph nodes, by

TGFβ-dependent cells (thought to be dendritic cells), without provoking an immune response[219]. This demonstrates both a role for LCs in the trafficking of antigen from skin to the lymph node and indicates that the conditions in which antigen is encountered may alter the response generated. Hawiger et al used a mouse model to deliver antigen directly to dendritic cells (DCs), via a monoclonal antibody (i.e., without an associated injury)[220]. Whilst they noted initial proliferation of T cells, these did not become polarized to a Th1 response and within 7 days numbers of antigen specific T cells were significantly reduced. However, when they delivered antigen along with an anti-CD40 agonist antibody (i.e., a stimulated environment) this resulted in T cell activation. From this they surmised that in the absence of additional stimuli DCs trafficking to lymph nodes result in peripheral tolerance. Further research has demonstrated the important role that context plays in how LCs respond. Seneschal et al isolated human LCs, dermal DCs and skin resident memory T cells, and cultured them together[67]. They found that LCs but not dermal DCs resulted in a proliferation of the skin resident memory T cells. On further characterisation a significant proportion of these proliferating skin resident memory T cells were $CD4^+$, $CD25^+$, $FOXP3^+$, $CD127^-$, $CTLA4^+$, $GITR^+$ consistent with a regulatory phenotype. When tested in a secondary mixed lymphocyte reaction, these Tregs suppressed proliferation of skin resident memory T effector cells. They used immunofluorescence to demonstrate co-localisation of LCs and skin resident regulatory T cells in human skin samples. However, they found that if *C.albicans* (a skin commensal that when intradermal can cause delayed hypersensitivity) is added to cultures, the LCs induce both regulatory and effector memory T cells. Higher doses of *C.albicans* induce higher proportions of effector memory T cells, whereas at lower doses this switches to higher proportion of the Tregs. In summary they demonstrated that the environmental context changed how the

LCs responded, with a more tolerogenic outcome at "steady state" compared to when an insult is detected, which led to effector activation.

While significant progress has been made in understanding the role of LCs in normal skin immunity, there are still questions remaining. In part this is because the mouse models that are routinely used to explore the mechanisms underlying the immune response do not fully reflect human skin antigen presenting cells[221]. Of note humans express five isoforms of the CD1 antigen presenting system, which is comprised of three groups: group 1 (CD1a, CD1b, CD1c), group 2 (CD1d) and group 3 (CD1e)[221]. Mice do not express any of the group 1 isoforms[221]. CD1 receptors are related to MHC Class I receptors and have been found to present lipid to T cells[222,223]. The CD1 receptors are less polymorphic than the MHC receptors, with limited variation between people, making them an interesting potential therapeutic target[221]. They are also mostly expressed on antigen presenting cells, with CD1a highly expressed on LCs[224]. Mice lack these CD1 molecules and are therefore unlikely to give a complete view of how lipid antigen presentation may affect the alloresponse. Of interest, a recent study of gene expression analysis in human face transplant biopsies found a significant increase in genes associated with lipid presentation (*CD1B, CD1C, CD1D*) in the skin at rejection (grade 3 Banff)[96]. Using high throughput TCR sequencing they demonstrated an increase in CD1b and CD1c receptors in the skin (but not blood) at rejection, suggesting a possible role for lipid presentation in mediating rejection in the skin.

The last 10 years has seen the development of human CD1 transgenic mouse models. Felio et al reported on a transgenic mouse model, which included the entire coding region

of human CD1a – d[225]. Using this model, they demonstrated the group 1 CD1 receptors presented mycobacterial lipid antigens to T cells resulting in their activation. It has also been found (using the same model) that group 1 CD1 molecules play a role in recognising *Staph. aureus* – derived lipids and developing a specific T cell response[226]. Kobayashi et al developed a similar mouse model, but specifically including only the human CD1a gene[227]. This model was then used to demonstrate a key role for CD1a in the skin inflammation caused by the plant lipid urushiol, with the development of skin inflammation abrogated when CD1a was blocked[228]. More recently Hardman et al have developed a human CD1a transgenic mouse model and used this to demonstrate that systemic effects of cutaneous inflammation are mediated by CD1a[229]. They showed that CD1a-transgenic mice, treated with imiquimod (a TLR7 agonist), developed significant splenomegaly and expansion of peripheral blood and spleen T cell compartments, compared to their wild type counterparts, which could be prevented by use of a CD1a blocking antibody.

6.2 Chapter 6 aims and hypothesis.

In this chapter the aim is to explore the role of the antigen presentation pathway in a human transgenic mouse model of skin transplantation. In this model, with collaborators, we have developed a transgenic mouse in which a human Langerhans cell-associated allorecognition pathway has been expressed although due to non-disclosure agreements, it is not possible to provide further details of the precise molecule being targeted. In this preliminary study, this model is used to investigate the contribution of this specific component of the antigen presentation pathway to acute rejection of skin. We hypothesise

that modifying a Langerhans cell-specific component of the antigen presentation pathway will promote skin graft survival in a human transgenic mouse model.

6.3 Results

All mice received a tail skin graft taken from a human transgenic donor mouse. Donor mice were treated preoperatively with IP injections of either an antibody to modify the LC-associated pathway or placebo. After skin transplantation, recipient mice continued to receive IP injections of antibody every 72h and the other half received a placebo (n=11 mice/group), **Figure 6-1**.

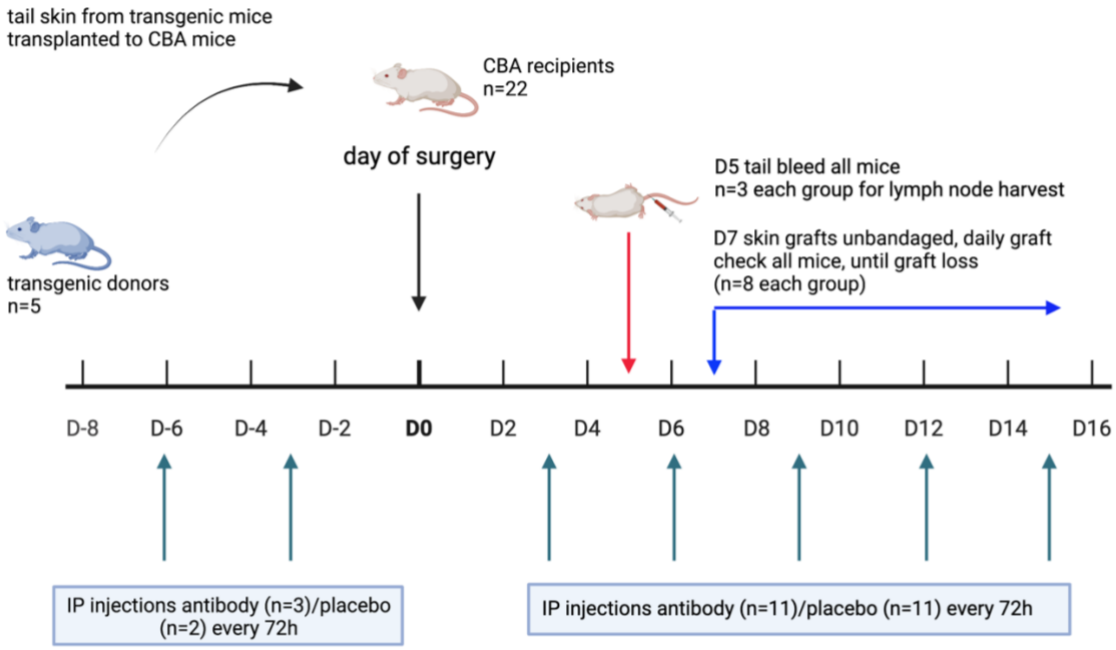

Figure 6-1. Overview of experimental design. *Tail skin from transgenic mice transplanted to CBA recipients. IP injections were given every 72h, there were two experimental groups, one received placebo the other the antibody. On day 5, tail bleeds of all transplant recipient mice were taken, and flow cytometric analysis undertaken to characterise the immune response. At the same time a subset of three of these mice in each group underwent lymph node harvest. The remaining 16 mice were followed up*

until all the skin grafts had failed, which occurred by day 16. Created with BioRender.com

6.3.1 Modifying a Langerhans cell-related antigen presentation pathway leads to decreased skin graft survival.

Skin grafts were monitored daily from day 7 post-operatively for signs of acute rejection and scored according to Zhao et al[141], with high scores indicating a healthy graft and low scores increasing graft loss, 0 indicating complete loss. Next, the two groups of mice were monitored for skin graft survival. As shown in **Figure 6-2**, the placebo group demonstrated longer skin graft survival than the antibody. Median survival time of skin grafts in the antibody group was 12 days versus 14 days for the placebo group. This was an unexpected finding given that modifying this antigen presentation pathway was hypothesised to promote graft survival.

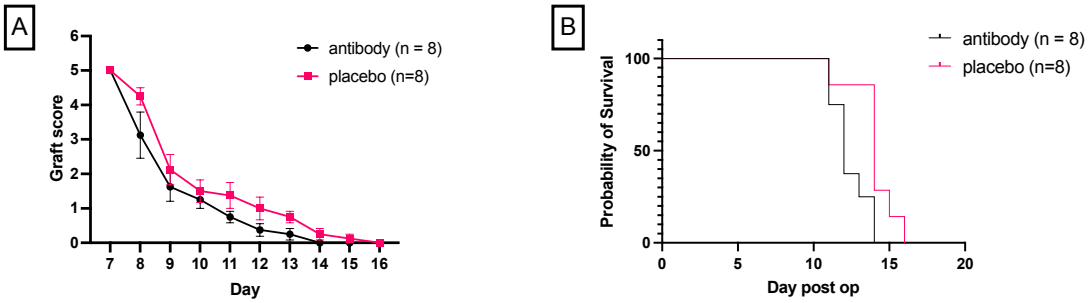

Figure 6-2. Modifying a Langerhans-related antigen presentation pathway leads to decreased skin graft survival. *CBA recipient mice were grafted with tail skin from donor transgenic human mice from one of two groups. Half had received an antibody which blocked part of the antigen presentation pathway, the other half had received a placebo. These two groups were maintained in the recipient mice, who also received IP injections every 72h of either antibody to block part of the antigen presentation pathway or placebo. Monitoring of skin grafts commenced at day 7. A. shows the skin*

graft scores for the two groups, demonstrating lower scores (indicating more rejection) for the equivalent time points in the antibody group. However, no significant difference was found between the two groups (two-way repeated measure ANOVA). The mean +/- standard error of mean is shown. B. includes the skin graft survival curves for mice receiving both the antibody (which blocks a skin-specific antigen presentation pathway) and placebo. It demonstrates decreased survival for the antibody group. The curves were found to be significantly different from each other (Log-rank test p = 0.04). n=8 mice/group.

6.3.2 Circulating T cell numbers and subsets were similar between the two experimental groups prior to acute rejection.

Blood samples were taken from all mice at day 5. This was chosen as previous experience with this model had indicated that rejection would start from day 7-8. The goal was to identify if modifying the antigen presentation pathway led to changes in circulating T cell expansion. As shown in **Figure 6-3**, there were no significant differences in the number of $CD4^+$ T cells, $CD8^+$ T cells or Treg cells between the two groups. Furthermore, there was no difference in proliferation ($Ki67^+$ cells) between the two groups, as shown in **Figure 6-3**.

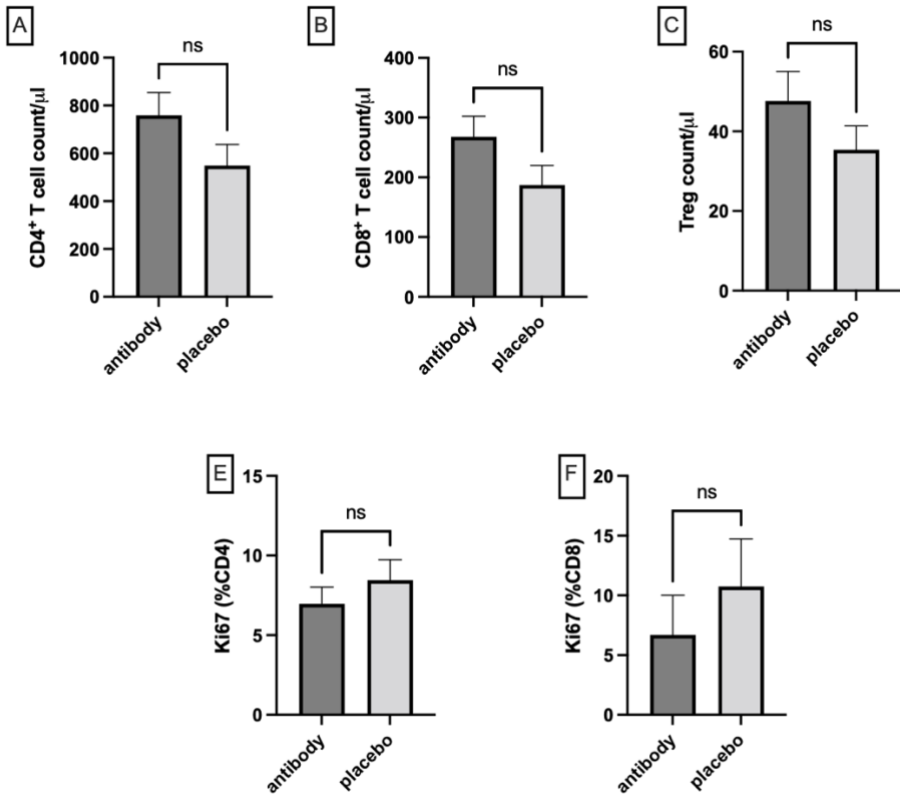

Figure 6-3. Circulating T cell subsets in blood at day 5 post skin transplantation. *A. CD4$^+$ T cell counts. B. CD8$^+$ T cell counts. C. Treg counts. D. % Ki67$^+$CD4$^+$ T cells. E. % Ki67$^+$CD8$^+$ T cells. Graphs show mean count + standard error of the mean (SEM). There were no significant differences found between the two groups. n=11 mice/group. Unpaired t-test p > 0.05. The FACS analysis of these samples was undertaken by Dr C. Hardman, one of our collaborators.*

6.3.3 Modifying a part of the antigen presentation pathway did not change T cell counts or activation in either draining or contralateral lymph nodes.

APCs migrate from skin to the draining lymph nodes, leading to activation of T cells. To determine if the antibody results in reduced T cell activation in draining lymph nodes, a subset of six mice (three from each group) were sacrificed at day 5 post-transplantation and the draining and contralateral lymph nodes were harvested for flow cytometric

analysis, **Figure 6-4**. There were no significant differences found in either the total T cell count, $CD4^+$ T cells or $CD8^+$ T cells in the draining lymph nodes between the two groups, or the contralateral lymph nodes between the two groups. Furthermore, there were no significant differences in the number of activated $CD4^+$ or $CD8^+$ T cells (identified by $CD69^+$). As would be expected the draining lymph nodes had higher numbers of T cells, in both groups when compared to the contralateral side. Overall, these findings suggest that treatment did not affect T cell activation in the lymph nodes at this early time point.

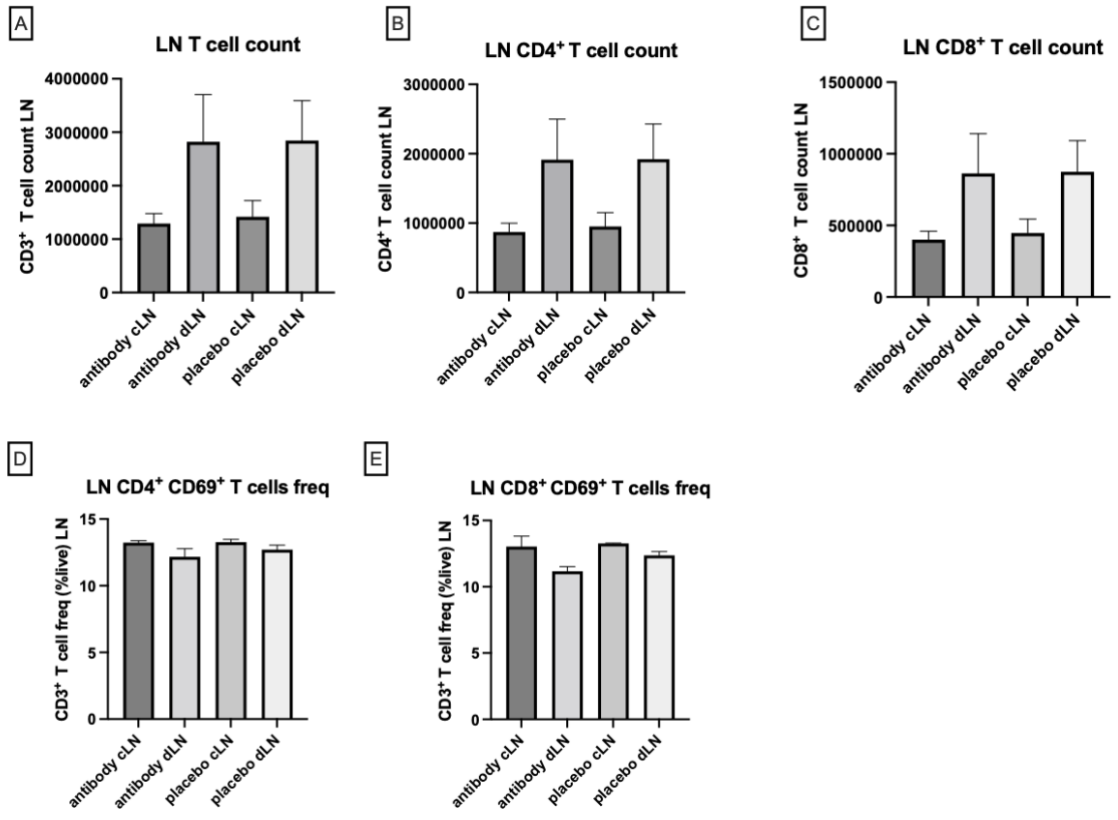

Figure 6-4. T cell counts and frequency of activated T cells in lymph nodes at day 5 post-transplantation. *Flow cytometric analysis of T cell numbers and subsets in the draining and contralateral lymph nodes at 5 days post-transplantation. Each graph shows data for group given the antibody to modify the antigen presentation pathway ("antibody") and placebo groups for the draining (dLN) and contralateral (cLN) lymph*

nodes. The mean count or frequency is shown +/- standard error of the mean, n=3 mice/group. There are clear differences in numbers seen between the draining and contralateral lymph node, as would be expected. There were no significant differences noted between the placebo and antibody group. The FACS analysis of these samples was undertaken by Dr C. Hardman, one of our collaborators.

6.3.4 Fewer Langerhans cells were noted in the contralateral lymph node of mice when the antigen presentation pathway was modified.

We next asked whether treatment reduces the number of LCs migrating to the lymph nodes. However, as shown in **Figure 6-5**, this was only found to hold true for the contralateral lymph nodes, indicating that treatment only seemed to have an effect at steady state.

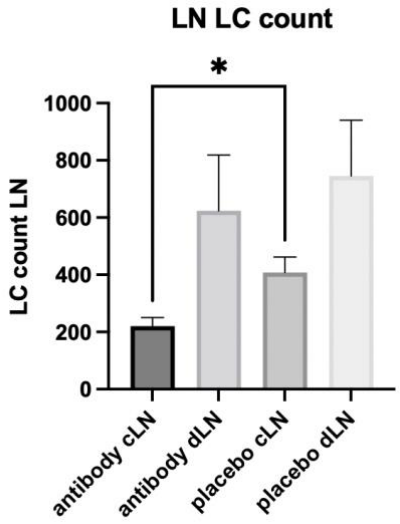

Figure 6-5. Langerhans cell count in lymph nodes at day 5 post-transplantation. *Flow cytometric analysis of Langerhans cells (CD207^{+}, human CD1a $^{+}$) in the lymph nodes. The graph shows data for antibody and placebo groups for the draining (dLN) and contralateral (cLN) lymph nodes. The mean count or frequency is shown +/- standard error of the mean. Data is based on six mice, three from each group. There are clear*

differences in numbers seen between the draining and contralateral lymph node, as would be expected. Of note there was a significant difference ($p<0.05$) in number of Langerhans cells in the contralateral lymph nodes between the two groups. The FACS analysis of these samples was undertaken by Dr C. Hardman, one of our collaborators.

6.4 Discussion

The results in this chapter show that contrary to our original hypothesis, modifying the Langerhans cell-related antigen presentation pathway led to a decrease in survival of a skin graft, from a median survival time of 14 days to 12 days. There were no significant differences in circulating T cells at day 5 post-transplantation between the two experimental groups. There were also no significant differences in T cell numbers within the lymph nodes at this point. This is consistent with data from Obhrai et al, who found that blocking Langerhans cells did not prevent rejection, likely due to other antigen presentation cells causing activation of T cells[212]. However, it is interesting that in this study, modifying the antigen presentation pathway has resulted in faster rejection. It is becoming clear that the skin resident immune cells form a complex regulatory system to maintain skin homeostasis[230]. Seneschal et al have demonstrated that when cultured together human LCs stimulate skin-resident memory T cells to proliferate, a proportion of which have been characterised as regulatory in function[67]. It is possible that modifying the pathway in this model has disrupted the ability of the LCs to stimulate skin-resident memory T cells, resulting in a pro-effector memory T cell proliferation and therefore earlier rejection. This hypothesis[8] is supported by the finding of Obhrai et al that blocking LCs in a minor mismatch transplant model prevented the development of tolerance[212].

To explore this further, in the future we plan to repeat these experiments and focus on characterising the LC and resident memory T cell populations in the skin. We will use a combination of FACS analysis and immunohistochemistry/fluorescence to identify differences that occur when modifying the LCs-related antigen presentation pathway. We predict that there will be fewer skin resident memory Tregs in the group where this pathway is modified, along with increases in skin resident effector T cells. We will look for co-localisation of LCs and memory T cells within the skin prior to rejection, and the numbers of these cells and their location within the skin.

In this study it was demonstrated that modifying the LCs-related antigen presentation pathway resulted in fewer LCs in the contralateral lymph node. This may be a result of less trafficking to the lymph nodes, less proliferation of the LCs, less migration of the LCs or more cell death. To investigate this further we plan to use FACS analysis of the skin, to include markers of cell proliferation (Ki67) and cell death (Live/Dead), along with maturation markers (CD86, CD40) to look for differences between the two groups. It would be interesting to repeat this study, transplanting male transgenic skin grafts to female recipient mice. This would allow tracking of donor LCs and T cells, utilising the XY differences for identification, to see if there are differences in the donor or recipient cells between groups and to visualise where they go.

These preliminary findings suggest the LC-related antigen presentation pathway is contributing to the alloresponse in skin graft rejection. As has been discussed in the introduction it has been recognised that lipid presentation by CD1a plays an important role in several inflammatory and infectious skin disorders[223,225,226,228]. The finding by Win

et al that *CD1B*, *CD1C* and *CD1D* were elevated at rejection in face transplant skin biopsies supports the idea that the lipid presentation pathway may contribute to the alloresponse[96]. The role of lipid presentation in transplantation has not been explored in this model before and offers a new therapeutic target for future assessment.

7 Chapter 7. Discussion and future directions

7.1 Introduction

The concept of a sentinel skin flap was developed to provide a way to continuously monitor transplanted tissues, whether solid organs, or vascularised composite allografts. Rather than waiting for evidence of graft dysfunction to prompt a test, or regularly taking blood samples at protocol time points, the sentinel skin flap acts as a "window" into the recipient's alloresponse to the transplant[127]. Skin develops a rash on rejection, that is visible to both the patient and medical team. This then acts as a prompt to investigate further or alter the immunosuppression being given. The sentinel skin flap also offers an easily accessible site for biopsies, with the potential to avoid morbidity from a biopsy of the transplanted organ.

Our team in Oxford has undertaken the first clinical trial of sentinel skin flaps for immune monitoring of simultaneous kidney pancreas, or pancreas alone transplants. It has been found to be safe for patients and of interest there are reduced rates of acute rejection in the first 12 months in both the skin and the solid organ transplant. As part of this study, samples were collected including blood samples and sentinel skin flap biopsies. These were taken at clinical trial protocol time points and when rejection was suspected. Oxford is also the only centre in the UK to perform combined abdominal wall and small bowel transplants. This has enabled the collection of a unique biobank of samples from patients who have undergone combined skin and solid organ transplants. These samples have been used in this thesis to perform the first in depth immunophenotyping of the response to a combined skin and solid organ transplant. A

pilot study, in a human transgenic mouse model has also been included. This focussed on the role of Langerhans cell-related pathways in skin graft rejection.

7.2 Summary of key findings

7.2.1 This thesis is the first in-depth immunological study of combined skin and solid organ transplants.

In this thesis a combination of flow cytometry, gene expression analysis and spatially resolved protein analysis has been used, to characterise the immune response in a combination of blood, skin and small bowel samples from patients who have had a combined skin and solid organ transplant. Less than 40 cases of this type of combined transplant have been reported[231]. This is a novel cohort of patients, for which in-depth immunological studies both longitudinally post-transplantation and at acute rejection have been reported on for the first time.

7.2.2 Repopulation of immune cell subsets post-transplantation are consistent with the reported literature.

The addition of a sentinel skin flap does not appear to have altered the immune cell repopulation in the blood samples of patients undergoing combined skin and SPK transplantation, when compared to the literature for kidney transplantation, where the same immunosuppression has been used (Chapter 3). There has been discussion regarding the potential for the SSF to sensitise patients to their solid organ transplant, but no evidence to support this based on these results.

7.2.3 CXCL9 and CXCL10 are elevated in the skin at rejection in combined skin and solid organ transplants.

CXCL9 and *CXCL10* were found to be the most significantly differentially expressed genes in the skin at rejection. Furthermore, CXCL9 protein expression was significantly differentially expressed in perivascular regions in the skin at rejection (Chapter 5). This supports a role for CXCL9 and CXCL10 in acute rejection and suggests this pathway may be a future therapeutic target.

7.2.4 A potential role for cGAS-STING pathway in acute rejection in skin and small bowel transplants

Levels of the protein STING were found to be elevated in both crypt AOIs (small bowel samples) and epidermal ROIs (skin samples) at rejection (Chapters 4 and 5). Increased expression of *CGAS* and *IRF1*, genes related to the cGAS-STING pathway were also found in skin samples at rejection (Chapter 5). This pathway has been suggested as a possible mediator for the effects of donor-derived cell free DNA[190]. This is the first-time upregulation of this pathway has been found in transplantation and it offers a potentially novel therapeutic target for further investigation.

7.2.5 Modifying the Langerhans-cell related antigen presentation pathway decreases skin allograft survival in a mouse model.

This is the first time the role of lipid presentation in skin allograft survival has been explored. The preliminary findings from this model demonstrate decreased skin graft survival when this pathway is modified (Chapter 6) and suggest understanding this pathway in more detail may lead to new therapeutic targets in the future.

7.3 Discussion

There were initially concerns that the addition of a skin transplant would alter the immune response and potentially sensitise patients to the solid organ transplant. However, our hypothesis was that when given alemtuzumab induction immunotherapy the immune cell repopulation in these combined transplants would be very similar to that reported by several other groups in the literature, for cohorts with kidney transplants alone[144,146,149]. This was explored in Chapter 3 and found to be true. Significant depletion of T and B cells is noted at 6 weeks post-transplant and while B cell numbers show signs of recovery by 6 months, the T cells had not recovered to pre-transplant levels by 12 months post-transplant (Chapter 3). This thesis is one of few studies in the literature to provide in depth phenotyping of immune compartments over time post-transplant, for patients who have received induction immunosuppression with alemtuzumab and maintenance with mycophenolate mofetil and tacrolimus. In this cohort there is a skewing of T cells towards memory phenotypes post-transplantation, with an increase in $CD4^+$ effector memory T cells and $CD8^+$ TEMRA T cells (Chapter 3). This was also found by Bouvy et al (n=12)[148] and Trzonkowski et al (n=13)[149] in smaller cohorts of kidney patients and Borges et al in three patients who had a hand transplant[150]. This is therefore one of the larger studies of immune cell repopulation post-transplant, for patients receiving alemtuzumab induction immunotherapy and then tacrolimus and mycophenolate mofetil maintenance.

It is also one of the few studies to explore changes in gene expression over time post-transplantation in protocol blood samples. In keeping with the flow cytometry data there is significant downregulation of genes associated with T cell pathways at 3 months

post-transplant (Chapter 3). This was consistent with findings reported by Dorr et al who performed RNAseq analysis of PBMCs from kidney transplant patients[163]. This data will form the basis for ongoing investigations into the immune response to combined transplants. There is also no evidence from this analysis of the blood samples that there is an upregulation of the immune response at protocol time points resulting from the addition of skin compared to the immune repopulation reported in the literature.

However, it is interesting to note that there were differences in the gene expression post-transplantation found in the skin and blood from matched patients (Chapter 5). At three months post-transplantation in blood samples there were 29 genes significantly downregulated, in comparison in the skin samples there were only 10 genes significantly downregulated. Furthermore, these were different genes, with a predominance of T cell pathway related genes in the blood and innate immunity-related genes in the skin. Whilst gene expression seemed to recover in the blood at six months post-transplantation (only 5/29 genes remained downregulated), more genes (25) were downregulated in the skin at this time. This suggests that monitoring the immune response in the blood does not necessarily reflect the immune response in the skin. Understanding both will give a more complete picture of the alloresponse to transplantation and perhaps identify novel therapeutic targets.

Although in this thesis there was only a small group who had rejection, it was possible to see differences in immune cell subsets and gene expression in blood samples taken at protocol time points, compared to those who did not develop rejection in the first 12

months post-transplantation. There were differences visible even at pre-transplant time points before the patients had received any immunosuppression or a transplant. Notably the patients who did not have a rejection episode had a higher proportion of TEMRA $CD8^+$ T cells pre-transplantation, persisting post-transplantation (Chapter 3). This is consistent with a study from Betjes et al who studied a population of kidney transplant patients and found an increased number of TEMRA $CD8^+$ T cells was associated with decreased late allograft rejection[232]. These TEMRA $CD8^+$ T cells increase in number in healthy individuals as they age and are thought to be less alloreactive[232,233]. Of course, these results are caveated by the small numbers in the study, but if it were possible to identify those more at risk of rejection, pre-transplantation, this would be very beneficial for clinicians and patients and lead to the development of more personalised medicine.

Much of the transplant literature focuses on what is happening at the time of rejection. This has a significant impact on the outcomes of both the patient and the graft. There is an increasing understanding of the common pathways involved in rejection[8,9]. Although there is growing interest in the potential for non-invasive genetic biomarkers, it has proven difficult to develop reliable tests. Deng et al developed an 11 gene test (*PDCD1, SEMA7A, ITGA4, RHOU, MARCH8, WDR40A, ITGAM, FLT3, IL1R2, PF4, C6orf25*) to differentiate grade 0 from grade 3 acute rejection in heart transplantation[234]. They utilised known allotransplantation pathways and leucocyte microarrays to identify 252 candidate genes in PBMCs from patients with a heart transplant, enrolled in the CARGO (Cardiac Allograft Rejection Gene expression Observational) study. The aim was to reduce the need for heart transplant biopsy, a low test score meant a low chance

of grade 3 rejection. It was also noted that differences in test score related to time post-transplant, possibly related to steroid weaning in first 12 months. It should be noted that the validation sets were enriched for rejection samples compared to the prevalence that would be seen in normal population post-transplant. However, when tested with a more lifelike ratio of rejection samples to check the cut-off score, the test result was still applicable. This gene test has subsequently been commercialised and is available as the AlloMap™ test. All these genes, except *WDR40A* and *C6orf25*, are included in the NanoString HOT panel that has been used in this thesis. However, none were elevated in the blood at rejection, although it should be noted that these genes were validated on PBMC rather than whole blood, which may contribute to this finding. In the skin samples *SEMA7A* was found to be significantly upregulated at rejection, but none of the other genes from this test were upregulated. *SEMA7A* is a member of the semaphorin family and is thought to have a role in immune cell function, with expression increased on $CD4^+$ T cells and dendritic cells when activated[235].

Akalin et al used a subset of five genes based on the AlloMap test (*DCAF12, MARCH8, FLT3, IL1R2, PDCD1)* and explored their role in differentiating immune quiescence from acute cellular rejection in kidney transplant patients[236]. Patients in the DART (Diagnosing Acute Rejection in kidney Transplant recipients) study were enrolled, into both training and validation sets. Using the AlloMap test they found significant differences between samples with acute T cell mediated rejection and those which were quiescent (from stable patients). Although the gene test score did not significantly correlate with the AlloSure test (for dd-cfDNA), they found that both together had superior performance for discriminating between quiescent and acute cellular rejection

in whole blood samples. None of these genes were found to be upregulated in either blood or skin samples at rejection in the results reported in this thesis.

Li et al also reported their gene assay for identification of acute rejection, in kidney transplant patients[237]. Once again, they used whole blood samples, this time from a paediatric cohort of renal transplant patients, along with paired renal biopsies to diagnose rejection. Five genes *(DUSP1, MAPK9, NKTR, PBEF1,* and *PSEN1)*, central to leukocyte trafficking and T/B cell activation were found to be significantly differentially expressed at rejection, with reported 91% sensitivity and 94% specificity. This five gene panel was then validated in an independent cohort of samples. Only *PSEN1* was included in the NanoString HOT panel, and it was not found to be upregulated in either the blood or skin at rejection in the SSF patients. This work was then extended, looking in a larger population of mainly adult patients, recruited as part of the AART (Assessment of Acute Rejection in kidney Transplantation) study, from eight different centres[238]. A similar strategy was used, to identify differentially expressed genes at rejection versus stable time points, as diagnosed by kidney biopsy. In this study a 13 gene panel was identified (the kSORT assay), which was able to discriminate between acute rejection and stable samples with a sensitivity of 83% and specificity of 91%. The genes included were related to regulation of apoptosis and immune phenotype, with inclusion of pathways related to monocytes, T cells and endothelial cells. This was then validated in an independent set of samples, where it maintained the ability to identify acute rejection, up to 3 months prior to biopsy proven rejection. This seemed to hold promise as a potential non-invasive test for acute rejection in kidney transplantation.

However, this was challenged by Van Loon et al who independently assessed the validity of the kSORT assay in an undefined cohort of kidney transplant patients[239]. The goal was to determine the ability of the kSORT assay to detect acute rejection compared to a biopsy. This is in contrast to the original paper which had embarked on the initial study using only case-controls, and thereby missed out indeterminate samples. The authors performed a large multicentre cohort study (over 1000 samples), where both clinicians and those who ran the test were blinded and results were analysed by independent statisticians. The kSORT score was not significantly different between groups with or without acute rejection on biopsy, furthermore the kSORT risk categories were not associated with risk of acute rejection. In summary they were unable to validate its use. This study highlighted the challenges of developing a non-invasive biomarker test for rejection. The predictive ability of the test is affected both by the samples it is tested on (for example how rejection is defined, the number of rejection samples included, timing of the samples post transplantation) and the assumptions made about factors such as the prevalence of rejection in the population being tested (which would affect positive and negative predictive values). It also may partly explain why these genes were not found to be upregulated in the samples in this thesis.

Whilst this thesis did not identify any significantly differentially expressed genes in the blood samples, there were several differences found in the skin samples. Although taking a skin biopsy involves a procedure, it may be considered less invasive than a pancreas or kidney biopsy, with less morbidity associated with it, offering potential for

immune monitoring[127]. Borges et al found 57 genes that were differentially expressed at rejection, in skin biopsies from hand transplant patients[150]. The most upregulated genes included chemokines and chemokine-mediated signalling (*CXCL13, CCL18, CXCL9* and *CCL17*). They also noted an increase in T cell co-stimulatory molecules and effector immune molecules such as granzymes. Of note their study only included three patients. Furthermore, they did not adjust the reported p values to account for multiple comparisons. It is generally suggested that when performing gene expression analysis with panels of this size some form of adjustment is made to mitigate for false discoveries, hence in this thesis the Benjamini-Hochberg method was used (as detailed in Chapter 2). Win et al found 79 genes that were upregulated in rejection in skin samples from a single patient who had a face VCA[240]. Consistent with the findings from Borges et al[150] the interferon-γ signalling pathway was found to be upregulated at the time of rejection, with increases in *IRF1* and *STAT-1*[240]. There was an increase in *CXCL9* and *CCL5* and effector molecules including granzyme[240]. In this thesis 134 genes were found to be differentially expressed in skin samples at rejection, with *CXCL9* and *CXCL10* the most upregulated. Chemokine signalling pathway *(CXCL1/2, CXCR4, CCL2, CCL19, CXCL16)*, effector molecule (*KLRK1)* and antigen presenting and processing pathway (*HLA-DPB, HLA-DMB, PSMB, TAP1/2)* genes were also all found to be significantly upregulated at rejection in these samples, consistent with the previously reported literature.

Chemokines are known to play a role in the migration of leucocytes. Animal studies, utilising both gene knockouts and CXCR3 antagonists, have shown that CXCR3, the receptor for CXCL9 and CXCL10 is required for both cardiac, small intestine and skin

allograft rejection[241–243]. Intragraft levels of both CXCR3 and CXCL10 have been found to be elevated at rejection in endomyocardial biopsies from heart transplant patients, and human kidney and lung transplant biopsies[244–247]. Levels of *CXCR3* and *CXCL10* mRNA have also been found to be elevated in urine samples from patients with renal transplant rejection[248]. This was of note as collecting a urine sample is a non-invasive way to monitor for rejection, in contrast to taking a kidney biopsy. Furthermore, high pre-transplant serum levels of CXCL9 and CXCL10 have been associated with an increased risk of kidney allograft failure and rejection[249,250]. Therefore, the findings in this thesis of elevated CXCL9 and CXCL10 in skin samples at rejection are consistent with findings across different organ types in the literature.

Khatri et al performed a metanalysis of gene expression in tissue samples from 8 independent datasets, including four organ types (heart, kidney, lung and liver)[251]. They found a set of 11 genes (*BASP1, CD6, CXCL10, CXCL9, INPP5D, ISG20, LCK, NKG7, PSMB9, RUNX3*, and *TAP1*) which were consistently upregulated in acute rejection across all groups[251]. These genes were typically involved in T cell activation, migration or antigen presentation. Of these eleven genes, 5 (*CXCL10, CXCL9, INPP5D, PSMB9, TAP1*) were significantly upregulated in rejection in the skin samples in this thesis (Chapter 5), *BASP1* did not reach significance (adj p value 0.056). Four of these core genes were not expressed highly enough in skin to be included in analysis (*CD6, ISG20, NKG7, LCK*) and one (*RUNX3*) was not included in the nCounter HOT panel. This study is the first to report on the use of the common rejection module in vascularised skin transplants. Whilst this is a small dataset that has not been validated it provides useful information that can be used to guide further studies.

It is interesting to note that there are pathways, such as the CXCR3/CXCL9/10 axis or interferon-γ signalling, that are consistently elevated in acute allograft rejection, including in this thesis. However, it should be noted that these are not specific to transplantation but are also recognised in autoimmunity, tumour recognition and the immune response to infection[252]. When activated these genes lead to immune-mediated tissue specific destruction[252]. Therefore, finding an elevated CXCL9 level is not necessarily specific for allograft rejection, rather it indicates activation of a conserved response to damage. Furthermore, there are a number of factors that may alter the response to the initial immune trigger (whether that's recognition of an allograft or tumour) which make interpreting this data challenging. In their paper focusing on tumour biology, Wang et al propose a framework, where host factors, environmental factors and tumour factors all combine to alter the outcome of immune activation[252]. In the context of transplantation, it may be that donor factors (such as major or minor antigen expression, ischaemic period), environmental factors (concurrent infection, differing immunosuppression) or host factors (previous immune exposure, genetic polymorphisms) all combine to influence the outcome of allograft transplantation. This may also be why it has proved challenging to identify a biomarker for rejection, as many factors influence the immune response, and these are likely to be different between individuals.

Win et al, reporting on nine skin samples from seven face VCA patients found that *GZMB* was the most upregulated gene at rejection in the skin[96]. They noted upregulation of genes involved in interferon-γ pathways and T cell activation[96]. They

also found upregulation of immune checkpoint inhibitor genes such as *CTLA4* and immunoregulatory pathways including *FOXP3*. In general, the studies looking at gene expression analysis in VCA patients have small sample sizes, in part due to the low number of patients who have had a VCA, to date only 40 face VCAs have been reported[96]. Therefore, this thesis which includes 12 individual patients, and 23 samples is one of the largest reporting on gene expression in skin post-transplantation (Chapter 5). In this thesis *GZMB* was not found to be significantly elevated at rejection. There are several possible reasons for this, including differences in immunosuppression and the timing of sample biopsies. However, in common these were all skin samples showing grade 3 rejection, so it may be expected that a similar immune response would be found. Granzyme B is an effector molecule released by cytotoxic T cells, resulting ultimately in cell death. It has been associated with acute allograft rejection in many animal and human studies[253], therefore it is interesting that it has not been found to be elevated in this cohort, perhaps suggesting there may be an alternative pathway involved in mediating rejection in these combined transplants.

Both blood and small bowel samples were also analysed using the same NanoString HOT panel for gene expression analysis as the skin samples, but no significant differences were found when comparing rejection to protocol time points. This has been discussed in detail in the respective chapters (3 and 4). To summarise it is likely due to the small sample size available for analysis, along with heterogeneity in time point of samples, reducing the power of the study to identify differences.

As has been described elsewhere in this thesis (Chapter 1), the patient cohort studied in this thesis is extremely rare and there are very few samples for analysis. To try and mitigate for this spatial proteomics has been used to analyse samples from the skin and small bowel. This was to gain as much information as possible from the archived samples available. Spatial proteomics is an exciting new technique which provides an insight into how protein expression varies across the histological topography. It is of particular use in transplant samples, as the immune response is known to directly target the transplanted tissue, but up to now spatially resolved information has mostly come from immunohistochemistry studies. It is established that in different parts of the tissue different infiltrating cells are present, for example in skin rejection perivascular infiltrates are one of the first characteristics of rejection[92,94]. Spatial proteomics enables the analysis of upwards of 40 protein markers in an area <300μm in diameter. It was also used to confirm findings from the gene expression analysis. This is the first time this technique has been used to investigate rejection in transplanted skin and small bowel samples.

This thesis demonstrates that at rejection the perivascular ROIs in skin samples had enrichment of proteins related to T cell and monocyte activation as well as upregulation of CXCL9 (Chapter 5). These findings support the hypothesis that these regions are the site of the initial alloresponse. It also validates the findings of the gene expression analysis. However, it is not possible to be sure whether these cells are tissue resident or have migrated from the peripheral circulation. It is likely that it may be a combination of the two, as it is known that macrophages can be found in the perivascular regions and are capable of activating tissue resident T cells[71]. It is possible that macrophages

producing CXCL9 also result in T cells from the periphery being recruited to the perivascular regions.

It is interesting to note that the small bowel crypt AOIs also demonstrated upregulation of proteins related to monocyte activation at rejection. Furthermore, they were noted to have upregulation of proteins relating to interferon pathways, including STING. STING was also found to be upregulated in epidermal AOIs in skin samples at rejection. This finding was validated by the gene expression analysis of skin samples which found upregulation in *CGAS*, at rejection. As discussed in Chapter 4, cGAS is a sensor of cell free DNA and activates STING, leading to activation of the interferon pathway[191]. It has previously been suggested that the cGAS-STING pathway may be activated by donor-derived cell free DNA[190], but this is the first time this has been shown in human transplant samples.

The $CD45^+$ areas of interest from perivascular ROIs in the skin were compared to $CD45^+$ AOIs from crypt regions of interest in the small bowel (Chapters 4 and 5). Histological studies have suggested that these two areas are the principal areas that rejection takes place in the transplanted organs[35,92]. It was interesting to note that there was not a significant difference in the immune component at rejection in these two areas. This adds further support to the theory that the sentinel skin may be used as a surrogate marker for rejection taking place in the solid organ transplant.

Whilst it is important to understand the mechanisms of rejection, it is also interesting to attempt to understand why some patients had no rejection episodes when rates of skin

rejection are reported to be 85% in the first 12 months in the hand transplant population[55]. In this cohort of SSF and SPK patients the rate of acute rejection in the first 12 months was 20% for skin and 0% for the pancreas allografts. Not only is this reduced rate of rejection of benefit for patients, but it would also be of clinical relevance to know which patients are more at risk of developing rejection in the future. If it were possible to identify the patients most at risk of acute rejection, they could be monitored more closely, or potentially have adjusted immunosuppression. Similarly, understanding which patients are at low risk for rejection may provide the opportunity to tailor their immunosuppression accordingly.

There is the intriguing suggestion that the combination of primarily vascularised skin with a solid organ transplant is immunomodulatory is some way, as evidenced by the lower rates of rejection observed. The concept of a protective effect of certain solid organ transplants has been around for over 50 years. It was initially noticed in animal models of liver transplantation[254], but as experience grew in transplantation it was found to translate to humans. It was thought that this tolerance was due to chimerism between the donor and recipient, with the liver being an organ with many passenger leucocytes. Starzl et al were able to demonstrate this chimerism in a study of nine female patients who had received male liver transplants[255]. As more complex combined solid organ transplants began to take place it was observed that liver-kidney[256], multivisceral[257], heart-lung[258] and heart-kidney transplants[259] all had reduced rates of rejection, compared to single organ transplant. Rana et al analysed a large dataset from the United Network of Organ Sharing which confirmed the protective effect of combining either liver, heart, or kidney transplants with another organ. Interestingly this effect was not

seen with pancreas or intestine transplants, in fact the addition of these seemed to lead to worse outcomes[260].

Gerlach et al reported on the early Oxford experience of AWTx and small bowel (+/- modified multivisceral transplant) transplantation, reporting outcomes compared with a matched cohort of patients without an AWTx. These patients were managed within the same teams and given the same immunosuppression. They observed equivalent patient survival, fewer intestinal rejection episodes in the combined transplants and there was a decrease in misdiagnosis of viral infection (instead of rejection) in the combined transplant group, overall suggesting a protective effect of the combined skin and small bowel transplant[134].

In a larger review of the worldwide experience of AWTx and small bowel transplants (including the Oxford data), Honeyman et al also concluded that patient survival was equivalent to those patients who have small bowel transplant alone. They found that acute rejection rates for combined transplants in the first year were 35% for the AWTx and 22% for the small bowel transplant, comparing favourably to hand transplant and small bowel alone, 87.8% and 30-50% respectively. This supports the view that adding the AWTx may have a protective effect on transplant survival[52].

At present there are several hypotheses for why there may be a protective effect to combined transplants, but no definitive answer. It has been postulated that the size of the transplant affects the level of chimerism seen in the blood (with this being a positive effect, linked to tolerance)[261]. It has also been suggested that an increased antigenic load

(because of multiple transplants) may lead to immune "exhaustion". This concept was originally described in association with chronic viral infections but is increasingly being recognised in other contexts[262]. Crane et al propose the concept of "immune triage", when the immune system is faced with more than one insult, it may be required to prioritise. In their mouse model, they demonstrate that wound healing is delayed in the presence of a respiratory viral infection and suggest this may be due to prioritisation of the lung infection over the wound healing[263]. It is feasible to consider the dual transplant of skin and a solid organ may lead to a similar mechanism.

7.4 Future work

The main limitations to this thesis have been the sample size available and the lack of control groups. This is difficult to address as neither pancreas nor small bowel transplants are commonly performed in the UK. To increase the dataset, a successful application has been made both to the NIHR for funding of a case-controlled trial of sentinel skin flaps for immune monitoring of lung transplants and for HRA and ethical approval (see appendix 4, 20/WM/0026). The goal is to recruit 46 patients to have a combined SSF and lung transplant. These patients will have routine samples taken at the same time points as in the SSF and SPK study (pre-transplantation and 6 weeks, 3-, 6- and 12-months post-transplantation), as well as at rejection, **Figure 7-1**. Biopsies will also be taken from the lung transplant itself, as these patients routinely undergo bronchoscopy for immune monitoring as part of their follow up. This will provide matched blood, skin, and lung samples for analysis. Patients who have a lung transplant without a SSF will also be recruited, to undergo the same sample testing and provide a control group. Both groups will receive the standard post-operative management for

lung transplant recipients, including immunosuppression. Clinical data will be collected for both groups, including number of rejection episodes in the first year (lung and/or SSF), allograft survival (lung and/or SSF) and patient survival. These groups can then be compared, and it will be possible to see if the addition of a SSF affects the rejection rate in lung transplantation, or indeed influences allograft or patient survival.

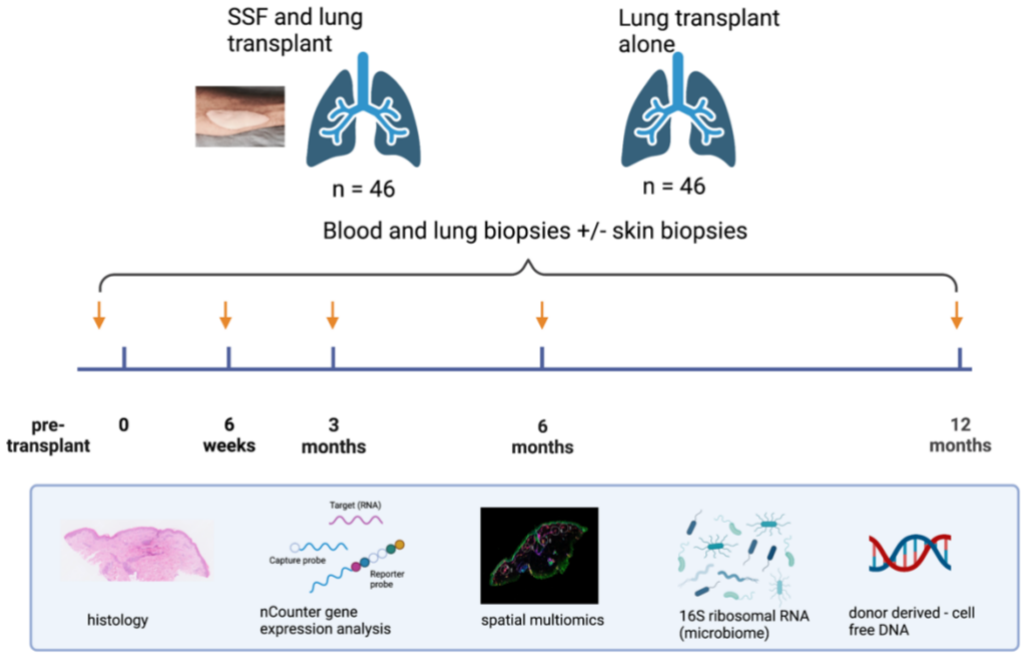

Figure 7-1. Overview of SSF and lung transplantation study*. The aim of this study is to recruit 46 patients to have a SSF and lung transplantation, along with a control group who have a lung transplant alone. Blood samples, lung biopsies +/- SSF biopsies will be taken at protocol time points, pre-transplantation, and 6 weeks, 3-, 6- and 12-months post-transplant. They will also be taken if a rejection episode occurs. A combination of techniques will be used, to analyse these samples, including histology, nCounter gene expression analysis, spatial multiomics,16S ribosomal RNA analysis and dd-cfDNA levels.*

The samples that are taken in this trial will provide further information about the immune response to a combined SSF and solid organ transplant. Rejection will be defined using the current gold standard of histological assessment, based on biopsies taken from the lung or SSF. It will be possible to assess whether rejection occurs concurrently by looking at matched SSF and lung transplant samples. The nCounter HOT panel will be used to analyse gene expression over time post-transplantation and at rejection, in blood, skin and lung biopsy samples. The results presented in this thesis suggest it is likely that differences will be found between the blood and tissue samples at protocol times post-transplantation. Furthermore, at rejection it is expected that chemokines such as CXCL9 and 10 will be elevated. The cGAS-STING/interferon-γ pathway will also be investigated further. As part of this the levels of dd-cfDNA will be measured at each of the protocol and rejection time points in these patients. The microbiome in the skin and lung samples will also be explored, by 16S ribosomal RNA sequencing. There is increasing evidence that the interaction between the microbiome and immune system plays a role in the immune response[264]. This cohort of samples taken prior to transplant and then at protocol and rejection time points post-transplantation will be used to explore the changes that occur due to transplant and that may be associated with rejection. Finally, a subset of the SSF and lung transplant biopsies will be analysed using spatial multiomics (either protein or mRNA expression), comparing rejection to protocol time points, as well as lung samples from combined transplants (with an SSF) and the control group (without an SSF). As demonstrated in this thesis, it is possible to collect data from very specific areas within tissues and then see what proteins are being expressed. In this thesis a protein panel consisting of 44

markers was used. It is possible to look at the mRNA being expressed in these regions, rather than proteins, and to assess the whole transcriptome. This would allow for more detailed deconvolution of which cell types and pathways are being activated in the chosen regions of interest. It may be possible, for example, to work out exactly what kind of T cell is present at rejection in the perivascular $CD45^+$ areas of interest. With a larger sample size and an appropriate control group it will be possible to explore whether the SSF is an accurate monitor for a matched lung transplant, and potentially whether it is having an immunomodulatory effect on solid organ transplantation. Furthermore, there is the opportunity to uncover the underlying mechanisms and identify new therapeutic targets.

To improve the analysis of the results presented in this thesis a further study has been proposed (REC 21/EE/0213, appendix 4) which will collect blood samples from patients who have either an SPK or pancreas alone transplant. These samples will be taken at the same protocol time points (pre-transplantation and 6 weeks, 3,6- and 12-months post-transplantation) and if rejection occurs. Clinical data including rates of rejection in the first 12 months, allograft and patient survival will also be collected. Participants will receive the same immunosuppression and other treatment as those who had a SSF and SPK. These samples will be analysed using the same flow cytometry panels and the nCounter HOT panel for gene expression analysis that were used in this thesis, to allow comparison to take place between participants who had a SSF and those who did not at both protocol and rejection time points. As lower rates of rejection were seen in the patients who had a SSF, it is anticipated there may be differences in the immune response between the two groups.

The methods described in this thesis generate large amounts of data. This provides the opportunity to uncover new mechanisms or pathways but requires careful analysis. One such method that has been developing in recent years is machine learning. This harnesses the power of mathematical algorithms, to simplify down large data sets to the points that contribute the most difference. This is likely to be a powerful method for identifying and validating markers of rejection. It will be possible to combine both the data gathered for this thesis, with the results from the proposed trials and use both to look for further common markers of rejection.

A larger sample size will allow us to confirm the findings we have seen so far and hopefully to uncover more details of the mechanisms involved. It will be particularly interesting to find out if the lower rates of rejection we have seen in the small bowel and pancreas transplants translates to lung transplantation. This would change the aim of the sentinel skin flap from immune monitoring to immune modulating. This could be ground-breaking for patients, as reducing rejection will protect their life-saving transplant.

In summary there is huge potential for sentinel skin flaps to both change the clinical management and outcomes of transplant patients and to help elucidate the mechanisms contributing to rejection or even tolerance. The data in this thesis have characterised in detail the immune phenotype of combined skin and solid organ transplants and will act as pilot data to guide analyses in the proposed randomised controlled trial of sentinel skin flaps for immune monitoring of lung transplantation.

8 Chapter 8: References

1. Robinson, D. H. & Toledo, A. H. Historical development of modern anesthesia. *Journal of Investigative Surgery* **25**, 141–149 (2012).
2. Schlich, T. The origins of organ transplantation. *The Lancet* **378**, 1372–1373 (2011).
3. Carrel, A. The Transplantation of Organs. A Preliminary Communication. *JAMA: The Journal of the American Medical Association* **XLV**, 1645 (1905).
4. Barker, C. F. & Markmann, J. F. Historical overview of transplantation. *Cold Spring Harb Perspect Med* **3**, (2013).
5. Merrill, J. P., Murray, J., Hartwell-Harrison, J. & Guild, W. Successful Homotransplantation of the Human Kidney Between Identical Twins. *J Am Med Assoc* **160**, 277 (1956).
6. Calne, R. Y. The Rejection of Renal Homografts Inhibition in Dogs by 6-Mercatpopurine. *The Lancet* **275**, 417–418 (1960).
7. Starzl, T. E., Marchioro, T. L. & Waddell, W. R. The Reversal of Rejection in Human Renal Homografts with Subsequent Development of Homograft Tolerance. *Surg Gynecol Obstet* **117**, 385–95 (1963).
8. Chaudhry, D., Chaudhry, A., Peracha, J. & Sharif, A. Survival for waitlisted kidney failure patients receiving transplantation versus remaining on waiting list: systematic review and meta-analysis. *BMJ* **376**, e068769 (2022).
9. Wilhelm, M. J. Long-term outcome following heart transplantation: Current perspective. *J Thorac Dis* **7**, 549–551 (2015).
10. Mulvihill, M. S., Hartwig, M. G. & Daneshmand, M. A. Lung transplantation in the most critically-III: Forging ahead. *J Thorac Dis* **9**, 3430–3432 (2017).

11. Halloran, P. F. Immunosuppressive Drugs for Kidney Transplantation. *New England Journal of Medicine* **351**, 2715–2729 (2004).

12. Claeys, E. & Vermeire, K. Immunosuppressive drugs in organ transplantation to prevent allograft rejection: Mode of action and side effects. *J Immunol Sci* **3**, 14–21 (2019).

13. Allison, A. C. *Immunosuppressive drugs: the first 50 years and a glance forward*. *Immunopharmacology* vol. 47 www.elsevier.comrlocaterimmpharm (2000).

14. Starzl, T. E., Groth, C. G. & Brettschneider, L. The Use of Heterologous Antilymphocyte Globulin (ALG) in Human Renal and Liver Transplantation. *Int Congr Ser* **162**, 83–90 (1967).

15. Starzl, T. E. *et al.* Cyclophosphamide and whole organ transplantation in human beings. *Surg Gynecol Obstet* **133**, 981–91 (1971).

16. Starzl, ThomasE. *et al.* FK 506 FOR LIVER, KIDNEY, AND PANCREAS TRANSPLANTATION. *The Lancet* **334**, 1000–1004 (1989).

17. European Mycophenolate Mofetil Cooperative Study Group. Placebo-controlled study of mycophenolate mofetil combined with cyclosporin and corticosteroids for prevention of acute rejection. *The Lancet* **345**, 1321–1325 (1995).

18. Groth, C. G. *et al.* Sirolimus (Rapamycin)-Based Therapy in Human Renal Transplantation. *Transplantation* **67**, 1036–1042 (1999).

19. Calne, R. *et al.* Prope tolerance, perioperative campath 1H, and low-dose cyclosporin monotherapy in renal allograft recipients. *The Lancet* **351**, 1701–1702 (1998).

20. Nashan, B. *et al.* Randomised trial of basiliximab versus placebo for control of acute cellular rejection in renal allograft recipients. *The Lancet* **350**, 1193–1198 (1997).

21. Vincenti, F. *et al.* Costimulation Blockade with Belatacept in Renal Transplantation. *New England Journal of Medicine* **353**, 770–781 (2005).

22. Dean, P. G., Kukla, A., Stegall, M. D. & Kudva, Y. C. Pancreas transplantation. *BMJ (Online)* vol. 357 Preprint at https://doi.org/10.1136/bmj.j1321 (2017).

23. Margreiter, C., Pratschke, J. & Margreiter, R. Immunological monitoring after pancreas transplantation. *Curr Opin Organ Transplant* **18**, 71–75 (2013).

24. Wan, J. *et al.* Pancreas allograft biopsies procedure in the management of pancreas transplant recipients. *Gland Surg* **8**, 794–798 (2019).

25. Noronha, I. L. *et al.* Analysis of the inflammatory infiltrate in pancreas allograft biopsies: 033. *Transplantation* **76**, S28–S29 (2003).

26. Cashion, A. K. *et al.* Serial analysis of biomarkers of acute pancreas allograft rejection. *Clin Transplant* **24**, 214–222 (2010).

27. Boggi, U. *et al.* First World Consensus Conference on pancreas transplantation: Part II – recommendations. *American Journal of Transplantation* **21**, 17–59 (2021).

28. Mittal, S., Page, S. L., Friend, P. J., Sharples, E. J. & Fuggle, S. V. De Novo Donor-Specific HLA Antibodies: Biomarkers of Pancreas Transplant Failure. *American Journal of Transplantation* **14**, 1664–1671 (2014).

29. NHS England. Annual Report on Pancreas and Islet Transplantation. *National Health Service Blood and Transplant* **2020**, 1–82 (2020).

30. Gruessner, A. C., Sutherland, D. E. R. & Gruessner, R. W. G. Long-term outcome after pancreas transplantation. *Curr Opin Organ Transplant* **17**, 100–105 (2012).

31. S.V., N. *et al.* Acute cellular and antibody-mediated rejection of the pancreas allograft: Incidence, risk factors and outcomes. *American Journal of Transplantation* **13**, 2945–2955 (2013).

32. Dong, M. *et al.* Acute pancreas allograft rejection is associated with increased risk of graft failure in pancreas transplantation. *American Journal of Transplantation* **13**, 1019–1025 (2013).

33. Middleton, S. J. *et al.* Adult small intestinal transplantation in England and Wales. *British Journal of Surgery* **90**, 723–727 (2003).

34. Middleton, S. J. & Jamieson, N. v. The current status of small bowel transplantation in the UK and internationally. *Gut* **54**, 1650–1657 (2005).

35. Ruiz, P. *et al.* Histological criteria for the identification of acute cellular rejection in human small bowel allografts: results of the pathology workshop at the VIII International Small Bowel Transplant Symposium. *Transplant Proc* **36**, 335–337 (2004).

36. Gürkan, A. Advances in small bowel transplantation. *Turk J Surg* **33**, 135–141 (2017).

37. Cheng, E. Y. *et al.* Prevalence and Clinical Impact of Donor-Specific Alloantibody among Intestinal Transplant Recipients. *Transplantation* **101**, 873–882 (2017).

38. Ehrenfried, A. Reverdin and Other Methods of Skin-Grafting. *Boston Med Surg J* **161**, 911–917 (1909).

39. Kilner, T. P. The Full-Thickness Skin Graft. *Postgrad Med J* **11**, 279–282 (1935).

40. Janzekovic, Z. A new concept in the early excision and immediate grafting of burns. *The Journal of Trauma: Injury, Infection, and Critical Care* **10**, 1103–1108 (1970).

41. Gottlieb, L. J. & Krieger, L. M. From the Reconstructive Ladder to the Reconstructive Elevator. *Plast Reconstr Surg* **93**, 1503 (1994).

42. Heuke, S. *et al.* Multimodal mapping of human skin. *British Journal of Dermatology* **169**, 794–803 (2013).

43. Ryan, T. J. Structure and function of lymphatics. *Journal of Investigative Dermatology* **93**, (1989).

44. Wong, R., Geyer, S., Weninger, W., Guimberteau, J. C. & Wong, J. K. The dynamic anatomy and patterning of skin. *Exp Dermatol* **25**, 92–98 (2016).

45. Dunn, R. Grafts and flaps. *Surgery (Oxford)* **24**, 27–32 (2006).

46. Fang, F. & Chung, K. C. An evolutionary perspective on the history of flap reconstruction in the upper extremity. *Hand Clinics* vol. 30 109–122 Preprint at https://doi.org/10.1016/j.hcl.2013.12.001 (2014).

47. Andrew Lee, W. P. *et al.* Relative antigenicity of components of a vascularized limb allograft. *Plast Reconstr Surg* **87**, 401–411 (1991).

48. Honeyman, C. & Fries, C. A. Vascularised Composite Allotransplantation – Basic Science and Clinical Applications. *International Journal of Orthoplastic Surgery* **2**, 13–22 (2019).

49. Carty, M. J. *et al.* Lessons learned from simultaneous face and bilateral hand allotransplantation. *Plast Reconstr Surg* **132**, 423–432 (2013).

50. Cooney, C. M. *et al.* The Ethics of Hand Transplantation: A Systematic Review. *Journal of Hand Surgery* **43**, 84.e1-84.e15 (2018).

51. Magill, G. *et al.* Existing and evolving bioethical dilemmas, challenges, and controversies in vascularized composite allotransplantation: An international perspective from the Brocher Bioethics Working Group. in *Transplantation* vol. 103 1746–1751 (Lippincott Williams and Wilkins, 2019).

52. Honeyman, C. *et al.* Abdominal Wall Transplantation: Indications and Outcomes. *Curr Transplant Rep* **7**, 279–290 (2020).

53. Honeyman, C. *et al.* Biomarker and surrogate development in vascularised composite allograft transplantation: Current progress and future challenges. *Journal of Plastic, Reconstructive & Aesthetic Surgery* **74**, 711–717 (2021).

54. Cendales, L. C. *et al.* The Banff 2007 working classification of skin-containing composite tissue allograft pathology. *American Journal of Transplantation* **8**, 1396–1400 (2008).

55. Petruzzo, P. *et al.* The international registry on hand and composite tissue transplantation. *Transplantation* **90**, 1590–1594 (2010).

56. Levi, D. M. *et al.* Transplantation of the abdominal wall. *Lancet* **361**, 2173–2176 (2003).

57. Nestle, F. O., di Meglio, P., Qin, J.-Z. & Nickoloff, B. J. Skin immune sentinels in health and disease. *Nat Rev Immunol* **9**, 679–691 (2009).

58. Wayne Streilein, J. Skin-Associated Lymphoid Tissues (SALT): Origins and Functions. *Journal of Investigative Dermatology* **80**, S12–S16 (1983).

59. Kabashima, K., Honda, T., Ginhoux, F. & Egawa, G. The immunological anatomy of the skin. *Nat Rev Immunol* **19**, 19–30 (2019).

60. West, H. C. & Bennett, C. L. Redefining the role of langerhans cells as immune regulators within the skin. *Front Immunol* **8**, 1–8 (2018).

61. Paus, R., Ito, N., Takigawa, M. & Ito, T. The Hair Follicle and Immune Privilege. *Journal of Investigative Dermatology Symposium Proceedings* **8**, 188–194 (2003).

62. Riol-Blanco, L. *et al.* Nociceptive sensory neurons drive interleukin-23-mediated psoriasiform skin inflammation. *Nature* **510**, 157–161 (2014).

63. Leonard, D. A., Amin, K. R., Giele, H., Fildes, J. E. & Wong, J. K. F. Skin Immunology and Rejection in VCA and Organ Transplantation. *Curr Transplant Rep* (2020) doi:10.1007/s40472-020-00310-1.

64. Clark, R. A. *et al.* The Vast Majority of CLA + T Cells Are Resident in Normal Skin. *The Journal of Immunology* **176**, 4431–4439 (2006).

65. Watanabe, R. *et al.* Human skin is protected by four functionally and phenotypically discrete populations of resident and recirculating memory T cells. *Sci Transl Med* **7**, 139–148 (2015).

66. Clark, R. A. & Kupper, T. S. IL-15 and dermal fibroblasts induce proliferation of natural regulatory T cells isolated from human skin. *Blood* **109**, 194–202 (2007).

67. Seneschal, J., Clark, R. A., Gehad, A., Baecher-Allan, C. M. & Kupper, T. S. Human Epidermal Langerhans Cells Maintain Immune Homeostasis in Skin by Activating Skin Resident Regulatory T Cells. *Immunity* **36**, 873–884 (2012).

68. Picker, L. J., Michie, S. A., Rott, L. S. & Butcher, E. C. *A Unique Phenotype of Skin-associated Lymphocytes in Humans*. *AmericanJournal ofPathology* vol. 136 (1990).

69. Hirahara, K. *et al.* The Majority of Human Peripheral Blood CD4+CD25highFoxp3+ Regulatory T Cells Bear Functional Skin-Homing Receptors. *The Journal of Immunology* **177**, 4488–4494 (2006).

70. Issa, F., Hester, J., Milward, K. & Wood, K. J. Homing of Regulatory T Cells to Human Skin Is Important for the Prevention of Alloimmune-Mediated Pathology in an In Vivo Cellular Therapy Model. *PLoS One* **7**, (2012).

71. Natsuaki, Y. *et al.* Perivascular leukocyte clusters are essential for efficient activation of effector T cells in the skin. *Nat Immunol* **15**, 1064–1069 (2014).

72. Parkin, J. & Cohen, B. An overview of the immune system. *The Lancet* **357**, 1777–1789 (2001).

73. Marino, J., Paster, J. & Benichou, G. Allorecognition by T Lymphocytes and Allograft Rejection. *Front Immunol* **7**, (2016).

74. Wood, K. J. & Goto, R. Mechanisms of rejection: Current perspectives. *Transplantation* vol. 93 1–10 Preprint at https://doi.org/10.1097/TP.0b013e31823cab44 (2012).

75. Kim, I. K., Bedi, D. S., Denecke, C., Ge, X. & Tullius, S. G. Impact of innate and adaptive immunity on rejection and tolerance. *Transplantation* **86**, 889–894 (2008).

76. Goldstein, D. R., Tesar, B. M., Akira, S. & Lakkis, F. G. Critical role of the Toll-like receptor signal adaptor protein MyD88 in acute allograft rejection. *Journal of Clinical Investigation* **111**, 1571–1578 (2003).

77. Matzinger, P. The Danger Model: A Renewed Sense of Self. *Science (1979)* **296**, 301–305 (2002).

78. Todd, J. L. & Palmer, S. M. Danger signals in regulating the immune response to solid organ transplantation. *Journal of Clinical Investigation* **127**, 2464–2472 (2017).

79. Tammaro, A., Kers, J., Scantlebery, A. M. L. & Florquin, S. Metabolic Flexibility and Innate Immunity in Renal Ischemia Reperfusion Injury: The Fine Balance Between Adaptive Repair and Tissue Degeneration. *Front Immunol* **11**, 1346 (2020).

80. Oberbarnscheidt, M. H. *et al.* Non-self recognition by monocytes initiates allograft rejection. *Journal of Clinical Investigation* **124**, 3579–3589 (2014).

81. Hara, M. *et al.* IL-10 Is Required for Regulatory T Cells to Mediate Tolerance to Alloantigens In Vivo. *The Journal of Immunology* **166**, 3789–3796 (2001).

82. Siu, J. H. Y., Surendrakumar, V., Richards, J. A. & Pettigrew, G. J. T cell allorecognition pathways in solid organ transplantation. *Front Immunol* **9**, 1–14 (2018).

83. Duneton, C., Winterberg, P. D. & Ford, M. L. Activation and regulation of alloreactive T cell immunity in solid organ transplantation. *Nat Rev Nephrol* (2022) doi:10.1038/s41581-022-00600-0.

84. Charmetant, X. *et al. Inverted direct allorecognition triggers early donor-specific antibody responses after transplantation*. *Sci. Transl. Med* vol. 14 https://www.science.org (2022).

85. Billingham, R. & Medawar, P. The Technique of Free Skin Grafting in Mammals. *Journal of Experimental Biology* **28**, 385–402 (1951).

86. Medawar, P. B. The Behaviour and Fate of Skin Autografts and Skin Allografts in Rabbits (A Report to the War Wounds Committee of the Medical Research Council). *J Anat* **78**, 176–199 (1944).

87. Billingham, R., Brent, L. & Medawar, P. B. 'Actively Acquired Tolerance' of Foreign Cells. *Nature* **172**, 603–606 (1953).

88. Gibson, T. & Medawar, P. B. The Fate of Skin Homografts in Man. *J Anat* **77**, 299–310 (1943).

89. Moseley, R. v., Sheil, A. G. R., Mitchell, R. M. & Murray, J. E. Immunologic relationships between skin and kidney homografts in dogs on immunosuppressive therapy. *Transplantation* **4**, 678–687 (1966).

90. Dvorak, H. F., Mihm, M. C., Dvorak, A. M., Barnes, B. A. & Galli, S. J. The Microvasculature is the Critical Target of the Immune Response in Vascularized Skin Allograft Rejection. *Journal of Investigative Dermatology* **74**, 280–284 (1980).

91. Hautz, T. *et al.* Indoleamine 2,3-Dioxygenase and Foxp3 Expression in Skin Rejection of Human Hand Allografts. *Transplant Proc* **41**, 509–512 (2009).

92. Cendales, L. C., Kirk, A. D., Moresi, J. M., Ruiz, P. & Kleiner, D. E. Composite tissue allotransplantation: Classification of clinical acute skin rejection. *Transplantation* **81**, 418–422 (2006).

93. Kanitakis, J. *et al.* Clinicopathologic monitoring of the skin and oral mucosa of the first human face allograft: Report on the first eight months. *Transplantation* **82**, 1610–1615 (2006).

94. Kanitakis, J. *et al.* Clinicopathologic features of graft rejection of the first human hand allograft. *Transplantation* **76**, 688–693 (2003).

95. Bhan, A. K., Mihm, M. C. & Dvorak, H. F. T cell subsets in allograft rejection. In situ characterization of T cell subsets in human skin allografts by the use of monoclonal antibodies. *J Immunol* **129**, 1578–83 (1982).

96. Win, T. S. *et al.* Immunoregulatory and lipid presentation pathways are upregulated in human face transplant rejection. *Journal of Clinical Investigation* **131**, 7250–7 (2021).

97. Hautz, T. *et al.* Molecular markers and targeted therapy of skin rejection in composite tissue allotransplantation. *American Journal of Transplantation* **10**, 1200–1209 (2010).

98. Lian, C. G. *et al.* Biomarker evaluation of face transplant rejection: Association of donor T cells with target cell injury. *Modern Pathology* **27**, 788–799 (2014).

99. Levenson, R. M., Borowsky, A. D. & Angelo, M. Immunohistochemistry and mass spectrometry for highly multiplexed cellular molecular imaging. *Laboratory Investigation* **95**, 397–405 (2015).

100. Shetty, V., Subramaniam, K. & Rao, R. Utility of immunofluorescence in dermatology. *Indian Dermatol Online J* **8**, 1 (2017).

101. Black, S. *et al.* CODEX multiplexed tissue imaging with DNA-conjugated antibodies. *Nature Protocols* vol. 16 3802–3835 Preprint at https://doi.org/10.1038/s41596-021-00556-8 (2021).

102. Giesen, C. *et al.* Highly multiplexed imaging of tumor tissues with subcellular resolution by mass cytometry. *Nat Methods* **11**, 417–422 (2014).

103. Agar, N. S., Halliday, G. M., Barnetson, R. S. C. & Jones, A. M. A novel technique for the examination of skin biopsies by laser capture microdissection. *J Cutan Pathol* **30**, 265–270 (2003).

104. Ung, N. *et al.* Adaptation of Imaging Mass Cytometry to Explore the Single Cell Alloimmune Landscape of Liver Transplant Rejection. *Front Immunol* **13**, (2022).

105. Trailin, A. *et al.* Chronic Active Antibody-Mediated Rejection Is Associated With the Upregulation of Interstitial But Not Glomerular Transcripts. *Front Immunol* **12**, (2021).

106. Vergani, A. *et al.* Laser capture microdissection as a new tool to assess graft-infiltrating lymphocytes gene profile in islet transplantation. *Cell Transplant* **18**, 827–832 (2009).

107. Ståhl, P. L. *et al.* Visualization and analysis of gene expression in tissue sections by spatial transcriptomics. *Science (1979)* **353**, 78–82 (2016).

108. Marx, V. Method of the Year: spatially resolved transcriptomics. *Nat Methods* **18**, 9–14 (2021).

109. Li, J. S. Y. *et al.* The Utility of Spatial Transcriptomics for Solid Organ Transplantation. *Transplantation* (2022) doi:10.1097/TP.0000000000004466.

110. Salem, F. *et al.* The spatially resolved transcriptional profile of acute T cell–mediated rejection in a kidney allograft. *Kidney Int* **101**, 131–136 (2022).

111. Rosales, I. A. *et al.* Novel intragraft regulatory lymphoid structures in kidney allograft tolerance. *American Journal of Transplantation* **22**, 705–716 (2022).

112. Sheil, A. G., Moseley, R. v & Murray, J. E. Differential skin and renal homograft survival in dogs on immunosuppressive therapy. *Surg Forum* **15**, 166–8 (1964).

113. Jones, N. D. *et al.* Differential Susceptibility of Heart, Skin, and Islet Allografts to T Cell-Mediated Rejection. *The Journal of Immunology* **166**, 2824–2830 (2001).

114. Issa, F. Vascularized composite allograft-specific characteristics of immune responses. *Transplant International* **29**, 672–681 (2016).

115. Fuchimoto, Y. *et al.* Skin-specific alloantigens in miniature swine. *Transplantation* **72**, (2001).

116. Wendt, J. R., Ulich, T. & Rao, P. N. Long-term survival of human skin allografts in patients with immunosuppression. *Plast Reconstr Surg* **113**, 1347–1354 (2004).

117. Daniel, R. K. *et al.* Tissue transplants in primates for upper extremity reconstruction: A preliminary report. *Journal of Hand Surgery* **11**, 1–8 (1986).

118. Horner, B. M. *et al.* In vivo observations of cell trafficking in allotransplanted vascularized skin flaps and conventional skin grafts. *Journal of Plastic, Reconstructive and Aesthetic Surgery* **63**, 711–719 (2010).

119. Leonard, D. A. *et al.* Cutaneous leukocyte lineages in tolerant large animal and immunosuppressed clinical vascularized composite allograft recipients. *American Journal of Transplantation* **21**, 582–592 (2021).

120. Kant, C. D. *et al.* Primary Vascularization of Allografts Governs Their Immunogenicity and Susceptibility to Tolerogenesis. *The Journal of Immunology* **191**, 1948–1956 (2013).

121. Barker, C. F. & Billingham, R. E. The Role of Afferent Lymphatics in the Rejection of Skin Homografts. *Journal of Experimental Medicine* **128**, 197–221 (1968).

122. Marino, J. *et al.* Donor exosomes rather than passenger leukocytes initiate alloreactive T cell responses after transplantation. *Sci Immunol* **1**, (2016).

123. Zamfirescu, D. G. *et al.* Sentinel Skin Allograft-A Reliable Marker for Monitoring of Composite Tissue Transplant Rejection. *Transplant Proc* **41**, 503–508 (2009).

124. Lanzetta, M. *et al.* Human hand transplantation: What have we learned? *Transplant Proc* **36**, 664–668 (2004).

125. Diefenbeck, M. *et al.* Outcome of allogeneic vascularized knee transplants. *Transplant International* **20**, 410–418 (2007).

126. Kueckelhaus, M. *et al.* Discerning Rejection After Facial Allotransplantation by Utilization of Sentinel Flaps. *Vascularized Composite Allotransplantation* **1**, 55–55 (2014).

127. Dunning, J. *et al.* Could Sentinel Skin Transplants Have Some Utility in Solid Organ Transplantation? *Transplant Proc* **48**, 2565–2570 (2016).

128. Knight, S. R., Thorne, A. & lo Faro, M. L. Donor-specific Cell-free DNA as a Biomarker in Solid Organ Transplantation. A Systematic Review. *Transplantation* **103**, 273–283 (2019).

129. Deng, M. C. The AlloMap™ genomic biomarker story: 10 years after. *Clin Transplant* **31**, (2017).

130. Gerlach, U. A. *et al.* Skype clinics after intestinal transplantation – follow-up beyond post codes. *Clin Transplant* **30**, 760–766 (2016).

131. Wendt, J. R., Ulich, T. R., Ruzics, E. P. & Hostetler, J. R. Indefinite Survival of Human Skin Allografts in Patients with Long-term Immunosuppression. *Ann Plast Surg* **32**, 411–417 (1994).

132. Haberal, M. *et al.* ABO-incompatible kidney transplantation with donor-specific skin graft. *Ren Fail* **13**, 103–110 (1991).

133. Allin, B. S. R. *et al.* A single center experience of abdominal wall graft rejection after combined intestinal and abdominal wall transplantation. *American Journal of Transplantation* **13**, 2211–2215 (2013).

134. Gerlach, U. A. *et al.* Abdominal Wall Transplantation: Skin as a Sentinel Marker for Rejection. *American Journal of Transplantation* **16**, 1892–1900 (2016).

135. Weissenbacher, A. *et al.* De novo donor-specific HLA antibodies after combined intestinal and vascularized composite allotransplantation — a retrospective study. *Transplant International* **31**, 398–407 (2018).

136. Barnes, J., Friend, P. & Sharples, E. Novel Approaches To Pancreas Allograft Surveillance. (University of Oxford, 2019).

137. NHSBT. *Annual Report on Intestine Transplantation 2020/2021, NHS Blood and Transplant.* (2021).

138. Streitz, M. *et al.* Standardization of whole blood immune phenotype monitoring for clinical trials: panels and methods from the ONE study. *Transplant Res* **2**, 17 (2013).

139. Asare, A. L. *et al.* Differential gene expression profiles are dependent upon method of peripheral blood collection and RNA isolation. *BMC Genomics* **9**, (2008).

140. Mengel, M. *et al.* Banff 2019 Meeting Report: Molecular diagnostics in solid organ transplantation–Consensus for the Banff Human Organ Transplant (B-HOT) gene panel and open source multicenter validation. *American Journal of Transplantation* **20**, 2305–2317 (2020).

141. Zhao, X. *et al.* Delayed allogeneic skin graft rejection in CD26-deficient mice. *Cell Mol Immunol* **16**, 557–567 (2019).

142. Gauthier, J. M. *et al.* Mechanisms of graft rejection and immune regulation after lung transplant. *Ann Am Thorac Soc* **14**, S216–S219 (2017).

143. Heidt, S., Hester, J., Shankar, S., Friend, P. J. & Wood, K. J. B cell repopulation after alemtuzumab induction - Transient increase in transitional B cells and long-term dominance of naïve B cells. *American Journal of Transplantation* **12**, 1784–1792 (2012).

144. Noris, M. *et al.* Regulatory T cells and T cell depletion: Role of immunosuppressive drugs. *Journal of the American Society of Nephrology* **18**, 1007–1018 (2007).

145. Trzonkowski, P., Zilvetti, M., Friend, P. & Wood, K. J. Recipient memory-like lymphocytes remain unresponsive to graft antigens after CAMPATH-1H induction with reduced maintenance immunosuppression. *Transplantation* **82**, 1342–1351 (2006).

146. Bloom, D. D., Hu, H., Fechner, J. H. & Knechtle, S. J. T-lymphocyte alloresponses of campath-1H-treated kidney transplant patients. *Transplantation* **81**, 81–87 (2006).

147. Knechtle, S. J. *et al.* Campath-1H induction plus rapamycin monotherapy for renal transplantation: Results of a pilot study. *American Journal of Transplantation* **3**, 722–730 (2003).

148. Bouvy, A. P. *et al.* Alemtuzumab as Antirejection Therapy. *Transplant Direct* **2**, e83 (2016).

149. Trzonkowski, P. *et al.* Homeostatic repopulation by CD28-CD8+ T cells in alemtuzumab-depleted kidney transplant recipients treated with reduced immunosuppression. *American Journal of Transplantation* **8**, 338–347 (2008).

150. Borges, T. J. *et al.* T cell-attracting CCL18 chemokine is a dominant rejection signal during limb transplantation. *Cell Rep Med* **3**, 100559 (2022).

151. Duggleby, R., Danby, R. D., Madrigal, J. A. & Saudemont, A. Clinical grade regulatory CD4+ T cells (Tregs): Moving toward cellular-based immunomodulatory therapies. *Frontiers in Immunology* vol. 9 Preprint at https://doi.org/10.3389/fimmu.2018.00252 (2018).

152. Lam, A. J., Uday, P., Gillies, J. K. & Levings, M. K. Helios is a marker, not a driver, of human Treg stability. *Eur J Immunol* **52**, 75–84 (2022).

153. Bloom, D. D. *et al.* CD4+CD25+FOXP3+ regulatory T cells increase de novo in kidney transplant patients after immunodepletion with campath-1H. *American Journal of Transplantation* **8**, 793–802 (2008).

154. Sullivan, L. C. *et al.* The complex existence of γδ T cells following transplantation: the good, the bad and the simply confusing. *Clin Transl Immunology* **8**, 1–10 (2019).

155. Newell, K. A. *et al.* Identification of a B cell signature associated with renal transplant tolerance in humans. *Journal of Clinical Investigation* **120**, 1836–1847 (2010).

156. Borges, T. J. *et al.* Codominant Role of Interferon-γ– and Interleukin-17–Producing T Cells During Rejection in Full Facial Transplant Recipients. *American Journal of Transplantation* **16**, 2158–2171 (2016).

157. Redfield, R. R. *et al.* Essential role for B cells in transplantation tolerance. *Curr Opin Immunol* **23**, 685–691 (2011).

158. Williams, K. M., Hakim, F. T. & Gress, R. E. T cell immune reconstitution following lymphodepletion. *Semin Immunol* **19**, 318–330 (2007).

159. Bloom, D. D. *et al.* CD4+CD25+FOXP3+ regulatory T cells increase de novo in kidney transplant patients after immunodepletion with campath-1H. *American Journal of Transplantation* **8**, 793–802 (2008).

160. Macedo, C. *et al.* Long-term effects of alemtuzumab on regulatory and memory T-cell subsets in kidney transplantation. *Transplantation* **93**, 813–821 (2012).

161. Law, B. M. P. *et al.* Effector γδ T cells in human renal fibrosis and chronic kidney disease. *Nephrology Dialysis Transplantation* **34**, 40–48 (2019).

162. Zhang, H. *et al.* Transcriptional dissection of differentially expressed long non-coding RNAs and messenger RNAs reveals the potential molecular mechanism after kidney transplantation. *Ann Transl Med* **7**, 458–458 (2019).

163. Dorr, C. *et al.* Differentially expressed gene transcripts using RNA sequencing from the blood of immunosuppressed kidney allograft recipients. *PLoS One* **10**, (2015).

164. Schluns, K. S., Kieper, W. C., Jameson, S. C. & Lefrançois, L. Interleukin-7 mediates the homeostasis of naïve and memory CD8 T cells in vivo. *Nat Immunol* **1**, 426–432 (2000).

165. Wang, Y. *et al.* A conserved CXXC motif in CD3ε is critical for T cell development and TCR signaling. *PLoS Biol* **7**, (2009).

166. Shan, Q. *et al.* Tcf1 and Lef1 provide constant supervision to mature CD8+ T cell identity and function by organizing genomic architecture. *Nat Commun* **12**, (2021).

167. Benichou, G., Gonzalez, B., Marino, J., Ayasoufi, K. & Valujskikh, A. Role of memory T cells in allograft rejection and tolerance. *Front Immunol* **8**, (2017).

168. Betjes, M. G. H., Meijers, R. W. J., de Wit, E. A., Weimar, W. & Litjens, N. H. R. Terminally differentiated CD8 + temra cells are associated with the risk for acute kidney allograft rejection. *Transplantation* **94**, 63–69 (2012).

169. Mowat, A. M. & Agace, W. W. Regional specialization within the intestinal immune system. *Nat Rev Immunol* **14**, 667–685 (2014).

170. Lee, R. *et al.* Pathology of human intestinal transplantation. *Gastroenterology* **110**, 1820–1834 (1996).

171. Hayashi, M., Martinez, O., Krams, S., Burns, W. & Equivel, C. Characterization of allograft rejection in an experimental model of small intestinal transplantation. *Journal of Gastrointestinal Surgery* **2**, 325–332 (1998).

172. Toogood, G. J., Rankin, A. M., Tam, P. K. H., Morris, P. J. & Dallman, M. J. The Immune Response Followoing Small Bowel Transplantation. I. An Unusual Pattern of Cytokine Expression. *Transplantation* **62**, 851–855 (1996).

173. Newell, K. A., He, G., Hart, J. & Thistlethwaite, J. R. Jr. Treatment with either anti-CD4 or anti-CD8 monoclonal antibodies blocks αβ T cell-mediated rejection of intestinal allografts in mice. *Transplantation* **64**, (1997).

174. Zhang, Z. *et al.* Donor T Cell Activation Initiates Small Bowel Allograft Rejection Through an IFN-γ-Inducible Protein-10-Dependent Mechanism. *The Journal of Immunology* **168**, 3205–3212 (2002).

175. Zambernardi, A. *et al.* Immunosuppressive therapies after intestinal transplant modulate the expression of Th1 signature genes during acute cellular rejection. Implications in the search for rejection biomarkers. *Clin Transplant* **28**, 1365–1371 (2014).

176. Bradley, S. P. *et al.* Genetic Expression Profile During Acute Cellular Rejection in Clinical Intestinal Transplantation. *Transplantation* **86**, 998–1001 (2008).

177. Asaoka, T. *et al.* Characteristic immune, apoptosis and inflammatory gene profiles associated with intestinal acute cellular rejection in formalin-fixed paraffin-embedded mucosal biopsies. *Transplant International* **24**, 697–707 (2011).

178. Selvaggi, G. *et al.* Abdominal Wall Transplantation: Surgical and Immunologic Aspects. *Transplant Proc* **41**, 521–522 (2009).

179. Weissenbacher, A. *et al.* De novo donor-specific HLA antibodies after combined intestinal and vascularized composite allotransplantation - a retrospective study. *Transplant International* **31**, 398–407 (2018).

180. Ruiz, P. *et al.* Histological criteria for the identification of acute cellular rejection in human small bowel allografts: Results of the pathology workshop at the VIII International Small Bowel Transplant Symposium. *Transplant Proc* **36**, 335–337 (2004).

181. Li, X. & Wang, C.-Y. From bulk, single-cell to spatial RNA sequencing. *Int J Oral Sci* **13**, 36 (2021).

182. Colvin, R. B. *CELLULAR AND MOLECULAR MECHANISMS OF ALLOGRAFT REJECTION*. *Annu. Rev. Med* vol. 41 www.annualreviews.org (1990).

183. Özdemir, B. H., Aksoy, P. K., Haberal, A. N., Demirhan, B. & Haberal, M. Relationship of HLA-DR expression to rejection and mononuclear cell infiltration in renal allograft biopsies. *Ren Fail* **26**, 247–251 (2004).

184. Bishop, G. A. *et al. Immunopathology of renal allograft rejection analyzed with monoclonal antibodies to mononuclear cell markers*. *Kidney International* vol. 29 (1986).

185. Mcdonald, G. B. & Jewell, D. P. *Class II antigen (HLA-DR) expression by intestinal epithelial cells in inflammatory diseases of colon*. *J Clin Pathol* vol. 40 (1987).

186. Spencer, J. & Sollid, L. M. The human intestinal B-cell response. *Mucosal Immunol* **9**, 1113–1124 (2016).

187. Schroder, K., Hertzog, P. J., Ravasi, T. & Hume, D. A. Interferon-γ: an overview of signals, mechanisms and functions. *J Leukoc Biol* **75**, 163–189 (2004).

188. Zambernardi, A. *et al.* Immunosuppressive therapies after intestinal transplant modulate the expression of Th1 signature genes during acute cellular rejection. Implications in the search for rejection biomarkers. *Clin Transplant* **28**, 1365–1371 (2014).

189. Bader, C. S., Jin, L. & Levy, R. B. STING and transplantation: can targeting this pathway improve outcomes? *Blood* **137**, 1871–1878 (2021).

190. Dholakia, S., De Vlaminck, I. & Khush, K. K. Adding Insult on Injury: Immunogenic Role for Donor-derived Cell-free DNA? *Transplantation* **104**, 2266–2271 (2020).

191. Decout, A., Katz, J. D., Venkatraman, S. & Ablasser, A. The cGAS–STING pathway as a therapeutic target in inflammatory diseases. *Nature Reviews Immunology* vol. 21 548–569 Preprint at https://doi.org/10.1038/s41577-021-00524-z (2021).

192. Kanitakis, J. *et al.* Pathological score for the evaluation of allograft rejection in human hand (composite tissue) allotransplantation. *European Journal of Dermatology* **15**, 235–238 (2005).

193. Murray, J. E. Organ transplantation (skin, kidney, heart) and the plastic surgeon. *Plast Reconstr Surg* **47**, 425–31 (1971).

194. Chen, X. *et al.* Inhibition of autophagy prolongs recipient survival through promoting CD8+ T cell apoptosis in a rat liver transplantation model. *Front Immunol* **10**, (2019).

195. Lin, J. C. *et al.* Sorafenib induces autophagy in human myeloid dendritic cells and prolongs survival of skin allografts. *Transplantation* **95**, 791–800 (2013).

196. Li, C. *et al.* Mechanism of indoleamine 2, 3-dioxygenase inhibiting cardiac allograft rejection in mice. *J Cell Mol Med* **24**, 3438–3448 (2020).

197. Rowshanravan, B., Halliday, N. & Sansom, D. M. CTLA-4: a moving target in immunotherapy. *Blood* **131**, 58–67 (2018).

198. Sharpe, A. H. & Pauken, K. E. The diverse functions of the PD1 inhibitory pathway. *Nat Rev Immunol* **18**, 153–167 (2018).

199. Gnanaprakasam, J. N. & Wang, R. MYC in Regulating Immunity: Metabolism and Beyond. *Genes (Basel)* **8**, 88 (2017).

200. Clark, R. A. Skin-Resident T Cells: The Ups and Downs of On Site Immunity. *Journal of Investigative Dermatology* **130**, 362–370 (2010).

201. Romagnani, P. & Crescioli, C. CXCL10: A candidate biomarker in transplantation. *Clinica Chimica Acta* **413**, 1364–1373 (2012).

202. Spivey, T. L. *et al.* Gene expression profiling in acute allograft rejection: challenging the immunologic constant of rejection hypothesis. *J Transl Med* **9**, 174 (2011).

203. Bhat, M. Y. *et al.* Comprehensive network map of interferon gamma signaling. *J Cell Commun Signal* **12**, 745–751 (2018).

204. Kuo, P. T. *et al.* The Role of CXCR3 and Its Chemokine Ligands in Skin Disease and Cancer. *Front Med (Lausanne)* **5**, (2018).

205. Brandacher, G. *et al.* Non-invasive monitoring of kidney allograft rejection through IDO metabolism evaluation. *Kidney Int* **71**, 60–67 (2007).

206. Clausen, B. E. & Kel, J. M. Langerhans cells: critical regulators of skin immunity? *Immunol Cell Biol* **88**, 351–360 (2010).

207. Schuler, G. & Steinman, R. M. Murine epidermal Langerhans cells mature into potent immunostimulatory dendritic cells in vitro. *Journal of Experimental Medicine* **161**, 526–546 (1985).

208. Tang, A., Amagai, M., Granger, L. G., Stanley, J. R. & Uddy, M. C. Adhesion of epidermal Langerhans cells to keratinocytes mediated by E-cadherin. *Nature* **361**, 82–85 (1993).

209. Kubo, A., Nagao, K., Yokouchi, M., Sasaki, H. & Amagai, M. External antigen uptake by Langerhans cells with reorganization of epidermal tight junction barriers. *Journal of Experimental Medicine* **206**, 2937–2946 (2009).

210. Nishibu, A. *et al.* Behavioral responses of epidermal Langerhans cells in situ to local pathological stimuli. *Journal of Investigative Dermatology* **126**, 787–796 (2006).

211. Ohl, L. *et al. CCR7 Governs Skin Dendritic Cell Migration under Inflammatory and Steady-State Conditions naive T cells as well as other DC through the interaction with CCR7 (Luther et al., 2000; Sallusto et al., 1998). In contrast to the widely accepted model for lymphocyte*. *Immunity* vol. 21 (2004).

212. Obhrai, J. S. *et al.* Langerhans cells are not required for efficient skin graft rejection. *Journal of Investigative Dermatology* **128**, 1950–1955 (2008).

213. Lakkis, F. G., Arakelov, A., Konieczny, B. T. & Inoue, Y. Immunologic 'ignorance' of vascularized organ transplants in the absence of secondary lymphoid tissue. *Nat Med* **6**, 686–688 (2000).

214. Hoefakker, S. *et al.* Migration of human antigen-presenting cells in a human skin graft onto nude mice model after contact sensitization. *Immunology* **86**, 296–303 (1995).

215. Richters, C. D., van Gelderop, E., du Pont, J. S., Hoekstra, M. J. & Kamperdijk, E. W. A. Migratory properties of skin dendritic cells of the rat. *Transplant Proc* **29**, 1745–1747 (1997).

216. Benichou, G. *et al.* Immune recognition and rejection of allogeneic skin grafts. *Immunotherapy* **3**, 757–770 (2011).

217. Chen, H.-D. & Silvers, W. K. Influence of Langerhans Cells on the Survival of H-Y Incompatible Skin Grafts in Rats. *Journal of Investigative Dermatology* **81**, 20–23 (1983).

218. He, C. *et al.* Effects of T Cell Frequency and Graft Size on Transplant Outcome in Mice. *The Journal of Immunology* **172**, 240–247 (2004).

219. Hemmi, H. *et al.* Skin antigens in the steady state are trafficked to regional lymph nodes by transforming growth factor-β1-dependent cells. *Int Immunol* **13**, 695–704 (2001).

220. Hawiger, D. *et al.* Dendritic Cells Induce Peripheral T Cell Unresponsiveness under Steady State Conditions in Vivo. *Journal of Experimental Medicine* **194**, 769–780 (2001).

221. Eckhardt, E. & Bastian, M. Animal models for human group 1 CD1 protein function. *Mol Immunol* **130**, 159–163 (2021).

222. van Rhijn, I. & Moody, D. B. CD1 and mycobacterial lipids activate human T cells. *Immunol Rev* **264**, 138–153 (2015).

223. Beckman, E. M. *et al.* Recognition of a lipid antigen by CD1-restricted αβ+ T cells. *Nature* **372**, 691–694 (1994).

224. de Jong, A. Activation of human T cells by CD1 and self-lipids. *Immunol Rev* **267**, 16–29 (2015).

225. Felio, K. *et al.* CD1-restricted adaptive immune responses to Mycobacteria in human group 1 CD1 transgenic mice. *Journal of Experimental Medicine* **206**, 2497–2509 (2009).

226. Visvabharathy, L. *et al.* Group 1 CD1-restricted T cells contribute to control of systemic Staphylococcus aureus infection. *PLoS Pathog* **16**, (2020).

227. Kobayashi, C. *et al.* GM-CSF-independent CD1a expression in epidermal langerhans cells: Evidence from human CD1A genome-transgenic mice. *Journal of Investigative Dermatology* vol. 132 241–244 Preprint at https://doi.org/10.1038/jid.2011.280 (2012).

228. Kim, J. H. *et al.* CD1a on Langerhans cells controls inflammatory skin disease. *Nat Immunol* **17**, 1159–1166 (2016).

229. Hardman, C. S. *et al.* CD1a promotes systemic manifestations of skin inflammation. *Nat Commun* **13**, (2022).

230. Polak, M. E. & Singh, H. Tolerogenic and immunogenic states of Langerhans cells are orchestrated by epidermal signals acting on a core maturation gene module. *BioEssays* **43**, (2021).

231. Honeyman, C. *et al.* Vascularised composite allotransplantation in solid organ transplant recipients: A systematic review. *Journal of Plastic, Reconstructive and Aesthetic Surgery* 1–11 (2020) doi:10.1016/j.bjps.2020.08.052.

232. Betjes, M. G. H. & Litjens, N. H. R. High numbers of differentiated CD28null CD8+ T cells are associated with a lowered risk for late rejection and graft loss after kidney transplantation. *PLoS One* **15**, 1–11 (2020).

233. Dedeoglu, B. *et al.* Lo of CD28 on peripheral T cells decreases the risk for early acute rejection after kidney transplantation. *PLoS One* **11**, (2016).

234. Deng, M. C. *et al.* Noninvasive Discrimination of Rejection in Cardiac Allograft Recipients Using Gene Expression Profiling. *American Journal of Transplantation* **6**, 150–160 (2006).

235. Dedrick, R. L. Understanding Gene Expression Patterns in Immune-Mediated Disorders. *J Immunotoxicol* **4**, 201–207 (2007).

236. Akalin, E. *et al.* Clinical Validation of an Immune Quiescence Gene Expression Signature in Kidney Transplantation. *Kidney360* **2**, 1998–2009 (2021).

237. Li, L. *et al.* A peripheral blood diagnostic test for acute rejection in renal transplantation. *American Journal of Transplantation* **12**, 2710–2718 (2012).

238. Roedder, S. *et al.* The kSORT Assay to Detect Renal Transplant Patients at High Risk for Acute Rejection: Results of the Multicenter AART Study. *PLoS Med* **11**, (2014).

239. Van Loon, E. *et al.* Diagnostic performance of kSORT, a blood-based mRNA assay for noninvasive detection of rejection after kidney transplantation: A retrospective multicenter cohort study. *American Journal of Transplantation* **21**, 740–750 (2021).

240. Win, T. S. *et al.* Longitudinal immunological characterization of the first presensitized recipient of a face transplant. *JCI Insight* **2**, 1–10 (2017).

241. Hancock, W. W. *et al.* Requirement of the Chemokine Receptor CXCR3 for Acute Allograft Rejection. *Journal of Experimental Medicine* **192**, 1515–1520 (2000).

242. Jiankuo, M. *et al.* Peptide Nucleic Acid Antisense Prolongs Skin Allograft Survival by Means of Blockade of CXCR3 Expression Directing T Cells into Graft. *The Journal of Immunology* **170**, 1556–1565 (2003).

243. Zhang, Z. *et al.* IP-10-Induced Recruitment of CXCR3+ Host T Cells Is Required for Small Bowel Allograft Rejection. *Gastroenterology* **126**, 809–818 (2004).

244. Fahmy, N. M. *et al.* Chemokine and receptor-gene expression during early and late acute rejection episodes in human cardiac allografts. *Transplantation* **75**, 2044–2047 (2003).

245. Melter, M. *et al.* Expression of the Chemokine Receptor CXCR3 and Its Ligand IP-10 During Human Cardiac Allograft Rejection. *Circulation* **104**, 2558–2564 (2001).

246. Segerer, S. *et al.* Expression of chemokines and chemokine receptors during human renal transplant rejection. *American Journal of Kidney Diseases* **37**, 518–531 (2001).

247. Agostini, C. *et al.* CXCR3 and its ligand CXCL10 are expressed by inflammatory cells infiltrating lung allografts and mediate chemotaxis of T cells at sites of rejection. *American Journal of Pathology* **158**, 1703–1711 (2001).

248. Tatapudi, R. R. *et al. Noninvasive detection of renal allograft inflammation by measurements of mRNA for IP-10 and CXCR3 in urine*. *Kidney International* vol. 65 (2004).

249. Rotondi, M. *et al.* High pretransplant serum levels of CXCL9 are associated with increased risk of acute rejection and graft failure in kidney graft recipients. *Transplant International* **23**, 465–475 (2010).

250. Rotondi, M. *et al.* High pretransplant serum levels of CXCL10/IP-10 are related to increased risk of renal allograft failure. *American Journal of Transplantation* **4**, 1466–1474 (2004).

251. Khatri, P. *et al.* A common rejection module (CRM) for acute rejection across multiple organs identifies novel therapeutics for organ transplantation. *Journal of Experimental Medicine* **210**, 2205–2221 (2013).

252. Wang, E., Bedognetti, D., Tomei, S. & Marincola, F. M. Common pathways to tumor rejection. *Ann N Y Acad Sci* **1284**, 75–79 (2013).

253. Choy, J. C. Granzymes and perforin in solid organ transplant rejection. *Cell Death Differ* **17**, 567–576 (2010).

254. Kamada, N., Brons, G., Davies, S. & Hugh, F. Fully allogeneic liver grafting in rats induces a state of systemic noreactivity to donor transplantation antigens. *Transplantation* **29**, 429–431 (1980).

255. Starzl, T. E. *et al.* Systemic chimerism in human female recipients of male livers. *The Lancet* **340**, 876–877 (1992).

256. Fung, J., Griffin, M., Duquesnoy, R., Shaw, B. & Starzl, T. Successful sequential liver-kidney transplantation in a patient with preformed lymphocytotoxic antibodies. *Transplant Proc* **19**, 767–768 (1987).

257. Tzakis, A. G. *et al.* 100 Multivisceral transplants at a single center. *Ann Surg* **242**, 480–493 (2005).

258. Sarris, G. E. *et al.* Long-term results of combined heart-lung transplantation: the Stanford experience. *J Heart Lung Transplant* **13**, 940–9 (1994).

259. Narula, J. *et al.* Outcomes in recipients of combined heart-kidney transplantation. *Transplantation* **63**, 861–867 (1997).

260. Rana, A. *et al.* The Combined Organ Effect. *Ann Surg* **248**, 871–879 (2008).

261. Nasir, S., Bozkurt, M., Klimczak, A. & Siemionow, M. Large antigenic skin load in total abdominal wall transplants permits chimerism induction. *Ann Plast Surg* **61**, 572–579 (2008).

262. Sanchez-Fueyo, A. & Markmann, J. F. Immune Exhaustion and Transplantation. *American Journal of Transplantation* **16**, 1953–1957 (2016).

263. Crane, M. J. *et al.* Pulmonary influenza A virus infection leads to suppression of the innate immune response to dermal injury. *PLoS Pathog* **14**, 1–24 (2018).

264. Tabibian, J. H. & Kenderian, S. S. The microbiome and immune regulation after transplantation. *Transplantation* **101**, 56–62 (2017).

9 Appendices

9.1 Appendix 1. Gating strategy

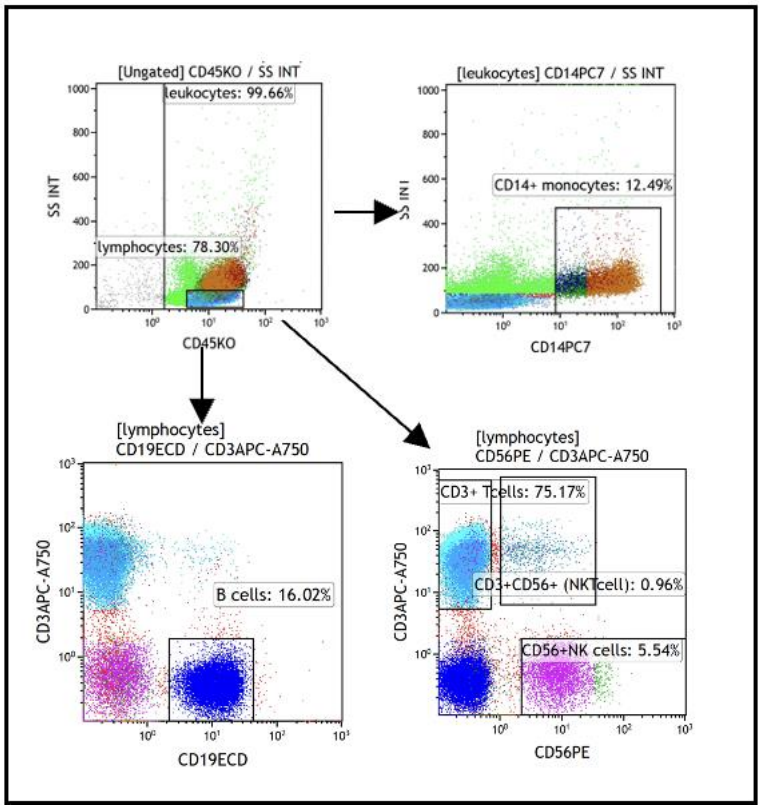

A1.1: Gating strategy for Duraclone basic phenotype panel. Lymphocytes were identified using a combination of side scatter (SS) and CD45. Taking this as a parent gate a combination of CD3, CD19, CD14 and CD56 were used to identify $CD3^+$ T cells, $CD19^+$ B cells, $CD14^+$ monocytes and $CD56^+$ NK cells.

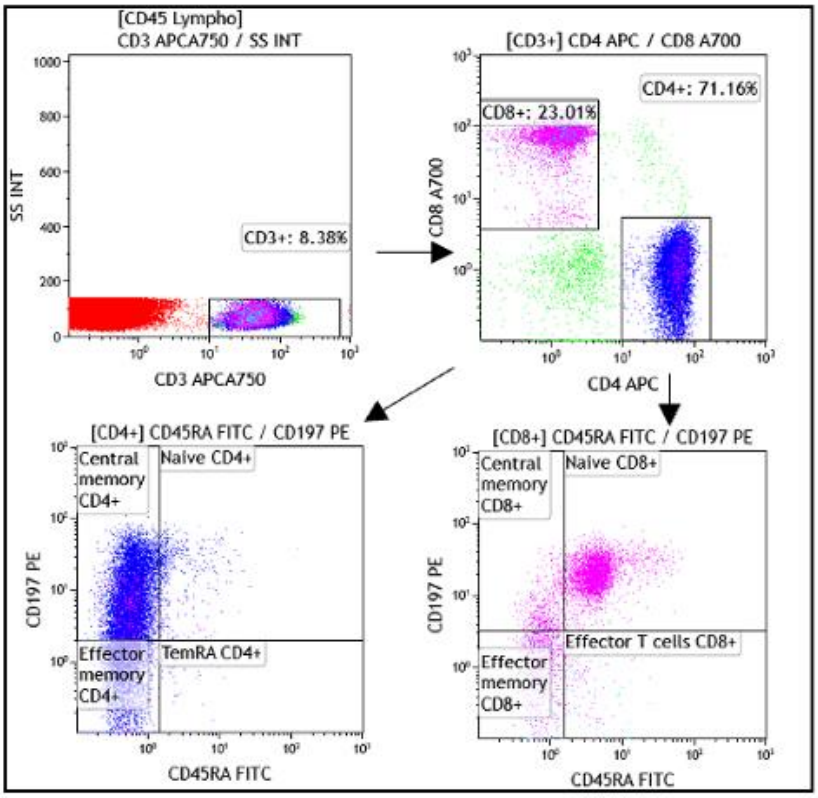

A1.2: Gating strategy for Duraclone T cell panel. Lymphocytes were identified using a combination of side scatter (SS) and CD45 (as shown in A1.1.). Taking this as a parent gate a combination of CD3 and SS were used to identify $CD3^+$ T cells. With $CD3^+$ T cells as the parent gate a combination of CD4 and CD8 were used to identify T helper ($CD4^+$) and T effector ($CD8^+$) populations. Taking the $CD4^+$ gate as a parent a combination of CD45RA and CD197 (CCR7) were used to subset the $CD4^+$ population into naïve ($CD45RA^+$ $CCR7^+$), central memory ($CD45RA^-$ $CCR7^+$), effector memory ($CD45RA^-CCR7^-$) and terminally differentiated or TEMRA ($CD45RA^+$ $CCR7^-$). The same strategy was used with $CD8^+$ T cells as the parent gate.

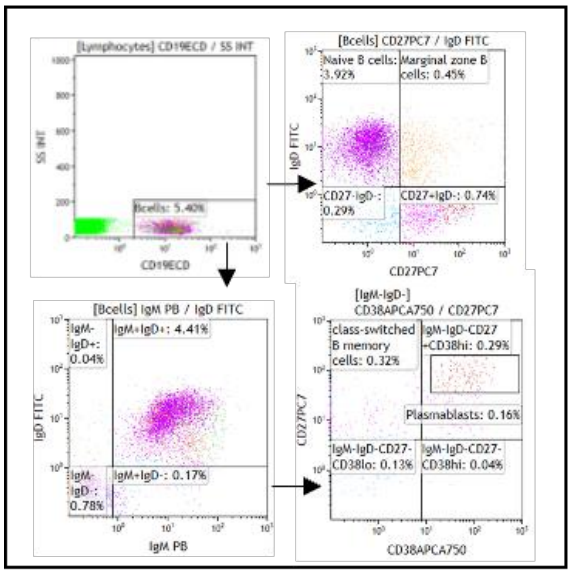

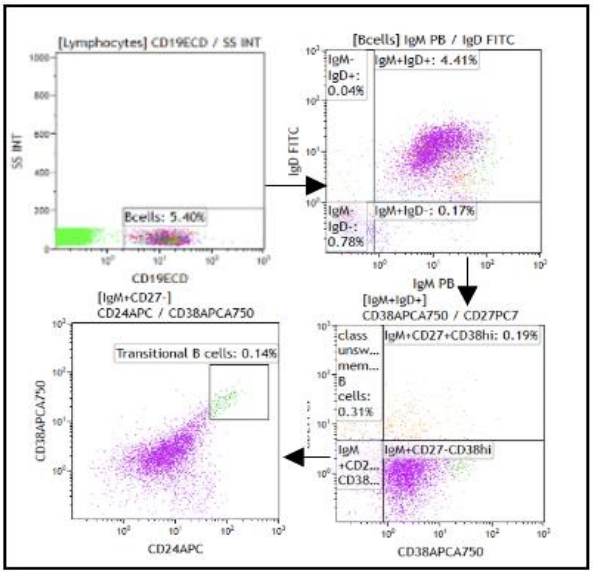

A1.3 Gating strategy for Duraclone B cell panel. Lymphocytes were identified using a combination of side scatter (SS) and CD45, as shown in A1.1. With this as the parent gate a combination of CD19 and SS were used to identify $CD19^+$ B cells. Taking B cells as the new parent gate a combination of CD27 and IgD were used to identify naïve B cells (IgD^+CD27^-) and marginal zone B cells (IgD^+CD27^+). IgD and IgM were used to identify IgD^+IgM^+ and IgD^-IgM^- B cell populations. Each of these was taken as a parent

gate and combination of CD38 and CD27 was used to identify class-switched memory B cells ($IgD^{-}IgM^{-}CD38^{-}CD27^{+}$), class unswitched memory B cells ($IgD^{+}IgM^{+}CD38^{-}CD27^{+}$) and plasmablasts ($IgD^{-}IgM^{-}CD38^{hi}CD27^{+}$). Finally, the $IgD^{+}IgM^{+}CD27^{+}$ subset was taken as a parent gate and a combination of CD24 and CD38 used to identify a population of transitional B cells ($CD38^{hi}CD24^{hi}$).

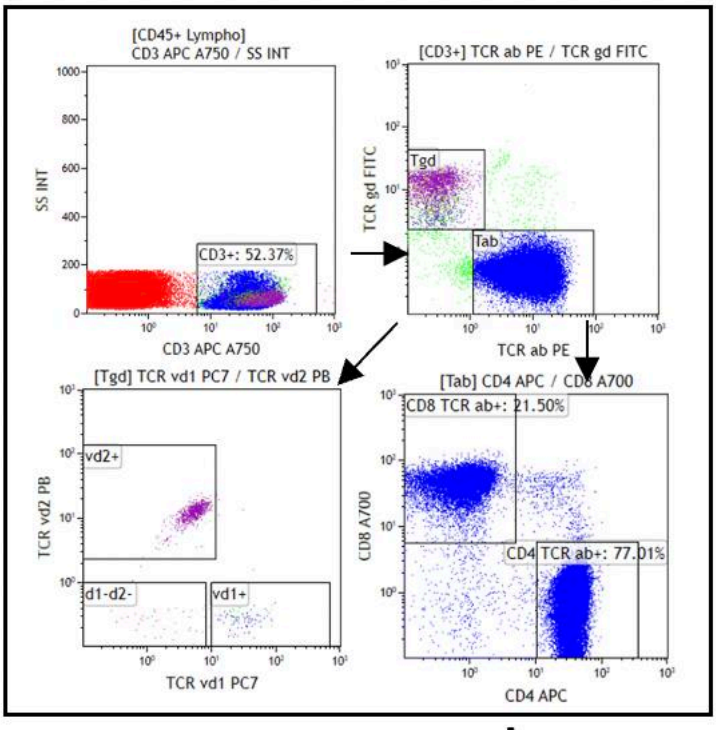

A1.4. Gating strategy for Duraclone TCR panel. Lymphocytes were identified using a combination of side scatter (SS) and CD45, as shown in A1.1. With lymphocytes as the parent gate a combination of SS and CD3 were used to identify $CD3^{+}$ T cells. This population were then used as the parent gate and TCR αβ and TCR γδ were used to identify $CD3^{+}$ TCR αβ and TCR γδ T cells. The TCR αβ population were taken as the parent gate and a combination of CD4 and CD8 were used to identify the $CD4^{+}$ TCR αβ

T cells and $CD8^+$ TCR αβ T cells. The TCR γδ T cells were taken as the parent gate and a combination of vδ1 and vδ2 was used to identify the TCR γvδ1 and TCR γvδ2 T cell subsets.

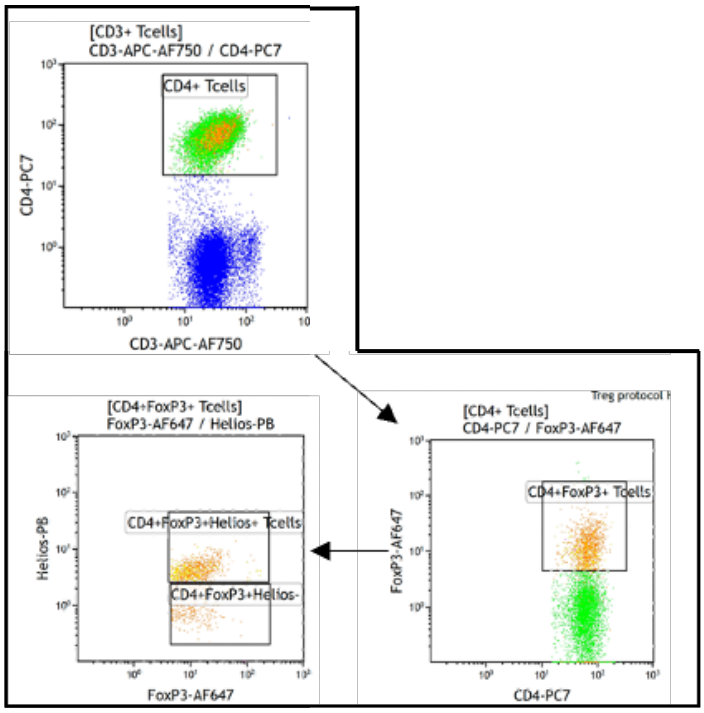

A1.5. Gating strategy for Duraclone Treg panel. Lymphocytes were identified using a combination of side scatter (SS) and CD45, as shown in A1.1. This was taken as the parent gate and then a combination of SS and CD3 used to identify $CD3^+$ T cells, as shown in A1.2. Taking $CD3^+$ T cells as the parent gate a combination of CD3 and CD4 was used to identify $CD4^+$ T cells. This population was taken as the parent gate and FoxP3 was used to identify $CD4^+$ $FoxP3^+$ T regs. This population was then taken as the parent gate and Helios was used to subset the T reg population into $Helios^+$ and $Helios^-$ groups.

9.2 Appendix 2. Human Organ Transplant Panel

ABCA1	BATF3	CCL3/L1	CD70	CTNNB1	FCAR	HLA-DPB1	IKBKB	IMPDH2	LEF1	MS4A4A	PDCD1LG2	RELA	SLC12A3	TIGIT	VSIR
ABCB1	BAX	CCL4	CD72	CTSL	FCER1A	HLA-DQA1	IKBKG	INHBC	LGALS3	MS4A6A	PDGFA	RELB	SLC19A3	TIMP1	VWF
ABCC2	BCL2	CCL5	CD74	CTSS	FCER1G	HLA-DQB1	IKZF1	INPP5D	LHX6	MS4A7	PDGFRB	RGN	SLC22A2	TIPARP	WARS
ABCE1	BCL2A1	CCR1	CD79A	CTSW	FCGR1A	HLA-DRA	IKZF2	IRF1	LIF	MT1A	PDPN	RGS5	SLC25A15	TLR2	WNT9A
ACKR1	BCL2L1	CCR10	CD80	CX3CL1	FCGR2A	HLA-DRB1	IL10	IRF4	LILRB1	MT2A	PECAM1	RHOJ	SLC4A1	TLR3	XAF1
ACTA2	BCL2L11	CCR2	CD81	CX3CR1	FCGR2B	HLA-DRB3	IL10RA	IRF6	LILRB2	MTOR	PF4	RHOU	SLPI	TLR4	XBP1
ACVR1	BCL3	CCR3	CD82	CXCL1/2	FCGR3A/B	HLA-E	IL10RB	IRF7	LILRB4	MUC1	PHEX	RNF149	SMAD2	TLR5	XCL1/2
ACVRL1	BCL6	CCR4	CD83	CXCL10	FCRL2	HLA-F	IL12A	IRF8	LOX	MX1	PIK3CD	ROBO4	SMAD3	TLR7	ZAP70
ADAM8	BDNF	CCR5	CD84	CXCL11	FGD2	HLA-G	IL12B	IRS1	LRP2	MX2	PIK3CG	RORA	SMAD4	TLR8	ZEB1
ADAMDEC1	BIRC3	CCR6	CD86	CXCL12	FGFBP2	HMGB1	IL12RB1	ISG15	LRRC32	MYB	PIN1	RORC	SMAD5	TLR9	Internal Refer
ADAMTS1	BK VP1	CCR7	CD8A	CXCL13	FJX1	HNF1A	IL12RB2	ISG20	LST1	MYBL1	PLA1A	RPL19	SMARCA4	TM4SF1	ABCF1
ADGRL4	BK large T Ag	CD14	CD8B	CXCL14	FKBP1A	HPRT1	IL13	ITGA4	LTA	MYC	PLAAT4	RPS6	SOCS1	TM4SF18	G6PD
ADORA2A	BLK	CD160	CD96	CXCL16	FLT3	HSD11B1	IL15	ITGAM	LTB	MYD88	PLAT	RPS6KB1	SOCS3	TMEM178A	GUSB
AGER	BLNK	CD163	CDH13	CXCL2	FN1	HSP90AA1	IL16	ITGAX	LTBR	MYL9	PLAU	RTN4	SOD2	TNC	NRDE2
AGR2	BMP2	CD19	CDH5	CXCL5	FOS	HSPA12B	IL17A	ITGB2	LTF	MYOM2	PLAUR	RUNX1	SOST	TNF	OAZ1
AGR3	BMP4	CD1D	CDKN1A	CXCL8	FOSL1	HYAL1	IL17F	ITGB6	LY96	NCAM1	PLK2	RXRA	SOX7	TNFAIP3	POLR2A
AGT	BMP6	CD2	CEACAM3	CXCL9	FOXO1	HYAL2	IL17RA	JAK1	LYVE1	NCR1	PNOC	S100A12	SP100	TNFAIP6	PPIA
AHR	BMP7	CD207	CETP	CXCR3	FOXP3	ICAM1	IL17RB	JAK2	MAF	NFAM1	POU2AF1	S100A8	SP140	TNFRSF14	SDHA
AICDA	BMPER	CD209	CFB	CXCR4	FPR1	ICAM2	IL17RC	JAK3	MALL	NFATC1	PPBP	S100A9	SPIB	TNFRSF17	STK11IP
AIM2	BMPR1A	CD22	CFH	CXCR5	FYN	ICOS	IL18	JUN	MAP3K1	NFATC2	PPM1F	S100B	SPRY4	TNFRSF18	TBC1D10B
AIRE	BMPR1B	CD24	CFI	CXCR6	GAPDH	ICOSLG	IL18BP	KAAG1	MAPK11	NFIL3	PPP3CA	S1PR1	SRC	TNFRSF1A	TBP
AKR1C3	BRWD1	CD244	CFLAR	DCAF12	GATA3	IDO1	IL18RAP	KDR	MAPK12	NFKB1	PRDM1	SAMHD1	ST5	TNFRSF1B	UBB
ALAS1	BST2	CD247	CGAS	DDX50	GBP1	IER5	IL1A	KIR3DL1	MAPK13	NFKB2	PRF1	SCGB1A1	ST8SIA4	TNFRSF4	
ALDH3A2	BTG2	CD27	CH25H	DEFB1	GBP2	IFI27	IL1B	KIR3DL2	MAPK14	NFKBIA	PROX1	SDC1	STAT1	TNFRSF9	
ALOX15	BTK	CD274	CHCHD10	DNMT1	GBP4	IFI30	IL1R1	KIR_Activatin	MAPK3	NFKBIZ	PSEN1	SELE	STAT3	TNFSF10	
ALOX5	BTLA	CD276	CHUK	DNMT3A	GBP5	IFI44	IL1R2	KIR_Activatin	MAPK8	NKG7	PSMB10	SELL	STAT4	TNFSF14	
ANKRD1	C1QA	CD28	CIITA	DUSP2	GDF15	IFI6	IL1RAP	KIR_Inhibitin	MARCH8.	NLRC5	PSMB8	SELP	STAT5A	TNFSF18	
ANKRD22	C1QB	CD34	CITED4	EBI3	GEMIN7	IFIT1	IL1RL1	KIR_Inhibitin	MASP1	NLRP3	PSMB9	SELPLG	STAT5B	TNFSF4	
ANXA1	C1S	CD38	CLEC4C	EBV LMP2	GIMAP5	IFITM1	IL1RN	KIT	MASP2	NNMT	PSME1	SEMA7A	STAT6	TNFSF8	
AOAH	C3	CD3D	CMKLR1	ECSCR	GNG11	IFITM2	IL2	KITLG	MBP	NOD1	PSME2	SERINC5	SYK	TNFSF9	
APOE	C3AR1	CD3E	CMV UL83	EDA	GNLY	IFITM3	IL21	KLF2	MCAM	NOD2	PSTPIP1	SERPINA3	TANK	TOX2	
APOL1	C5	CD3G	COL13A1	EEF1A1	GZMA	IFNA1	IL21R	KLF4	MCM6	NOS2	PTGER4	SERPINE1	TAP1	TP53	
APOL2	C5AR1	CD4	COL1A1	EGFR	GZMB	IFNAR1	IL22	KLHL13	MEF2C	NOS3	PTGS2	SERPING1	TAP2	TPMT	
APOLD1	C9	CD40	COL3A1	EGR1	GZMH	IFNAR2	IL23A	KLRB1	MEGF11	NOTCH1	PTPN2	SERTAD1	TAPBP	TPSAB1/B2	
AQP1	CALHM6	CD40LG	COL4A1	EHD3	GZMK	IFNG	IL23R	KLRC1	MEOX1	NOTCH2	PTPN22	SFTPA2	TBK1	TRAF4	
AQP2	CARD16	CD44	COL4A3	EMP3	HAVCR1	IFNGR1	IL27	KLRD1	MERTK	NOX4	PTPN6	SFTPB	TBX21	TRAF6	
AREG	CARD8	CD45R0	COL4A4	ENG	HAVCR2	IFNGR2	IL27RA	KLRF1	MET	NPDC1	PTPN7	SFTPC	TCF7	TRAT1	
ARG1	CASP1	CD45RA	COL4A5	EOMES	HDAC3	IGF1	IL2RA	KLRG1	MICA	NPHS1	PTPRC	SFTPD	TCL1A	TRDC	
ARG2	CASP3	CD45RB	CPA3	EPAS1	HDAC6	IGF1R	IL2RB	KLRK1	MICB	NPHS2	PTPRO	SH2D1A	TEK	TRDN	
ARHGDIB	CASP4	CD46	CR1	EPO	HDC	IGF2R	IL2RG	KRT19	MIF	NPPA	PTX3	SH2D1B	TFF3	TRDV3	
ARRB2	CASP8	CD47	CRHBP	ERG	HEG1	IGFBP1	IL33	KRT8	MIR155HG	NPPB	PVR	SHROOM3	TFRC	TREM1	
ASB15	CAV1	CD48	CRIP2	ERRFI1	HFE	IGFL1	IL4	LAG3	MME	NR4A1	RAB40C	SIGIRR	TGFB1	TRIB1	
ATF3	CCL13	CD5	CRP	EVA1C	HIF1A	IGHA1	IL4R	LAIR1	MMP12	OASL	RAF1	SIGLEC5	TGFB2	TRIM22	
ATM	CCL15	CD55	CSF1	EZH2	HK2	IGHG1	IL5	LAMP1	MMP14	OR2I1P	RAG2	SIRPG	TGFBI	TYK2	
ATXN3	CCL18	CD58	CSF2	F3	HLA-A	IGHG2	IL6	LAP3	MMP9	OSMR	RAMP3	SKI	TGFBR1	UMOD	
AXL	CCL19	CD59	CSF2RB	FABP1	HLA-B	IGHG3	IL6R	LAYN	MMRN2	P2RX4	RAPGEF5	SLA	TGFBR2	VCAM1	
B2M	CCL2	CD6	CSF3	FADD	HLA-C	IGHG4	IL6ST	LCK	MPIG6B	PADI4	RARRES1	SLAMF6	TGIF1	VCAN	
B3GAT1	CCL20	CD68	CSF3R	FAM30A	HLA-DMA	IGHM	IL7	LCN2	MRC1	PALMD	RASIP1	SLAMF7	THBD	VEGFA	
BASP1	CCL21	CD69	CTLA4	FAS	HLA-DMB	IGKC	IL7R	LCP2	MS4A1	PAX5	RASSF9	SLAMF8	THBS1	VEGFC	
BATF	CCL22	CD7		FASLG	HLA-DPA1	IGLC1	IMPDH1	LDLR	MS4A2	PDCD1	REL	SLC11A1	THEMIS	VMP1	

A.2.2. List of all the genes included in the NanoString Technologies Banff Human Organ Transplant Panel.

9.3 Appendix 3. NanoString GeoMx Protein Panel

Immune cell Profiling Panel	beta-2-microglobulin
	CD3
	CD4
	CD45
	CD11c
	CD20
	CD56
	CD68
	CD8
	CTLA4
	pan-cytokeratin
	fibronectin
	GZMB
	HLA-DR
	Ki-67
	PD-1
	PD-L1
	SMA
IO Drug Target Panel	4-1BB
	ARG1
	B7-H3
	GITR
	IDO1
	LAG3
	OX40L
	STING
	TIM-3
	VISTA
Immune Cell Typing Panel	CD14
	CD163
	CD34
	CD45RO
	CD66b
	FAPalpha
	FOXP3
Human Activation Status Pan	CD127
	CD25
	CD27
	CD40
	CD44
	CD80
	ICOS
	PD-L2
Custom	CXCL9
Negative controls	Ms IgG2a
	MS igG1
	Rb IgG
Housekeepers	Histone H3
	S6
	GAPDH

A3.1. Full list of NanoString Technologies GeoMx DSP protein panels.

9.4 Appendix 4. Ethical approvals

NHS
Health Research Authority
South West - Central Bristol Research Ethics Committee
Whitefriars
Level 3, Block B
Lewin's Mead
Bristol BS1 2NT
Email: nrescommittee.southwest-bristol@nhs.net

18 December 2015

Professor Peter Friend
Oxford Transplant Centre
Churchill Hospital
Oxford
OX3 7LE

Dear Professor Friend

Study title:	**Vascularised sentinel skin flaps to detect rejection in pancreas transplantation**
REC reference:	**15/SW/0333**
IRAS project ID:	**185583**

Thank you for your letter of 15th December 2015, responding to the Committee's request for further information on the above research and submitting revised documentation.

The further information has been considered on behalf of the Committee by the alternate Vice-Chair.

We plan to publish your research summary wording for the above study on the HRA website, together with your contact details. Publication will be no earlier than three months from the date of this opinion letter. Should you wish to provide a substitute contact point, require further information, or wish to make a request to postpone publication, please contact the REC Manager, Mrs Nazneen Nathoo at nrescommittee.southwest-bristol@nhs.net.

Confirmation of ethical opinion

On behalf of the Committee, I am pleased to confirm a favourable ethical opinion for the above research on the basis described in the application form, protocol and supporting documentation as revised, subject to the conditions specified below.

Conditions of the favourable opinion

The REC favourable opinion is subject to the following conditions being met prior to the start of the study.

Management permission must be obtained from each host organisation prior to the start of the study at the site concerned.

Management permission should be sought from all NHS organisations involved in the study in accordance with NHS research governance arrangements. Each NHS organisation must confirm through the signing of agreements and/or other documents that it has given permission for the research to proceed (except where explicitly specified otherwise).

Guidance on applying for NHS permission for research is available in the Integrated Research Application System, www.hra.nhs.uk or at http://www.rdforum.nhs.uk.

Where a NHS organisation's role in the study is limited to identifying and referring potential participants to research sites ("participant identification centre"), guidance should be sought from the R&D office on the information it requires to give permission for this activity.

For non-NHS sites, site management permission should be obtained in accordance with the procedures of the relevant host organisation.

Sponsors are not required to notify the Committee of management permissions from host organisations

Registration of Clinical Trials

All clinical trials (defined as the first four categories on the IRAS filter page) must be registered on a publically accessible database within 6 weeks of recruitment of the first participant (for medical device studies, within the timeline determined by the current registration and publication trees).

There is no requirement to separately notify the REC but you should do so at the earliest opportunity e.g. when submitting an amendment. We will audit the registration details as part of the annual progress reporting process.

To ensure transparency in research, we strongly recommend that all research is registered but for non-clinical trials this is not currently mandatory.

If a sponsor wishes to contest the need for registration they should contact Catherine Blewett (catherineblewett@nhs.net), the HRA does not, however, expect exceptions to be made. Guidance on where to register is provided within IRAS.

It is the responsibility of the sponsor to ensure that all the conditions are complied with before the start of the study or its initiation at a particular site (as applicable).

Ethical review of research sites

NHS sites

The favourable opinion applies to all NHS sites taking part in the study, subject to management permission being obtained from the NHS/HSC R&D office prior to the start of the study (see "Conditions of the favourable opinion" below).

Approved documents

The final list of documents reviewed and approved by the Committee is as follows:

Document	*Version*	*Date*
Covering letter on headed paper [REC Response Letter]	1	11 December 2015
Evidence of Sponsor insurance or indemnity (non NHS Sponsors only) [SSF Sponsor Letter]		26 October 2015
GP/consultant information sheets or letters [SSF GP Letter]	1	26 October 2015
IRAS Checklist XML [Checklist_02112015]		02 November 2015
IRAS Checklist XML [Checklist_11122015]		11 December 2015
Letter from sponsor [SSF Sponsor Letter]		26 October 2015
Letters of invitation to participant [SSF Patient Invite Letter]	1	26 October 2015
Participant consent form [SSF Participant Consent Form]	2	11 December 2015
Participant information sheet (PIS) [SSF Patient Information Leaflet]	2	11 December 2015
REC Application Form [REC_Form_02112015]		02 November 2015
Referee's report or other scientific critique report [SSF Independent Peer Review Form]		08 October 2015
Research protocol or project proposal [SSF Protocol]	1.0	26 October 2015
Summary CV for Chief Investigator (CI) [Peter Friend Short CV]		08 September 2015
Summary CV for student [James Barnes Short CV]		08 September 2015
Summary CV for supervisor (student research) [Peter Friend Short CV]		08 September 2015

Statement of compliance

The Committee is constituted in accordance with the Governance Arrangements for Research Ethics Committees and complies fully with the Standard Operating Procedures for Research Ethics Committees in the UK.

After ethical review

<u>Reporting requirements</u>

The attached document *"After ethical review – guidance for researchers"* gives detailed guidance on reporting requirements for studies with a favourable opinion, including:

- Notifying substantial amendments

- Adding new sites and investigators
- Notification of serious breaches of the protocol
- Progress and safety reports
- Notifying the end of the study

The HRA website also provides guidance on these topics, which is updated in the light of changes in reporting requirements or procedures.

User Feedback

The Health Research Authority is continually striving to provide a high quality service to all applicants and sponsors. You are invited to give your view of the service you have received and the application procedure. If you wish to make your views known please use the feedback form available on the HRA website:
http://www.hra.nhs.uk/about-the-hra/governance/quality-assurance/

HRA Training

We are pleased to welcome researchers and R&D staff at our training days – see details at http://www.hra.nhs.uk/hra-training/

15/SW/0333	**Please quote this number on all correspondence**

With the Committee's best wishes for the success of this project.

Yours sincerely

Mr Brian Pixton
Chair

Enclosures: "After ethical review – guidance for researchers" *[SL-AR2]*

Copy to: *Ms Heather House, R&D Department, Oxford University Hospitals NHS Trust, Churchill Hospital*

Oxford Radcliffe Biobank
NDCLS, Level 4, Academic Block
University of Oxford
John Radcliffe Hospital, Headley Way
Headington Oxford OX3 9DU

T +44 (0) 1865 220550
E orbmanager@ndcls.ox.ac.uk

Prof. Henk Giele

20/05/2021

Department of Plastic Surgery
John Radcliffe Infirmary
Headley Way
Oxford
OX3 9DU

Re Biobank reference **ORB 21/A037**

Dear Prof Giele & Miss Stark

Sentinel skin flaps for immune monitoring in solid organ transplantation

I am writing to inform you that the above named project is approved under the Oxford Radcliffe Biobank (ORB) research tissue bank ethics, reference 19/SC/0173. Please find attached a copy of the ORB approval letter from NRES Committee South Central – Oxford C as confirmation of this approval.

The favourable ethical opinion applies to this research project conducted in the UK using the material supplied by the tissue bank, provided that the release of material complies with the attached NRES conditions. Also attached is your finalised OCHRe application form with the ORB/OCHRe Terms and Conditions as an appendix (note in particular sections 3.3, 3.4 and 3.11).

Please note that this approval applies to this specific research project only. Any further work or deviation from the project as outlined in the application form would require further committee review and approval. Examples of changes that would require further review would include sharing the samples with other researchers or performing a different test or assay.

We ask that any publication or presentation that is based (in whole or in part) on materials obtained via the Oxford Centre for Histopathology Research (OCHRe) or ORB will include the following standard acknowledgement: "We acknowledge the contribution to this study made by the Oxford Centre for Histopathology Research and the Oxford Radcliffe Biobank, which are funded by the University of Oxford, the Oxford CRUK Cancer centre, the NIHR Oxford Biomedical Research Centre (BRC) (Molecular Diagnostics Theme/Multimodal Pathology Subtheme and the NIHR CRN Thames Valley network." You should provide to ORB a copy of any publication(s) based on work derived from the material provided.

Please note it is your responsibility to ensure you destroy all remaining human tissue at the end of the project, or return it to us. Failure to do this is a breach of the Human Tissue Act and the terms of the University of Oxford's Human Tissue Authority licence. All University of Oxford staff working with human tissue must complete HTA training, refer to the University's webpage: https://researchsupport.admin.ox.ac.uk/governance/human-tissue/training

Yours sincerely

Stephanie Jones
Oxford Radcliffe Biobank Collections Governance Manager

Professor Henk Giele
Consultant plastic and transplant surgeon
Oxford University Hospitals
Department of plastic and reconstructive surgery
Level LG1, west wing, Oxford University Hospitals
Headington, Oxford
OX3 9DU

Email: approvals@hra.nhs.uk
HCRW.approvals@wales.nhs.uk

17 April 2020

Dear Professor Giele

HRA and Health and Care Research Wales (HCRW) Approval Letter

Study title:	**Vascularised sentinel skin flaps to monitor for rejection in lung transplantation**
IRAS project ID:	**262849**
Protocol number:	**1**
REC reference:	**20/WM/0026**
Sponsor	**CTRG**

I am pleased to confirm that **HRA and Health and Care Research Wales (HCRW) Approval** has been given for the above referenced study, on the basis described in the application form, protocol, supporting documentation and any clarifications received. You should not expect to receive anything further relating to this application.

Please now work with participating NHS organisations to confirm capacity and capability, in line with the instructions provided in the "Information to support study set up" section towards the end of this letter.

How should I work with participating NHS/HSC organisations in Northern Ireland and Scotland?
HRA and HCRW Approval does not apply to NHS/HSC organisations within Northern Ireland and Scotland.

If you indicated in your IRAS form that you do have participating organisations in either of these devolved administrations, the final document set and the study wide governance report (including this letter) have been sent to the coordinating centre of each participating nation. The relevant national coordinating function/s will contact you as appropriate.

Please see IRAS Help for information on working with NHS/HSC organisations in Northern Ireland and Scotland.

How should I work with participating non-NHS organisations?
HRA and HCRW Approval does not apply to non-NHS organisations. You should work with your non-NHS organisations to obtain local agreement in accordance with their procedures.

What are my notification responsibilities during the study?

The standard conditions document "*After Ethical Review – guidance for sponsors and investigators*", issued with your REC favourable opinion, gives detailed guidance on reporting expectations for studies, including:

- Registration of research
- Notifying amendments
- Notifying the end of the study

The HRA website also provides guidance on these topics, and is updated in the light of changes in reporting expectations or procedures.

Who should I contact for further information?
Please do not hesitate to contact me for assistance with this application. My contact details are below.

Your IRAS project ID is **262849**. Please quote this on all correspondence.

Yours sincerely,

Helen Penistone
Approvals Specialist

Email: approvals@hra.nhs.uk
Telephone: 0207 104 8010

Copy to: *mrs aaa CTRG*

Ymchwil Iechyd a Gofal Cymru
Health and Care Research Wales

NHS
Health Research Authority

Miss Helen L Stark
DPhil student
University of Oxford
Transplantation Research and Immunology Group
John Radcliffe Hospital
Oxford
OX3 9DU

Email: approvals@hra.nhs.uk
HCRW.approvals@wales.nhs.uk

16 June 2022

Dear Miss Stark

HRA and Health and Care Research Wales (HCRW) Approval Letter

Study title:	**Investigating the immune response in pancreas transplantation alone compared to pancreas and sentinel skin flap transplantation combined.**
IRAS project ID:	**292049**
Protocol number:	**1**
REC reference:	**21/EE/0213**
Sponsor	**University of Oxford/Clinical Trials and Research Governance**

I am pleased to confirm that **HRA and Health and Care Research Wales (HCRW) Approval** has been given for the above referenced study, on the basis described in the application form, protocol, supporting documentation and any clarifications received. You should not expect to receive anything further relating to this application.

Please now work with participating NHS organisations to confirm capacity and capability, in line with the instructions provided in the "Information to support study set up" section towards the end of this letter.

How should I work with participating NHS/HSC organisations in Northern Ireland and Scotland?
HRA and HCRW Approval does not apply to NHS/HSC organisations within Northern Ireland and Scotland.

If you indicated in your IRAS form that you do have participating organisations in either of these devolved administrations, the final document set and the study wide governance report

(including this letter) have been sent to the coordinating centre of each participating nation. The relevant national coordinating function/s will contact you as appropriate.

Please see IRAS Help for information on working with NHS/HSC organisations in Northern Ireland and Scotland.

How should I work with participating non-NHS organisations?
HRA and HCRW Approval does not apply to non-NHS organisations. You should work with your non-NHS organisations to obtain local agreement in accordance with their procedures.

What are my notification responsibilities during the study?

The standard conditions document "*After Ethical Review – guidance for sponsors and investigators*", issued with your REC favourable opinion, gives detailed guidance on reporting expectations for studies, including:

- Registration of research
- Notifying amendments
- Notifying the end of the study

The HRA website also provides guidance on these topics, and is updated in the light of changes in reporting expectations or procedures.

Who should I contact for further information?
Please do not hesitate to contact me for assistance with this application. My contact details are below.

Your IRAS project ID is **292049**. Please quote this on all correspondence.

Yours sincerely,

Mathew Barnes
Approvals Specialist

Email: approvals@hra.nhs.uk

Copy to: *CTRG*

9.5 Appendix 5. Full list of differentially expressed genes in skin at rejection.

Gene	Log2 fold change	BH.p.value	Gene	Log2 fold change	BH.p.value	Gene	Log2 fold change	BH.p.value
CXCL10-mRNA	-6.29	0.0011	**CD68-mRNA**	-2.66	0.00432	**CXCL16-mRNA**	-2	0.0179
CXCL9-mRNA	-5.93	0.0022	**NFIL3-mRNA**	-2.61	0.00545	**HLA-DRB3-mRNA**	-1.98	0.00267
S100A9-mRNA	-4.59	0.0011	**LY96-mRNA**	-2.61	0.00752	**OSMR-mRNA**	-1.98	0.00815
FOS-mRNA	-4.16	0.000696	**IL10RA-mRNA**	-2.6	0.00239	**APOLD1-mRNA**	-1.98	0.0231
S100A8-mRNA	-3.96	0.0156	**CGAS-mRNA**	-2.59	0.000331	**NFKBIA-mRNA**	-1.97	0.00613
ATF3-mRNA	-3.94	0.001	**IRF8-mRNA**	-2.59	0.00186	**SAMHD1-mRNA**	-1.97	0.00867
CXCL1/2-mRNA	-3.78	0.000696	**CCL19-mRNA**	-2.59	0.00335	**HLA-DRB1-mRNA**	-1.96	0.00176
JUN-mRNA	-3.78	0.00119	**CD45R0-mRNA**	-2.56	0.0081	**HLA-F-mRNA**	-1.96	0.0125
SERPINE1-mRNA	-3.76	0.00111	**FGD2-mRNA**	-2.55	0.00387	**TGFB1-mRNA**	-1.94	0.00377
FCER1G-mRNA	-3.66	0.00188	**GBP4-mRNA**	-2.55	0.00389	**THBS1-mRNA**	-1.94	0.00754
C1QB-mRNA	-3.62	0.00164	**RELB-mRNA**	-2.53	0.00228	**HLA-DRA-mRNA**	-1.92	0.0011
CD209-mRNA	-3.58	0.00137	**BCL3-mRNA**	-2.51	0.00313	**TAPBP-mRNA**	-1.9	0.0081

LCP2-mRNA	-3.51	0.000696	**PSMB9-mRNA**	-2.49	0.0033	**LST1-mRNA**	-1.88	0.00509
IGKC-mRNA	-3.41	0.0221	**CSF1-mRNA**	-2.42	0.00389	**IFI6-mRNA**	-1.86	0.0348
CFB-mRNA	-3.38	0.00178	**TIMP1-mRNA**	-2.39	0.00165	**ADAMTS1-mRNA**	-1.85	0.0168
CALHM6-mRNA	-3.28	0.00242	**CD84-mRNA**	-2.38	0.017	**PDPN-mRNA**	-1.84	0.0236
FCGR3A/B-mRNA	-3.27	0.00149	**HLA-DMB-mRNA**	-2.35	0.00629	**PLAU-mRNA**	-1.82	0.0163
IDO1-mRNA	-3.26	0.00153	**KLRK1-mRNA**	-2.34	0.0092	**IFI27-mRNA**	-1.82	0.046
MS4A6A-mRNA	-3.22	0.00178	**CTSS-mRNA**	-2.32	0.000876	**SEMA7A-mRNA**	-1.81	0.0071
CD14-mRNA	-3.2	0.00189	**EGR1-mRNA**	-2.31	0.0127	**TRIB1-mRNA**	-1.79	0.00826
CD163-mRNA	-3.2	0.00243	**CD4-mRNA**	-2.28	0.00242	**SERTAD1-mRNA**	-1.77	0.00593
IKZF1-mRNA	-3.13	0.00132	**IFITM1-mRNA**	-2.28	0.00243	**CDKN1A-mRNA**	-1.76	0.0148
MS4A4A-mRNA	-3.12	0.00267	**PSMB10-mRNA**	-2.25	0.00267	**FN1-mRNA**	-1.76	0.0154
TNFRSF1B-mRNA	-3.08	0.0011	**TNC-mRNA**	-2.25	0.0165	**CD40-mRNA**	-1.75	0.0171
CXCR4-mRNA	-3.06	0.00189	**BST2-mRNA**	-2.23	0.0267	**PTPN6-mRNA**	-1.71	0.011
IRF1-mRNA	-2.97	0.00197	**STAT1-mRNA**	-2.21	0.00242	**C3-mRNA**	-1.71	0.0403
TLR2-mRNA	-2.96	0.001	**FCGR2B-mRNA**	-2.21	0.0122	**IL4R-mRNA**	-1.69	0.00168

SOD2-mRNA	-2.96	0.0011	**HLA-DPA1-mRNA**	-2.19	0.00716	**SERPING1-mRNA**	-1.68	0.00567
MT2A-mRNA	-2.91	0.00139	**HLA-DMA-mRNA**	-2.18	0.00509	**PTGER4-mRNA**	-1.66	0.00389
IL18BP-mRNA	-2.9	0.0011	**NFKB2-mRNA**	-2.17	0.00867	**SLPI-mRNA**	-1.66	0.0334
TRIM22-mRNA	-2.89	0.00119	**PIK3CG-mRNA**	-2.17	0.0161	**VCAN-mRNA**	-1.65	0.0428
CD83-mRNA	-2.87	0.00279	**TLR4-mRNA**	-2.16	0.00867	**IFNAR2-mRNA**	-1.64	0.00863
PTPRC-mRNA	-2.85	0.00282	**WARS-mRNA**	-2.14	0.00509	**TAP1-mRNA**	-1.63	0.00242
ICAM1-mRNA	-2.83	0.001	**CTSL-mRNA**	-2.14	0.00752	**GIMAP5-mRNA**	-1.6	0.0435
APOL1-mRNA	-2.82	0.0011	**HLA-DPB1-mRNA**	-2.11	0.00792	**RUNX1-mRNA**	-1.59	0.0335
IL2RG-mRNA	-2.81	0.00242	**IFITM3-mRNA**	-2.09	0.00484	**ARHGDIB-mRNA**	-1.58	0.017
MRC1-mRNA	-2.81	0.00754	**IL15-mRNA**	-2.09	0.00844	**IFITM2-mRNA**	-1.57	0.00422
TNFAIP3-mRNA	-2.8	0.00149	**CIITA-mRNA**	-2.07	0.00346	**HLA-C-mRNA**	-1.55	0.00173
GBP1-mRNA	-2.8	0.00377	**CD74-mRNA**	-2.06	0.000876	**PSME2-mRNA**	-1.54	0.00256
IFI30-mRNA	-2.79	0.00389	**CMKLR1-mRNA**	-2.06	0.0081	**MYD88-mRNA**	-1.53	0.0115
VCAM1-mRNA	-2.75	0.00752	**BTG2-mRNA**	-2.06	0.0179	**VEGFA-mRNA**	-1.53	0.0338

PLAAT4-mRNA	-2.74	0.00377	**PIK3CD-mRNA**	-2.05	0.00377	**TLR3-mRNA**	-1.52	0.0468
CCL2-mRNA	-2.73	0.00165	**APOL2-mRNA**	-2.05	0.0038	**HLA-B-mRNA**	-1.51	0.0092
NNMT-mRNA	-2.73	0.00274	**TAP2-mRNA**	-2.05	0.00545	**IGHM-mRNA**	1.86	0.044
ST8SIA4-mRNA	-2.68	0.00394	**GBP2-mRNA**	-2.03	0.000341			

9.6 Appendix 6. Differentially expressed genes in blood and skin samples

DEG skin 3m post Tx	DEG skin 6m post Tx	DEG blood 3m post Tx	DEG blood 6m post Tx
BCL3	ADAMTS1	BCL2	**CCR7**
CD163	**BCL3**	CCR4	**CD40LG**
CD44	CCL2	CCR7	**IL7R**
FOS	**CD44**	CD2	**LEF1**
ITGB2	CDH13	CD27	**TCF7**
MT2A	CITED4	CD28	
MYC	COL4A5	CD3D	
SOD2	FKBP1A	CD3E	
STAT6	**FOS**	CD3G	
THBD	IER5	CD40LG	
	IGLC1	CD5	
	LCN2	CXCR3	
	LTBR	CXCR6	
	MICA	GATA3	
	MT2A	GIMAP5	
	MYC	ICOS	
	NFIL3	IGHA1	
	NFKBIZ	IGHG2	
	NOTCH1	IGHG3	
	NPDC1	IL7R	
	SOD2	KLRG1	
	STAT6	LCK	
	TAP1	LEF1	
	THBD	MYC	

	THBS1	RORA	
		SIRPG	
		TCF7	
		THEMIS	
		TRAT1	

A.6.1. Full list of the genes found to be differentially expressed at 3- and 6-months post-transplantation. Genes in bold are downregulated at both 3- and 6-months post-transplant. Gene highlighted in yellow are downregulated in both skin and blood at 3 months post- transplant. DEG = differentially expressed gene.

9.7 Appendix 7. Impact of COVID-19

I started my DPhil Trinity Term 2019. My original research plan was to carry out a clinical trial of sentinel skin flaps for immune monitoring in lung transplantation. I spent the first 12 months of my DPhil working towards this aim, which included being successful in applying for HRA and REC committee approval (REC ref 20/WM/0026, IRAS 262849). Unfortunately, due to COVID-19 I have been unable to start this trial. I therefore had to develop and plan a new thesis. I was able to access samples from a previous trial carried out in Oxford of sentinel skin flaps for immune monitoring in pancreas transplantation and I also wrote and applied for ethics to access samples from patients with abdominal wall and small bowel transplants. I was then required to learn new laboratory techniques to process these samples. Once again COVID-19 impacted the time available for this, as there was a period of 6 months from March 2020- August 2020 when we were not able to go into the lab. Not only did this impair my ability to learn and carry out experiments, it also reduced the opportunities I had for discussion with both peers and senior scientists within the lab, often vital educational opportunities. Despite these challenges I think there has also been a positive impact of COVID-19. I have learnt to be more adaptable and to have multiple lines of enquiry open to build resilience within my research. It has also given me the opportunity to enhance my laboratory skills with new techniques and to develop my bioinformatic skills.